

POST-TENSIONING THE INVERTED-T BRIDGE SYSTEM FOR IMPROVED
DURABILITY AND INCREASED SPAN-TO-DEPTH RATIO

by

RIM M. NOUREDDIN NAYAL

B. SC., ALEPPO UNIVERSITY, SYRIA, 2000
M.S., KANSAS STATE UNIVERSITY, 2003

AN ABSTRACT OF A DISSERTATION

submitted in partial fulfillment of the requirements for the degree

DOCTOR OF PHILOSOPHY

DEPARTMENT OF CIVIL ENGINEERING
COLLEGE OF ENGINEERING

KANSAS STATE UNIVERSITY
Manhattan, Kansas

2006

Abstract

Possibly the most pressing need in highway construction today is the repair or replacement of existing bridges. Due to increased needs and growing traffic, in addition to aging and extensive use, more than 2000 bridges in Kansas alone need to be replaced during the next decade. The majority of these bridges has spans of 100 ft or less, and has relatively shallow profiles. It is becoming increasingly important to implement a standard method for replacement in which the process is expedited and accomplished in cost-effective manner.

Requirements for design and construction of concrete bridges have drastically changed during recent years. A main change in design is live-load requirements.

Nebraska inverted-T bridge system has gained increasing popularity for its lower weight compared to I-girder bridges. However, there are some limiting issues when using IT system in replacing existing CIP bridges.

Implementation of a post-tensioned IT system, which is the focus of this research, is believed to be one excellent solution for the IT deficiencies. Post-tensioning is added by placing a draped, post-tensioning duct in the stems of the IT members. Post-tensioning will lead to a higher span-to-depth ratio than IT system, and will reduce the potential transverse cracks in the (CIP) deck. Finally, the undesired cambers of pretensioned beams will be reduced, because fewer initial prestressing will be needed.

This study was intended to explore the behavior of the PT-IT system, identify major parameters that control and limit the design of this system, and investigate different construction scenarios. This was achieved by conducting an extensive parametric study. For that purpose, PT-IT analysis program was developed and written using C++ programming language. The program was used to analyze various post-tensioning procedures for the post-tensioned inverted-T system. A Visual Basic friendly interface was provided to simplify the data input process.

The findings of this research included recommendation of construction scenario for PT-IT system, as well as examining different methods for estimating time-dependent restraining moments. Effect of different concrete strengths on the behavior of PT-IT system was also

determined. Most importantly, the effect of timing on different construction stages was also evaluated and determined.

POST-TENSIONING THE INVERTED-T BRIDGE SYSTEM FOR IMPROVED
DURABILITY AND INCREASED SPAN-TO-DEPTH RATIO

by

RIM M. NOUREDDIN NAYAL

B. SC., ALEPPO UNIVERSITY, SYRIA, 2000
M.S., KANSAS STATE UNIVERSITY, 2003

A DISSERTATION

submitted in partial fulfillment of the requirements for the degree

DOCTOR OF PHILOSOPHY

DEPARTMENT OF CIVIL ENGINEERING
COLLEGE OF ENGINEERING

KANSAS STATE UNIVERSITY
Manhattan, Kansas

2006

Approved by:

Major Professor
ROBERT J. PETERMAN

Copyright

RIM NAYAL

2006

Abstract

Possibly the most pressing need in highway construction today is the repair or replacement of existing bridges. Due to increased needs and growing traffic, in addition to aging and extensive use, more than 2000 bridges in Kansas alone need to be replaced during the next decade. The majority of these bridges has spans of 100 ft or less, and has relatively shallow profiles. It is becoming increasingly important to implement a standard method for replacement in which the process is expedited and accomplished in cost-effective manner.

Requirements for design and construction of concrete bridges have drastically changed during recent years. A main change in design is live-load requirements.

Nebraska inverted-T bridge system has gained increasing popularity for its lower weight compared to I-girder bridges. However, there are some limiting issues when using IT system in replacing existing CIP bridges.

Implementation of a post-tensioned IT system, which is the focus of this research, is believed to be one excellent solution for the IT deficiencies. Post-tensioning is added by placing a draped, post-tensioning duct in the stems of the IT members. Post-tensioning will lead to a higher span-to-depth ratio than IT system, and will reduce the potential transverse cracks in the (CIP) deck. Finally, the undesired cambers of pretensioned beams will be reduced, because fewer initial prestressing will be needed.

This study was intended to explore the behavior of the PT-IT system, identify major parameters that control and limit the design of this system, and investigate different construction scenarios. This was achieved by conducting an extensive parametric study. For that purpose, PT-IT analysis program was developed and written using C++ programming language. The program was used to analyze various post-tensioning procedures for the post-tensioned inverted-T system. A Visual Basic friendly interface was provided to simplify the data input process.

The findings of this research included recommendation of construction scenario for PT-IT system, as well as examining different methods for estimating time-dependent restraining moments. Effect of different concrete strengths on the behavior of PT-IT system was also

determined. Most importantly, the effect of timing on different construction stages was also evaluated and determined.

Table of Contents

List of Figures	xii
List of Tables	xx
Acknowledgements.....	xxi
Dedication	xxii
CHAPTER 1 - Introduction	1
Overview.....	1
Objectives	2
Outline	4
CHAPTER 2 - Literature Review	5
General Description	5
Available Methods for Evaluating Time-Dependent Losses	8
Time-Step Prestress Loss Methods.....	9
Refined Prestress Loss Methods	10
Lump-Sum Methods	12
Methods to Calculate Time-Dependent Restraining Moments.....	12
PCA Method	13
Texas Transportation Institute	15
CTL Method.....	16
P Method.....	18
Creep-Transformed Section Properties Method	20
Positive Moment Connection for Girders Made Continuous with CIP Deck.....	23
CHAPTER 3 - Analysis of Post-Tensioned Prestressed Inverted T System	30
Time-Dependent Material Properties.....	31
Concrete Compressive Strength.....	31
Modulus of Elasticity	33
Shrinkage Strain.....	34
Creep Coefficient	39
Relaxation of Steel.....	43

Instantaneous Losses in Post-tensioning.....	45
Design-Limit State.....	46
Strength I Limit State.....	46
Service I Limit State.....	47
Service III Limit State.....	47
Flexural Design and Capacity Check.....	47
Vertical Shear Design and Capacity Check.....	48
Allowable Stresses.....	50
Vehicular Live-load.....	51
Algorithm.....	51
Comparison with Consplice.....	55
Example 1: IT-700.....	55
Example 2: IT-500.....	60
Discussion of P Method and CTL Method.....	61
CHAPTER 4 - RESULTS OF PARAMETRIC STUDY.....	103
Scope of Parametric Study.....	103
Parametric Study Results.....	104
Different Construction Scenarios.....	104
Effect of Concrete Strength.....	109
Effect of girder concrete strength.....	109
Effect of deck concrete.....	110
Effect of Different Creep and Shrinkage Models.....	110
Effect of Timing.....	111
Effect of time of cutting prestressing strands.....	111
Effect of time of establishing continuity and casting the deck.....	111
Effect of time of establishing continuity.....	111
Effect of time of casting the deck.....	112
Effect of time of post-tensioning.....	112
Comparison with Experimental Data.....	112
Experiment 1: Mattock.....	113
Experiment 2: Peterman and Ramirez.....	113

CHAPTER 5 - CONCLUSION AND RECOMMENDATIONS	157
Conclusion	157
Recommendation	159
Notations	161
References	164
Appendix A - Details of Reinforcement	168
Concrete Cover	168
Minimum Spacing of Prestressing Tendons	168
Maximum Number of Post-Tensioning Tendons and Duct Size	168
Design and Detailing of Anchorage Zone	169
Appendix B - Program Documentation	176
Class "Data"	177
Class "Solve"	181
Class "Element"	183
Class "Element2"	184
Class "Diaphragm"	185
Class "Node"	185
Class "ESM"	186
Class "BCEssential"	187
Class "DOF"	187
Class "FixedEM"	188
Class "BCNodalLoad"	189
Class "MomentandShear"	190
Class "Concrete Stresses"	190
Class "Meterial"	192
Class "Steel"	192
Class "Concrete"	193
Class "PreStrands"	194
Class "PostTend"	195
Class "Straight"	197
Class "ParabolicPT"	197

Class “Section”	198
Class “TimeDepLosses”	200
Class “Time”	201
Class “Matrix”	201

List of Figures

Figure 2. 1 PT-IT bridge system under construction	25
Figure 2. 2 PT-IT bridge system under construction	25
Figure 2. 3 IT section and modified IT section.....	26
Figure 2. 4 PT-IT bridge system.....	27
Figure 2. 5 Realtive humidity correction factor (Texas Technology Institute method) ...	28
Figure 2. 6 Volume-to-surface ratio correction factor (Texas Technology Institute method)	28
Figure 2. 7 (a) Deformation due to differential shrinkage, (b) Restraining moments in continuous prestressed, precast beams made continuous by CIP deck.....	29
Figure 3. 1 Experimental shrinkage strain versus predicted strain for SCC.....	66
Figure 3. 2 Experimental creep coefficient versus predicted creep coefficient for specimen loaded at Day 1	66
Figure 3. 3 SCC-Experimental creep coefficient versus predicted creep coefficient for specimen loaded at day 29	67
Figure 3. 4 Experimental creep coefficient versus predicted creep coefficient using equation for specimen loaded at day 1 and corrected for loading age of 29 days.....	67
Figure 3. 5 Structural analysis model	68
Figure 3. 6 Example 1. IT 700 section properties.....	68
Figure 3. 7 Example 1. beam layout	69
Figure 3. 8 Post-tensioning tendons profile	69
Figure 3. 9 Example 1-PT-IT front page	70
Figure 3. 10 Example 1-concrete properties form	70
Figure 3. 11 Example 1-beam layout.....	71
Figure 3. 12 Example 1-section properties	71
Figure 3. 13 Example 1-deck dimensions and material.....	72
Figure 3. 14 Example 1-strands properties	72
Figure 3. 15 Example 1-post-tensioned tendons.....	73

Figure 3. 16 Example 1-supports	73
Figure 3. 17 Example 1-externally applied loads	74
Figure 3. 18 Example 1-staging	74
Figure 3. 19 Example 1-stress in prestressed strands along the bridge	75
Figure 3. 20 Example 1-stress in post-tensioned tendons along the bridge.....	75
Figure 3. 21 Example 1-moments resulting from girder and deck weight	76
Figure 3. 22 Example 1-moments resulting from prestressing forces	76
Figure 3. 23 Example 1-moments due to post-tensioning forces.....	77
Figure 3. 24 Example 1-moments resulting from differential shrinkage between deck and girder	77
Figure 3. 25 Example 1-moments resulting from barrier weight.....	78
Figure 3. 26 Example 1-positive moments due to lane load.....	78
Figure 3. 27 Example 1-negative moments due to lane load.....	79
Figure 3. 28 Example 1-positive moments due to design tandem	79
Figure 3. 29 Example 1-negative moments due to design tandem	80
Figure 3. 30 Example 1-positive moments due to design truck.....	80
Figure 3. 31 Example 1-Negative moments due to design truck.....	81
Figure 3. 32 Example 1-Negative moments due to double tandem.....	81
Figure 3. 33 Example 1-Negative moments due to double truck	82
Figure 3. 34 Example 1-HL-93 Positive moment.....	82
Figure 3. 35 Example 1-HL-93 Negative moment	83
Figure 3. 36 Example 1-Factored required moment	83
Figure 3. 37 Example 1-(1.2 Times cracking moment).....	84
Figure 3. 38 Example 1- ΦM_n (Nominal resistance moment).....	84
Figure 3. 39 Example 1-Time-dependent deflection due to prestressing	85
Figure 3. 40 Example 1-Time-dependent deflection due to component weight and shrinkage	85
Figure 3. 41 Example 1-Time-dependent deflection due to post-tensioning.....	86
Figure 3. 42 Example 1-Time-dependent deflection due to barriers weight	86
Figure 3. 43 Example 2 IT 500 section properties.....	87
Figure 3. 44 Example 2-Beam layout	88

Figure 3. 45 Example 2-Post-tensioning tendons profile.....	88
Figure 3. 46 Example 2-Stresses in prestressed strands along the bridge	89
Figure 3. 47 Example 2- Stresses in post-tensioned tendons along the bridge.....	89
Figure 3. 48 Example 2- Moments resulting from girder and deck weights	90
Figure 3. 49 Example 2- Moments resulting from prestressing forces.....	90
Figure 3. 50 Example 2-Moments due to post-tensioning forces	91
Figure 3. 51 Example 2- Moments resulting from differential shrinkage between deck and girder	91
Figure 3. 52 Example 2- Moments resulting from barriers weight.....	92
Figure 3. 53 Example 2-HL-93 Positive moment.....	92
Figure 3. 54 Example 2- HL-93 Negative moment	93
Figure 3. 55 Example 2-Factored required moment	93
Figure 3. 56 Example 2- Φ times nominal resistance moment.....	94
Figure 3. 57 Example 2-time-dependent deflection due to prestressing.....	94
Figure 3. 58 Example 2-time-dependent deflection due to component weight and shrinkage	95
Figure 3. 59 Example 2-time-dependent deflection due to post-tensioning	95
Figure 3. 60 Example 2-time-dependent deflection due to barrier weight	96
Figure 3. 61 Forces in deck and girder due to differential shrinkage	96
Figure 3. 62 Deformations affecting both deck and girder	97
Figure 3. 63 Example 1-prediction of restraining moment due to differential shrinkage using published versus suggested CTL equation.....	97
Figure 3. 64 Example 1-prediction of restraining moment due to differential shrinkage using published versus suggested P equations	98
Figure 3. 65 Example 1-prediction of restraining moment due to differential shrinkage using PCA, suggested CTL, and suggested P expressions.....	98
Figure 3. 66 Example 2-prediction of restraining moment due to differential shrinkage using published versus suggested CTL equations	99
Figure 3. 67 Example 2-prediction of restraining moment due to differential shrinkage using published versus suggested P equation.....	99

Figure 3. 68 Example 2-prediction of restraining moment due to differential shrinkage using PCA, suggested CTL, and suggested P expressions	100
Figure 4. 1 Maximum spans for different IT sections for different construction scenarios, for girder concrete strength of 8 ksi.....	115
Figure 4. 2 Time-dependent restraining moments using different methods for Dia & Deck-PT construction scenario; continuity established @ 14 days of girder's age.....	115
Figure 4. 3 Time-dependent restraining moments using different methods for Dia - Deck-PT construction scenario; continuity established @ 14 days of girder age.....	116
Figure 4. 4 Time-dependent restraining moments using different methods for Dia -PT - Deck construction scenario; continuity established @ 14 days of girder age.....	116
Figure 4. 5 Time-dependent restraining moments using different methods for (two-stage PT) construction scenario; continuity established @ 14 days of girder age.....	117
Figure 4. 6 Secondary moment due to post-tensioning for different construction scenarios; continuity established @ 14 days.....	117
Figure 4. 7 Post-tensioning tendon path with respect to C.G. of the girder and C.G. of the composite section.....	118
Figure 4. 8 Maximum positive restraining moment in the pier including LL, for different construction scenario according to CTL method; continuity established @ 14 days of girder age	118
Figure 4. 9 Maximum positive restraining moment in the pier including LL, different construction scenarios, P method; continuity established @ 14 days of girder age	119
Figure 4. 10 Maximum negative restraining moment in the pier, for Dia & Deck-PT construction scenario, P method; continuity established @ 14 days of girder age	119
Figure 4. 11 Maximum negative restraining moment in the pier for Dia - Deck-PT construction scenario, P method; continuity established @ 14 days of girder age	120
Figure 4. 12 Time-dependent restraining moment in the pier for Dia - Deck -PT construction scenario according to P method	120
Figure 4. 13 Restraining moment in the pier for Dia - Deck -PT construction scenario resulting from time-dependent effect and secondary moment due to post-tensioning	121

Figure 4. 14 Maximum negative restraining moment in the pier for Dia -PT - Deck construction scenario, P method; continuity established @ 14 days of girder age	121
Figure 4. 15 Time-dependent restraining moment in the pier for Dia -PT - Deck construction scenario according to P method	122
Figure 4. 16 Restraining moment in the pier for Dia – PT - Deck construction scenario resulting from time-dependent effect and secondary moment due to post-tensioning	122
Figure 4. 17 Maximum negative restraining moment in the pier for two-stage PT construction scenario, P method; continuity established @ 14 days of girder age	123
Figure 4. 18 Time-dependent restraining moments using different methods for Dia & Deck-PT construction scenario; continuity established @ 224 days of girder age.....	123
Figure 4. 19 Time-dependent restraining moments using different methods for Dia - Deck-PT construction scenario; continuity established @ 224 days of girder age.....	124
Figure 4. 20 Time-dependent restraining moments using different methods for Dia-PT - Deck construction scenario; continuity established @ 224 days of girder age.....	124
Figure 4. 21 Time-dependent restraining moments using different methods for two-stage PT construction scenario; continuity established @ 224 days of girder age.....	125
Figure 4. 22 Secondary moment due to post-tensioning for different construction scenarios; continuity established @ 224 days of girder age	125
Figure 4. 23 Maximum negative restraining moment in the pier for Dia & Deck-PT construction scenario, P method; continuity established @ 224 days of girder age	126
Figure 4. 24 Maximum negative restraining moment in the pier for Dia- Deck- PT construction scenario, P method; continuity established @ 224 days of girder age	126
Figure 4. 25 Time-dependent restraining moment in the pier for Dia - Deck -PT construction scenario according to P method	127
Figure 4. 26 Restraining moment in the pier for Dia - Deck -PT construction scenario resulting from time-dependent effect and secondary moment due to post-tensioning	127
Figure 4. 27 Maximum negative restraining moment in the pier for Dia- PT- Deck construction scenario, P method; continuity established @ 224 days of girder age	128
Figure 4. 28 Time-dependent restraining moment in the pier for Dia-PT- Deck construction scenario according to P method	128

Figure 4. 29 Restraining moment in the pier for Dia -PT- Deck construction scenario resulting from time-dependent effect and secondary moment due to post-tensioning	129
Figure 4. 30 Maximum negative restraining moment in the pier for two-stage PT construction scenario, P method; continuity established @ 224 days of girder age	129
Figure 4. 31 Shear reinforcement detailing for Dia & Deck-PT construction scenario .	130
Figure 4. 32 Shear reinforcement detailing for Dia & Deck-PT construction scenario .	130
Figure 4. 33 Shear reinforcement detailing for Dia -Deck-PT construction scenario	131
Figure 4. 34 Shear reinforcement detailing for Dia -Deck-PT construction scenario	131
Figure 4. 35 Shear reinforcement detailing for Dia –PT - Deck construction scenario..	132
Figure 4. 36 Shear reinforcement detailing for Dia –PT - Deck construction scenario..	132
Figure 4. 37 Shear reinforcement detailing for two-stage PT construction scenario.....	133
Figure 4. 38 Shear reinforcement detailing for two-stage PT construction scenario.....	133
Figure 4. 39 Time-dependent restraining moment in the pier for different concrete strength of the girder using PCA method.....	134
Figure 4. 40 Time-dependent restraining moment in the pier for different concrete strength of the girder using CTL method.....	134
Figure 4. 41 Time-dependent restraining moment in the pier for different concrete strength of the girder using P method	135
Figure 4. 42 Time-dependent restraining moment in the pier for different concrete strength of the girder using creep-transformed section properties method.....	135
Figure 4. 43 Time-dependent restraining moment due to creep under prestressing, according to CTL method.....	136
Figure 4. 44 Time-dependent restraining moment due to creep under girder weight, according to CTL method.....	136
Figure 4. 45 Time-dependent restraining moment due to differential shrinkage, according to CTL method.....	137
Figure 4. 46 Losses in prestressing strands for different concrete strengths	137
Figure 4. 47 Losses in post-tensioning tendons for different concrete strengths.....	138
Figure 4. 48 Time-dependent restraining moment for different concrete strengths of the deck using CTL method	138

Figure 4. 49 Time-dependent restraining moment for different concrete strengths of the deck using P method.....	139
Figure 4. 50 Prediction of shrinkage strain using different models for 6-ksi concrete...	139
Figure 4. 51 Prediction of creep coefficient using different models for 6-ksi concrete .	140
Figure 4. 52 Prediction of shrinkage strain using different models for 10-ksi concrete.	140
Figure 4. 53 Prediction of creep coefficient using different models for 10-ksi concrete	141
Figure 4. 54 Predicted losses in pretensioned strands using different models.....	141
Figure 4. 55 Predicted losses in post-tensioning using different models.....	142
Figure 4. 56 Time-dependent restraining moment for different creep-and-shrinkage models using PCA method.....	142
Figure 4. 57 Time-dependent restraining moment for different creep-and-shrinkage models using CTL method.....	143
Figure 4. 58 Time-dependent restraining moment for different creep-and-shrinkage models using P method	143
Figure 4. 59 Time-dependent restraining moment for different creep-and-shrinkage models using creep-transformed section properties method.....	144
Figure 4. 60 Effect of time of cutting strands on losses in prestressing	144
Figure 4. 61 Time-dependent restraining moment in the pier for continuity established @ 14 days of girder age	145
Figure 4. 62 Time-dependent restraining moment in the pier for continuity established @ 28 days of girder age	145
Figure 4. 63 Time-dependent restraining moment in the pier for continuity established @ 56 days of girder age	146
Figure 4. 64 Time-dependent restraining moment in the pier for continuity established @ 112 days of girder age.....	146
Figure 4. 65 Time-dependent restraining moment in the pier for continuity established @ 224 days of girder age.....	147
Figure 4. 66 Secondary moments due to post-tensioning for different times of establishing continuity	147
Figure 4. 67 Restraining moment in the pier for continuity established @ 14 days of girder age	148

Figure 4. 68 Restraining moment in the pier for continuity established @ 28 days of girder age	148
Figure 4. 69 Restraining moment in the pier for continuity established @ 56 days of girder age	149
Figure 4. 70 Restraining moment in the pier for continuity established @ 112 days of girder age	149
Figure 4. 71 Restraining moment in the pier for continuity established @ 224 days of girder age	150
Figure 4. 72 Effect of time of casting the deck on time-dependent restraining moment using CTL method.....	150
Figure 4. 73 Effect of time of casting the deck on time-dependent restraining moment using P method.....	151
Figure 4. 74 Effect of time of casting the deck on the restraining moment in the pier ..	151
Figure 4. 75 Cross section for experiment conducted by (4).....	152
Figure 4. 76 Comparison with experimental data (4).....	152
Figure 4. 77 Cross section of panels tested by (7).....	153
Figure 4. 78 Comparison with experimental data from (7)	153
Figure A. 1 General zone and local zone.....	174
Figure A. 2 Bearing plate dimension for tendons consisting of 5-0.6” strands.....	174
Figure A. 3 Detailing of anchorage zone for tendons consisting of 5-0.6” strands.....	174
Figure A. 4 Bearing plate dimension for tendons consisting of 5-0.6” strands.....	175
Figure A. 5 Detailing of anchorage zone for tendons consisting of 5-0.6” strands.....	175

List of Tables

Table 3. 1 Values of the constants α and β and the time ratio for the concrete compressive strength ⁽²⁴⁾	101
Table 3. 2 Values for K_1 and K_2 ⁽¹⁴⁾	102
Table 3. 3 Shrinkage factor γ_{cp} ⁽¹⁴⁾	102
Table 3. 4 Recommended values for friction and wobble coefficient	102
Table 4. 1 Variation of parameters	154
Table 4. 2 Maximum spans for different construction scenarios for IT 500-IT 1000	155
Table 4. 3 Maximum span-to-depth ratio for different construction scenarios for IT 700155	
Table 4. 4 Details for IT 500 for different concrete strengths	156
Table 4. 5 Restraining moment in the pier due to girder weight	156
Table 4. 6 Effect of time of establishing continuity (casting diaphragm) on maximum span-to-depth ratio	156

Acknowledgements

I express my appreciation and thanks to Dr. Robert J. Peterman, for giving me this opportunity and supporting me during the course of this research.

I'd like to extend my appreciation and thanks to Dr. asadollah Esmaeily, his inspiration and encouragement strengthened my ability to tackle the difficulties encountered during my graduate study.

I'm grateful to Dr. Hayder Rasheed who prepared me and guided me to the successful path of graduate studies; his advising and teachings formed my strong background in structural engineering.

Special thanks to Dr. Youqi wang and Dr. Malgorzata J. Rys for being members in my dissertation committee and generously giving their time to better this work.

This work would have not been possible without the generous support and funding from Kansas Department of Transportation.

I'd like to acknowledge Mr. Kenneth F. Hurst, Mr. Loren Risch, and Mr. Steve Burnette, for their help during this research.

Dedication

To my parents,

M.Noureddin Nayal and Lamis Kudsi

This would have not been possible without their sacrifices, encouragement, patience and endless love.

Thanks for their sincere prayers and blessing

To my father, and mother in law

Farouk Charkas and Amira Bayaa

For all love and care they gave to me

and to

my husband

Hasan Charkas

For his continued support, understanding, love, and care

To my sister and brother

Lama and Tawfiq Nayal

For their love and support

For my son

Farouk Charkas

For being the light and blessing of my life

To my Friends in Manhattan, Ks

Especially Safa Attassi and Sara Asmar

For making me feel family as part of their families.

CHAPTER 1 - Introduction

Overview

Bridges are a key element in transportation systems, if for any reason a bridge is unable to meet traffic needs, it becomes a constriction to the flow of traffic, and needs to be replaced. The requirements for the design and construction of reinforced concrete bridges in terms of live-load requirements, material properties, structural shapes, etc. has evolved based on both increased needs and available materials. For example, these bridges were often designed for a live-load less than HL-93 as determined by AASHTO LRFD ⁽¹⁾. Due to the aforesaid facts, and also due to aging of and extensive use, there are a number of bridges in Kansas need to be replaced. The majority of these bridges has spans of 100 ft or less, and relatively shallow profiles.

It is apparent that when a bridge is taken out-of-service for repair or replacement, it causes major inconveniency for traffic passing through that area. As there are many options for replacement of existing bridges or construction of new ones, a wise decision must be made when selecting a specific bridge system. A balance must be achieved among strength, cost, and construction time factors, while not compromising safety.

Introduction of the prestressed reinforced concrete concept in 1950 paved the way for a revolution in bridge design. More than 50% of bridges are now constructed of prestressed concrete ⁽²⁾.

In prestressed concrete, the steel reinforcement is tensioned against the concrete, which precompresses the surrounding concrete, giving it the ability to resist higher loads prior to cracking.

Practical prestressed concrete was introduced in 1928 by Eugene Feysient of France, who recommended use of high-strength steel wires and high strength-concrete to provide higher levels of precompression ⁽²⁾.

Two different procedures for prestressing concrete were developed: post-tensioning, (used by Feysient) in which the steel is tensioned after the concrete has been cast and hardened; and prestressing (developed by the German engineer E.Hoyer in 1938), in which the steel is tensioned prior to casting of the concrete. Currently, in North America, about two-thirds of

prestressed steel is used to manufacture precast, pretensioned products, with the remaining one-third used for post-tensioning ⁽²⁾.

Cast-in-place (CIP) reinforced concrete slab has been the typical replacement option for short spans of approximately 30-60 ft. Post-tensioned concrete-haunched slab bridges have become an increasingly popular option within the last few years for medium spans between 60-100 ft, but these are relatively complicated to design and expensive to build. These strategies are also weather-dependent and require intensive labor, which extends road-closure time for construction. In addition, availability of large volumes of consistently good-quality, ready-mixed concrete required for these bridges can be a problem in rural areas.

Precast members are widely used in construction. Obviously, prefabrication of components provides significant reduction in construction or replacement time, and cost savings because of the reduced field labor employed. However, challenges to meet high span-to-depth ratio with prestressed, precast I-girders motivated researchers to come up with lighter and more cost-effective solutions. Recently, the inverted-T (IT) bridge system has become more popular for short-to medium-span bridges during the past few years. The IT system consists of longitudinal prestressed concrete members having an “Inverted-Tee” shaped cross section. Inverted-T girders are adjacently placed and serve as stay-in-place formwork for a composite CIP topping. This reduces the construction time and labor work as it eliminates a large portion of false work required in CIP systems. These girders support their own weight and the weight of the composite topping. The girders act compositely with the CIP topping to carry the live-load. Despite the advantages and merits of IT system, there are some limiting issues when using the IT beams in replacing existing bridges. First, the span-to-depth ratio which cannot compete with that of post-tensioned concrete haunched bridges. Currently IT members are constructed continuous only for live-load. In addition IT members contain only straight pre-tensioned strands that are contained in the bottom flanges. This fact often necessitates the use of de-bonding of the strands to control top tensile stresses at the members ends. In addition, the top tension can lead to increased transverse cracking of the composite top deck slab over the piers when experiencing a combination of live loads and the loads induced by the restraint of time-dependent deformations.

Objectives

The post-tensioned, inverted-T bridge system (PT-IT) is believed to be a good option for new system construction or replacing existing bridges. Construction of the PT-IT system involves post-tensioning of the pretensioned, Inverted-T beam sections. Adding post-tensioning to the IT system increases the durability of the section so it can handle more loads. In addition, post-tensioning allows reduction of the span-to-depth ratio of the beam, and reduces cracks in the deck over the piers.

The objective of this research was to provide guidelines for designing the PT-IT system, this was achieved by conducting an extensive and detailed analytical study in which major parameters influencing the design of these post-tensioned structures were determined, this included considering of different scenarios for construction. The effect of these parameters on the system response at different construction stages was also explored and the optimal values and conditions for successful post-tensioning scheme for the IT system were determined. The main challenge in this study was to account for the effect of creep and shrinkage on the stresses in the strands, and the continuity of the bridge structure. Different creep and shrinkage models were considered in the study, including and not limited to AASHTO LRFD, ACI, and NCHRP models. Shrinkage and creep of the girder not only affect the stresses in the strands, but also affect continuity of the entire structure. Since the precast girders and CIP topping are of different ages, the time-dependent restraining moment tends to form at the piers. Generally, the CIP concrete tends to shrink more than that of precast girders. Differential shrinkage between the deck and girder, along with creep of the girder under prestressing and post-tensioning, affects the development of restraining moments at interior piers of the bridge. This effect might become critical when it leads to cracking of the diaphragm over the piers and consequently deterioration of post-tensioning tendons, thereby reducing the life of the entire structure.

Current AASHTO provisions for the design of prestressed girders made continuous do not specify how to consider the effects of creep and shrinkage on the restraining moments. If this case is not carefully considered in design, premature cracking of concrete may occur.

Different methods have been proposed to calculate restraining moments, such as the Portland Cement Association (PCA) method by Mattock and Freyermuth ⁽³⁾ and ⁽⁴⁾ (1961), Construction Technology Laboratories (CTL) method developed by Oesterle et al. ⁽⁵⁾ and ⁽⁶⁾ (1989), P method developed by Peterman and Ramirez ⁽⁷⁾ (1998), and creep-transformed-section properties method by Dilger ⁽⁸⁾ (1982).

Outline

The study and results are presented within the following scope:

Chapter two includes a literature review discussing different bridge replacement options, and pros and cons of each option. The review also includes different prestress loss calculation methods. This chapter discusses different methods for calculating creep and shrinkage effect on restraining moments at interior piers.

Chapter three discusses the analogy used in analysis and design of the post-tensioned, inverted-T system, including different material, creep, shrinkage, and relaxation models. This chapter three also includes two examples comparing results from the commercial program Consplace with results obtained from PT-IT, highlighting major differences by analysis. A discussion about CTL and P methods used in the analysis is presented at the end of this chapter, along with proposed modifications for these methods.

Chapter four specifies main parameters affecting the design of PT-IT along with the results of parametric study including the effects of each of these parameters on the response of the system

Chapter five includes conclusions and recommendations for future research.

Appendix A Includes detailing of reinforcement for PT-IT system

Appendix B presents documentation for the program developed to analyze and simulate the behavior of the structure; user instructions are also provided

CHAPTER 2 - Literature Review

General Description

Precast prestressed concrete bridges constitute an increasingly large share of the total bridge market, because they are economical, durable, and elegant. There are many different forms of prestressed concrete bridges. The most common form in small-to-medium-span-range bridges is the precast, pretensioned standard I-girder with a cast-in-place deck slab. For longer spans, the precast prestressed concrete I-girder can be made continuous by using reinforcement over the supports in the cast-in-place deck slab.

Inverted-T beams have been used in bridges as bentcap beams to support precast stringers. The stringers are supported on the flange of the IT section. Mirza and Furlung ⁽⁹⁾ performed a study on this type of inverted-T beams. Based on observations from laboratory tests and analysis of IT sections, they proposed a procedure for proportioning of cross-section dimensions as well as reinforcement detail for such sections.

The Precast, prestressed, Inverted-T (IT) bridge system was developed at the University of Nebraska-Lincoln ⁽¹⁰⁾. The IT system consists of longitudinal, prestressed concrete members with an inverted-T-shaped cross section. In this system, inverted-Ts are adjacently placed to serve as a stay-in-place formwork for a composite CIP topping. This reduces construction time and labor, as it eliminates the large portion of false work required in CIP systems. This is considered to be an important benefit for IT girders from construction point of view. Figure 2. 1 and Figure 2. 2 show photos of IT bridges during construction.

The IT system provides members that are relatively lightweight, which aids in handling and placement operations. While the IT system, similar to I-girder sections, can span longer, and it saves up to 20% in weight off the standard I-beam. According to Kamel and Derrick ⁽¹¹⁾, no other existing precast concrete or cast-in-place conventionally reinforced system has this capability.

The IT system was designed to be used by small contractors in sparsely populated areas where relatively modest erection equipment exists. The ITs were developed in "hard" metric units, i.e., using round-figure millimeters. They are 600 mm (23.5 in) wide. However, depth is

varied as needed per design. The fact that ITs have the same flange width makes it possible to use a single set of formwork when casting sections with varying depth.

Ambare and Peterman ⁽¹²⁾ (2001) at Kansas State University suggested modifications to the IT system. Modified IT sections have curved edges instead of the knife edges of the Inverted sections. This helps eliminate bug pores during casting of the section. Figure 2.3 shows a graphical comparison between an IT section and a modified IT section.

Ambare and Peterman ⁽¹²⁾ also studied live-load distribution factors for IT girders, as current codes don't address systems with adjacent composite precast girders like the IT bridge system. The study included computer modeling in order to evaluate the accuracy of current AASHTO LRFD equations for IT girders. They concluded that the AASHTO LRFD (2nd Edition) approximate equation gave live-load distribution factors that were higher than those obtained by refined methods for moments. Shear-load distribution factor values are generally conservative but may become unconservative at large skew angles. Ambare and Peterman recommended using the AASHTO standard specification formula for predicting live-load distribution factor for moments.

$$DF_{Moment} = \frac{S}{5.5} \quad (2.1)$$

where S is girder spacing (in).

For shear, the authors recommended a distribution factor of 0.42 be used for interior non-skew bridges, exterior non-skew bridges, interior skewed bridges, and exterior skewed bridges with skew angle less than 20 degrees. For exterior skew bridges with skew angle larger than 20, shear distribution factors should be taken as

$$DF_{Shear} = 0.42 + \frac{(skewangle - 20)}{100} \quad (2.2)$$

where skew angle is taken in degree.

Despite the advantages and merits of the IT system, there are some limiting issues when using IT beams in replacing existing bridges. First, the maximum span-to-depth ratio of the IT system (close to 30) cannot compete with post-tensioned, concrete-haunched bridges with span-to-depth ratios approaching 40. IT bridge systems are constructed continuously only for live-loads; the beams act as simple-supported members for dead loads, including the weight of the top CIP deck slab. In addition, IT members contain only straight pre-tensioned strands in the

bottom flanges. This causes the bottom of the beam to be under compression and the top of the beam to be under tension. However, in sections where moment due to self-weight of the beam or the applied loads is significant this tension in the top is reduced, while in sections where the moment is small, the tension causes cracks in the deck. This fact often necessitates de-bonding of the strands to control normal stresses and top-tensile stresses at the member ends. This in turn leads to a reduction in the shear capacity of these members. In addition, the top tension can lead to increased transverse cracking of the composite top deck slab over the piers when experiencing a combination of live-loads and loads induced by restraint of time-dependent deformations.

Longer spans can be achieved by post-tensioning the precast girders to form continuous spans by splicing together individual precast beams. Spliced girders that are continuous over interior supports may be constructed with many configurations; girders may be spliced at the interior supports, or continuous over the support and spliced within the span. Most common spliced girders are I-girders, which are relatively deep. For medium-span-length girders, spliced girders are not cost effective, as they need false work.

This study investigates the use of post-tensioning, prestressed inverted-T girders. The system is referred to as post-tensioned, inverted-T beams (PT-IT). Post-tensioning is believed to overcome the deficiencies of the IT system explained above and make it more structurally efficient. Post-tensioning effectively increases span ranges of IT systems and consequently, span-to-depth ratio. This helps in replacing existing bridges with bridges of more capacity and same or lower depth, without raising the finished roadway elevation or restricting the hydraulic flow. Post-tensioning is applied by threading tendons through a draped duct provided while casting the IT section. Figure 2. 4 shows a sketch of a PT-IT bridge system. The design implementation is accomplished by either applying one-stage post-tensioning before or after casting the CIP top-deck slab, or partially post-tensioning before casting the deck and apply second-stage post-tensioning afterwards.

Use of post-tensioning allows for flexibility in tendon placement with greater eccentricity at mid span and reduced eccentricity at the ends. Use of post-tensioning decreases the number of pre-tensioned straight strands required. Additional benefits of the PT-IT system are reducing top tension in these continuous structures and reducing the potential for transverse cracks in the CIP deck (thereby decreasing vulnerability of the bridges to deicing salts). An additional benefit of

the PT-IT system is that cambers of the pre-tensioned concrete members will be significantly reduced (since fewer pre-tensioned strands will be used).

Many points are to be carefully addressed in analyzing the PT-T system. Since construction of PT-IT is done in many stages, using different construction scenarios, and the factors causing losses in prestressing and post-tensioning are time-dependent, losses should be incrementally evaluated at the beginning and end of each stage. Accordingly stresses in the concrete should be checked at each stage so as not to exceed allowable stresses at any time during construction and service life of the bridge. Factors that are time-dependent and cause losses in prestressing are shrinkage of concrete, relaxation of prestressing and post-tensioning steel, as well as creep of the concrete under the pre-tensioning and post-tensioning, and dead load stresses.

When precast girders are made continuous using a cast-in-place deck and diaphragm, aforesaid time-dependent factors create restraint moments in the piers. Factors affecting and causing restraining moments are discussed later in this chapter.

A review of published literature was conducted focusing on methods for evaluating losses in prestressing and post-tensioning, as well as methods of estimating time-dependent moments developed at the cast-in-place (CIP) joints after girders are made continuous. The literature review includes different recommended types of positive moment connection over the piers.

Available Methods for Evaluating Time-Dependent Losses

Evaluating effective prestress force is of great importance in analysis of prestressed concrete structures. Effective prestress force is used to calculate stress in concrete and evaluate deformations under service loads. Loss of prestress is defined as loss of compressive force acting on the concrete component of a prestressed concrete section. Creep and shrinkage affect a prestressed concrete member, causing it to shorten. This results in loss of tension in prestressing strands. For prestressed members and grouted post-tensioning members, the sum of the reduction in tensile force in the strands is equal and opposite to the incremental loss of compression force in concrete. Two factors affect tension force in the strands: loss of prestress and elastic gain of prestress. Loss of prestress is a time-dependent loss counted from the time strands are tensioned until a certain time. Elastic loss or gain in prestress is an instantaneous change. As the prestressing force is released from the bed and transferred to the concrete member; the member

undergoes shortening and cambers upward between its two ends. The net elastic loss at transfer is equal to the stress loss due to prestress, combined with stress gain due to member self weight. The strands further elongate and undergo elastic gain as additional load is introduced to the member, such as deck weight or as post-tensioning is applied to the section.

Components of prestress losses ⁽¹³⁾:

1. Loss due to prestressing bed anchorage seating, and relaxation between the time of initial tensioning and transfer. For post-tensioned strands, there is an instantaneous loss due to friction.

2. Instantaneous prestress loss at transfer due to pre-stressing force and self-weight.

3. Prestress loss between transfer and deck placement due to shrinkage and creep of girder, and relaxation of prestressing strands.

4. Instantaneous prestress gain due to deck weight on the noncomposite section and superimposed dead loads on the composite section.

5. Long-term prestress losses after deck placement due to shrinkage and creep of girder concrete, and relaxation of prestressing strands.

Estimating prestress loss requires an accurate prediction of material properties, the interaction between creep and shrinkage of concrete, and the relaxation of steel ⁽¹³⁾. In addition, prestress losses are influenced by composite action between the cast-in-place concrete deck and the precast, prestressed concrete girder. Existing approaches for estimating prestress losses can be divided into three categories, listed as follows in descending order of complexity and accuracy.

Time-Step Prestress Loss Methods

These methods calculate prestress loss based on a step-by-step numerical procedure. This is usually implemented in computer programs for accurate estimation of long-term prestress losses. This approach is especially useful in multi-stage bridge construction, which is considered during the course of this study.

The interaction of relaxation of steel with creep and shrinkage is considered in such methods. As concrete creeps and shrinks, the prestressing strands shorten and decrease in tension. This, in turn, decreases relaxation of the steel. As tension in strands is decreased, compressive force applied on concrete sections is decreased, causing concrete to creep less.

To account for continuous interactions between creep and shrinkage of concrete and relaxation of strands with time, time will be divided into intervals. The duration of each time interval can be made larger as the concrete age increases ⁽¹³⁾. Stress in the strands at the end of each time interval equals stress in the strands at the beginning of that time interval, minus calculated prestress losses during the interval. Stresses and deformations at the beginning of an interval are the same as those at the end of the preceding interval. In this time-step method, the prestress level can be estimated at any critical time during the life of the structure.

Refined Prestress Loss Methods

In these methods, individual components of prestress loss are calculated separately, and the total prestress loss is then calculated by summing up the separate components.

However, none of these methods account for composite action between deck slabs and precast girders. Because the deck concrete shrinks more and creeps less than the precast girder concrete, prestress gain rather than prestress loss may occur.

In these methods, data representing the properties of materials, loading conditions, and environmental conditions have been incorporated into the prediction formulas used for computing individual prestress loss components.

Over the years, several methods have been developed. Among these are the current AASHTO-LRFD ⁽¹⁾ refined method and the AASHTO Standard Specifications method ⁽¹⁴⁾. In AASHTO LRFD, prestress losses are computed at release and at final time in the location of midspan section only. According to LRFD Art 5.9.5, prestress losses in pretensioned members, $\Delta f_p T$, at transfer is given as

$$\Delta f_p = \Delta f_{pES} + \Delta f_{pR1} \quad (2.3)$$

where

Δf_{pES} is the loss due to elastic shortening given as

$$\Delta f_{pES} = \frac{E_p}{E_{ci}} f_{cgp} \cdot \quad (2.4)$$

f_{cgp} is the sum of concrete stresses at the center of gravity of prestressing tendons due to the prestressing force at transfer and the self-weight of the member at the sections of maximum moments, E_p modulus of elasticity of prestressing steel, and E_{ci} modulus of elasticity of concrete at transfer.

Δf_{pR1} is the loss due to relaxation of steel at transfer, which is given according to the type of strands as follows:

For stress relieved strands,

$$\Delta f_{pR1} = \frac{\log(24.0 t)}{10.0} \left[\frac{f_{pj}}{f_{py}} - 0.55 \right] f_{pj}; \text{ and} \quad (2.5)$$

for low-relaxation strands,

$$\Delta f_{pR1} = \frac{\log(24.0 t)}{40.0} \left[\frac{f_{pj}}{f_{py}} - 0.55 \right] f_{pj} \quad (2.6)$$

where t is time estimated in days from stressing to transfer, f_{pj} is the initial stress in the tendon at the end of stressing, and f_{py} is specified yield strength of prestressing steel.

At the final stage, total loss is calculated at midspan only as the sum of individual components.

$$\Delta f_{pT} = \Delta f_{pES} + \Delta f_{pSH} + \Delta f_{pCR} + \Delta f_{pR2} \quad (2.7)$$

where

Δf_{pT} is total loss of prestress, and

Δf_{pES} is loss due to elastic shortening and is given in equation (2.4).

Δf_{pSH} is the loss due to concrete shrinkage and is given as follows:

For pretensioned members,

$$\Delta f_{pSH1} = (17.0 - 0.150H) \quad (ksi); \text{ And} \quad (2.8)$$

for post-tensioned members,

$$\Delta f_{pSH1} = (13.5 - 0.123H) \quad (ksi) \quad (2.9)$$

where H is the average annual ambient relative humidity (%).

Δf_{pCR} is the loss due to creep of concrete.

$$\Delta f_{pCR} = 12.0f_{cgp} - 7.0\Delta f_{cdp} \geq 0 \quad (ksi) \quad (2.10)$$

f_{cgp} is concrete stress at the center of gravity of prestressing steel at transfer.

Δf_{cdp} is change in concrete stress at the center of gravity of prestressing steel due to permanent loads.

Δf_{pR2} is loss due to relaxation of steel after transfer

for pretensioning with stress-relieved strands.

$$\Delta f_{pR2} = 20.0 - 0.4\Delta f_{pES} - 0.2(\Delta f_{pSR} + \Delta f_{pCR}) \quad (ksi); \text{ and} \quad (2.11)$$

for post-tensioning with stress-relieved strands

$$\Delta f_{pR2} = 20.0 - 0.3\Delta f_{pf} - 0.4\Delta f_{pES} - 0.2(\Delta f_{pSR} + \Delta f_{pCR}) \quad (ksi). \quad (2.12)$$

For low-relaxation, loss due to relaxation is taken as 30 % of the loss for stress-relieved strands.

Lump-Sum Methods

Lump-sum methods are commonly used in preliminary design. According to the AASHTO LRFD ⁽¹⁾ lump-sum method, prestress loss for girders with 270 ksi low-relaxation strands is given by the following formulas:

For box girders

$$19 + 4PPR - 4 \quad (ksi); \quad (2.13)$$

for rectangular beams and solid slabs

$$26 + 4PPR - 6 \quad (ksi); \text{ and} \quad (2.14)$$

for I-girders

$$33.0 \left[1.0 - 0.15 \frac{f'c - 6.0}{6.0} \right] + 6.0PPR - 6 \quad (ksi) \quad (2.15)$$

in the case of single t, double-T, hollow-core and voided slab

$$33.0 \left[1.0 - 0.15 \frac{f'c - 6.0}{6.0} \right] + 6.0PPR - 8 \quad (ksi) \quad (2.16)$$

where *PPR* is the partial prestress ratio, which is normally equal to 1 for precast, pretensioned members. These formulas reflect trends obtained from a computerized time-step analysis of different beam sections for ultimate creep coefficient ranging from 1.6 to 2.4, ultimate concrete shrinkage ranging from 0.0004 to 0.0006, and relative humidity ranging from 40% to 100%.

Methods to Calculate Time-Dependent Restraining Moments

Design of multi-span, continuous, precast, prestressed concrete bridges requires certain additional considerations which do not arise in the case of simple span. Concrete bridge structures are subject to time-dependent deformations produced by creep of the deck and beam concrete, and by differential shrinkage between the deck and beams. In continuous girders, these deformations cannot occur freely due to the restraint of continuity. As a result, additional moments and shear forces are produced in the beams, which must be considered during design. Since precast members are often fabricated several months before they are installed in the field, most concrete shrinkage due to drying has occurred before the CIP concrete is cast. As the fresh CIP concrete cures, its shrinkage will be partially restrained by the girders. In the case of a simply supported beam, the beam will be free to rotate at the ends. In the case of a continuous beam, the interior ends are not free to rotate. This produces negative restraint moments. The effect of creep under prestressing usually has an opposite effect to shrinkage. This will produce positive moments. Figure 2. 7(a) shows the effect of differential shrinkage on deformation of a two span continuous beam. Figure 2. 7(b) shows restraint moments due to differential shrinkage and creep on a two-span beam. The value of the resultant restraint moment should be considered in the design. According to the PCI bridge design manual ⁽¹⁵⁾ 8.13.4.3.2.1, “Only loads introduced before continuity can cause time-dependent restraint moments due to the time-dependent effects”.

Some of the methods available for estimating restraint moments are discussed below.

PCA Method

The PCA method was developed by Mattock ⁽⁴⁾ 1961. Adopted by the Portland Cement Association; in 1969, the method was investigated by Freyermuth ⁽¹⁾.

The Portland Cement Association conducted an experimental research program on precast I-girders with a continuous situ-cast deck, studied the influence of creep in precast girders and differential shrinkage between the precast girders and CIP deck slab on continuity behavior after an extended period of time. The experimental study was restricted to observation and evaluation of the behavior of two half-scale, two-span continuous bridge girders over a period of approximately two years from the time of construction. The girders were identical in all particulars, except that one girder incorporated positive-moment connection at the interior support, while the other did not. Long-term variations of support reactions and deflections due to

creep and differential shrinkage effects were measured. The continuity behavior of the girders were investigated at intervals by loading them within service-load range. Finally, the girders were loaded to destruction in order to determine the effect, if any, of creep and shrinkage on the ultimate strength of the girders.

In this method, the uniform differential shrinkage moment in a composite concrete section at any time is given by

$$M_s = \varepsilon_s E_d A_d \left(e_c + \frac{h}{2} \right) \quad (2.17)$$

where ε_s is the differential shrinkage strain;

E_d is the modulus of elasticity of CIP concrete;

A_d is the cross-sectional area of CIP slab;

h is CIP thickness; and

e_c is the distance between the top of the precast member and the centroid of the composite section.

In the first step, the restraint moments are calculated as if the prestress, dead load, and shrinkage moments had been applied to the continuous girder and not to the individual spans. In the second step, the restraint moments calculated in the first step are multiplied by $(1-e^{-\phi})$ for prestress and dead load, and by $(1-e^{-\phi})/\phi$ for moments due to shrinkage.

The restraint moment at the center support of the two-span continuous beam is given as

$$M_r = \left(\frac{3}{2} M_p + M_d \right) (1 - e^{-\phi}) + \frac{3}{2} M_s \left(\frac{1 - e^{-\phi}}{\phi} \right) \quad (2.18)$$

where M_p is the moment caused by prestressing force around the centroid of the composite member;

M_d is midspan moment due to dead load;

e is the base of the Napierian logarithm; and

ϕ is the creep coefficient (ratio of creep strain to elastic strain at time of investigation).

The study by Mattock concluded that deformations due to creep and differential shrinkage do not influence the ultimate load-carrying capacity of a continuous I-girder. The influence of creep and shrinkage is restricted to deformations and the possibility of cracking at the service-load level.

Texas Transportation Institute

In 1974 the Texas Transportation Institute ⁽¹⁶⁾ and Texas A&M University performed a study about precast, prestressed concrete girders made continuous by CIP deck. This included developing a computer program to perform calculations for design of such girders.

In this method, the restraining moments resulting from creep under self weight, weight of deck, and prestressing along with moments resulting from differential shrinkage between the girder and the deck are computed by the slope-deflection method of elastic analysis and then scaled by proper factors.

Restraint moments resulting from creep are multiplied by the factor SF_{creep}

$$SF_{creep} = \frac{\phi}{1 + \phi} \quad (2.19)$$

while restraint moments resulting from shrinkage are multiplied by the factor $SF_{shrinkage}$

$$SF_{shrinkage} = \frac{1}{1 + \phi} \quad (2.20)$$

where fixed end moments for shrinkage are given as

$$M_s = \varepsilon_{SD} EA e \quad (2.21)$$

ε_{SD} is the differential shrinkage strain between deck and beam concrete at the time connection was established.

E is the modulus of elasticity of deck concrete.

A is the cross sectional area of deck.

e is the distance between mid-depth of the deck and the centroid of the composite section.

$$\varepsilon_{SD} = 525 \times 10^{-6} \alpha_H \frac{t}{20 + t} \quad (2.22)$$

where t is age of the beam in days when the deck is cast, and α_H is the correction factor for humidity taken from.

Creep factor Φ is calculated as follows to

$$\phi = \frac{\varepsilon_c}{\varepsilon_e} (1 - \alpha) \quad (2.23)$$

ε_c =creep strain at time t due to unit stress.

ε_e =initial strain due to unit stress.

α =fraction of ε_c , which has occurred when continuity connection is established.

The deck and the beam are assumed to have the same creep and shrinkage behavior. Depending on laboratory experiments, expressions were developed to fit the shrinkage and unit creep strain data.

$$\varepsilon_c(t) = \frac{425t}{34+t} \quad (\text{in / in / ksi} \times 10^{-6}) \quad (2.24)$$

when $t = \infty$, $\varepsilon_c = 425$.

This basic unit creep strain is for concrete specimens with a volume/surface ratio of approximately 1.0. Correction factor is considered to account for different volume-to-surface ratios.

$$\varepsilon_c = 425 \times \alpha_{V/S} \quad (\text{in / in / ksi} \times 10^{-6}) \quad (2.25)$$

where $\alpha_{V/S}$ is taken from Figure 2. 6.

$$\varepsilon_e = \frac{1}{E_i} \quad \text{and} \quad (2.26)$$

$$\alpha = \frac{t}{34+t} \quad (2.27)$$

with substitution in equation (2.23)

$$\phi = 425 \times 10^{-6} \times \alpha_{V/S} \times E_i \times \left(1 - \frac{t}{34+t}\right) \quad (2.28)$$

where t is the age of concrete when connection was established.

This method is not believed to be as accurate as other methods for the following reasons. Since the concrete of the girder has different strength, curing type, and age than the deck concrete, shrinkage and creep properties, contrary to the method's assumption, will be different for the beam than for the deck. This method also assumes that the restraint moment will be the same from the day connection was made through the life of the structure, while it actually changes with time.

CTL Method

In 1989, Osterle, Glikin, and Larson ^{(5), (6)} proposed modifications to the PCA method. While PCA considered the continuity connections to have zero length and to be fully rigid, CTL considered the actual connections to have finite lengths and rotational stiffness. CTL developed the BRIDGERM program to carry out an incremental time-step solution, including separate

shrinkage functions for the deck and girder concrete, and time-dependent functions for the strength and stiffness of deck concrete.

Creep restraint moments were determined by multiplying the dead load and prestress moments by a coefficient $(1-e^{-\Phi T})$, where

$$\Phi T = \nu T - \nu T_0 \quad (2.29)$$

where

ν_T creep coefficient is at time T days, where T is the time after prestress release at which restraint moments are being calculated $T > T_0$; and

ν_{T_0} creep coefficient is at time T_0 days, where T_0 is the time after prestress release at which continuity is established.

Restraint moments due to differential shrinkage were determined using a multiplier of $(1-e^{-\Phi T})/\Phi$.

Change in restraint moment ΔM_i within each time step is calculated as follows:

$$\Delta M_i = (M_D' + M_{PT}') (1 - e^{-\phi_i'}) + \Delta M_{si}' (1 - e^{-\phi_i'}) / \phi_i' \quad (2.30)$$

where M_p' is restraint moment due to creep under prestress, M_D' is restraint moment due to dead load and M_{si}' is restraint moment due to differential shrinkage between the deck slab and girder.

For the calculation of restraint moment due to prestress-induced creep, the prestress force was adjusted at each time step to account for losses due to shrinkage, creep, and relaxation.

In this method, the moment due to differential shrinkage is

$$\Delta M_{si}' = \Delta F_{di} \left(e_c + \frac{t}{2} \right) \quad (2.31)$$

where ΔF_{di} is tension in the deck to establish compatibility with the girder

$$\Delta F_{di} = \frac{\delta \Delta \varepsilon_{si} E_{di} A_d}{1 + \frac{E_{di} A_d}{E_g A_g}} \quad (2.32)$$

$$\delta \Delta \varepsilon_{si} = (\varepsilon_{sdi} - \varepsilon_{sdi-1}) - (\varepsilon_{sgi} - \varepsilon_{sgi-1}). \quad (2.33)$$

ε_{sdi} is shrinkage strain in the CIP slab at time T_i .

ε_{sgi} is shrinkage strain in the girder at time T_i .

E_{di} is the modulus of elasticity of the deck concrete at time T_i .

E_g is the modulus of elasticity of the girder concrete.

A_d is the cross-sectional area of the CIP slab.

A_g is the area of the prestressed member.

$\left(e_c + \frac{t}{2} \right)$ = distance between mid-depth of the deck slab and centroid of the composite

section

in determining the deck shrinkage strain 30 days after casting the deck, the ultimate shrinkage strain of the deck was reduced by the Dischinger effect factor to account for the restraint from the reinforcing steel within the deck. This factor is given as follows:

$$Disch = \frac{1 - e^{-0.03\phi_u ni}}{1 + 0.03 \times n} \frac{1}{\phi_u \times ni \times 0.03} \quad (2.34)$$

Φ_u is the deck's ultimate shrinkage.

$$ni = \frac{Es}{E_d(28)}, \quad n = \frac{Es}{E_d(T)} \quad (2.35)$$

Results of computer analyses were compared to the PCA test observation conducted by Mattock⁽⁴⁾. The study concluded that continuity established at an early girder age will result in positive restraint moments developing in the pier.

P Method

Peterman and Ramirez⁽⁷⁾ conducted an experimental investigation to evaluate the restraint moment in the piers for bridges made continuous by a cast-in-place CIP deck.

Two full-span bridges were fabricated and tested at Purdue University. The bridges had two spans; each span consisted of two prestressed concrete form panels measuring 21 ft long and 4 ft wide. Each bridge was subjected to repeated loading using two hydraulic actuators located at a distance of 8 ft 3 in from the center of the middle pier. The experimentally obtained moments were compared with values calculated from PCA and CTL methods, which ignored cracking of the CIP topping and overestimated the negative restraint moments in composite construction with shallow prestressed members.

The authors proposed a modified restraint moment calculation method that accounts for length and stiffness of the diaphragm, different initiation times of creep, and restraint of CIP concrete shrinkage. The method was referred to as P method.

This method estimates the moment due to differential shrinkage as

$$M_s = \varepsilon_s E_d A_d \left(e_c + \frac{h}{2} \right) \left(\frac{1}{1 + \frac{E_p A_p}{E_d A_d}} \right) \left(\frac{1}{1 + \frac{E_s A_s}{E_d A_d}} \right) \quad (2.36)$$

E_p is the modulus of elasticity of the prestressed member.

A_p is the area of the prestressed member.

E_s is the modulus of elasticity of steel reinforcement in the CIP deck.

A_s is the cross-sectional area of steel reinforcement in the CIP deck.

E_d is the modulus of elasticity of the CIP concrete.

A_d is the cross-sectional area of the CIP slab.

Using the P method ⁽⁷⁾, the restraint moment at the center pier of a two-span, symmetric bridge is calculated as

$$M_r = \left[\frac{3}{2} \alpha M_p - \alpha (M_d)_{precast} \right] [\Delta(1 - e^{-\psi_1})] - \alpha (M_d)_{CIP} - \frac{3}{2} \alpha M_s \left(\frac{1 - e^{-\psi_2}}{\psi_2} \right) \quad (2.37)$$

where

$$\alpha = \frac{\frac{2I_d}{L_d}}{\frac{2I_d}{L_d} + \frac{3I_m}{L_m}} \quad (2.38)$$

I_d is the moment of inertia of the diaphragm region.

L_d is length of the diaphragm region.

I_m is the moment of inertia of the main span.

L_m is the length of the main span.

$(M_d)_{precast}$ is the midspan moment due to dead load of the girders.

$(M_d)_{CIP}$ is the midspan moment due to CIP deck weight.

ψ_1 is the creep coefficient for creep effects initiating when prestress force is transferred to the precast panel.

ψ_2 is the creep coefficient for creep effects initiating when the CIP topping is cast.

$\Delta(1 - e^{-\psi_1})$ is the change in expression $(1 - e^{-\psi_1})$ occurring from the time corresponding to restraint moment calculations.

Restraint moments are compared to cracking moments in the diaphragms. Once the diaphragm cracks, moment redistribution will occur and restraint moment will be calculated using stiffness of the cracked diaphragm section.

Discussion of PCA, CTL, and P methods is presented in chapter three, highlighting major differences mainly between CTL and P methods. Modifications for both methods are proposed as well.

Creep-Transformed Section Properties Method

The method developed by Dilger ⁽⁸⁾ is intended for time-dependent analysis for prestressed concrete structures, including evaluating prestress losses, restraint moments, time-dependent curvature, and deflection.

The method makes use of well-known methods of stress analysis and is, in principle, similar to the elastic stress analysis of a member consisting of two materials in which one component (concrete) changes its temperature while the temperature of the other (reinforcement) remains constant.

In this method, time-dependent analysis of prestressed concrete members, the cross-section properties include the effect of concrete creep.

The response of the concrete to gradually changing stress due to creep and shrinkage is best calculated by Bazant's ⁽¹⁷⁾ age-adjusted effective modulus formula:

$$E_c^* = E_c(t_0) / [1 + \chi \phi(t, t_0)] \quad (2.39)$$

where

$E_c(t_0)$ is the modulus of elasticity of concrete loaded at age t_0 .

$\Phi(t, t_0)$ is the creep coefficient at time t for concrete loaded at age t_0 .

χ is the aging coefficient.

The aging coefficient expresses the aging effect on creep of concrete loaded gradually and depends on the magnitude of the creep coefficient, age of the concrete at first loading, and time under load.

The forces corresponding to unrestrained creep, free shrinkage of the concrete, and reduced relaxation of the prestressing steel are applied to the creep-transformed section in which the steel is included with the modular ratio

$$n^* = \frac{E_s}{E_c^*} = n_0[1 + \chi\phi(t, t_0)] \quad (2.40)$$

For non-composite members, the change in strain due to unrestrained creep and free shrinkage at the tendon level is

$$\Delta\varepsilon_c^*(t) = \varepsilon_1\phi(t, t_0) + \varepsilon_{sh}(t, t_0) \quad (2.41)$$

where

$\varepsilon_1 = f_{c1}/E_c(t_0)$ elastic concrete strain at the level of the tendon due to load applied at age t_0 producing the stress f_{c1} , and

$\varepsilon_{sh}(t, t_0)$ free shrinkage since the time of prestressing.

The corresponding steel stress including reduced relaxation, is

$$f_s^*(t) = n_0 f_{c1} \phi(t, t_0) + \varepsilon_{sh}(t, t_0) E_s + f_r'(t); \quad (2.42)$$

and the corresponding normal force and bending moment is

$$\begin{aligned} N_s^* &= A_s f_s^*(t) \\ M_s^* &= N_s^* y_1^* \end{aligned} \quad (2.43)$$

where A_s is the steel area and

y_1^* is the distance between the centroid of the steel and the centroid of the creep-transformed section.

The stress corresponding from N_s^* and M_s^* in steel obtained from the relation is

$$\Delta f_s^*(t) = -\left(\frac{N_s^*}{A_c^*} + \frac{M_s^*}{I_c^*} y_1^*\right) n^* \quad (2.44)$$

The time-dependent change in steel stress is obtained by summing steel stresses in equations (2.42) and (2.44).

Solving for stresses in a composite member, the difference in time-dependent strains between the precast girder and cast-in-place deck is calculated at the level of the centroid of the concrete deck. All strains are determined for time after the beginning of composite action. Initial elastic strain ε_1 in any fiber of the precast section due to the weight of the girder and prestressing will increase due to unrestrained creep and free shrinkage from the beginning of the composite action t_1 until time t by

$$\Delta\varepsilon_1(t) = \varepsilon_1[\phi(t, t_0) - \phi(t_1, t_0)] + \varepsilon_{sh1}(t, t_1) \quad (2.45)$$

At the level of the centroid of the cast-in-place deck, the increase in strain is

$$\Delta\varepsilon_{1,2}(t) = \varepsilon_{1,2}[\phi(t, t_0) - \phi(t_1, t_0)] + \varepsilon_{sh1}(t, t_1) \quad (2.46)$$

where $\varepsilon_{1,2}$ is initial elastic strain due to the weight of the girder and prestressing at the level of the deck's centroid.

While the girder concrete develops the strain expressed by equation(2.46), the deck shrinks by an amount $\varepsilon_{sh2}(t, t_1)$, where t and t_1 are counted from the moment at which the composite action begins.

In addition to the steel forces, the deck generates a normal force corresponding to the difference between the free shrinkage of the deck $\varepsilon_{sh2}(t, t_1)$ and the strain due to unrestrained creep and free shrinkage at the level of the deck's centroid. In unshored construction, where the weight of the slab is carried by the precast girder, the difference in strain is

$$\Delta\varepsilon_2^*(t, t_1) = \varepsilon_{1,2}[\phi_1(t, t_0) - \phi_1(t_1, t_0)] + \varepsilon_{1,2}^{(2)}\phi(t, t_1) + \varepsilon_{sh1}(t, t_1) - \varepsilon_{sh2}(t, t_1) \quad (2.47)$$

where $\varepsilon_{1,2}^{(2)}$ is strain due to deck weight at the level of the deck's centroid.

The force and moment in the deck corresponding to the difference in strains expressed by equation (2.47) is

$$\begin{aligned} N_c^* &= \Delta\varepsilon_2^*(t, t_1)E_c^*A_c \\ M_c^* &= N_c^*y_c^* \end{aligned} \quad (2.48)$$

where y_c^* is the distance between the centroid of the creep-transformed section and the centroid of concrete deck; and

$$E_{c2}^* = E_{c2}(t_0)/[1 + \chi_2\phi_2(t, t_0)] \quad (2.49)$$

where subscript 2 in equation (2.49) refers to the deck's concrete properties.

Total forces acting on the creep-transformed concrete section are those developed in the steel and deck, adding the normal and moment forces from equations (2.43) and (2.48):

$$\begin{aligned} N^* &= N_s^* + N_c^* \\ M^* &= M_s^* + M_c^* \end{aligned} \quad (2.50)$$

The time-dependent stresses in steel are calculated by equation (2.44), replacing N_s^* and M_s^* by N^* and M^* .

In this method, the time-dependent moment developing at the cast-in-place joint can be determined by expanding the compatibility conditions to include the time-dependent curvature, where the change in curvature at time t is expressed by

$$\Delta\psi(t) = \psi_1^{(1)}[\phi_1(t, t_0) - \phi_1(t_1, t_0)] + \psi^{(2)}\phi_1(t, t_1) - \frac{M^*}{I_c^* E_{c1}^*} \quad (2.51)$$

where $\psi_1^{(1)}$ is the initial curvature of the precast girder weight and prestressing, $\psi^{(2)}$ is the curvature due to the deck weight moment, t_0 is time of prestressing, and t_1 is the time when composite action starts.

Positive Moment Connection for Girders Made Continuous with CIP Deck

The effectiveness of continuity in girders made continuous using CIP deck and diaphragms are the concern of many research studies. Arguments can be made that continuity becomes ineffective with the initiation of a small crack near the bottom of the diaphragm, forcing the girders to carry live-load as simple span and resulting in higher live-load moments. On the other hand, successful experience of agencies that regularly design such bridges under the assumption of full continuity for live-load counters the previous argument. “It is unlikely that this issue will be settled in the near future. In the meantime, on the basis of the excellent performance of structures of this type, it is recommended that designers continue to rely on continuous action for the design of routine bridges and use details at the piers that have proven to be successful”⁽¹⁵⁾. In this regard, and since positive moment connections are not the topic of the current study, a quick review will be presented, including commonly used connections as well as recommendations of recent studies. It is important to mention that during the course of this project, the amount of reinforcement in pier connections was evaluated to provide required strength in the diaphragms.

In 1989 Osterle and Glikin ^{(5), (6)} (NCHRP Report 322) investigated positive moment connections for precast girders made continuous using CIP slab and diaphragms. The study concluded that positive moments generated mainly by effect of creep under prestressing may crack the continuity connection. The study investigated use of bent bars in this type of connection and concluded that positive moment connections, besides being costly, difficult and time consuming, have no structural benefits. They will cause restraint moments to increase and that can lead to cracking of the connection.

Rabbat and Aswad ⁽¹⁸⁾ reviewed standard details for continuity diaphragms based on NCHRP Report 322 findings and the experience of Tennessee and many other states using this type of construction. Based on discussions held during the PCI Committee on Bridges meetings,

the authors recommended the dead load of the girders and the deck as acting on a simple span, analyzing the structure as continuous for live-load and superimposed loads, and providing a positive moment connection through reinforcing or prestressing steel to develop a design strength equal to or greater than 1.2 times the positive cracking moment. In so, no analysis for restraint moments due to time-dependent effects would be required.

Mirmiran, et al.⁽¹⁹⁾ carried out an analytical study to investigate the performance of reinforced continuity connections for precast, prestressed concrete girders with CIP decks. The study concluded that positive moment reinforcement in the continuity diaphragm has a significant effect on restraint moments when the continuity is established at early ages. The study also concluded that continuity behavior of the bridge is generally better when continuity is established at a later age of the girders. The authors recommended that practicing engineers should consider providing minimum reinforcement that prevents excessive cracking of the diaphragm section without crowding the connection.

In 2004, Miller et al.⁽²⁰⁾, under a National Cooperative Highway Research Program, conducted a survey of state DOTs concerning connections for precast, prestressed concrete bridge girders. The study concluded that the presence of positive-moment cracking at the diaphragm doesn't necessarily reduce continuity. The report proposed revisions to the AASHTO LRFD bridge design specifications, including details for fabricating positive-moment connections by either extending the prestressing strands from the end of the girder, bending it at 90° and embedding it in the diaphragm section, or by embedding mild steel at the ends of the girders with standard hooks at the protruding end of the bar to be embedded in the diaphragms.

In 2004, Saadeghvazini et al.⁽²¹⁾ proposed using flexible CFRP composites to improve continuity over fixed piers. The study concluded that bond between the concrete and the composite is the most critical element. It also concluded that wrapping and surface preparation have a significant effect against debonding the composite.

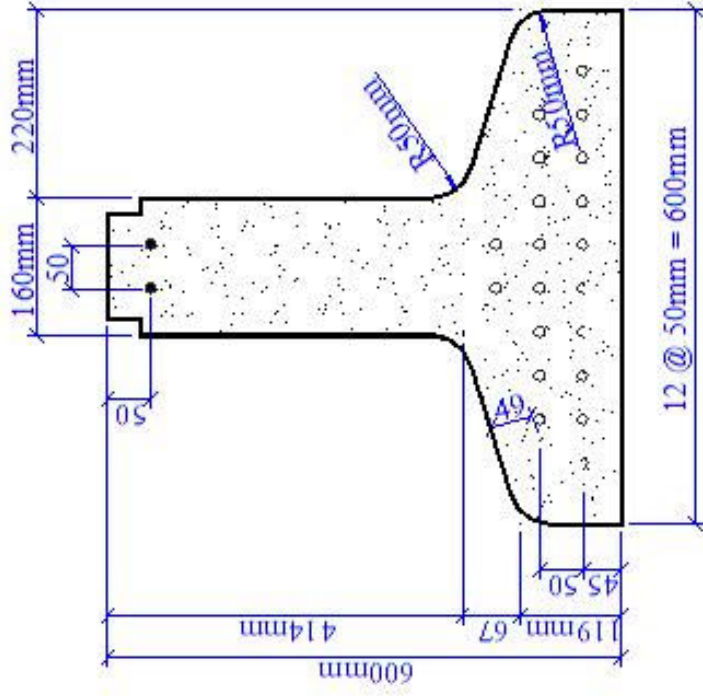
Figure 2. 1 PT-IT bridge system under construction



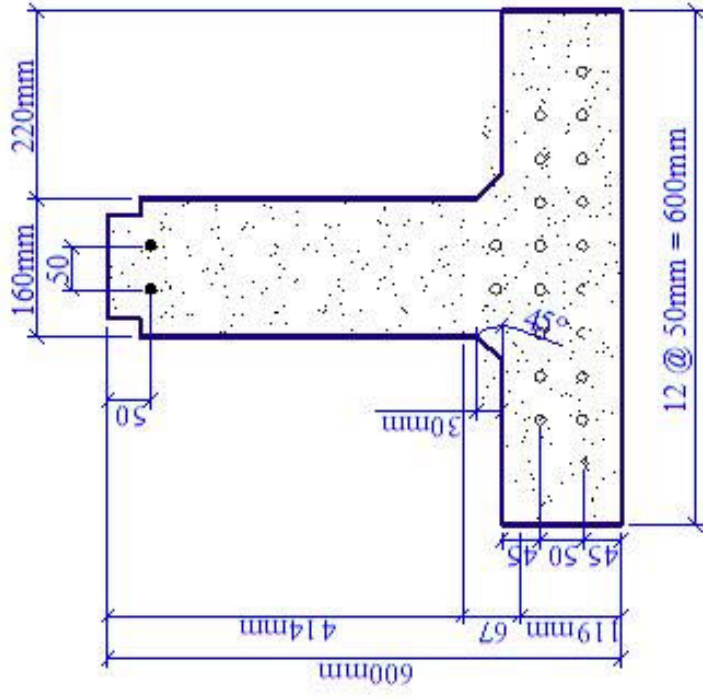
Figure 2. 2 PT-IT bridge system under construction



Figure 2. 3 IT section and modified IT section



IT600 (Modified)



IT600 (Standard)

Figure 2. 4 PT-IT bridge system

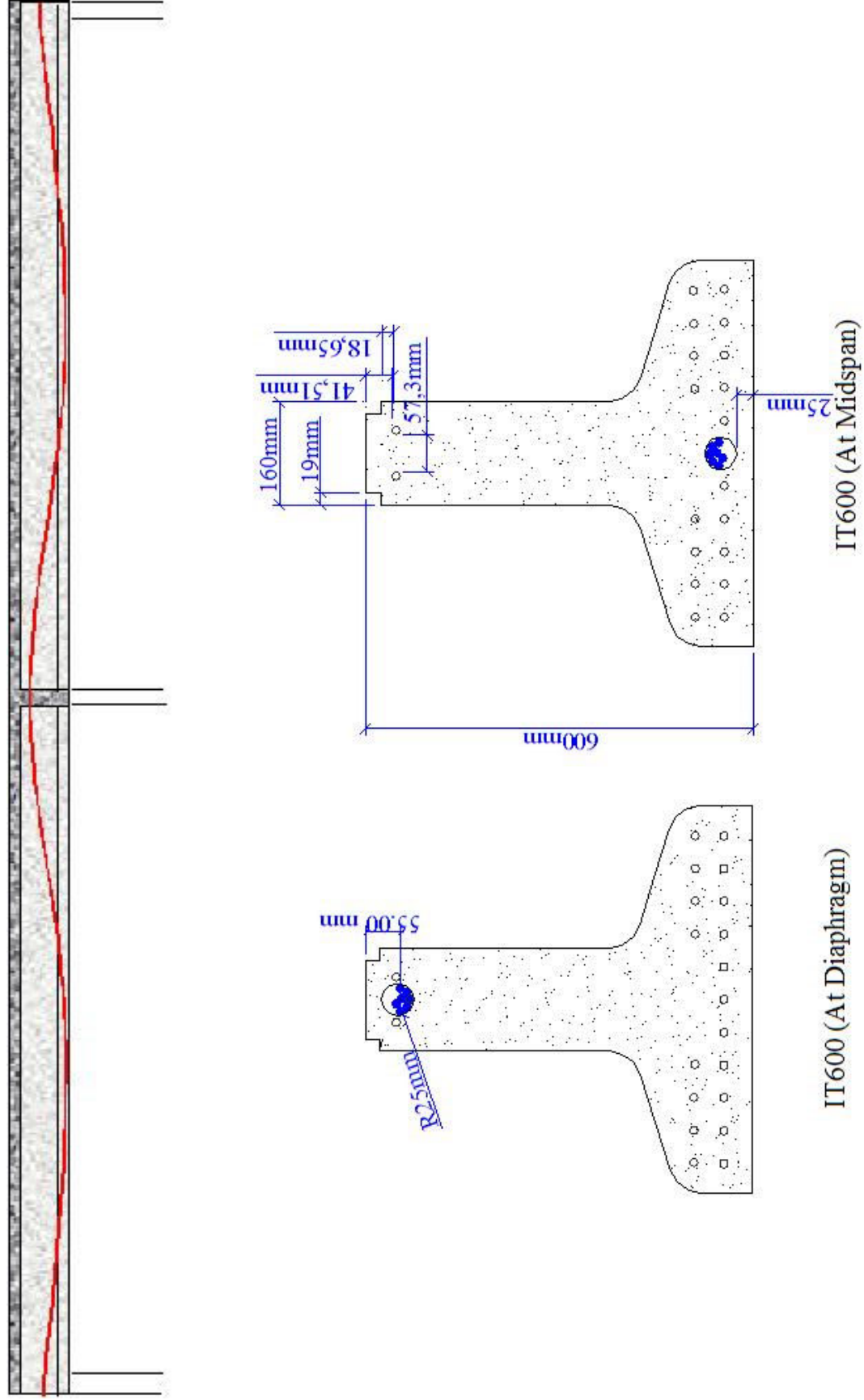


Figure 2. 5 Realtive humidity correction factor (Texas Technology Institute method)

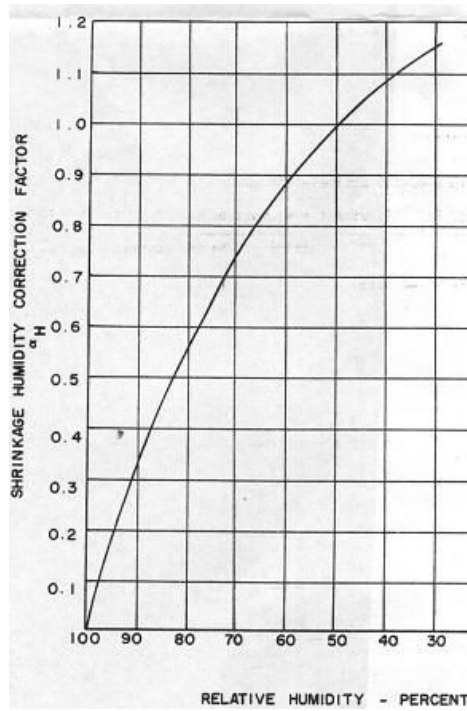


Figure 2. 6 Volume-to-surface ratio correction factor (Texas Technology Institute method)

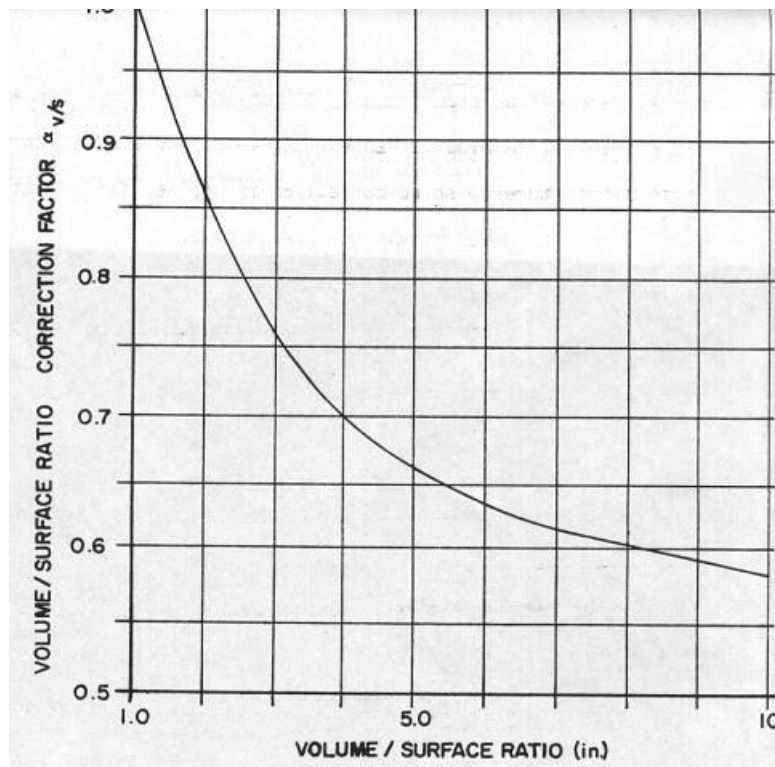
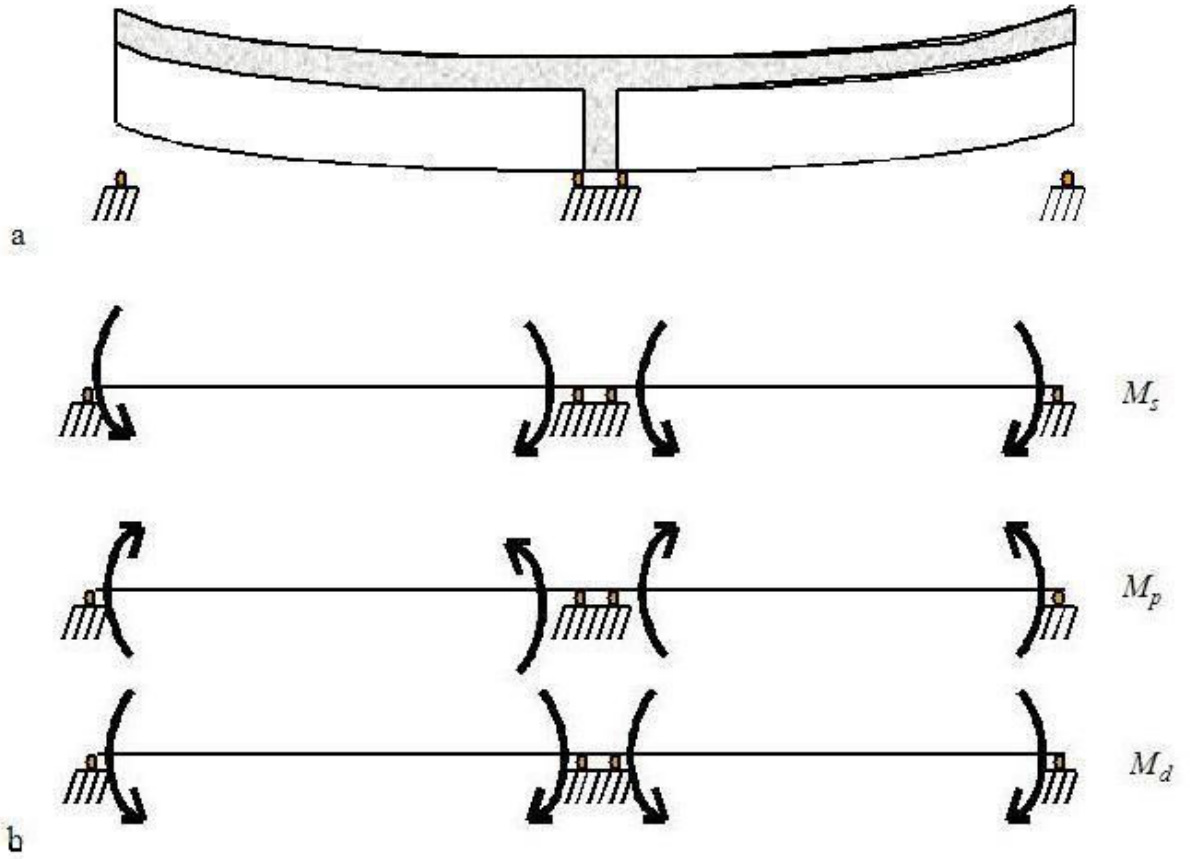


Figure 2.7 (a) Deformation due to differential shrinkage, (b) Restraining moments in continuous prestressed, precast beams made continuous by CIP deck



M_s Restraining moment due to differential shrinkage between deck and girders

M_p Restraining moment due to creep under prestressing

M_d Restraining moment due to creep under dead weight

CHAPTER 3 - Analysis of Post-Tensioned Prestressed Inverted T System

The PT-IT program was developed for the purpose of analyzing PT-IT systems. It is used as a tool to perform parametric study. Parameters varied in the parametric study are discussed in details in chapter 4. The program is written using C++ object-oriented language. The PT-IT program performs time-stepping analyses. Structural analysis is performed at each stage during and after construction. New stage is typically marked by adding structural component or load to the structure. For example events like casting deck, casting diaphragm, apply post-tensioning, install barriers, and apply live load mark the beginning of a new stage. Analysis includes evaluating moments and shears produced by self weight, deck weight, external applied loads, moment and shear internally produced by prestressing and post-tensioning, as well as time-dependent moment and shear caused by creep and shrinkage. The program also checks AASHTO LRFD service and strength limit. A Graphical interface is provided for the program using Visual Basic 6.

Analysis of moment and shear due to Live-load is performed using the Risa 2D program. Analysis includes generating influence lines for different moving loads according to AASHTO LRFD ⁽¹⁾, then manually creating the envelope for a maximum of positive moments, negative moments shear, and live-load deflection. Algorithm used in PT-IT is discussed in details later in this chapter.

To validate results of the program, results of the PT-IT program are checked versus Consplice ⁽²²⁾ utilizing major differences between Consplice and PT-IT. Consplice was developed by LEAP software to analyze spliced girders.

Spliced girders consist of precast prefabricated (usually prestressed) girder, transported to the construction site and joined together using splices, resulting in a continuous span structure. Ideally, spliced girders are post-tensioned to maximize span length. Spliced girders are typically joined within the span, unlike post-tensioned, prestressed IT systems where girders are joined at the pier.

This chapter discusses different material properties of models incorporated in the program and the algorithm used in the PT-IT program. Results of comparison between Consplice and the PT-IT program are also included in this chapter.

Time-Dependent Material Properties

Time effects are incorporated into the analysis by dividing the solution into discrete solution intervals, each with a finite amount of time (1 day). At early age of the girders, time step increases as age of the girders increases. In this analysis, time-dependent material properties are used. This includes concrete compressive strength, modulus of elasticity, creep, and shrinkage. Different models for estimating time-dependent material properties are incorporated in the program, including AASHTO LRFD (American Association of State Highway and Transportation Officials) Third Edition 2003 Interim⁽²³⁾, ACI (American Concrete Institute) 209⁽²⁴⁾, CEB-FIP 1990 (Comite Euro-International Du Beton-Federation Internationale Du Beton)⁽²⁵⁾, and NCHRP (National Cooperative Highway Research Program) Report 496⁽¹³⁾. Creep and shrinkage models for Self-Consolidating Concrete (SCC) are also included. The model was developed using ACI 209 general equations to fit experimental creep and shrinkage data from experiments on SCC performed by Ph.D. candidate Kyle Larson at Kansas State University laboratories⁽²⁶⁾.

Concrete Compressive Strength

The compressive strength of concrete is usually defined in terms of its strength at 28 days (f'_c) and a time function showing its variation with time.

AASHTO LRFD: AASHTO LRFD doesn't give a model for concrete compressive strength. The model proposed by ACI-209 is used for AASHTO.

ACI-209: ACI-209 estimates concrete compressive strength at time t (days) as follows:

$$(f'_c)_t = \frac{t}{\alpha + \beta t} (f'_c)_{28} \quad (3.1)$$

where α (in days) and β are constants,

t is the age of the concrete in days, and

$(f'_c)_{28}$ is the strength of the concrete at 28 days.

The ranges of α and β are given for normal weight, sand light-weight, and all light-weight concrete for both moist and steam-cured concrete.

The constants α and β are functions of both the type of cement used and the type of curing employed. Table 3. 1 shows the values for α and β as given by ACI-209.

NCHRP Report 496: NCHRP doesn't provide an equation to consider variation of concrete compressive strength with time. The ACI-209 equation is used in the program to estimate concrete strength at time (t). NCHRP proposed a formula to predict unit weight of the concrete in terms of its compressive strength as

$$W_c = 0.14 + \frac{f'_c}{1000} \leq 0.155 kcf \quad \backslash \quad (3.2)$$

CEB-FIP 90 ⁽²⁵⁾: This code is based on the uniaxial compressive strength f_c of cylinders, 150 mm in diameter and 300 mm in height, stored in water at $20 \pm 2^\circ\text{C}$, and tested at the age of 28 days in accordance with ISO 1920, ISO 2736/2, and ISO 4012. CEB-FIP evaluates concrete strength at time (t) in terms of mean value of compressive strength f_{cm} associated with the characteristic compressive strength f_{ck} .

$$f_{cm} = f_{ck} + \Delta f; \quad \Delta f = 8 \text{ MPa} \quad (3.3)$$

The mean compressive strength at an age of (t) days is given as function of cement type and time

$$f_{cm}(t) = \beta_{cc}(t) f_{cm} \quad (3.4)$$

where $\beta_{cc}(t)$ is a coefficient, which depends on the age of concrete (t);

$$\beta_{cc}(t) = \exp \left[s \left(1 - \sqrt{\frac{28}{t}} \right) \right]; \quad t_1 = 1 \text{ day} \quad (3.5)$$

where s is a coefficient, which depends on the type of cement.

S=0.2 for rapid-hardening high-strength cement; 0.25 for normal cement; 0.25 for rapid-hardening cements; and 0.38 for slowly hardening cements.

Modulus of Elasticity

AASHTO LRFD: The modulus of elasticity E_c for concrete with unit weights between 0.09 and 0.155 kcf is evaluated in terms of compressive strength and unit weight:

$$E_c = 33000 (W_c^{1.5}) \sqrt{f'_c} \quad (3.6)$$

where W_c is the unit weight in (kcf), and f'_c is specified strength of concrete (ksi).

ACI-209: Modulus of elasticity is given as

$$E_{ct} = g_{ct} [W_c^3 (f'_c)_t]^{1/2} \quad (3.7)$$

where $g_{ct}=33$, W_c is unit weight per pound of cubic foot (pcf), and compressive strength f'_c is compressive strength in pound per square inch (psi).

NCHRP Report 496: NCHRP proposes an equation to evaluate modulus of elasticity at 28 days. The equation incorporated two factors: K_1 representing the difference between national average and local average; and K_2 representing whether an upper-bound or lower-bound value is desired in the calculation, where an upper-bound value is usually used for crack-control analysis and lower-bound value would be appropriate for prestress loss and deflection calculations.

$$E_{ct} = 33,000 K_1 K_2 \left(0.14 + \frac{f'_c}{1000}\right)^{1.5} \sqrt{f'_c} \quad (3.8)$$

Table 3. 2 gives values for K_1 and K_2 predicted in the report. Values used in the program are $K_1=0.975$ and $K_2=0.788$.

NCHRP report 496 proposes an equation to evaluate the development of modulus of elasticity with time. This is given as

$$E_{ci}(t) = \beta_E(t) E_{ci} \quad (3.9)$$

with

$$\beta_E(t) = [\beta_{cc}(t)]^{0.5} \quad (3.10)$$

where

$E_{ci}(t)$ is the modulus of elasticity at an age of t days;

E_{ci} is the modulus of elasticity at an age of 28 days given as

$$E_{ci} = E_{c0} \left[\frac{f_{cm}}{f_{cm0}} \right]^{\frac{1}{3}}; \text{ and} \quad (3.11)$$

$E_{c0} = 2.15 \times 10^4$ MPa, $f_{cm0} = 10$ MPa, $\beta_{cc}(t)$ is given in equation (3.4).

Shrinkage Strain

Shrinkage of concrete is affected by many factors, these factors such as aggregate characteristics and proportions, average humidity at the bridge site, water-to-cement (W/C) ratio, type of cure, volume-to-surface area ratio of a member, and duration of drying period. Shrinkage strain is often defined in terms of ultimate shrinkage and time function to adjust for shrinkage up to a certain time.

AASHTO LRFD: AASHTO LRFD gives two equations to assess shrinkage strain— one for moist-cured concrete and the other for steam-cured concrete.

For moist-cured concretes and concrete devoid of shrinkage-prone aggregates, the strain due to shrinkage ϵ_{sh} at time t , is given by

$$\epsilon_{sh} = -k_s k_h \left(\frac{t}{35.0 + t} \right) 0.51 \times 10^{-3} \quad (3.12)$$

For steam-cured concrete devoid of shrinkage-prone aggregates

$$\epsilon_{sh} = -k_s k_h \left(\frac{t}{55.0 + t} \right) 0.56 \times 10^{-3} \quad (3.13)$$

where

t is the drying time (days).

k_s is size factor given as

$$k_s = \left[\frac{\frac{t}{26e^{0.36(V/S)} + t}}{\frac{t}{45 + t}} \right] \left[\frac{1064 - 94(V/S)}{923} \right] \quad (3.14)$$

k_h is humidity factor given as

for $H < 80\%$

$$k_h = \frac{140 - H}{70} \quad (3.15)$$

for $H \geq 80\%$

$$k_h = \frac{3(100-H)}{70} \quad (3.16)$$

ACI-209: ACI-209 predicts creep and shrinkage referring to “standard conditions” and correction factors for other than standard conditions. ACI-209 provides a model to evaluate shrinkage as follows:

$$(\epsilon_{sh})_t = \frac{t^\alpha}{f+t^\alpha} (\epsilon_{sh})_u \quad (3.17)$$

Where, f (in days) and α are considered constants for a given member is shape and size; $(\epsilon_{sh})_u$ is the ultimate shrinkage strain; and t is time from the end of initial curing. Values of f and α can be determined by fitting the data obtained from tests performed in accordance to ASTM C512. Normal ranges of f , α , and $(\epsilon_{sh})_u$ are

$$\begin{aligned} f &= 20 \text{ to } 30 \text{ days,} \\ \alpha &= 0.9 \text{ to } 1.10, \text{ and} \\ (\epsilon_{sh})_u &= 415 \times 10^{-6} \text{ to } 1070 \times 10^{-6} \end{aligned}$$

These constants are based on the standard conditions for normal weight, sand light-weight, and all light-weight, using both moist and steam-curing, and Types I and III cement.

ACI-209 recommends the following constant values be used in shrinkage calculations:

Shrinkage after seven days for moist-cured concrete

$$(\epsilon_{sh})_t = \frac{t}{35+t} (\epsilon_{sh})_u ; \quad (3.18)$$

Shrinkage after age one to three days for steam-cured concrete

$$(\epsilon_{sh})_t = \frac{t}{55+t} (\epsilon_{sh})_u \quad (3.19)$$

Where $(\epsilon_{sh})_u = 780\gamma_{sh} \times 10^{-6}$ in/in,(m/m),and

Where γ_{sh} represents the product of the applicable correction factors discussed below.

With initial moist-curing, for shrinkage of concrete moist-cured during a period of time other than seven days, the γ_{cp} factor is used and is given in Table 3. 3.

With ambient relative humidity, For ambient relative humidity greater than 40 %, the γ_h factor should be used, where

$$\begin{aligned}\gamma_h &= 1.40 - 0.010\lambda, \quad \text{for } 40 \leq \lambda \leq 80; \text{ and} \\ \lambda_h &= 3.00 - 0.030\lambda, \quad \text{for } 80 > \lambda \leq 100\end{aligned}\tag{3.20}$$

With average thickness of a member other than 1.5 in. ACI-209 offers two methods to estimate the effect of member size on shrinkage and creep—the average-thickness method and volume-surface ratio method. The volume-surface ratio method is discussed here as it was used in the course of study—

$$\gamma_{vs} = 1.2 \exp(-0.00472v / s) \text{ where } v / s \text{ (mm)}.\tag{3.21}$$

ACI-209 included correction factors for temperature and concrete mix other than 70F. These factors aren't included in the study. These parameters, however, must be accounted for as they are used in the final design where the temperature at the construction site is estimated, and concrete mix is designed.

CEB-FIP-90⁽²⁵⁾: Total shrinkage or swelling strains $\epsilon_{sc}(t, t_s)$ are calculated from

$$\epsilon_{cs}(t, t_s) = \epsilon_{cs0} \beta_s (t - t_s)\tag{3.22}$$

where ϵ_{sc0} is the notional shrinkage coefficient given in equation (3.23) below.

β_s is the coefficient to describe the development of shrinkage with time;

t is the age of concrete (days); and

t_s is the age of concrete (days) at the beginning of shrinkage or swelling.

The notional shrinkage coefficient may be obtained from

$$\epsilon_{cs0} = \epsilon_s(f_{cm}) \beta_{RH}, \text{ and}\tag{3.23}$$

$$\epsilon_s(f_{cm}) = [160 + 10\beta_{sc}(9 - f_{cm}/f_{cm0})] \times 10^{-6},\tag{3.24}$$

where

f_{cm} is the mean compressive strength of concrete at the age of 28 days (MPa);

f_{cm0} = 10 MPa;

β_{sc} is a coefficient which depends on the type of cement: β_{sc} = 4 for slowly hardening cements, β_{sc} = 5 for normal or rapid-hardening cements, and β_{sc} = 8 for rapid-hardening, high-strength cements;

$$\begin{aligned}\beta_{RH} &= -1.55\beta_{sRH} && \text{for } 40\% \leq RH < 99\%, \text{ and} \\ \beta_{RH} &= +0.25 && \text{for } RH \geq 99\%\end{aligned}\quad (3.25)$$

where

$$\beta_{sRH} = 1 - \left(\frac{RH}{RH_0} \right)^3 \quad (3.26)$$

with RH as the relative humidity of the ambient atmosphere (%);

$RH_0=100\%$.

The development of shrinkage with time is given by

$$\beta_s(t - t_s) = \left[\frac{(t - t_s)/t_1}{350(h/h_0)^2 + (t - t_s)/t_1} \right], \text{ and} \quad (3.27)$$

$h_0=100$ mm.

h is the notational size of member (mm) defined as

$$h = \frac{2A_c}{u}, \quad (3.28)$$

where A_c is the cross section and u is the perimeter of the member in contact with the atmosphere.

NCHRP Report 496: Using data collected from experiments on high-strength concrete, NCHRP Report 496 proposed factors to predict shrinkage in high-strength concrete, where ultimate shrinkage is assumed to be 0.000480:

$$(\epsilon_{sh}) = 480 \times 10^{-6} \gamma_{sh}; \quad (3.29)$$

γ_{sh} is given as

$$\gamma_{sh} = K_{td} K_s K_{hs} K_f; \quad (3.30)$$

K_{td} is the time development factor

$$K_{td} = \frac{t}{61 - 4f'_c + t}; \quad (3.31)$$

K_{hs} is the humidity factor

$$K_h = 2.00 - 0.0143H; \quad (3.32)$$

K_s is the size factor

$$K_s = \frac{1064 - 94V/S}{735}; \text{ and} \quad (3.33)$$

K_f is the concrete strength factor

$$K_f = \frac{5}{1 + f'_c} \quad (3.34)$$

The NCHRP model also suggested factors K_1 and K_2 to present average, upper, and lower bound values of shrinkage for local materials. Values for K_1 and K_2 were not developed in the project.

Self-Consolidating Concrete Model SCC: As mentioned earlier in this chapter, the model for predicting shrinkage of self-consolidating concrete is proposed in a study conducted in the laboratories of Kansas State University by Larson and Peterman ⁽²⁶⁾.

The ACI-209 model was used to fit the experimental data and come up with appropriate f and α factors to best represent shrinkage of SCC; ACI-209 correction factors were also used for other than standard conditions.

The specimen tested was a “4” x 4” x 24”” cube. Material properties of the concrete mix were as follows: concrete strength at two days was 6280 psi with a modulus of elasticity of 3687 ksi; concrete strength at 29 days was 7878 psi with a modulus of elasticity of 5306 ksi, unit weight of the mix was 140 pcf.

The specimens were steam-cured over night and left at room temperature for a day. Readings started two days after curing stopped.

The purpose for including the SCC model in this study was to furnish an estimate of feasibility of using SCC in fabricating IT members for future research.

The proposed equation to predict shrinkage at time t for SCC is given as:

$$(\epsilon_{sh})_t = \frac{t}{f + t} 550 \times 10^{-6} \times \gamma_h \times \gamma_{vs} \quad (3.35)$$

Where γ_h and γ_{vs} are given in equations (3.20) and (3.21) above. Figure 3. 1 shows predicted values versus shrinkage strain from the tested specimen.

Creep Coefficient

Creep coefficient is being defined as the creep strain divided by instantaneous (elastic) strain. The creep coefficient is applied to the instantaneous compressive strain caused by permanent loads in order to obtain the strain due to creep.

Creep is influenced by the same factors as for shrinkage, and also by magnitude and duration of the stress, maturity of the concrete at the time of loading, and temperature of concrete.

Creep shortening of concrete under permanent loads is generally in the range of 1.5 to 4 of the initial elastic shortening, depending primarily on concrete maturity at the time of loading.

Creep prediction models include an ultimate creep coefficient and time function to adjust for creep at certain times.

AASHTO LRFD: Methods of determining creep and shrinkage in AASHTO LRFD were taken from Collins and Mitchell (1991) ⁽²⁷⁾. These methods are based on the recommendation of ACI Committee 209, as modified by additional recently published papers.

The creep coefficient is given as

$$\psi(t, t_i) = 3.5k_c k_f \left(1.58 - \frac{H}{120}\right) t_i^{-0.118} \frac{(t - t_i)^{0.6}}{10.0 + (t - t_i)^{0.6}} \quad (3.36)$$

where

k_f is the factor of the effect of concrete strength given as

$$k_f = \frac{1}{0.67 + \left(\frac{f'_c}{9}\right)}; \quad (3.37)$$

H is relative humidity; and

k_c is the factor for the effect of the volume-to-surface ratio and is given as follows

$$k_c = \left[\frac{\frac{t}{26e^{0.36(V/S)} + t}}{\frac{t}{45 + t}} \right] \left[\frac{1.80 + 1.77e^{-0.54(V/S)}}{2.587} \right] \quad (3.38)$$

ACI-209: The design approach presented for predicting creep is the same as used for predicting shrinkage. ACI-209 estimates creep coefficient for standard conditions, then corrects for non-standard conditions.

$$(v)_t = \frac{t^\psi}{d + t^\psi} v_u . \quad (3.39)$$

where d is days, and ψ are considered constants for a given member shape and size which define the time-ratio part. Normal ranges of the constants were found to be as follows: $d = 6$ to 30 days, $\psi = 0.4$ to 0.8, $v_u = 1.3$ to 4.15.

This model also allows for fitting experimental data to come up with constants that mostly fit experimental results. This model will be used for predicting the SCC creep model.

ACI-209 recommended values for d , ψ , and v_u be used for predicting creep for normal weight, sand lightweight, and all lightweight concrete, using both moist and steam-curing, and Type I and III cement under standard conditions. Creep coefficient v_t for a loading age of seven days for moist-cured concrete and one to three days steam-cured concrete is given by

$$(v)_t = \frac{t^{0.6}}{10 + t^{0.6}} v_u \quad (3.40)$$

In the absence of specific creep data for local aggregates and conditions, ACI-209 suggested the value of $v_u = 2.35\gamma_c$, where γ_c represents the product of the applicable correction factors.

Correction factors for non-standard conditions are given as follows:

Loading age correction factor γ_{la} is applied for loading ages later than seven days for moist-cured concrete and later than one to three days for steam-cured concrete

$$\begin{aligned} \gamma_{la} &= 1.25(t_{la})^{-0.118} \quad \text{for moist-cured concrete, and} \\ \gamma_{la} &= 1.3(t_{la})^{-0.094} \quad \text{for steam-cured concrete.} \end{aligned} \quad (3.41)$$

For ambient relative humidity greater than 40%, a correction factor should be estimated as follows:

$$\gamma_\lambda = 1.27 - 0.00067\lambda, \quad \text{for } \lambda > 40. \quad (3.42)$$

To correct for volume-surface ratio, correction factor γ_{vs} is given as follows:

$$\gamma_{vs} = \frac{2}{3} [1 + 1.13 \exp(-0.54v/s)] . \quad (3.43)$$

Other correction factors for temperature, concrete composition, and slump are not considered in the study because their influence is very small, and are they not exactly known until the construction site and concrete mix design are decided.

CEB-FIP-90 ⁽²⁵⁾: The creep coefficient is given as

$$\phi(t, t_0) = \phi_0 \beta_c(t - t_0); \quad (3.44)$$

where

ϕ_0 is the notional creep coefficient given as

$$\phi_0 = \phi_{RH} \beta(f_{cm}) \beta(t_0); \quad (3.45)$$

with

$$\phi_{RH} = 1 + \frac{1 - RH / RH_0}{0.46(h / h_0)^{1/3}}, \quad (3.46)$$

$$\beta(f_{cm}) = \frac{5.3}{(f_{cm} / f_{cm0})^{0.5}}, \text{ and} \quad (3.47)$$

$$\beta(t_0) = \frac{1}{0.1 + (t_0 / t_1)^{0.2}}; \quad (3.48)$$

where h is defined in equation (3.28)

f_{cm} is the mean compressive strength of concrete at the age of 28 days (MPa);

$f_{cm0} = 10$ MPa;

RH is the relative humidity of the ambient environment (%);

$RH_0 = 100\%$; and

$t_1 = 1$ day.

The development of creep with time is given by

$$\beta_c(t - t_0) = \left[\frac{(t - t_0) / t_1}{\beta_H + (t - t_0) / t_1} \right]^{0.3}, \quad (3.49)$$

with

$$\beta_H = 150 \left[1 + \left(1.2 \frac{RH}{RH_0} \right)^{18} \right] \frac{h}{h_0} + 250 \leq 1500. \quad (3.50)$$

NCHRP Report 496: NCHRP Report 496 proposed a formula for estimating the creep coefficient for high-strength concrete. Standard conditions have been defined as $R.H.=70\%$, $V/S=3.5$ in, and $f'_{ci}=4$ ksi; loading age is one day for accelerated curing and seven days for normal curing. The ultimate creep coefficient for these standard conditions equals 1.90.

$$\psi(t, t_i) = 1.90\gamma_{cr}; \quad (3.51)$$

γ_{cr} is the product of the applicable correction factors; and

$$\gamma_{cr} = k_{td}k_{la}k_s k_{hc}k_f \quad (3.52)$$

where

k_{td} is time-development factor.

$$k_{td} = \frac{t}{61 - 4f'_c + t} \quad (3.53)$$

k_{la} is loading factor:

$$k_{la} = t^{-0.118}. \quad (3.54)$$

k_{hc} is the humidity factor for creep:

$$k_{hc} = 1.56 - 0.008H. \quad (3.55)$$

k_s is the size factor:

$$k_s = \frac{1064 - 94V/S}{735}. \quad (3.56)$$

k_f is the concrete strength factor:

$$k_f = \frac{5}{1 + f'_{ci}}. \quad (3.57)$$

Self-Consolidating Concrete (SCC): Experimental data from tests performed by Larson and Peterman in the laboratories of Kansas State University⁽²⁶⁾ are used to predict a model for SCC creep coefficient.

Two specimens were tested, the first loaded at the age of one day and the second loaded at the age of 29 days; the second specimen was moist-cured until the day of loading (29 days).

Using the ACI-209 model to fit experimental data, constants were found to be $d=16$ days, $\psi=0.7$, and $v_u=1.75$ for specimen loaded at an age of one day. Figure 3. 2 shows actual versus predicted creep coefficient

$$\psi = \frac{t^{0.7}}{16+t^{0.7}} \times 1.75. \quad (3.58)$$

For specimen loaded at the age of 29 days constants to fit data are $d=30$ days, $\psi=0.74$, and $v_u=1.6$. Figure 3. 3 shows the comparison between experimental versus predicted creep coefficient.

$$\psi = \frac{t^{0.74}}{30+t^{0.74}} \times 1.6. \quad (3.59)$$

Equation (3.58) is used to predict creep coefficient for specimen loaded at age 29 days by multiplying with correction factor γ_{la} for moist-cured specimen given in equation (3.41). Figure 3.4 shows comparison between measured and predicted creep coefficient

$$\psi = \frac{t^{0.7}}{16+t^{0.7}} \times 1.75 \times \gamma_{la}, \quad (3.60)$$

where : $\gamma_{la} = 1.25 \times (t_{la})^{-0.118}$.

Comparison shows that equation (3.58) could be used to predict creep of SCC, noting appropriate correction factors given by ACI (3.41), (3.42), and (3.43). ACI should be used for non-standard conditions.

Relaxation of Steel

Relaxation of steel is defined as the change in strand stress due to continued stress. Prestress losses due to steel relaxation and concrete creep and shrinkage are inter-dependent and also time-dependent. To account for changes of these effects with time, a step-by-step procedure in which the time interval increases with age of concrete is recommended ⁽²⁴⁾.

AASHTO LRFD: AASHTO LRFD estimates relaxation in two parts, relaxation at transfer and relaxation after transfer. Relaxation after transfer is calculated in terms of total creep and shrinkage.

Due to a lack of better estimation of time-dependent steel relaxation in AASHTO LRFD, relaxation of steel is predicted using a method explained in Consplice software theory ⁽²²⁾.

Consplice software ⁽²²⁾ proposed modifications for these equations. Consplice estimates relaxation in three parts: ultimate relaxation, change of relaxation with time, and interaction with creep and shrinkage.

Ultimate relaxation is a function of steel type, elastic shortening, initial stress, and yield stress, given as ultimate relaxation for stress-relieved strands:

$$R_u = f_{pi} \times 0.5 \times \left(\frac{f_{pi}}{f_y} - 0.55 \right) < 20 - 0.3(Fr) - 0.4(ES); \quad (3.61)$$

for low-relaxation strands

$$R_u = 0.25 \times f_{pi} \times 0.5 \times \left(\frac{f_{pi}}{f_y} - 0.55 \right) < 0.3 \times [20 - 0.3(Fr) - 0.4(ES)]; \text{ and} \quad (3.62)$$

relaxation variation with time

$$F(t) = 0.2 \times \log(24t) < 1, \quad (3.63)$$

where R_u is the ultimate relaxation,

f_{pi} is the stress in the strands at the beginning of each stage (ksi),

t is time in days from the day the strands were cut,

Fr is friction loss, and

ES is elastic shortening loss.

To account for interaction with creep and shrinkage a reduction factor is applied; steel relaxation at any time interval is given as

$$R_u(t) = R_u \times fr(t) - 0.2 \times Loss(CR + SH). \quad (3.64)$$

ACI-209: Intrinsic relaxation in ACI-209 is given as follows:

for stress relieved strands:

$$R(t) = 0.1 \times f_{pi} \times \left(\frac{f_{pi}}{f_y} - 0.55 \right) \times \log_{10} \left(\frac{t}{t_1} \right); \quad (3.65)$$

for low-relaxation strands:

$$R(t) = 0.0222 \times f_{pi} \times \left(\frac{f_{pi}}{f_y} - 0.55 \right) \times \log_{10} \left(\frac{t}{t_1} \right); \text{ and} \quad (3.66)$$

where t is estimated in hours, and $t_1 = 1$ hour.

CEB-FIP-90 ⁽²⁵⁾: CEB-FIP-90 divides steel into relaxation classes, which refers to the relaxation at 1000 hours (ρ_{1000}) for initial stresses equal to 0.6, 0.7, and 0.8 of tensile stress.

The code defines three relaxation classes:

Class 1: normal relaxation characteristics for wires and strands

Class 2: improved relaxation characteristics for wires and strands

Class 3: Relaxation characteristics for bars

For estimation of relaxation up to 30 years, the following formula may be applied:

$$\rho_t = \rho_{1000} \left(\frac{t}{1000} \right)^k \quad (3.67)$$

where $k=0.12$ for class 1, and 0.19 for class 2.

NCHRP Report 496: The report recommends estimation of steel relaxation at any time t using a formula based on the work of Magura et al. ⁽²⁸⁾

$$L_r = \frac{f_{pi}}{45} \left(\frac{f_{pi}}{f_{py}} - 0.55 \right) \log \left(\frac{24t_2 + 1}{24t_1 + 1} \right) \quad (3.68)$$

where L_r is intrinsic relaxation loss between t_1 and t_2 (days);

f_{pi} is stress in prestressing strands as the beginning of the period considered;

f_{py} is yield strength of the strand;

t_2 is age of concrete at the end of the period (days); and

t_1 is age of concrete at the beginning of the period (days).

Instantaneous Losses in Post-tensioning

When a tendon is tensioned using a jack, the force produced is not constant along the length of the tendon due to friction between the tendon and the duct. Typically the friction loss is estimated in two parts: the wobble curvature and the wobble frictional.

Both AASHTO LRFD and Post-Tensioning Manual ⁽¹⁵⁾ evaluate losses due to friction between the internal post-tensioned tendon and the duct wall as follows:

$$\Delta f_{pF} = f_{pj} (1 - e^{-(\mu\alpha + kx)}) \quad (3.69)$$

where

f_{pj} is the stress in the prestressing steel at jacking (ksi);

x is the length of a prestressing tendon from the jacking end to any point under consideration (ft);

k is wobble friction coefficient (per foot of tendon);

μ is the coefficient of friction; and
 α is the sum of the absolute values of angular change of the prestressing steel path from the jacking end, or from the nearest jacked end if tensioning is done equally at both ends, to the point under investigation (in RAD).

In the course of the study, post-tensioning tendons were assumed to be stressed from the left side. Tendon profile was assumed to be parabolic.

Both the friction coefficient μ and wobble coefficient k were specified as user input. Table 3. 4 shows values recommended by the Post-Tensioning Manual for μ and k . These values are taken into account while performing the parametric study. The effects of anchorage set on tendon stresses is calculated as recommended by the Post-Tensioning Manual as follows:

$$\Delta f = \sqrt{\frac{E \Delta L d}{3L}} \quad (3.70)$$

where E is tendon modulus of elasticity (ksi);

ΔL is anchor set (in);

d is friction loss in length L (ksi); and

L is length to the point where loss is known (ft).

Length influenced by the anchor set is given as

$$x = \sqrt{\frac{E \times \Delta L \times L}{12 \times d}} \quad (3.71)$$

where x is measured in (ft).

Design-Limit State

Design-limit stresses are checked according to AASHTO LRFD as follows:

Strength I Limit State

This limit state is related to load combination resulting from normal vehicular use of the bridge without wind.

Load factors are given as follows:

$$\text{Strength I: } (0.9_{\min} \text{ to } 1.25_{\max}) \times (DC + DW) + 1.75 \times LL, \quad (3.72)$$

where DC is dead load of structural components and nonstructural attachments, and

DW is dead load of wearing surfaces and utilities.

Service I Limit State

Load combination is related to the normal operational use of the bridge with a 55 MPH wind and all loads taken at their normal values:

$$\text{Service I: } DC + DW + LL . \quad (3.73)$$

Service III Limit State

Load combination is related only to tension in prestressed concrete superstructures with the objective of crack control.

Flexural Design and Capacity Check

Nominal flexural resistance is calculated according to AASHTO LRFD Interim 2006 ⁽²³⁾. Factored resistance components shall be based on conditions of equilibrium and strain compatibility; the resistance factor for flexure is taken as per LRFD 5.5.4.2, as $\phi=1$ for tensioned-controlled reinforced concrete sections, and $\phi=0.75$ for compression-controlled reinforced concrete sections, with spirals or ties. For sections in which the net tensile strain in the extreme tension steel at nominal resistance is between the limits of tension-controlled and compression-controlled sections, ϕ is linearly interpolated.

The variation in ϕ may be computed for prestressed members such that

$$0.75 \leq \phi = 0.583 + 0.25\left(\frac{d_t}{c} - 1\right) \leq 1 \quad (3.74)$$

where c is the distance from the extreme compression fiber to the neutral axis (in), and d_t is the distance from the extreme compression fiber to the centroid of the extreme tension steel element (in).

Minimum prestressed and non-prestressed reinforcement should be provided to develop a factored flexural resistance M_r at least equal to the lesser of $1.2 M_{cr}$ or $1.33 M_u$ where

- $1.2 M_{cr}$: as per LRFD equation 5.7.3.3.2-1 cracking moment M_{cr} is determined on the basis of elastic stress distribution and the modulus of rupture f_r of the concrete, where

$$M_{cr} = S_c (f_r + f_{cpe}) - M_{dnc} \left(\frac{S_c}{S_{nc}} - 1 \right) \leq S_c f_r ; \quad (3.75)$$

Where f_r is the modulus of rupture, for normal weight concrete given as $0.24\sqrt{f'_{ci}}$ (ksi);
 f_{cpe} is the compression stress in concrete due to effective prestress forces only at the extreme fiber of the section where tensile stress is caused by externally applied loads (ksi)

M_{dnc} is the total unfactored dead load moment acting on the monolithic or noncomposite section.

S_c is the section modulus for the extreme fiber of the composite section where tensile stress is caused by externally applied loads;

S_{nc} is the section modulus for the extreme fiber of the noncomposite section where tensile stress is caused by externally applied loads; and

- 1.33 M_u , where M_u is the factored moment required by the applicable strength combination.

Vertical Shear Design and Capacity Check

According to AASHTO, transverse reinforcement shall be provided where

$$V_u > 0.5\phi(V_c + V_p) ; \quad (3.76)$$

where V_u is factored shear force (kip), V_c is nominal shear resistance of the concrete given in (Kip) as

$$V_c = 0.0316\beta\sqrt{f'_c}b_v d_v ; \quad (3.77)$$

β is the factor indicating ability of diagonally cracked concrete to transmit tension; and

V_p is the component of prestressing force in the direction of the shear force (Kip) taken positive if resisting the applied shear, $\phi = 0.9$ for normal weight concrete.

The location for critical shear section is the larger of $0.5d_v \cot(\theta)$ or d_v from the internal face of the support, where d_v and θ are measured at the critical section for shear.

d_v is effective shear depth taken as the distance between the resultant of the tensile and compression forces due to flexure, but not less than the greater of 0.9, the distance between tension reinforcement and top of the section, or 0.72 of the overall section depth.

θ is the angle of inclination of diagonal compressive stresses. The procedure for determining shear critical section location is iterative, where a value for θ is assumed, longitudinal strain in web reinforcement ε_x is calculated, the ratio of shear stress on concrete-to-concrete compressive strength v_u/f'_c is obtained, new values for θ and β are obtained from the table AASHTO-LRFD-5.8.3.4.2-1, and iterations are carried on until the value for θ converges.

For locations other than shear critical section, the value for θ is directly obtained from AASHTO-LRFD-5.8.3.4.2-1 after determining ε_x and v_u/f'_c .

The longitudinal strain in the web reinforcement on the flexural tension side of the member for sections contains at least the minimum transverse reinforcement given as

$$\varepsilon_x = \frac{\frac{M_u}{d_v} + 0.5N_u + 0.5(V_u - V_p) \cot \theta - A_{ps}f_{po}}{2(E_s A_s + E_p A_{ps})} \leq 0.001 \quad (3.78)$$

where for simplification, $0.5 \cot(\theta) = 1$ according to the AASHTO 2003 Interim.

If ε_x is negative, the strain shall be taken as

$$\varepsilon_x = \frac{\frac{M_u}{d_v} + 0.5N_u + 0.5(V_u - V_p) \cot \theta - A_{ps}f_{po}}{2(E_c A_c + E_s A_s + E_p A_{ps})} \quad (3.79)$$

where M_u is the factored moment taken as positive quantity but not less than $V_u d_u$ (Kip.in), V_u factored shear force is taken as positive quantity (Kip), N_u is factored axial load (Kip), f_{po} is taken as $0.7f_{pu}$ for prestressing and post-tensioned members, and A_c is the area of concrete on the flexural tension side of the member below the mid-height of the section.

Shear stress on concrete v_u is calculated as

$$v_u = \frac{V_u - \phi V_p}{\phi b_v d_v} \quad (3.80)$$

where b_v is the effective web width.

Required transverse reinforcement shear resistance is calculated to satisfy

$$V_u \leq \phi(V_c + V_s + V_p) \quad (3.81)$$

Required stirrups area A_v in s inch is obtained as follows:

$$\frac{A_v}{s} = \frac{V_s}{f_y d_v \cot \theta} \quad (3.82)$$

Nominal shear resistance V_n is the lesser of

$$\begin{aligned} V_n &= V_c + V_s + V_p \\ V_n &= 0.25f'_c b_v d_v + V_p \end{aligned} \quad (3.83)$$

Minimum transverse reinforcement in areas where transverse reinforcement is required is

$$\frac{A_v}{s} = 0.0316 \sqrt{f'_c} \frac{b_v}{f_y} \quad (3.84)$$

If longitudinal reinforcement cannot resist required tension T , transverse shear reinforcement should be increased but not exceeding the section nominal shear capacity. In the case where longitudinal reinforcement cannot resist required tension T with maximum transverse shear reinforcement, longitudinal reinforcement shall be increased.

$$T = \frac{M_u}{d_v \phi} + 0.5 \frac{N_u}{\phi} + \left(\frac{V_u}{\phi} - 0.5 V_s - V_p \right) \cot \theta \quad (3.85)$$

Allowable Stresses

Stresses in the concrete are checked as specified by AASHTO LRFD per LRFD 5.9.4:

Stresses at transfer: Service load stresses due to beam self weight and prestressing are computed for precast during release conditions and checked versus allowable stresses. Allowable stresses are given as follows:

Compression stresses: The compressive stress limit for pretensioned and post-tensioned concrete components shall be taken as $0.6 f'_{ci}$ (ksi).

Tension stresses: In areas with bonded reinforcement, the stress is limited to $0.19 \sqrt{f'_{ci}}$ (ksi)

-For stresses at service limit state after losses:

Compression stresses: Compression stresses in segmentally constructed bridges are checked in accordance with LRFD 5.9.4.2.2-1 as follows:

- Stresses due to the sum of effective prestress and permanent loads should be limited to $0.45 f'_{ci}$ (ksi); and
- Stresses due to the sum of effective prestress, permanent loads, and transient loads and during shipping and handling should be limited to $0.4 f'_{ci}$ (ksi).

Tensile stress: Tensile stresses should be limited to $0.19 \sqrt{f'_{ci}}$ (ksi).

Vehicular Live-load

AASHTO LRFD HL-93 ⁽¹⁾ vehicular live-load is considered in design LRFD 3.6.1.2 which is a combination of:

- design truck or design tandem, and
- design lane load.

Application of design live-load is considered as per LRFD 3.6.1.3.

Distribution factors for live-load recommended by Ambare and Peterman⁽¹²⁾ are used in this study as discussed in chapter two, which is 0.42 for shear and 0.18 for moment.

Live-load deflection is estimated according to 3.6.1.3.2 to be the larger of those resulting from design truck alone or resulting from 25% of the design truck taken together with the design lane load.

Analysis of live-load is done separately using Risa 2D software. An envelope of positive and negative shear, positive and negative moment, as well as upward and downward deflections is obtained from Risa2D. The values of this envelope are multiplied by the distribution factors and saved in text file to be read by the PT-IT program.

Algorithm

PT-IT program can be used to analyze various construction sequences and scenarios. The analysis accounts for construction sequence such as simple span behavior of the girder before casting of the diaphragm and continuous behavior after that. Casting of the deck and diaphragm, as well as applying post-tensioning can be done in any sequence and at any age of the girder. Therefore, the program can be used to investigate behavior under a wide variety of conditions.

The program allows to track cracking of the deck and diaphragm under possible positive or negative moments, taking into account time-dependent material properties. The program specifies amounts of reinforcement required in the deck over the pier and in the bottom of the diaphragm to satisfy strength limit.

Analysis process consists of three main parts: input data, analysis (1-D linear analysis), and output data.

1. Input data are listed in different categories as follows:
 - a. Specification of methods and models used in analysis

- i. Losses calculation method: The user has the option to choose from the following two methods to calculate losses— AASHTO LRFD ⁽¹⁾ method and creep-transferred section properties method.
- ii. Shrinkage and creep models: The program incorporates different creep and shrinkage models, including AASHTO LRFD⁽¹⁾, ACI-209 ⁽²⁴⁾, CEB-FIP-90 ⁽²⁵⁾, NCHRP ⁽¹³⁾ model for high-strength concrete, and SCC model.
- iii. Methods for calculation of time-dependent restraint moment include PCA, TTI, CTL, P, and “creep-transformed-section properties” method.
- iv. Construction scenario: two main construction scenarios methods are possible:
 - 1. Using one-step post-tensioning, where post-tensioning is applied before or after casting the deck
 - 2. Using two-step post-tensioning, where the beam will be partially tensioned before casting the deck to carry the weight of the deck. At this point, the duct will remain ungrouted, and after the deck is cast, another tendon is added and duct is grouted.
- b. Define concrete material models that will be used. This includes material ID, curing type (steam or moist-curing), cement type (I or III), initial compression strength (ksi), compression strength at 28 days (ksi), unit weight (pcf), and humidity %.
- c. Define steel properties for pretensioning strands and post-tensioned tendons that include ID number, ultimate tensile stress (ksi), and yielding stress (ksi).
- d. Define layout properties which include number of spans, number of diaphragms by default is equal to the number of spans -1; define number of sections in the diaphragm at which stresses and forces will be assessed; define the following for each span: span ID number, number of section, material ID (assign one of the materials that are defined earlier), and assign material for the deck and diaphragm.

- e. Define nodes properties. Each span or diaphragm will have two nodes. The diaphragm will share the nodes with the two adjacent spans, and consequently, the number of nodes to be defined is equal to the number of spans \times 2. Coordinates are defined such as the left bottom corner of the first span is to be (0,0). For each node a defined node ID number and horizontal distance to the first node (ft) are specified.
- f. Define boundary conditions for each node. Translation (UX or UY) or rotation (Theta) can be locked.
- g. IT section properties are specified giving center of gravity location (distance from bottom of girders) (in), area of the section (in²), moment of inertia (in⁴), volume-to-surface ratio (in), section height (in), and web width (in)
- h. Specify deck's tributary width and thicknesses.
- i. Specify strand properties for each girder including number of pretensioning rows in the span, diameter, strand type (low-lax or stress-relieved), strand profile (straight or depressed with one or two depression points), number of strands, and distance of center of gravity of the strand to the bottom of the beam.
- j. Specify tendon properties: number of tendons (normally one tendon for one-stage post-tensioning and two strands for two-stage post-tensioning), tendon profile (parabolic or straight), tendon area (number of strands in the tendon), anchorage set, friction coefficient, and wobble coefficient. Defining tendon paths will be discussed later in this chapter.
- k. Specify the number of external dead loads applied to the bridge, uniform or concentrated force. For uniform load, specify the number of spans on which the load is applied, span IDs on which the load is applied, and magnitude (kip/ft). For point load, specify span on which load is applied, distance from the left support of the span (ft), and magnitude (kip/ft)
- l. Define construction stages and specify girder age at the beginning of each stage. Define number of elements forming the structure at this stage (where 1 refers to the girders, 2 refers to girders +diaphragms, 3 to the girders +diaphragms +deck, 4 to girders +diaphragms +deck +post-tensioning).

Define external load ID number if any load is applied at the structure at that specific stage (0 if no load is applied, load ID for other external loads, number of external loads+1 for live-load).

2. Live-load analysis is performed using Risa 2D, saved into text file and read by a PT-IT program. Live-load analysis results include maximum positive and negative shear envelope, positive and negative concurrent moments, maximum positive and negative moment envelope, and maximum positive and negative deflection.
3. Figure 3.5 shows the structural analysis model used in analyzing the bridge system. Each girder and each diaphragm has its own material properties, length, and strand profiles. Each girder shares its nodes with the adjacent diaphragm.
4. Analysis is performed using the matrix structural analysis approach. For each stage, stiffness matrices are recalculated depending on concurrent material properties and section properties. Global stiffness matrix is obtained by assembling element's stiffness matrices and applying boundary conditions.

Before establishing continuity (i.e., casting diaphragm), stiffness of diaphragm will be equal to zero; consequently, each girder will act as simply supported span. After continuity is established, simultaneous stiffness for the diaphragm is used to obtain the global assembled stiffness matrix.

Girders weights are carried by simply supported girders. For the one-stage, post-tensioning scenario, the deck's weight is carried by the simply supported girders too; while for the two-stage, post-tensioning scenario, the deck weight is carried by the continuous beam. External loads are also applied on the continuous beam. Time-dependent restraint moments are calculated and redistributed on the continuous beam.

The moments due to post-tensioning in continuous beams are not directly proportional to the tendon eccentricity, because deformations imposed by post-tensioning are resisted by the continuous member at continuity points. The restraint to post-tensioning deformations modifies the reactions and hence affects the elastic moments and shears. The restraint to the prestressing deformations are referred to as secondary moments. Usually secondary moments increase positive moments within the spans and reduce negative moments at interior supports. Conjugate beam analogy is used to estimate fixed-end secondary moments. These fixed-end moments are

used to calculate moments in interior supports. Moment and shear forces are then evaluated at each section along girders and diaphragms.

5. Losses in prestressing and post-tensioning stresses are incrementally evaluated for the duration between each of two consecutive stages. Time increments are considered to be equal to one day at the beginning and increase as age of the girders increases.
6. Concrete stresses are evaluated at each stage and at each section along the structural elements; stresses are checked versus allowable stresses.
7. Shear capacity is also checked at each stage and at each section; required vertical shear reinforcement is evaluated.
8. The program using provisions of AASHTO LRFD calculates required horizontal shear reinforcement.
9. Area of non-prestressed steel required in the deck to aid in resistance of negative moment over the pier is determined by the program in order to satisfy strength state limits in these sections.
10. Area of non-prestressed steel required to resist positive restraint moments in the pier is evaluated by the program based on strength limit.

Comparison with Consplice

A comparison between Consplice and PT-IT was performed. Consplice results were used to validate PT-IT results. The comparison highlighted major differences between Consplice and PT-IT analysis. Two examples for post-tensioned, prestressed, inverted-T beams were designed using PT-IT and compared with Consplice.

Example 1: IT-700

In considering two-span IT-700; each span is 88 ft long, with two-feet diaphragm connecting the two spans. Girders were assumed to be prestressed, precast and steam-cured using (8 ksi) strength concrete. The weight of the girders' concrete was (140 pcf). Prestressing strands were placed in two rows. The bottom row consisted of (11-1/2-270K-LL) low-relaxation straight strands at a distance of (1.77 in) from the bottom of the section. The second row consisted of (6-1/2-270K-LL) straight strands at a distance of 3.5 in from the bottom of the section. Jacking stress for the strands was ($0.75 f_{pu}$).

The construction scenario we considered to be such as deck and diaphragm were cast simultaneously; the girders were 56 days old when deck was cast, deck thickness was 5.98=6 in, deck's concrete strength at 28 days was 3.5 ksi with 140 pcf weight, and the deck was moist-cured. The diaphragm was assumed to have the same concrete of the deck.

Beams were post-tensioned 17 days after continuity was established, using a 4-0.5" tendon. The tendon had a parabolic profile. Figure 3. 7and Figure 3. 8 show bridge layout as well as tendon path along the bridge length. Anchorage set for the post-tensioning tendons was assumed to be 0.25 in, a friction coefficient of 0.25 was assumed, wobble coefficient was equal to 0.0002 1/ft, and the tendons were stressed to $0.75 f_{pu}$.

Barriers were installed 4 days after post-tensioning. The girder's age when barriers were installed was 77 days. Barriers weight was 61 lb/ft. The bridge was assumed to be open for traffic 10 days after installing the barriers (i.e., girders were 87 days old). Analysis of the system is performed for 20 years of girder age. Humidity was assumed to be 70%.

Figure 3.6 shows section properties and dimensions, including strands and tendon locations and numbers. Analysis was performed using AASHTO LRFD specifications. Restraint moments were calculated using both PCA and P methods.

The PT-IT main screen is shown in Figure 3.9. Main options for analysis are defined in the main screen. This includes loss calculation method, shrinkage and creep models, restraining moment calculation method, and construction scenario.

The second step for input data was to define different concrete materials and specify their properties. These materials will be later assigned to each element in the structure (i.e. each girder, deck, and diaphragm) to give flexibility in design by allowing use of different material properties for each girder or span. Figure 3. 10 shows a concrete properties input form. New material properties are defined in the text boxes. By clicking on the "Add" button, the material is added to the material list. The user has the option to modify or delete an existing material. Modifying properties of an existing material is done by clicking on a specified material row in the list. Properties of this material will be shown in the text boxes. Properties can be modified and the new properties will be saved by clicking on the Modify" button. An existing material is simply deleted by pointing to it in the material list and clicking on the "Delete" button. The same process is followed to add and edit materials and is followed for layout, prestressing, post-tensioning, loading, and staging.

Figure 3. 11 show the “Layout” screen, where girder lengths and diaphragm lengths are defined and materials are assigned from a dropdown list for each span and diaphragm. Number of sections along the beam at which analysis is performed is also defined for each span in the “Layout” screen.

Beam section is defined by clicking on the “Beam Section” button on the “Layout” screen. This will activate the girder section screen shown in Figure 3. 12 and the user can choose from the dropoff list different ITs as well as Modified ITs sections discussed in chapter two. By clicking “Deck Section Button” on the “Girder Section”, the deck section screen appears allowing user to specify arbitrary width of the deck thickness. Deck material is specified from the dropdown list. Figure 3. 13 shows the deck properties screen.

Clicking on the “Strands” button on the main screen activates that screen, in Figure 3. 14, the user has the option of using straight or draped strands. However, for PT-IT, only straight strands are used as post-tensioning tendons are placed in the stem of the section. Prestressing strands type is specified by clicking on the list containing available strand diameters.

Figure 3. 15 shows the “Post-Tensioning Tendons Properties” screen, which is activated by clicking on the “Tendons” button on the main screen. Tendons are combinations of single strands. A list of commonly used strand combinations is provided on the “Tendon” screen to choose from. Other properties such as friction and wobble coefficients, jacking stress, and anchor set are specified by the user. Two options for tendon profile are available— straight and parabolic. For the PT-IT parabolic profile, tendon path is described using maximum and minimum eccentricity points along the path, as well as the ratio of the distance between the contraflexure points and maximum eccentricity points (i.e., points over the pier). Tendon location along the beam is defined in terms of the distance from the centroid of the tendon to the bottom of the section.

By clicking on the “Supports” button on the main screen, the “Supports” screen is started. As default, all nodes are supported in the vertical direction. Figure 3. 16 shows the “Supports” screen. Clicking on the “Loads” button from the main screen (Figure 3. 17)– activates this screen. Two types of loads are available for the user— uniform and point loads.

Finally, Figure 3. 18 shows stages defined through the structure’s construction and lifetime. The “Construction Stages” screen is accessed by clicking on the “Stages” button from the main screen.

It is important to mention that in order to compare results with Consplice, output data from PT-IT had to be separated into different components to match the Consplice output data format. For example, Consplice output for forces (shear and moment) due to component weights includes time-dependent restraining moments resulting from creep under component weights; moments produced by prestressing include the effect of prestressing force multiplied by the eccentricity, in addition to the time-dependent restraining moment due to creep under prestressing; moments produced by post-tensioning include the moment due to the primary and secondary effect of post-tensioning. Consplice output also contained time-dependent restraint moments due to differential shrinkage.

Typically, PT-IT output data for forces (moment and shear) contain moment and shear due to self weight and deck weight separately, as well as time-dependent restraint moment which includes effect of creep-under-component weight, deck weight, creep under prestressing, and shrinkage all together. Secondary moments are also reported separately from primary moments (i.e. PT force multiplied by eccentricity). For the sake of comparison, only different components for time-dependent restraining moments are evaluated.

Comparison is carried out at a girder's age of 100 days; at this time, the bridge is assumed to be in service (open for traffic).

Figure 3. 19 shows stresses in the two layers of prestressing at that stage. A maximum difference of 3% was obtained. However, Consplice predicts that strands at the end of the girders are applying tension forces on the girders, while it is known that at the edges, stresses in the pretensioning strands are equal to zero. It is believed that this was generated in Consplice when adjusting stresses in the strands for the effect of applying post-tensioning.

Figure 3. 20 shows comparison of stresses in the tendons at the considered stage. Maximum difference is 0.7%. It is obvious that at the left end of the first span, PT-IT predicts the same stresses in tendons as Consplice does, However Consplice predicts a sudden increase in post-tensioning at that same point.

Figure 3. 21 shows a moment diagram resulting from both girder and deck weights acting on the simple span, along with the time-dependent restraining moments in the pier resulting from creep-under-component weights. Comparison included restraining moments calculated using both PCA and P methods. Excellent agreement is achieved especially using the P method, to estimate restraining moments due to creep under the effect of component weights.

Figure 3. 22 includes moments caused by prestressing strands on the structure; this includes moments caused by prestressing force eccentricity as well as time-dependent restraining moments due to the effect of creep under prestressing.

Figure 3. 23 show moments introduced by post-tensioning. This effect includes the primary effect of post-tensioning (due to tendon eccentricity) and secondary effect of post-tensioning (secondary moments). It is important to mention that post-tensioning doesn't cause time-dependent restraining moments due to creep, since it is applied on the structure after establishing continuity as discussed before.

Figure 3. 24 shows time-dependent restraining moments due to differential shrinkage between deck and girder. It is obvious that predictions vary using different methods. While PCA predicts high-restraining moments due to shrinkage, it is believed that the P method predicts quiet, low-restraining moments.

A discussion about the P method of prediction of moment due to differential shrinkage will be included at the end of this chapter.

Figure 3. 25 shows moments under barrier weight. Figure 3. 26 through Figure 3. 33 show comparison of live-load positive and negative moments for loading cases required by AASHTO LRFD. This includes lane load, tandem, truck load, double tandem, and double truck. Figure 3. 34 and Figure 3. 35 shows maximum positive and negative moments for vehicular live-loading specified by AASHTO LRFD designated as HL-93 which consists of design truck or design tandem along with design lane load. Application of design vehicular live-load is according to LRFD 3.6.1.3.1 for moments and reactions, and LRFD 3.6.1.3.2 for live-load deflection.

Figure 3. 36 shows factored, required positive and negative moments obtained from Consplice along with these moments obtained from PT-IT.

Figure 3. 37 compares the amount of 1.2 times cracking moments under positive and negative moments along the beam. Figure 3. 38 includes a comparison of factored flexural resistance. Analysis of PT-IT program included analysis of factored resistance according to the provisions of AASHTO LRFD 3rd Edition (2004) ⁽¹⁾, and provisions of AASHTO LRFD Interim 2006 ⁽²³⁾ using strain compatibility approach. Figure 3. 39 through Figure 3. 42 show a comparison for time-dependent deflection due to different components. PT-IT has two options to calculate deflection using PCI factors obtained from the PCI Design Handbook⁽²⁹⁾, Table 4.8.2.

The other option was to use the creep-transformed section properties method to calculate deflection. It is clear from graphs that deflection due to components or loads applied before continuity compared better with Consplice and PCI factor predictions, while for components and loads applied after establishing continuity (post-tensioning and barriers), the Creep-transformed section properties method predicted less deflection.

Example 2: IT-500

The second example is considered to be IT 500. The bridge consisted of two-spans; each span was (64 ft) in length, with a 2 ft diaphragm connecting the two spans. Girders were prestressed, precast, and moist-cured using 8 ksi strength concrete. A girder's concrete unit weight was considered to be 140 pcf. One layer of prestressing strands used consisted of 6-1/2-270K-LL low-relaxation straight strands at a distance of 1.77 in from the bottom of the section. Strands were jacked to a stress of $0.75 f_{pu}$.

Deck and diaphragm were cast simultaneously when the girders were 224 days old. The deck thickness was 5.98=6 in. Figure 3. 43 shows the bridge cross section including the deck. Concrete of the deck and diaphragms was 3.5 ksi strength at 28 days, with 140 pcf unit weight. The concrete was moist-cured.

The beams were post-tensioned (17 days) after the deck was cast using 4-0.6" tendon. The tendon has a parabolic profile, anchorage set for the tendons is (0.25 in), friction coefficient of 0.2 was assumed, wobble coefficient is equal to 0.0002 1/ft and the tendons are stressed to $0.75 f_{pu}$.

Barriers were installed four 4 days after post-tensioning, the girder's age when barriers were installed was 245 days. Barrier weight was assumed to be 61 lb/ft. The bridge was assumed to be open to traffic (10 days) after installing the barriers (i.e., girders are 255 days old). The bridge was analyzed for 20 years of girder age. Humidity was assumed to be (70%).

Analysis was performed using AASHTO LRFD specification; restraint moments were calculated using both PCA and P methods.

Comparison was carried on at girder's age of 300 days after the bridge was fully constructed and opened for traffic.

Figure 3. 44 and Figure 3. 45 show bridge layout and post-tensioned tendon path. shows stresses in prestressing strands along the bridge length at this stage. An excellent agreement is achieved, except for the girders end points, where the stresses in the strands should be equal to zero.

Figure 3. 47 represents comparison of stresses in post-tensioned tendons along the length of the bridge. Maximum difference between Consplice prediction and PT-IT prediction was 1.9%.

Figure 3. 48 shows moments resulting from girder and deck weights, and restraining moments in the pier resulting from creep-under-component weights.

Figure 3. 49 and Figure 3. 50 include comparison of moments induced by prestressing strands and post-tensioned tendons, respectively. For prestressing strands, moments include moment due to strand eccentricity as well as restraining moments resulting from creep under prestressing. For post-tensioning, moments included primary and secondary moments produced by post-tensioning.

Figure 3. 51 shows time-dependent restraining moments due to differential shrinkage between deck and girder.

Figure 3. 52 shows moments under barrier weight. Figure 3. 53 and Figure 3. 53 show maximum positive and negative moments for vehicular live-loading (HL-93).

Figure 3. 55 shows factored required positive and negative moments obtained from Consplice, along with the envelope of maximum positive and negative moments obtained from PT-IT.

Figure 3. 56 includes comparison of factored flexural resistance. The section is not overreinforced, but still Consplice predicts less flexural resistance than PT-IT.

Figure 3. 57 through Figure 3. 60 show comparisons for time-dependent deflection due to different components.

Discussion of P Method and CTL Method

Different methods were presented in chapter two for estimating time-dependent restraining moments. Comparing results obtained comparing these methods with Consplice analysis in Figure 3. 21, Figure 3. 22, Figure 3. 24, Figure 3. 48, Figure 3. 49, and Figure 3. 51. It is obvious that PCA, CTL, and P methods are almost predicting comparable time-dependent

restraining moments due to creep effect, while they vary in predicting restraining moments due to shrinkage.

Derivation of moments due to differential shrinkage was carried out for the purpose of comparing PCA, CTL, and P methods.

Since the deck and the diaphragm have different concrete properties and different ages, shrinkage occurred in each one differently. At equilibrium, both deck and girder will have the same deformation under differential shrinkage. This is Assuming P_d to be force applied at the center of gravity of the deck due to shrinkage strain in the girder, and P_g to be force applied at the center of gravity of the girder due to shrinkage strain in the deck. Figure 3. 61 is equivalent to the case where shrinkage strain in the deck is larger than shrinkage strain in the girder.

For equilibrium, the two forces should be equal:

$$P_d = P_g = P \quad (3.86)$$

Figure 3. 62 illustrates deformations encountered at both deck and girder where δSh_d and δSh_g are deformations due to shrinkage strain in the deck and the girder, respectively, while δP_d and δP_g are deformations due to the effect of shrinkage of the deck and the girder on each other.

$$\delta Sh_d - \delta P_d = \delta Sh_g + \delta P_g \quad (3.87)$$

$$\epsilon_{Shd} \times L - \frac{P \times L}{E_d A_d} = \epsilon_{Shg} \times L + \frac{P \times L}{E_g A_g} \quad (3.88)$$

where: ϵ_{shd} and ϵ_{shg} are shrinkage strain in deck and girder, respectively, at time T.

E_d and E_g are modulus of elasticity of deck and girder, respectively.

A_d and A_g are sectional area of deck and girder, respectively.

$$\epsilon_{Shd} - \epsilon_{Shg} = \frac{P}{E_d A_d} + \frac{P}{E_g A_g} \quad (3.89)$$

where $\epsilon_{shd} - \epsilon_{shg} = \epsilon_{sh}$

$$\delta \epsilon_{Sh} = P \left[\frac{E_g A_g + E_d A_d}{E_d A_d E_g A_g} \right] \quad (3.90)$$

$$P = \delta \epsilon_{Sh} E_d A_d \left[\frac{1}{1 + \frac{E_d A_d}{E_g A_g}} \right] \quad (3.91)$$

The moment resulting of that force P is equal to

$$M_s = P \times (C_g - C_d) = \delta \varepsilon_{sh} E_d A_d \left[\frac{1}{1 + \frac{E_d A_d}{E_g A_g}} \right] (C_g - C_d) \quad (3.92)$$

Where C_g and C_d are distances from the top of the composite section to the center of gravity of the girder and the deck, respectively.

The centroid of the composite section is at distance C_c from the top of the section, where

$$C_c = \frac{A_g C_g + n A_d C_d}{A_g + n A_d}; \quad n = \frac{E_d}{E_g} \quad (3.93)$$

$$C_c = \frac{A_g E_g C_g + A_d E_d C_d}{A_g E_g + A_d E_d} \quad (3.94)$$

Rearranging

$$C_c - C_d = \frac{1}{1 + \frac{A_d E_d}{A_g E_g}} (C_g - C_d), \text{ and} \quad (3.95)$$

Substituting in equation (3.92)

$$M_s = \delta \varepsilon_{sh} E_d A_d (C_c - C_d) \quad (3.96)$$

This equation is similar to the equation published by the PCA method to predict moment due to differential shrinkage, with a difference that in the PCA method, $\delta \varepsilon_{sh}$ is the differential shrinkage between deck and girder as time continuity is established.

CTL method predicts moment due to differential shrinkage as

$$M_s = \delta \varepsilon_{sh} E_d A_d \left[\frac{1}{1 + \frac{E_d A_d}{E_g A_g}} \right] (C_c - C_d) \quad (3.97)$$

Comparing equation (3.92) and equation (3.97), it is clear that the CTL method uses different expressions in terms of determining the arm of the moment resulting from differential shrinkage.

P method predicts moment due to differential shrinkage as

$$M_s = \delta\epsilon_{sh} E_d A_d \left[\frac{1}{1 + \frac{E_g A_g}{E_d A_d}} \right] \left[\frac{1}{1 + \frac{E_s A_s}{E_d A_d}} \right] (C_c - C_d) \quad (3.98)$$

Where according to Peterman and Ramirez ⁽⁷⁾, the two factors in equation (3.98) account for effect of restraining the girder and reinforcement on the shrinkage of the deck. Peterman and Ramirez ⁽⁷⁾ modeled this effect as the effect of a steel bar embedded in a concrete section in restraining the shrinkage of the concrete. While this assumption is valid for the steel reinforcement, since it is generally eccentric with the deck, it does not seem appropriate for the girder's concrete, which has a large eccentricity with respect to the center of gravity of the deck.

According to the aforesaid discussion, suggested corrections for CTL and P methods are presented. These corrections apply to the expression used to predict moment due to differential shrinkage, while estimation of creep coefficient and effect of deck reinforcement are considered the same as published for each method.

The suggested expression used to calculate moment due to differential shrinkage for the CTL method is recommended to be

$$\Delta M_s = \delta\epsilon_{sh} E_d A_d (C_c - C_d) \quad (3.99)$$

Figure 3. 63 and Figure 3. 66 compare published versus suggested equations to predict moment due to differential shrinkage according to CTL method for example 1 and example 2, respectively.

The suggested expression used to calculate moment due to differential shrinkage for the P method is recommended to be

$$M_s = \delta\epsilon_{sh} E_d A_d \left[\frac{1}{1 + \frac{E_s A_s}{E_d A_d}} \right] (C_c - C_d) \quad (3.100)$$

Figure 3. 64 and Figure 3. 67 show comparison of published versus suggested equations to predict moment due to differential shrinkage, according to the P method for example 1 and 2, respectively.

Figures 3.66 and 3.69 show comparison of restraining moment due to shrinkage predicted for Consplice, PCA, proposed CTL, and proposed P methods. It is clear that the suggested P method prediction is closer to the prediction of Consplice.

P method is believed to better estimate creep coefficient used in prediction of restraining moment due to shrinkage, because it uses creep coefficient for creep effect, initiating when CIP is cast. On the other hand, CTL uses creep coefficient at each stage, considering creep initiates at time of prestressing. That explains why for example 1, where continuity was established at age 56 days of girder's age, suggested CTL and P methods predict comparable shrinkage strain. While for example 2, where continuity is established at 224 days of girder's age, CTL noticeably predicts higher restraining moments due to differential shrinkage.

Figure 3. 1 Experimental shrinkage strain versus predicted strain for SCC

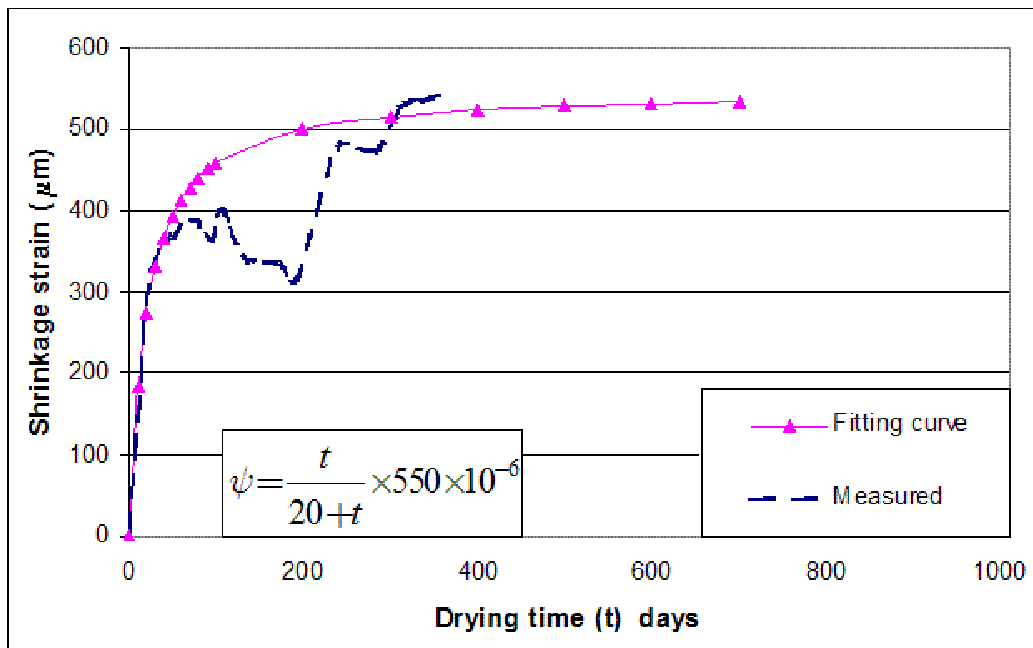


Figure 3. 2 Experimental creep coefficient versus predicted creep coefficient for specimen loaded at Day 1

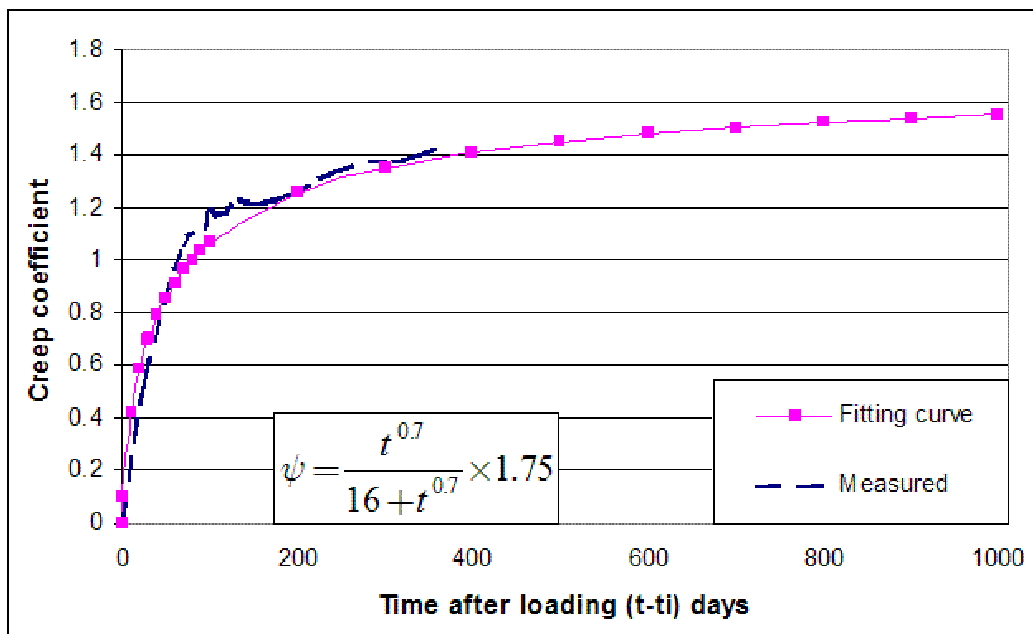


Figure 3. 3 SCC-Experimental creep coefficient versus predicted creep coefficient for specimen loaded at day 29

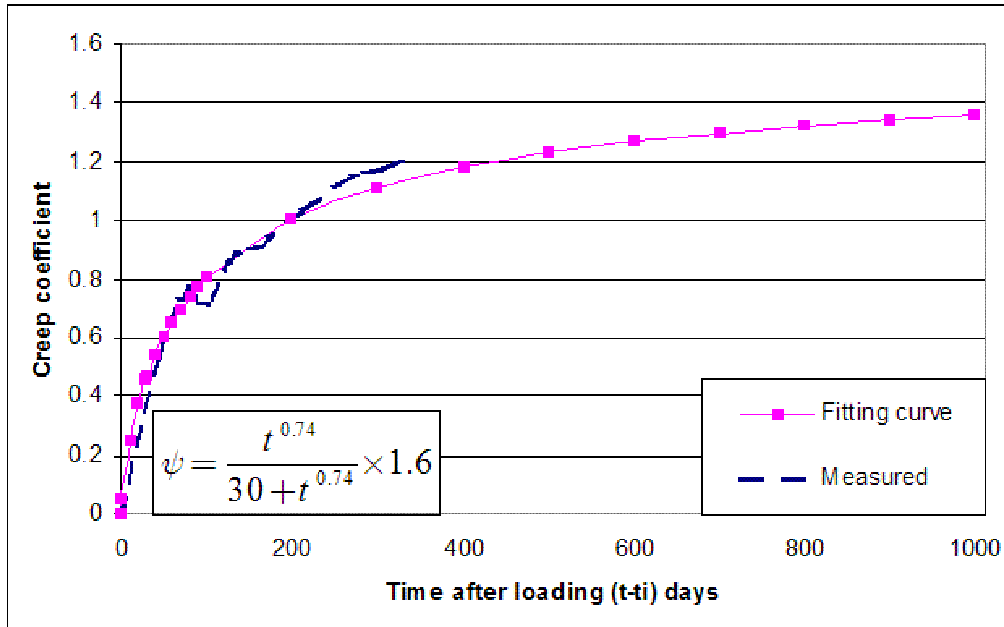


Figure 3. 4 Experimental creep coefficient versus predicted creep coefficient using equation for specimen loaded at day 1 and corrected for loading age of 29 days

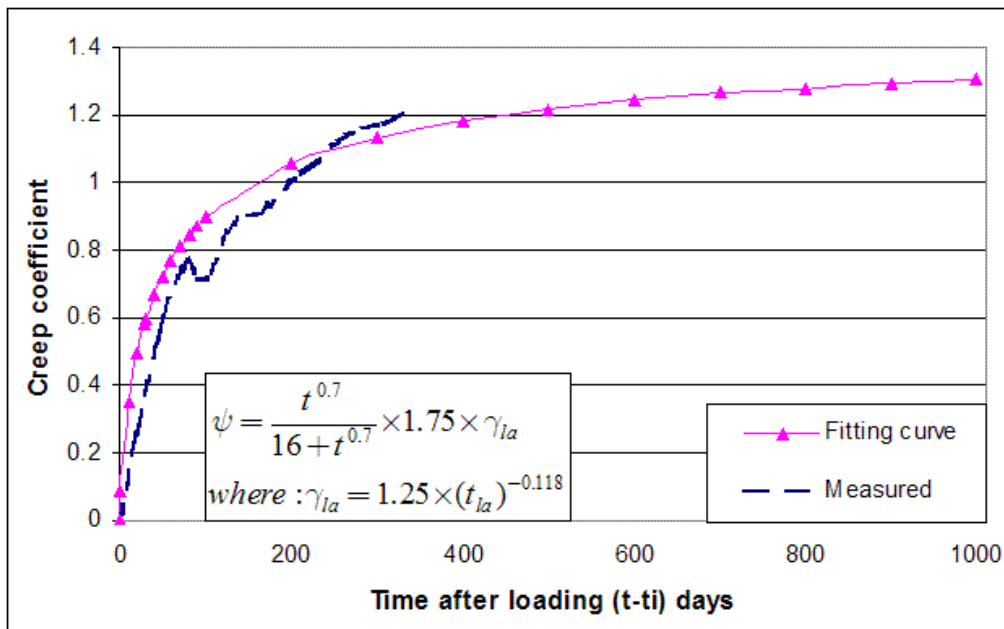


Figure 3. 5 Structural analysis model

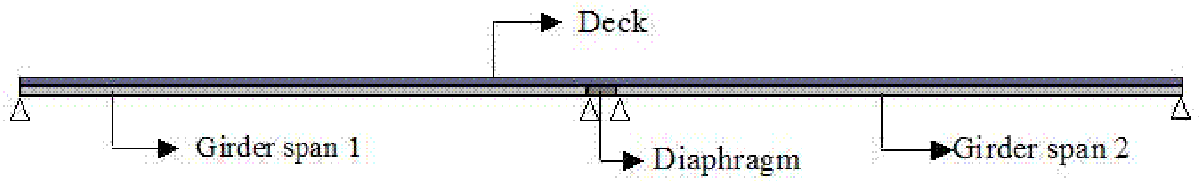


Figure 3. 6 Example 1. IT 700 section properties

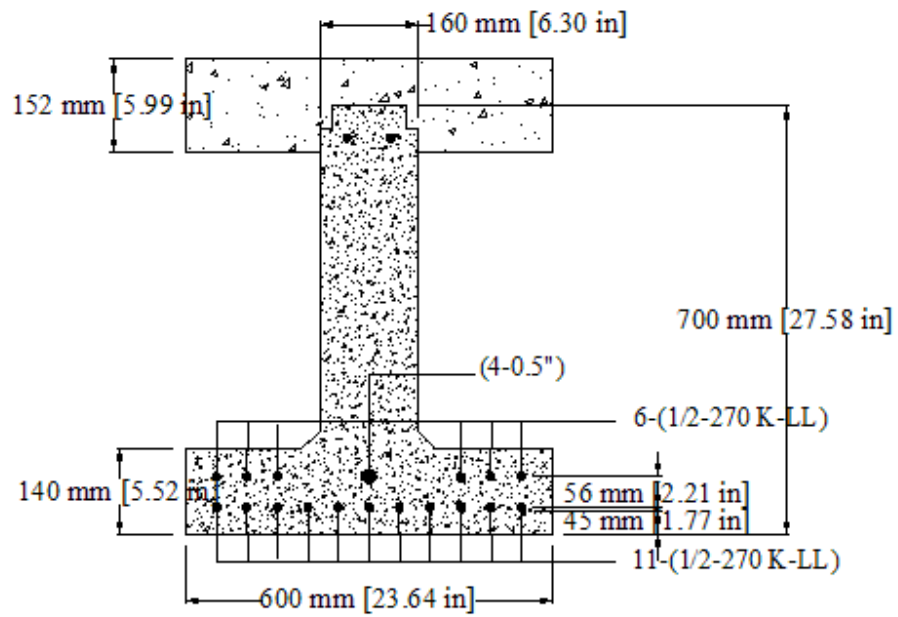


Figure 3. 7 Example 1. beam layout

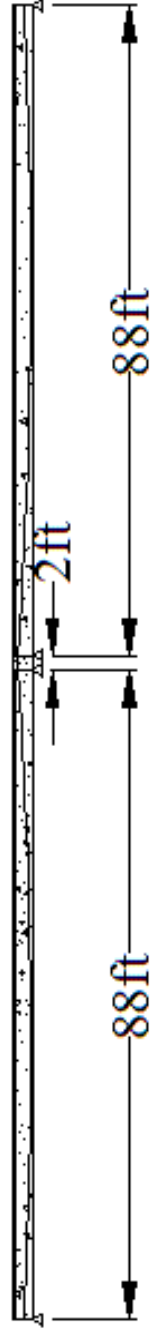


Figure 3. 8 Post-tensioning tendons profile

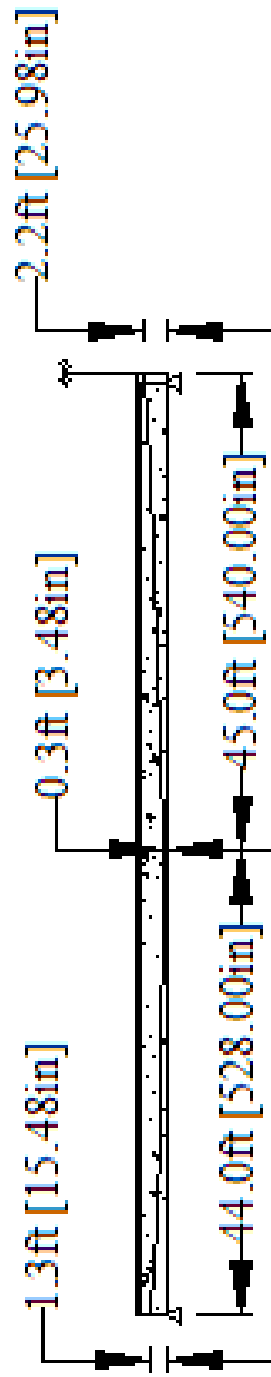


Figure 3. 9 Example 1-PT-IT front page

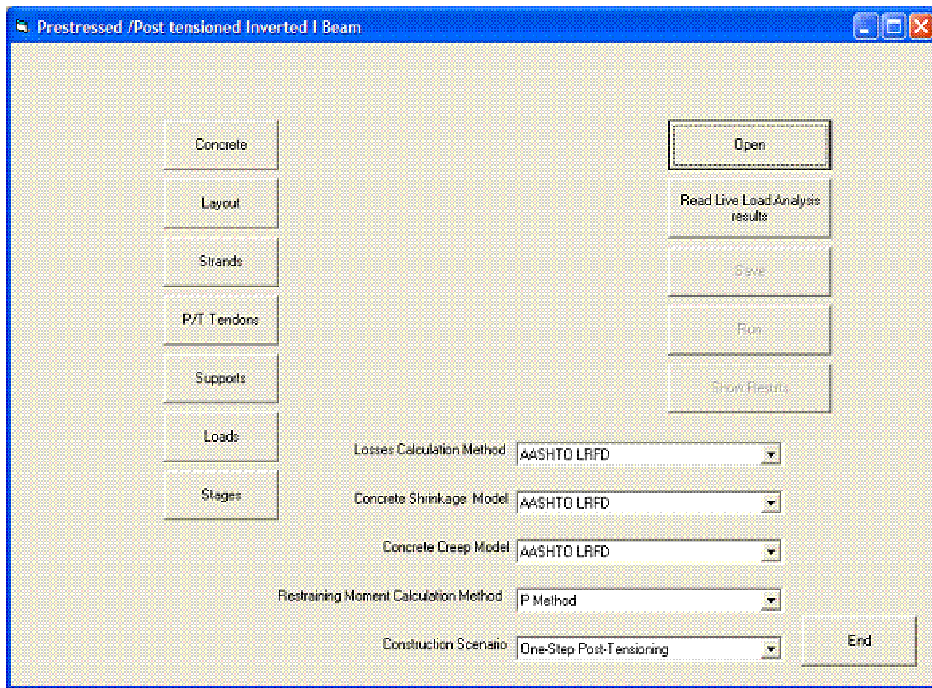


Figure 3. 10 Example 1-concrete properties form

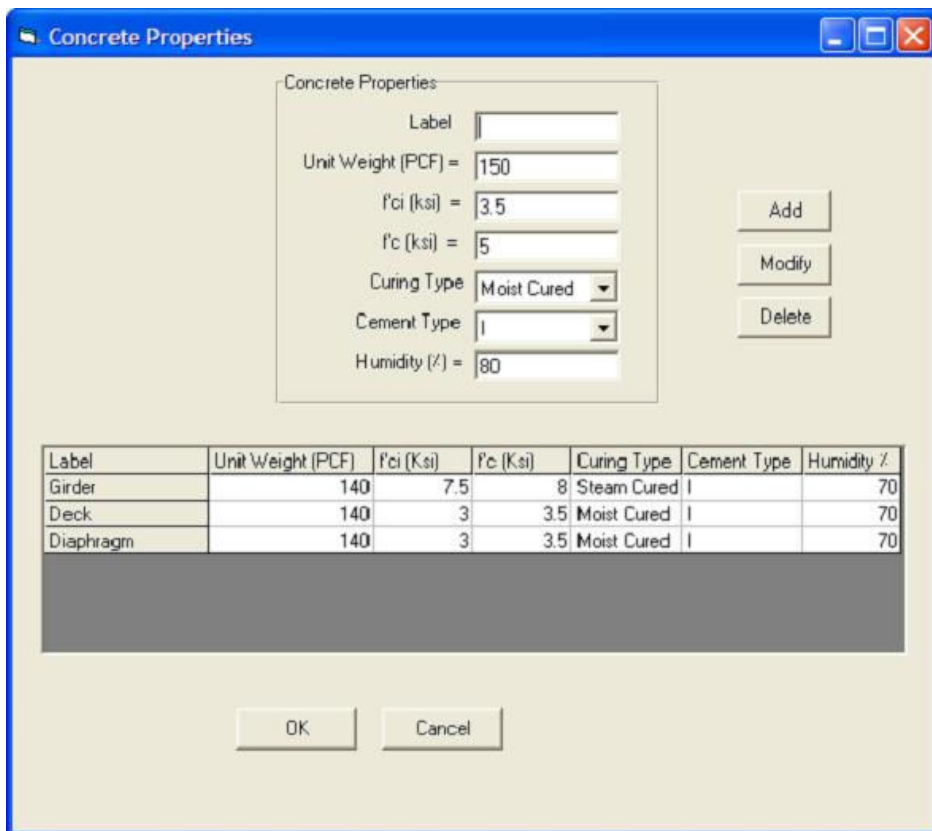


Figure 3. 11 Example 1-beam layout

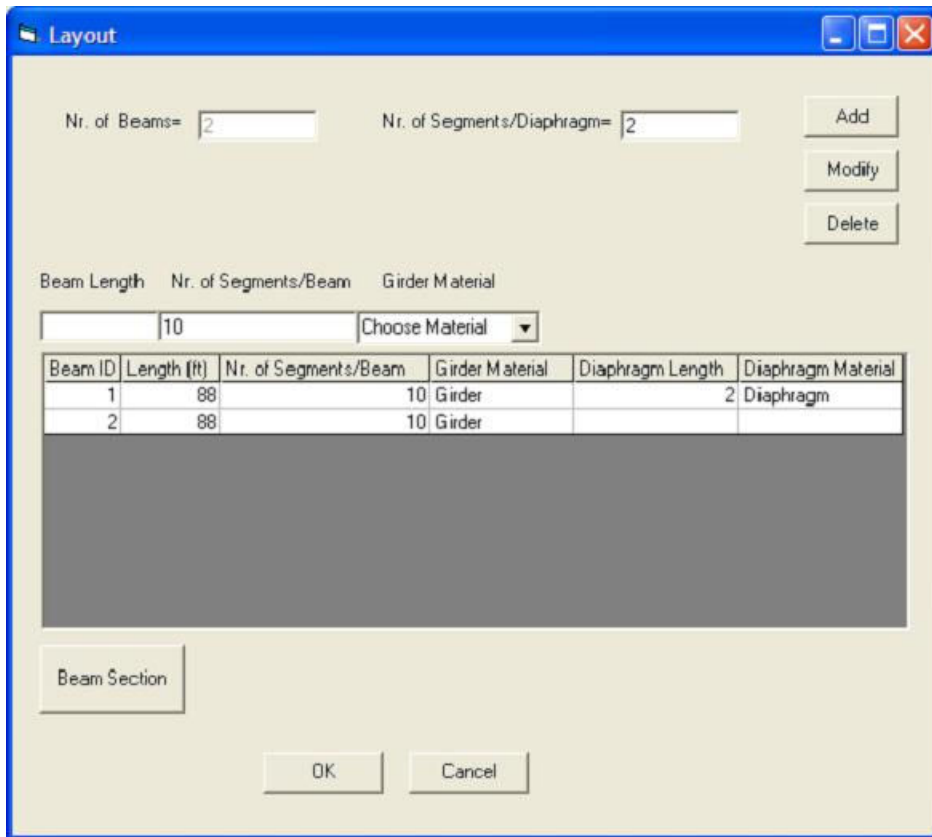


Figure 3. 12 Example 1-section properties

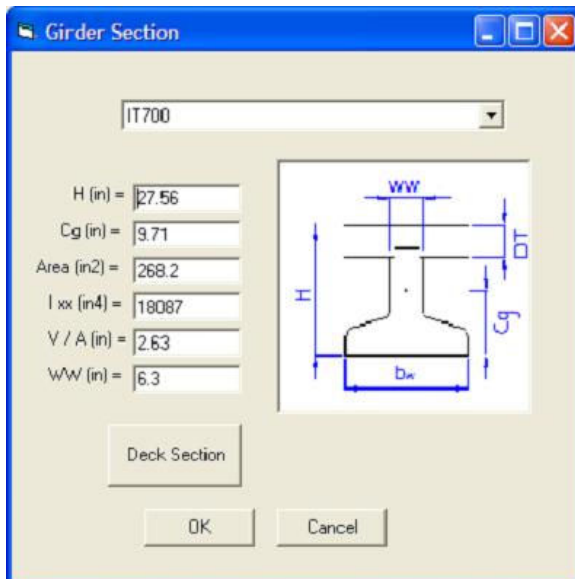


Figure 3. 13 Example 1-deck dimensions and material

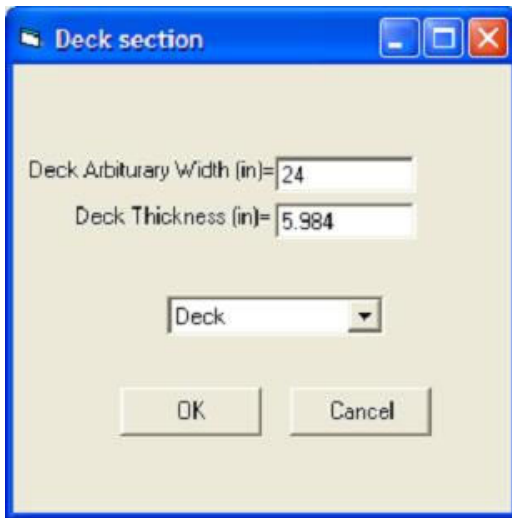


Figure 3. 14 Example 1-strands properties

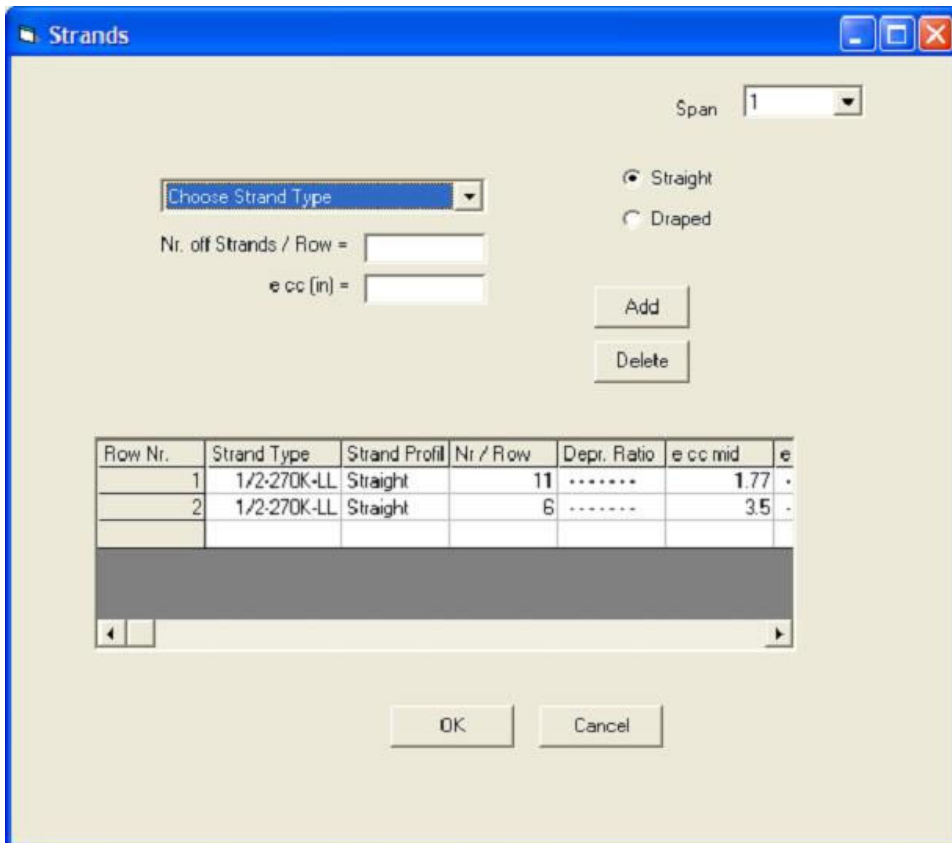


Figure 3. 15 Example 1-post-tensioned tendons

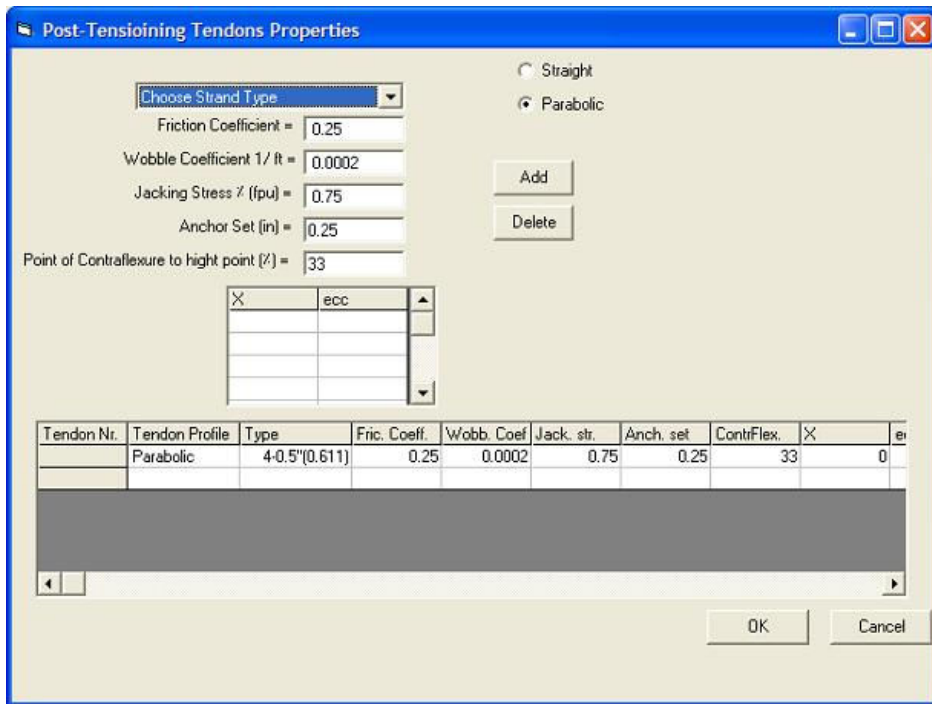


Figure 3. 16 Example 1-supports

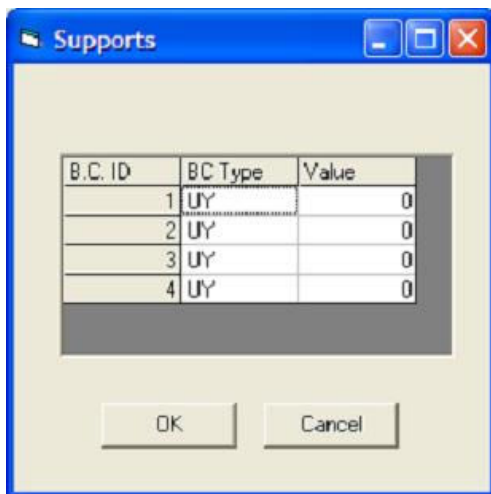


Figure 3. 17 Example 1-externally applied loads

Nr. of Applied Loads =

Load Type =

Magnitude(Kip.ft) =

Nr. of Elements under loading =

Load ID	Load Type	q or p	Elem. Nr.(C)	Left Dist.(C)	1	2
2	U	0.061	-----	-----	1	2

Buttons: Add, Delete, OK, Cancel

Figure 3. 18 Example 1-staging

Nr. of stages =

Stage Properties:

Stage Description =

Elements in the System at this stage =

Time (Days) =

External Load Nr. (If Applicable) =

Buttons: Modify, Add, Delete, OK, Cancel

St. Nr.	Stage Description	Elements in the System at this Stage	Time (Days)	Ext. Loads
		Prestressed Precast Beam	1	0
		Prestressed Precast Beam	10	0
		Prestressed Precast Beam	55.9	0
		Prestressed Precast Beam + Deck	56	0
		Prestressed Precast Beam + Deck	56.1	0
		Prestressed Precast Beam + Deck	72.9	0
		Prestressed Precast Beam + Deck + Post-Tensioning	73	0
		Prestressed Precast Beam + Deck + Post-Tensioning	73.1	0
		Prestressed Precast Beam + Deck + Post-Tensioning	76.9	0
		Prestressed Precast Beam + Deck + Post-Tensioning	77	1
		Prestressed Precast Beam + Deck + Post-Tensioning	77.1	0
		Prestressed Precast Beam + Deck + Post-Tensioning	86.9	0
		Prestressed Precast Beam + Deck + Post-Tensioning	87	Live Load

Figure 3. 19 Example 1-stress in prestressed strands along the bridge

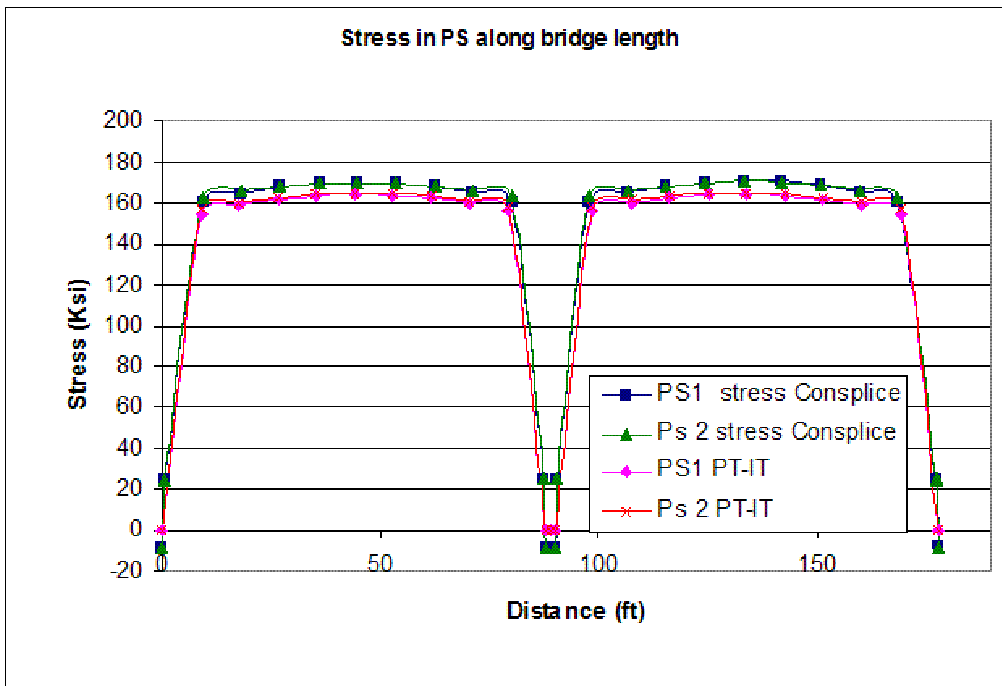


Figure 3. 20 Example 1-stress in post-tensioned tendons along the bridge

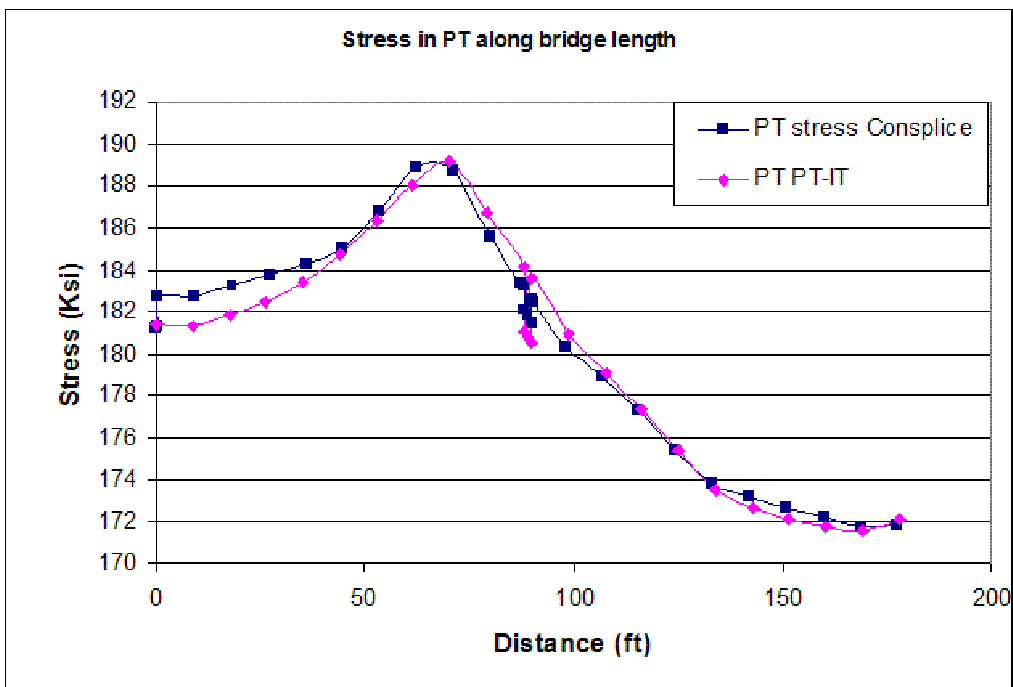


Figure 3. 21 Example 1-moments resulting from girder and deck weight

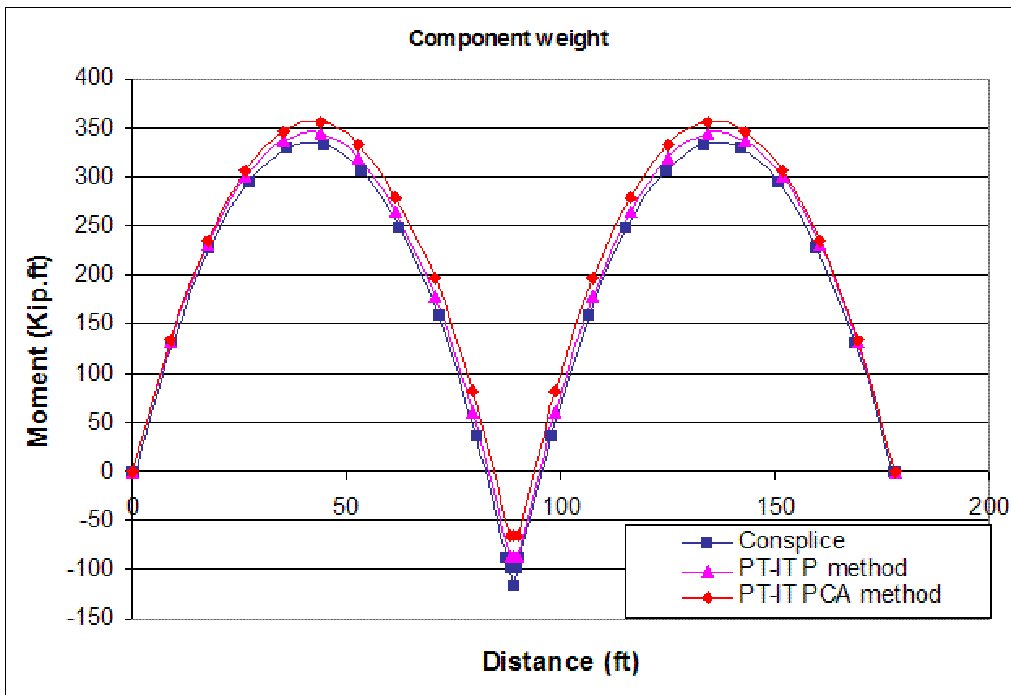


Figure 3. 22 Example 1-moments resulting from prestressing forces

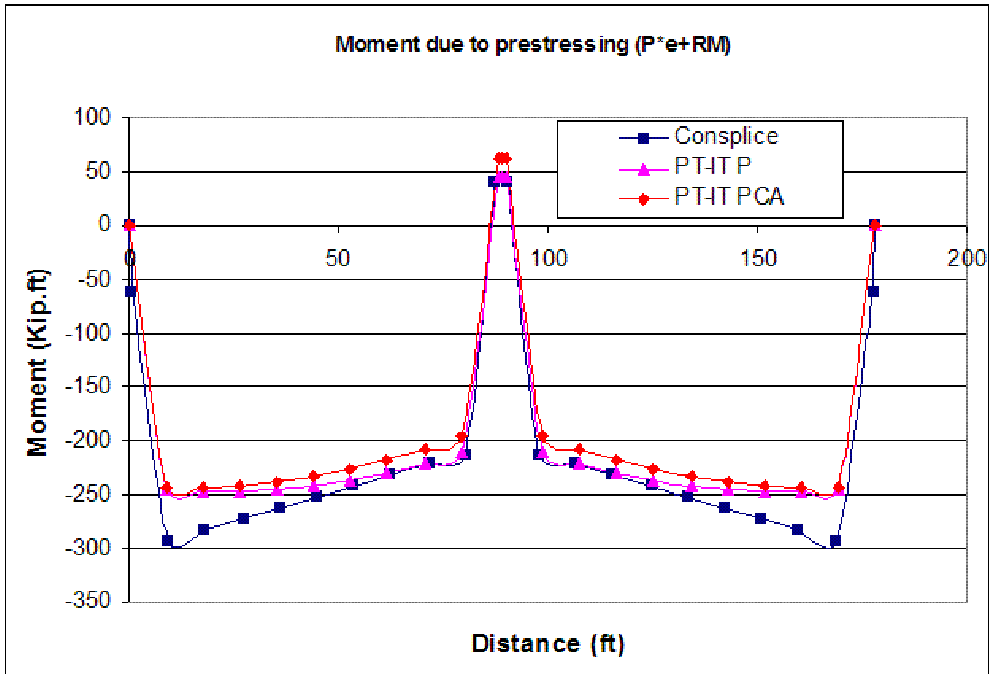


Figure 3. 23 Example 1-moments due to post-tensioning forces

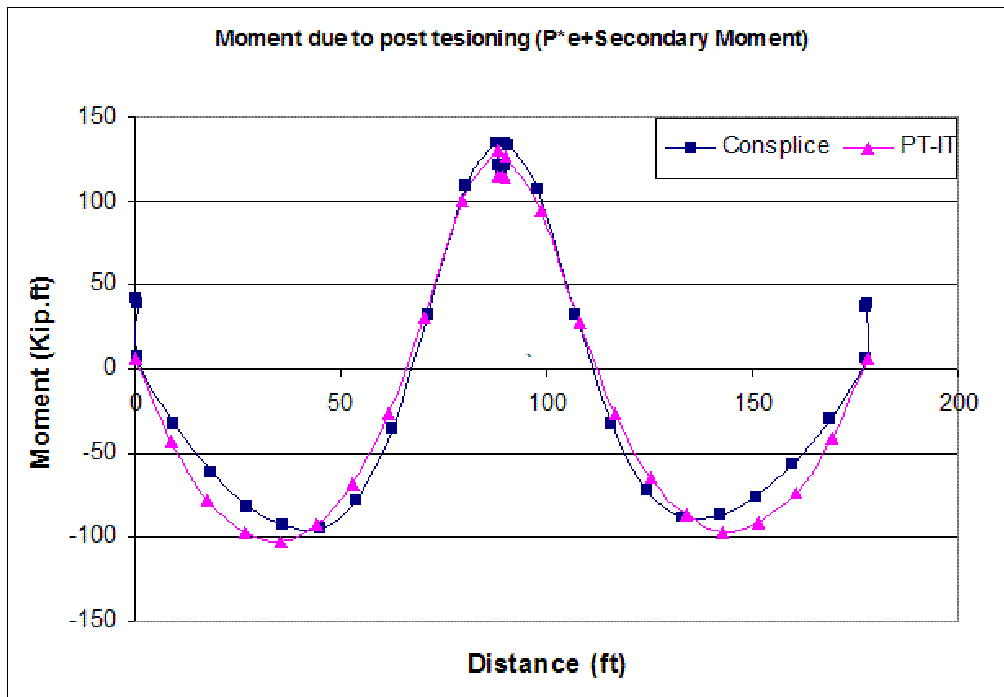


Figure 3. 24 Example 1-moments resulting from differential shrinkage between deck and girder

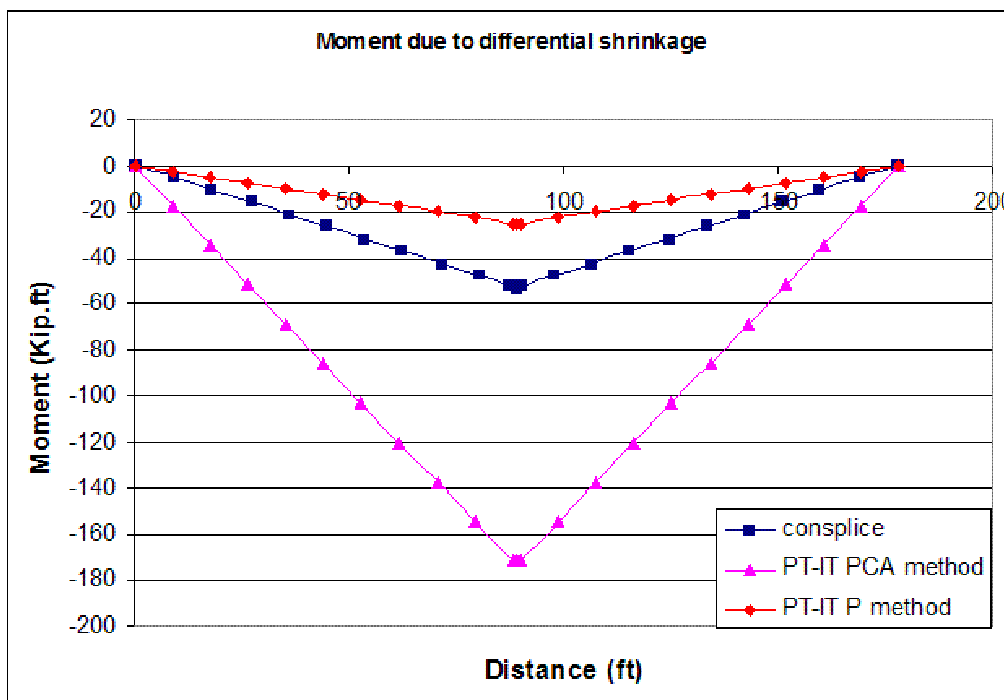


Figure 3. 25 Example 1-moments resulting from barrier weight

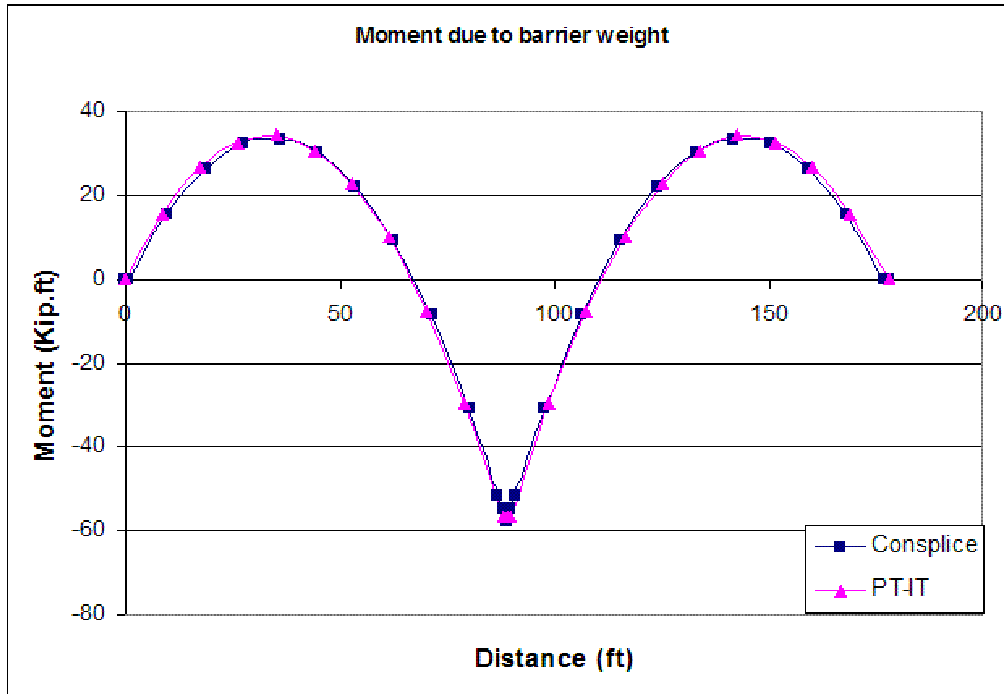


Figure 3. 26 Example 1-positive moments due to lane load

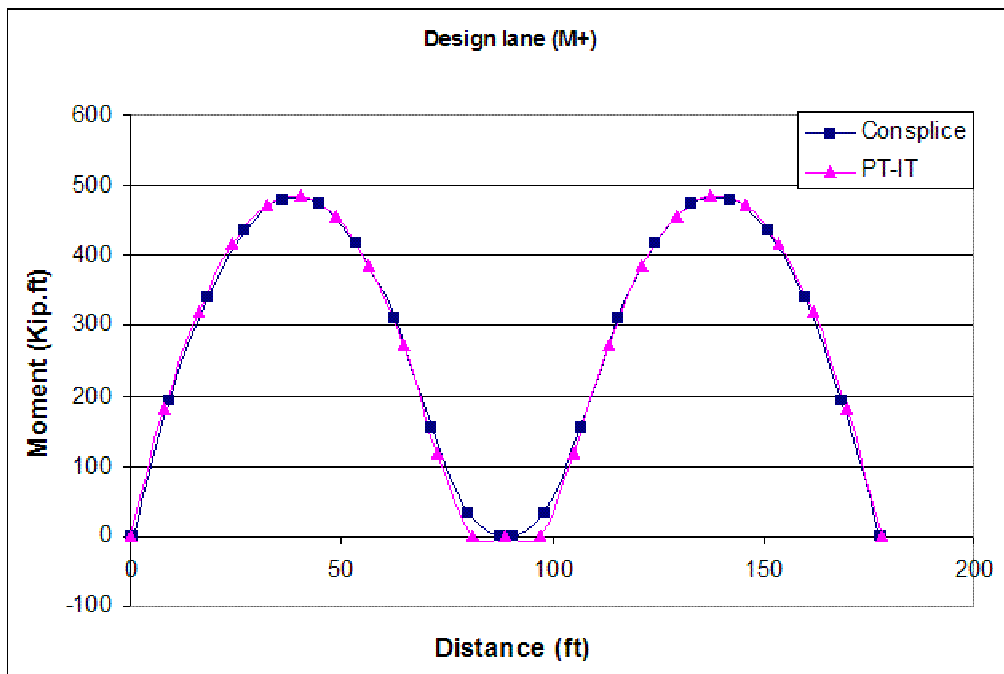


Figure 3. 27 Example 1-negative moments due to lane load

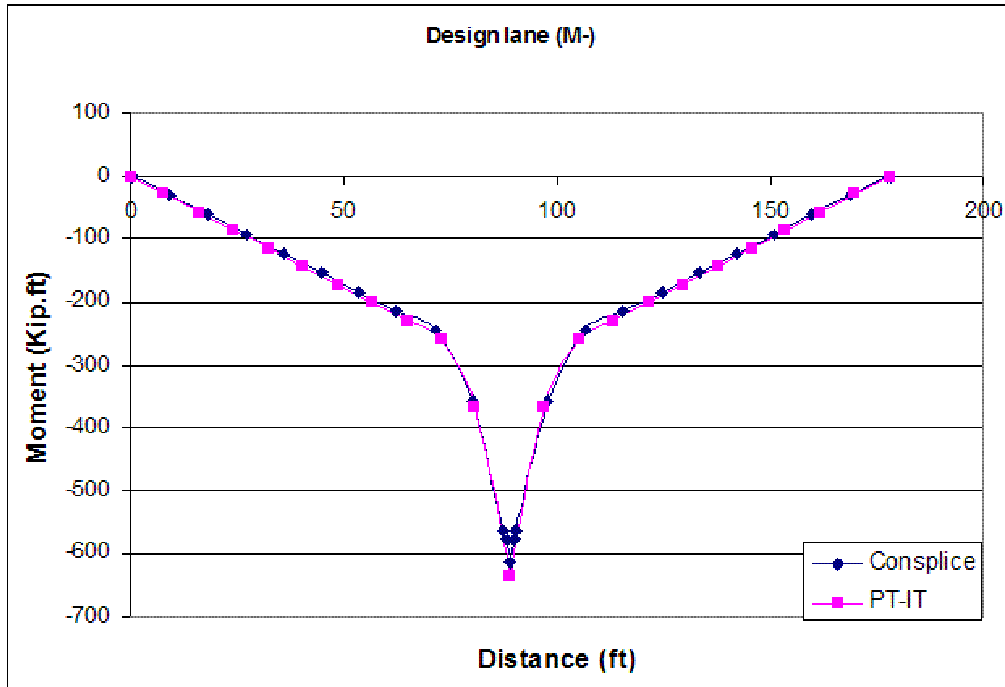


Figure 3. 28 Example 1-positive moments due to design tandem

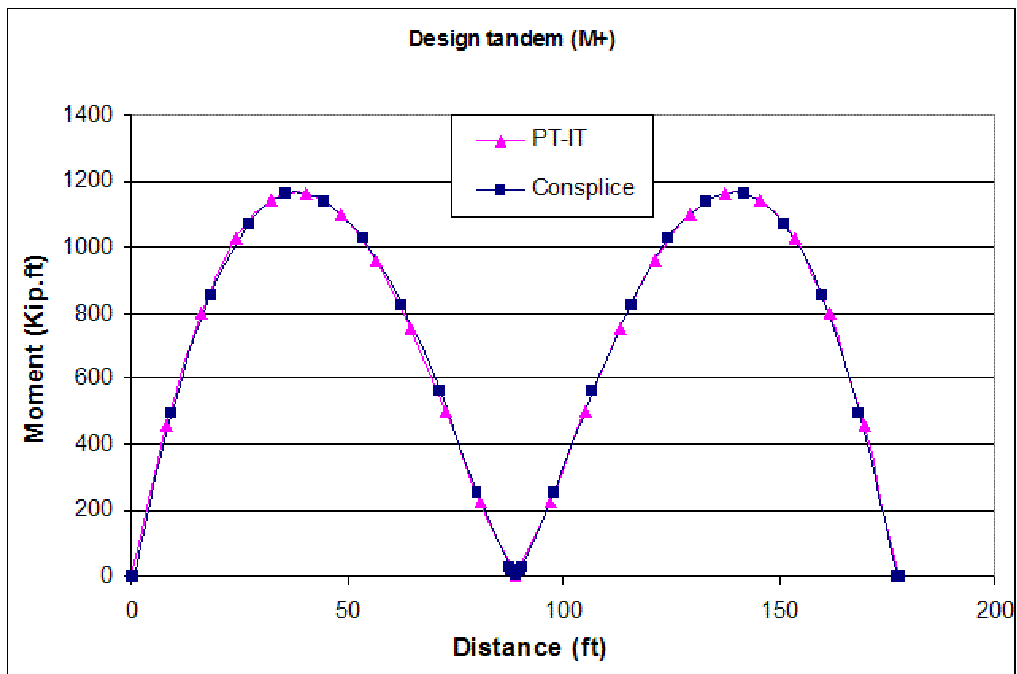


Figure 3. 29 Example 1-negative moments due to design tandem

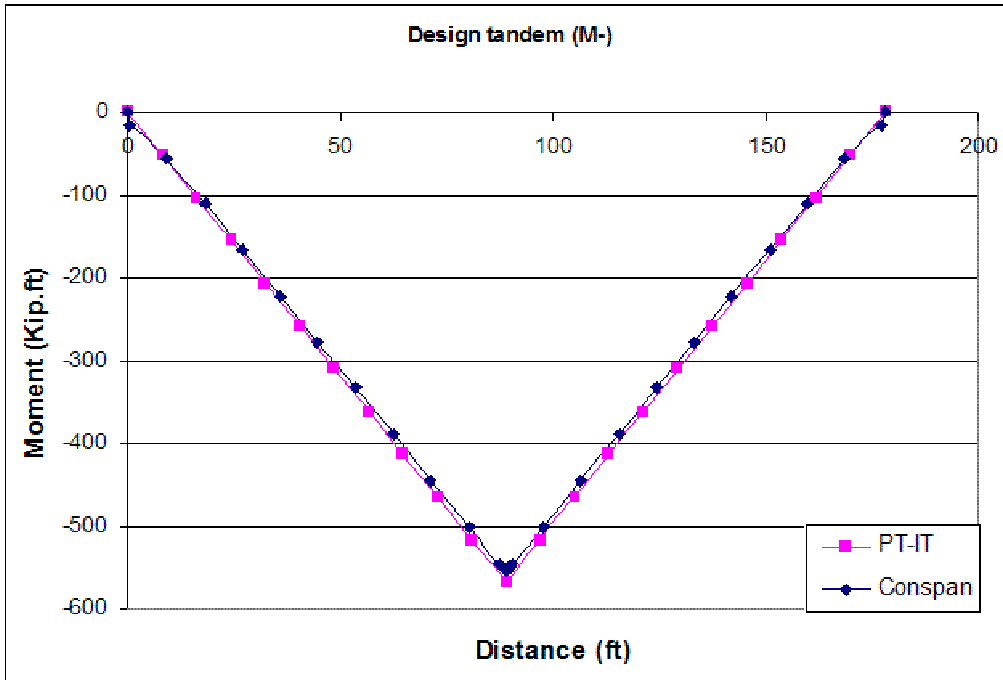


Figure 3. 30 Example 1-positive moments due to design truck

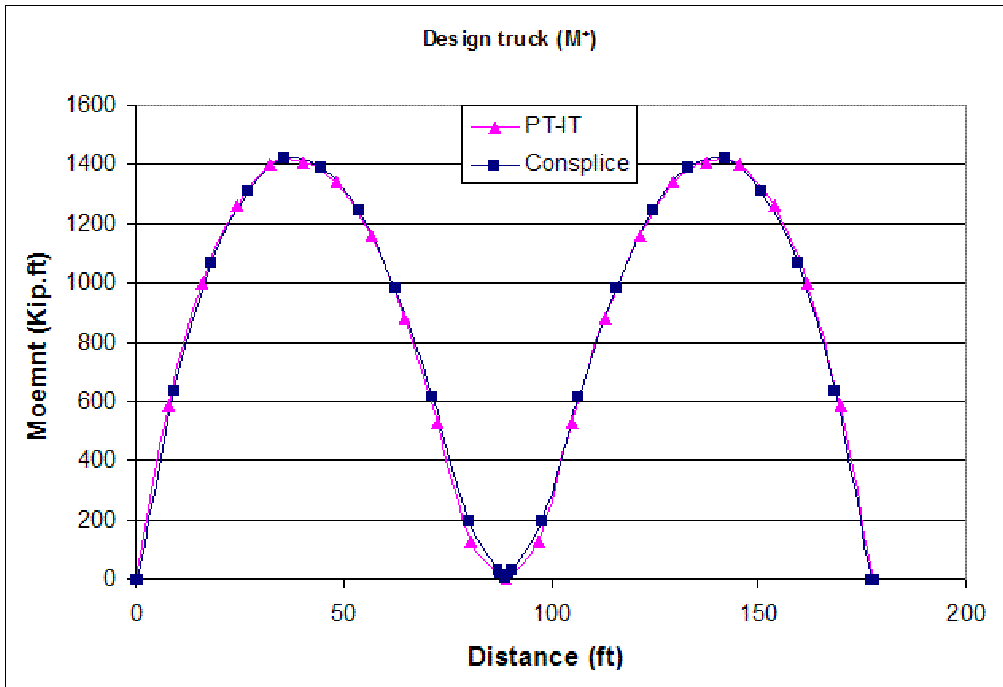


Figure 3. 31 Example 1-Negative moments due to design truck

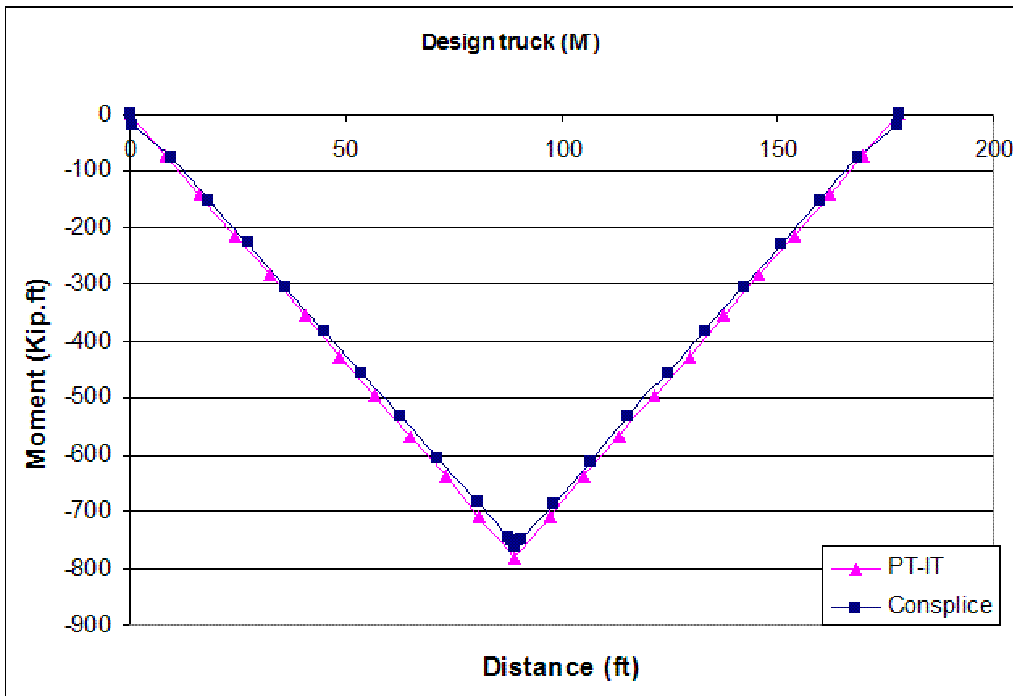


Figure 3. 32 Example 1-Negative moments due to double tandem

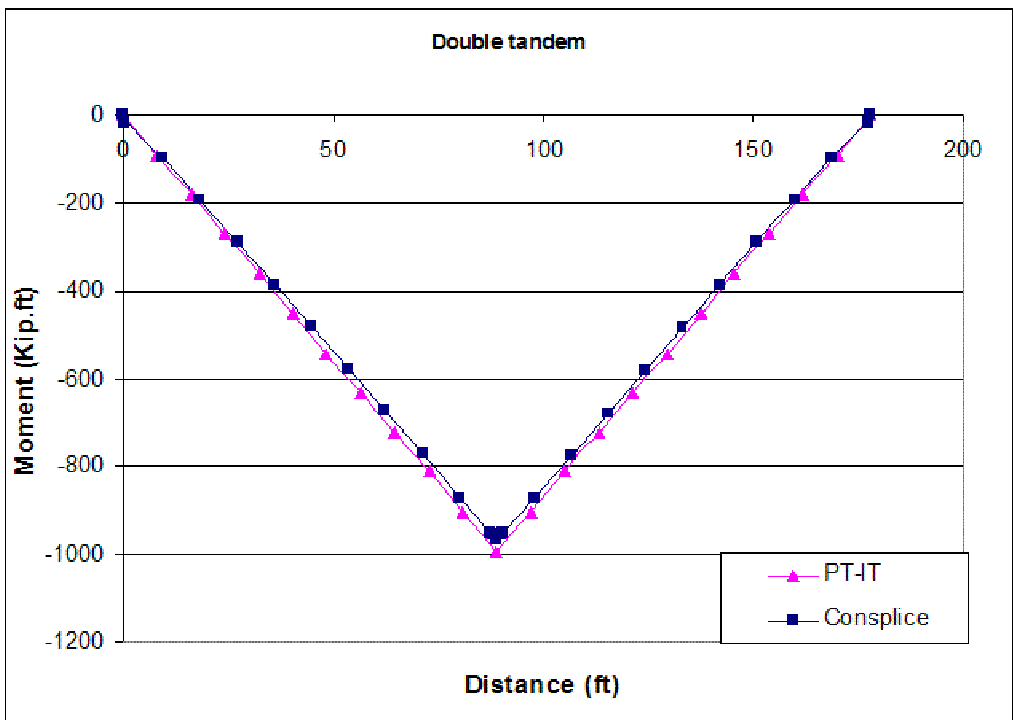


Figure 3. 33 Example 1-Negative moments due to double truck

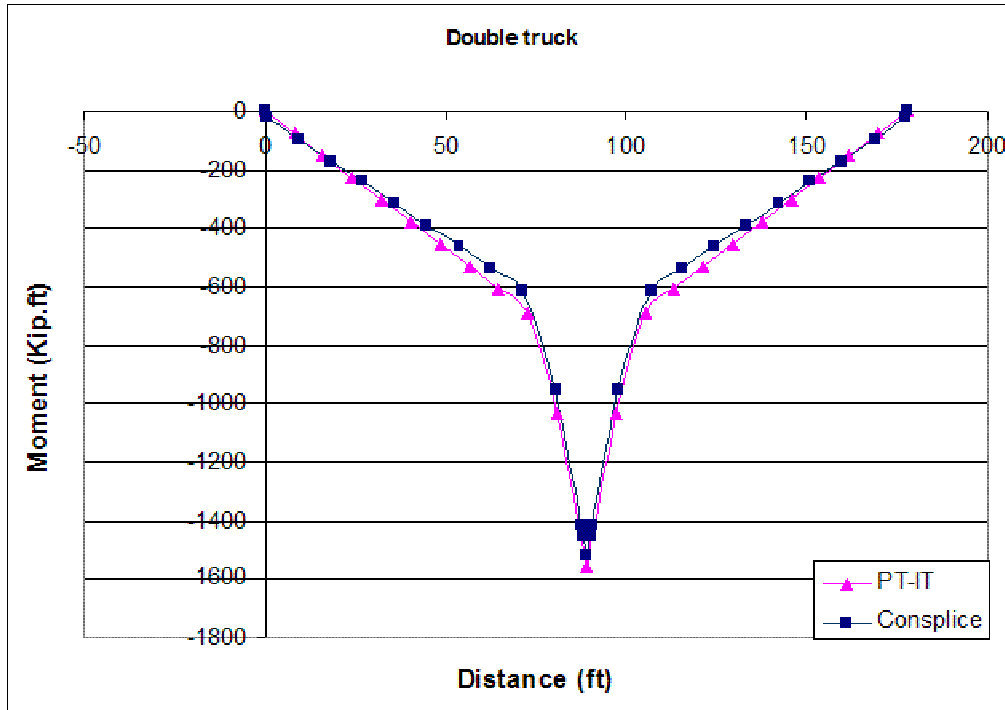


Figure 3. 34 Example 1-HL-93 Positive moment

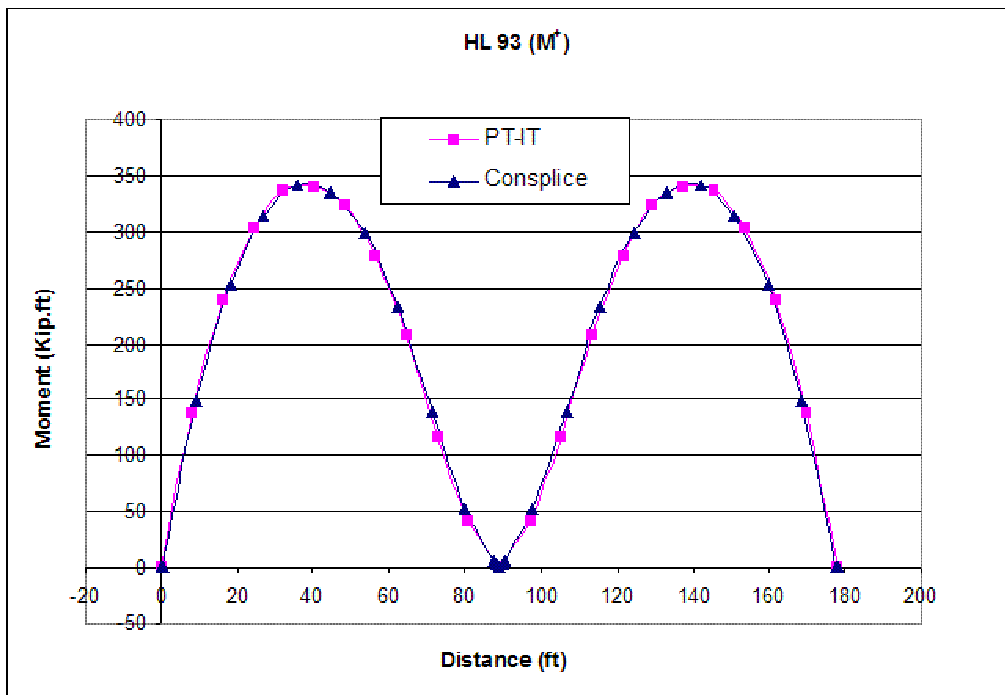


Figure 3. 35 Example 1-HL-93 Negative moment

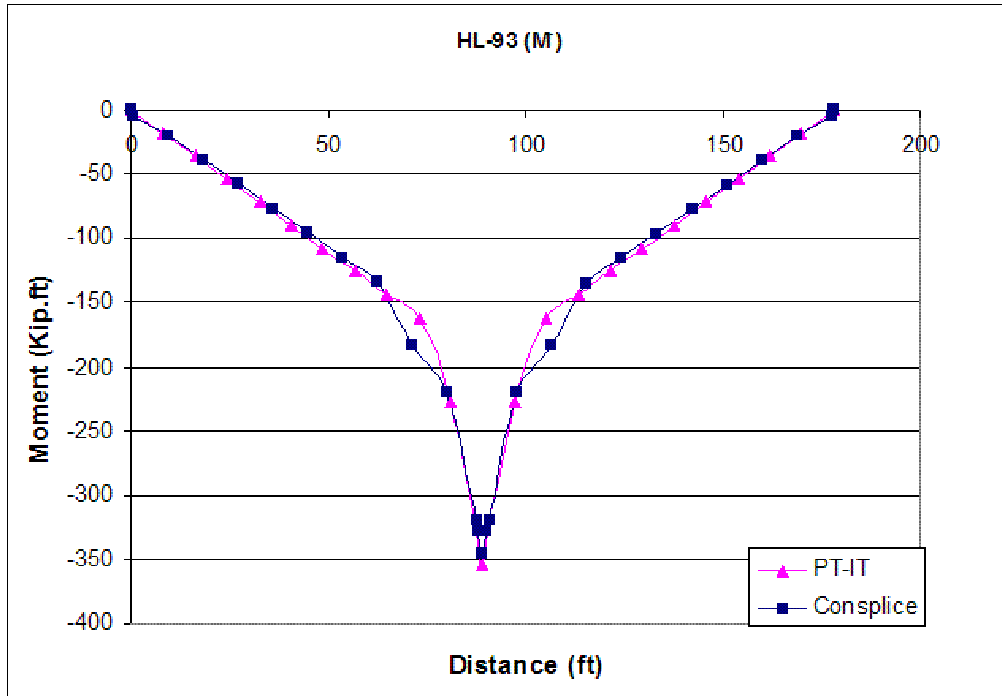


Figure 3. 36 Example 1-Factored required moment

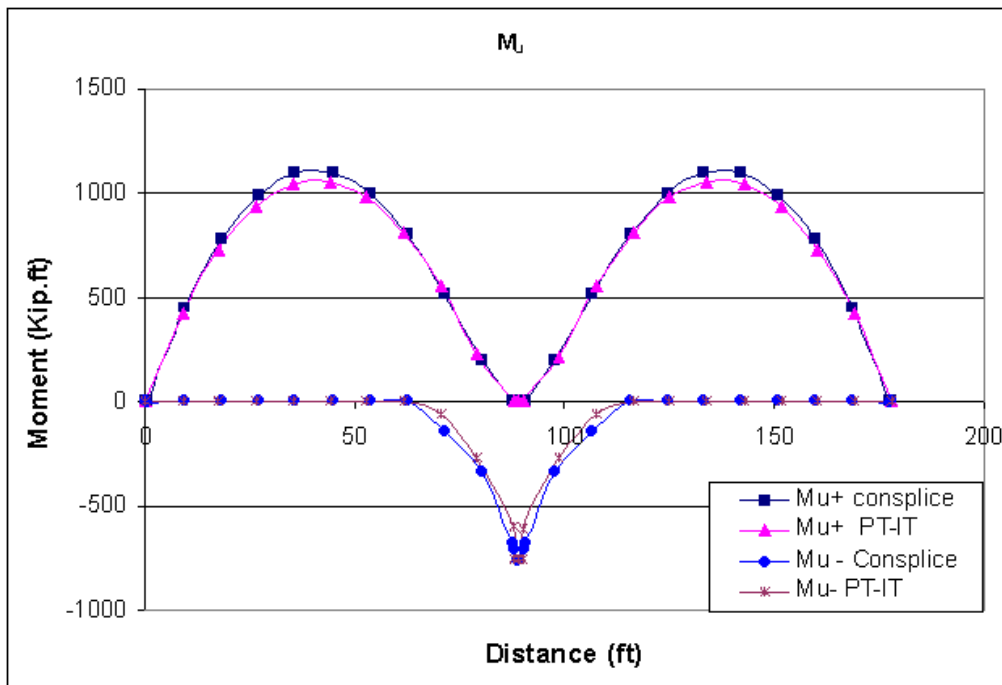


Figure 3. 37 Example 1-(1.2 Times cracking moment)

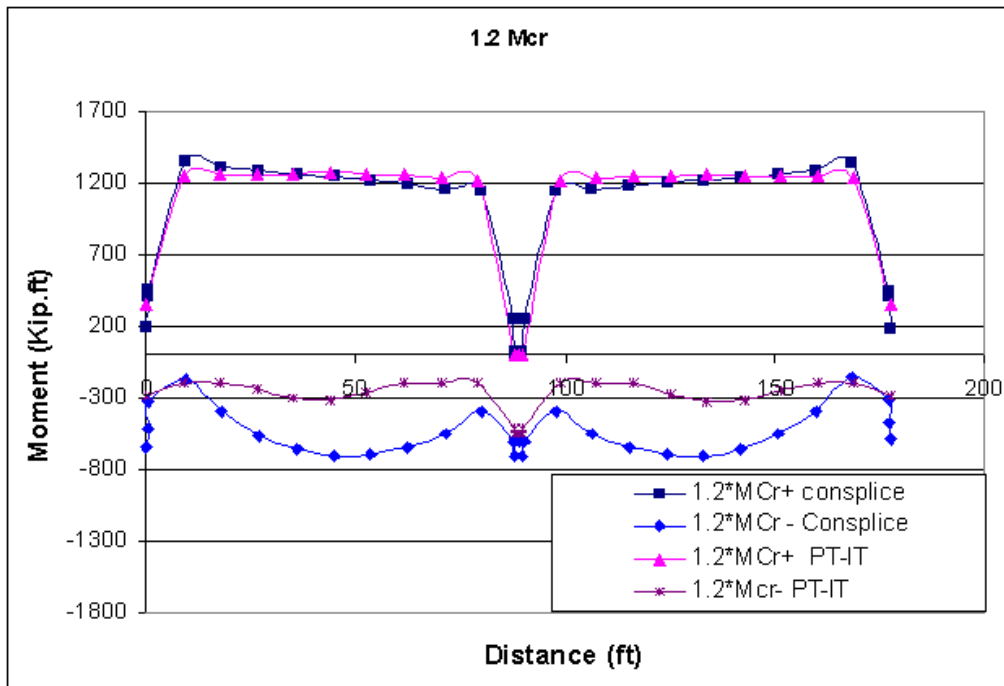


Figure 3. 38 Example 1- ΦM_n (Nominal resistance moment)

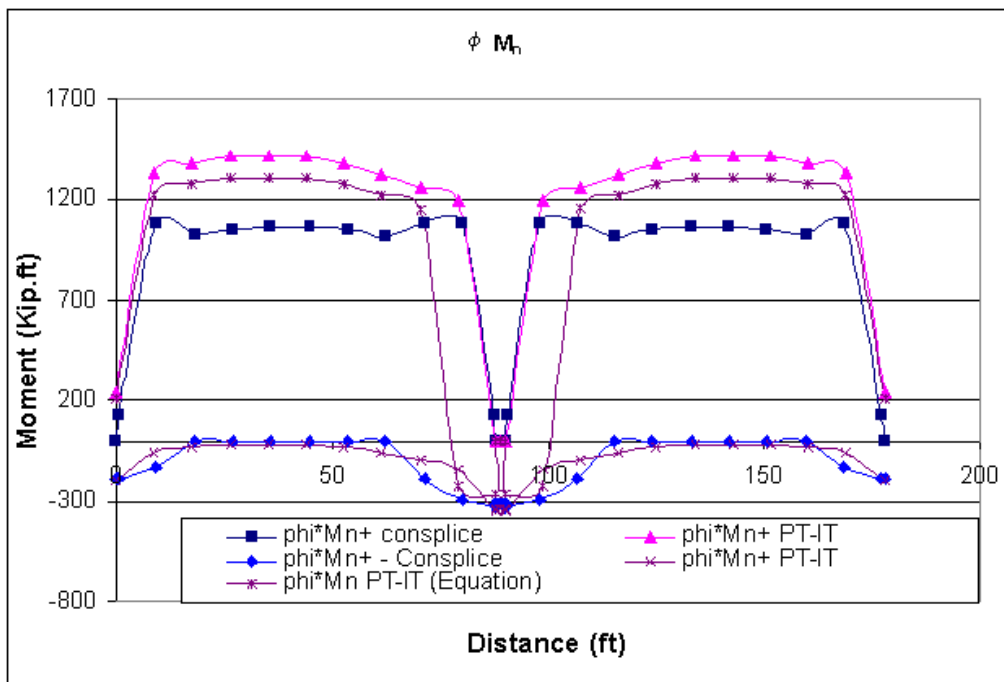


Figure 3. 39 Example 1-Time-dependent deflection due to prestressing

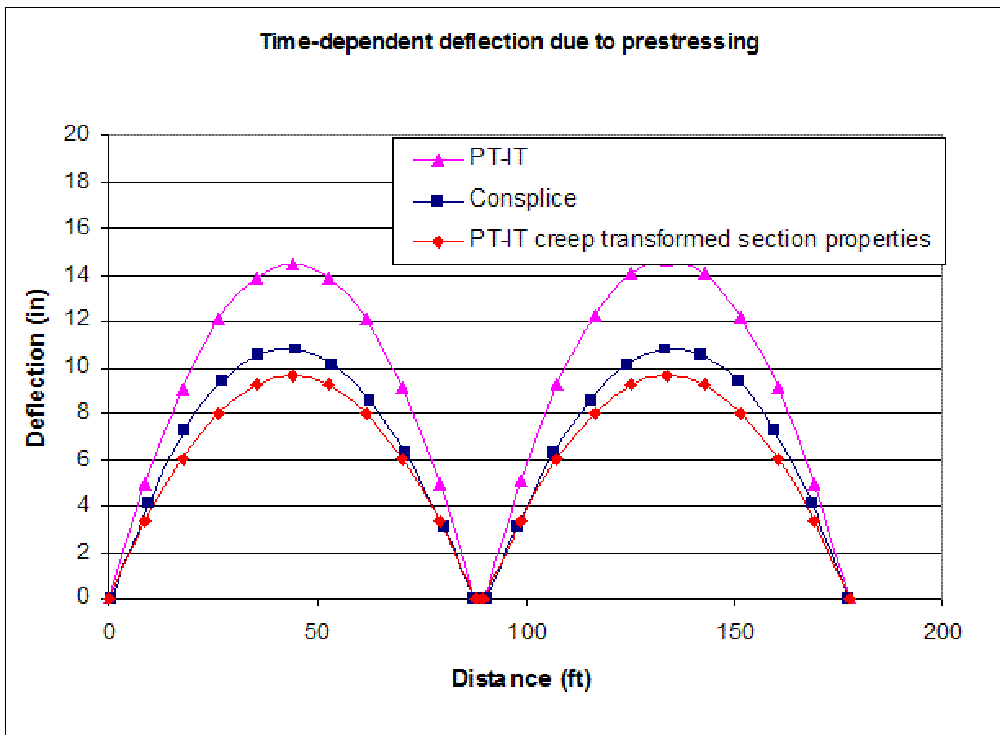


Figure 3. 40 Example 1-Time-dependent deflection due to component weight and shrinkage

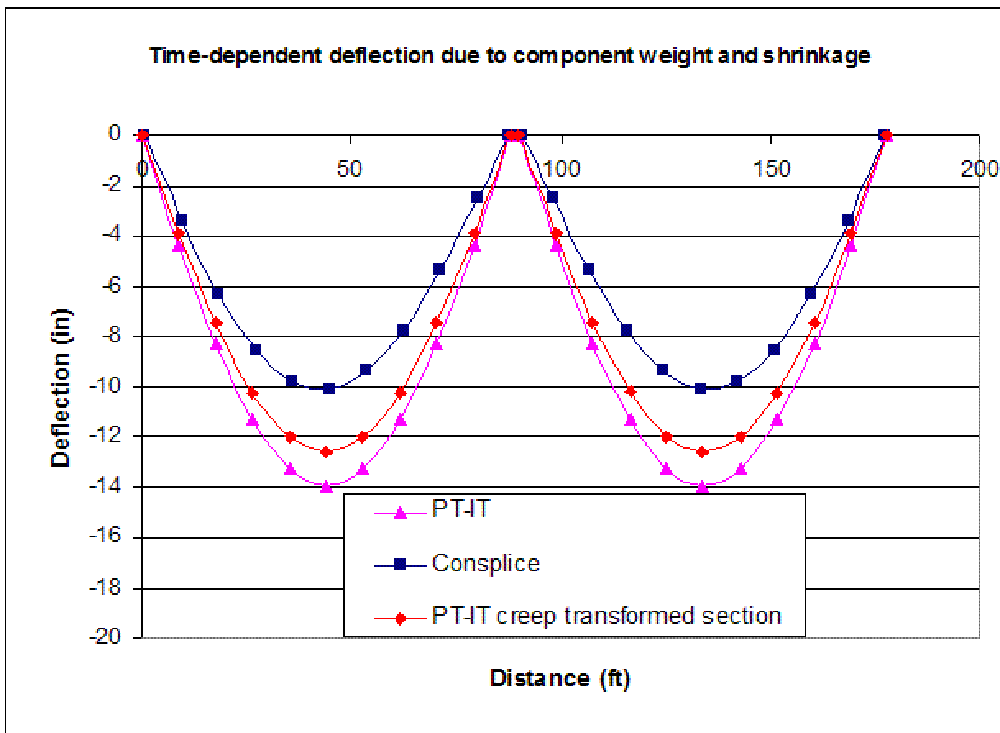


Figure 3. 41 Example 1-Time-dependent deflection due to post-tensioning

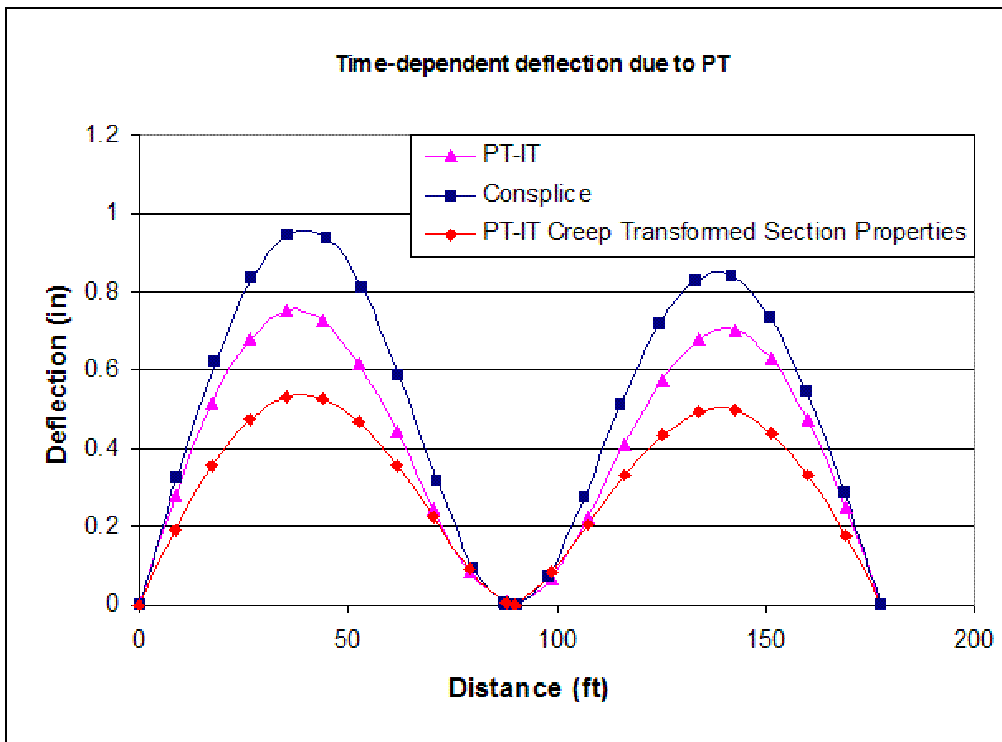


Figure 3. 42 Example 1-Time-dependent deflection due to barriers weight

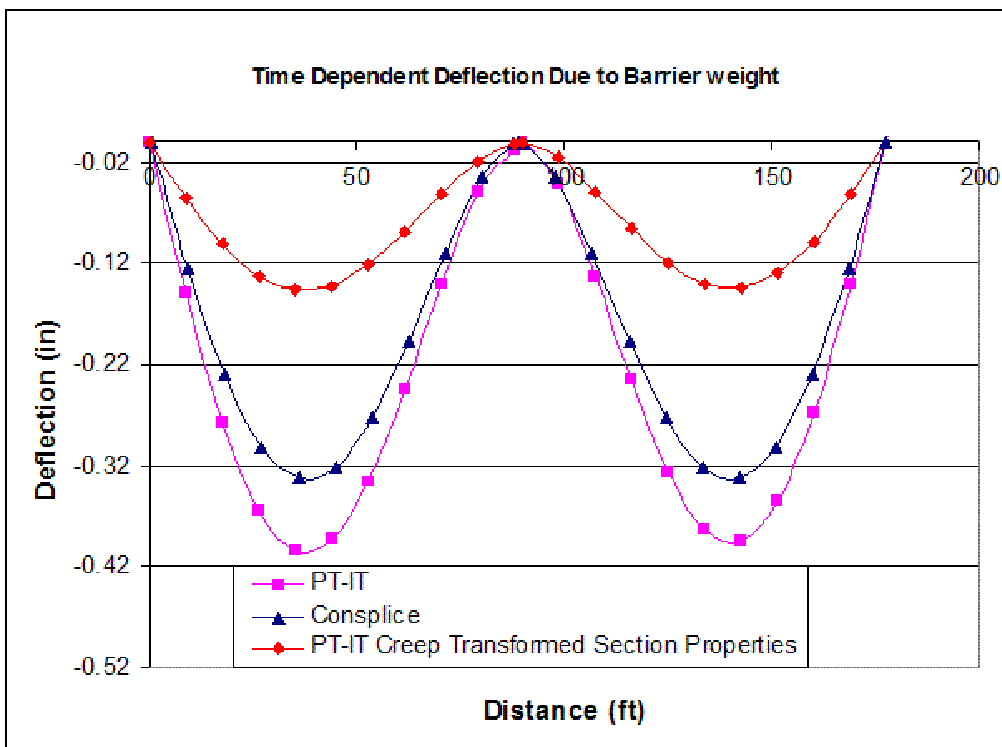


Figure 3. 43 Example 2 IT 500 section properties

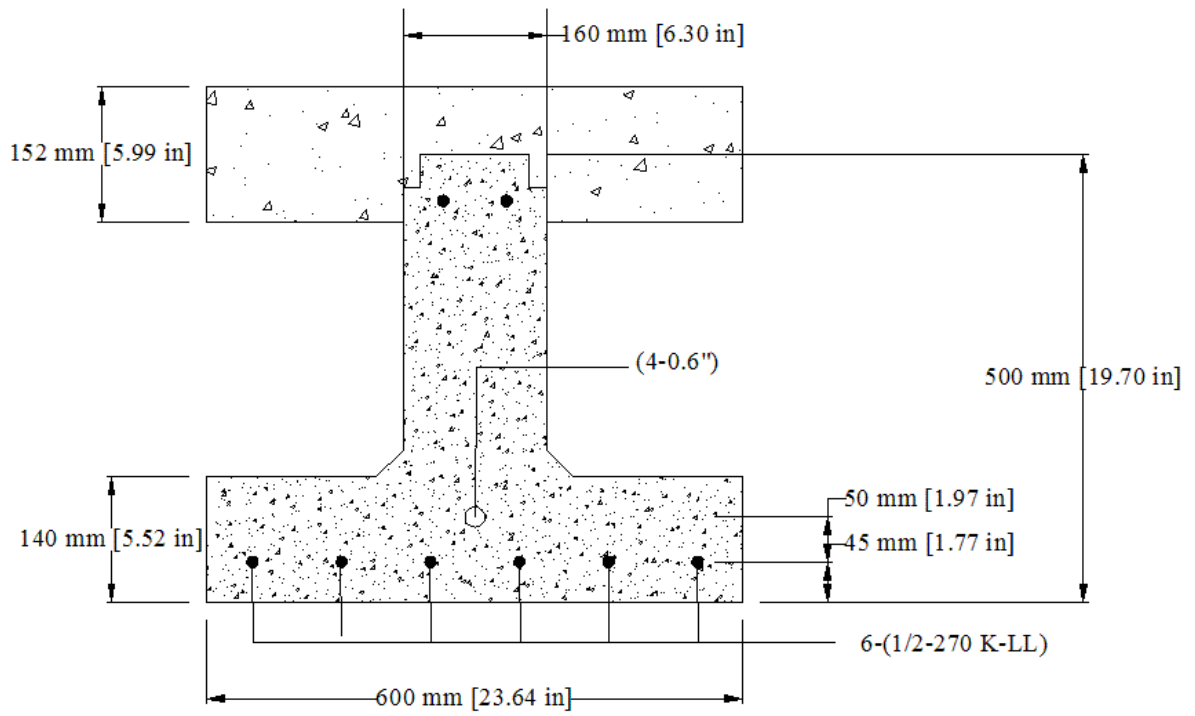


Figure 3. 44 Example 2-Beam layout

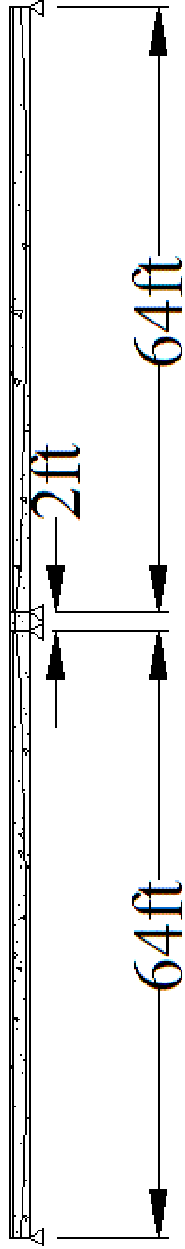


Figure 3. 45 Example 2-Post-tensioning tendons profile

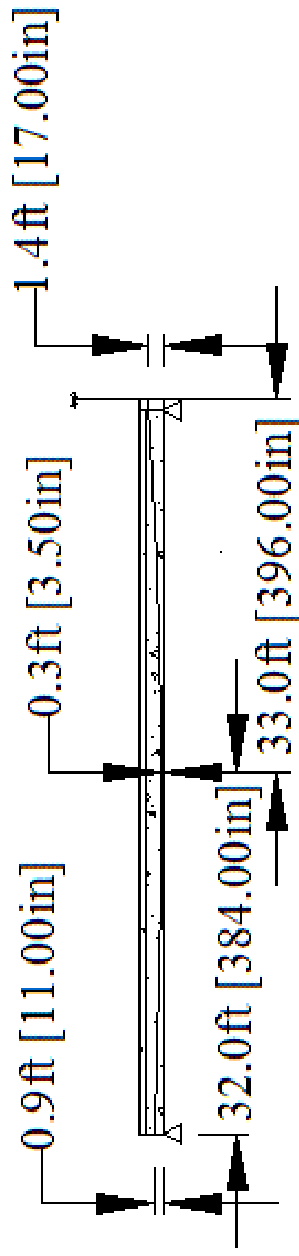


Figure 3. 46 Example 2-Stresses in prestressed strands along the bridge

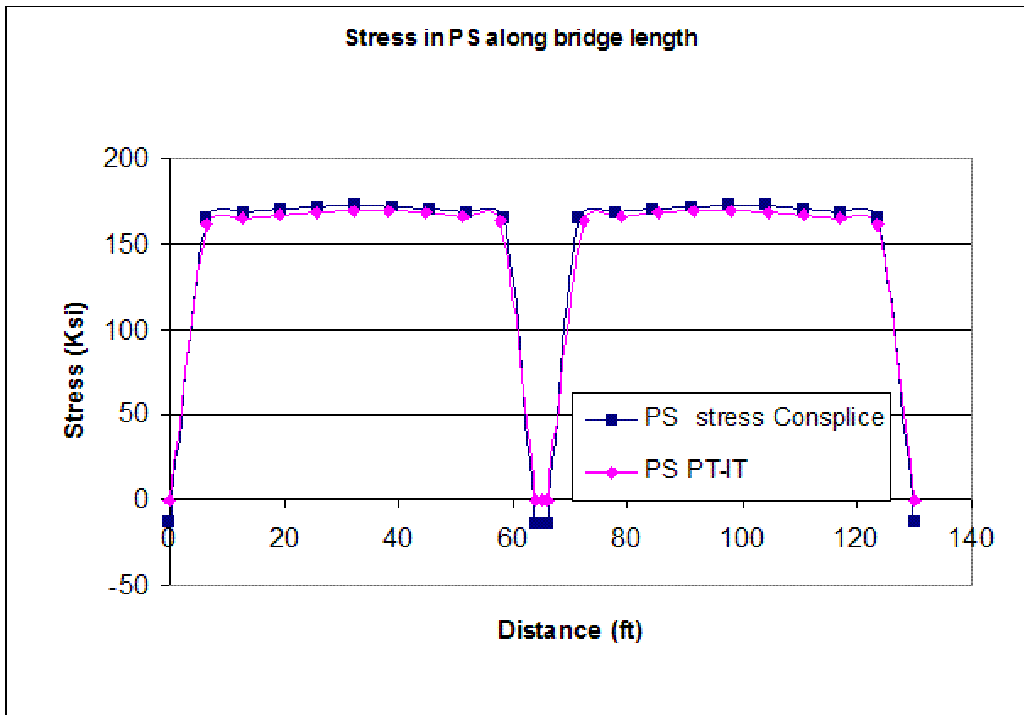


Figure 3. 47 Example 2- Stresses in post-tensioned tendons along the bridge

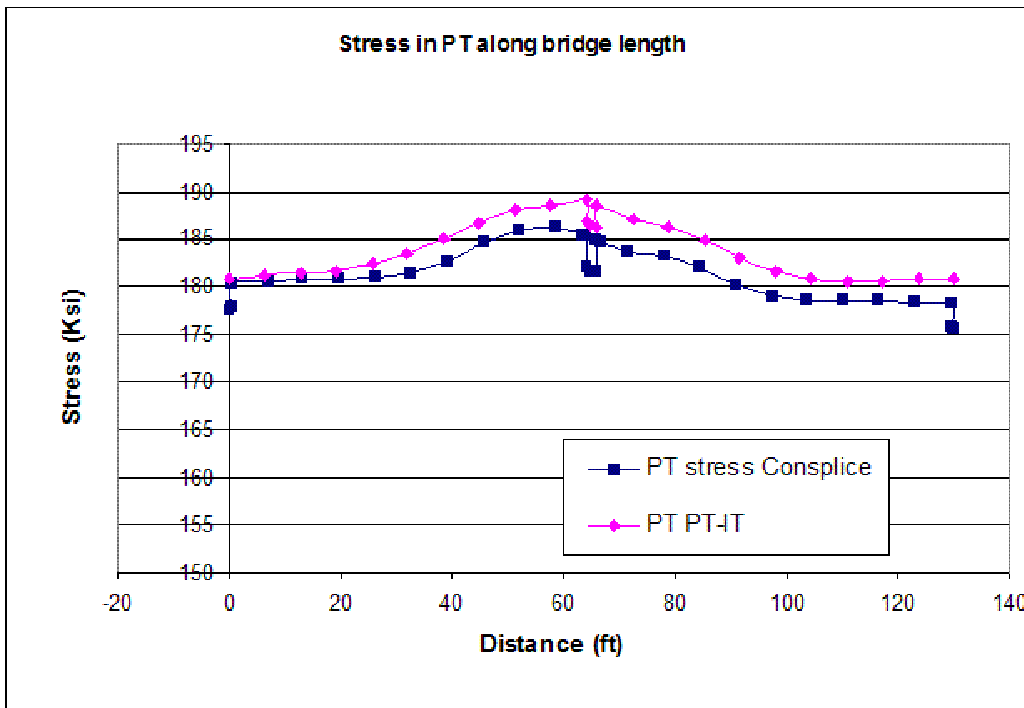


Figure 3. 48 Example 2- Moments resulting from girder and deck weights

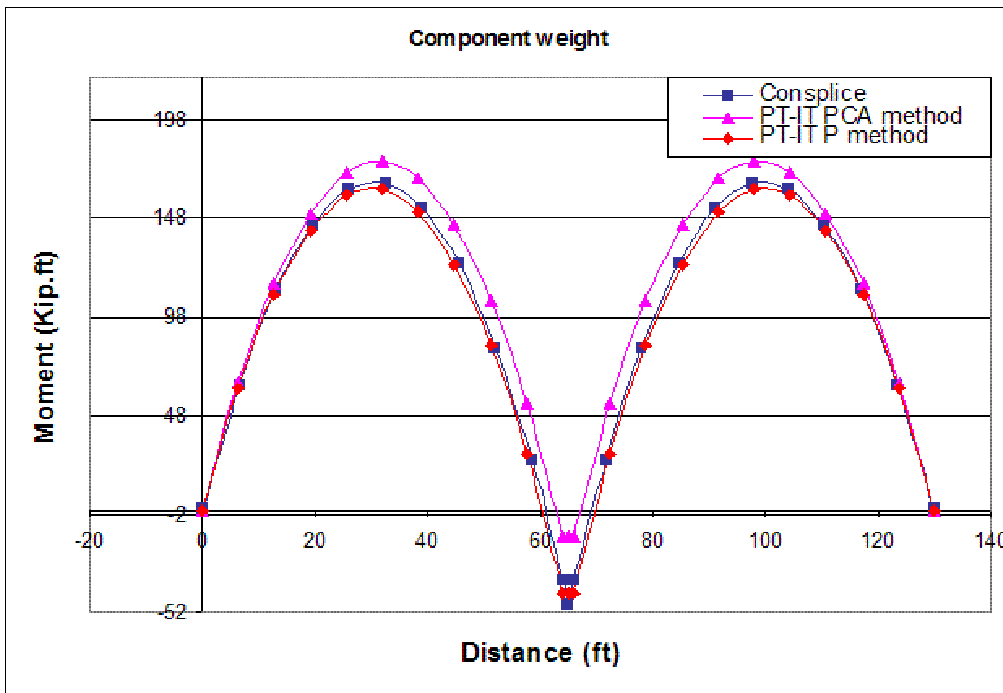


Figure 3. 49 Example 2- Moments resulting from prestressing forces

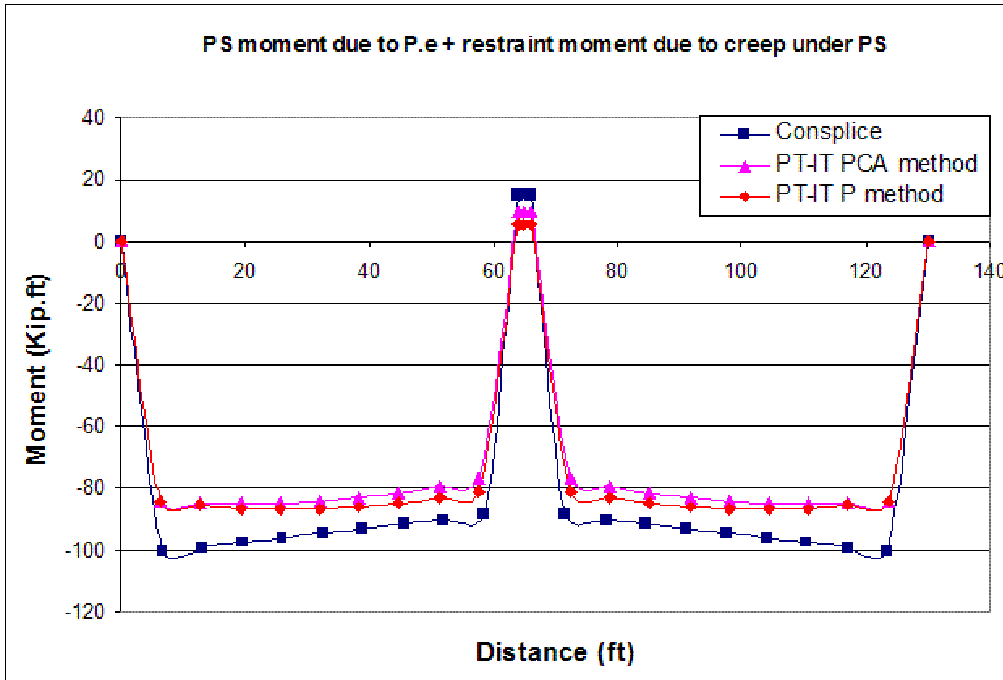


Figure 3. 50 Example 2-Moments due to post-tensioning forces

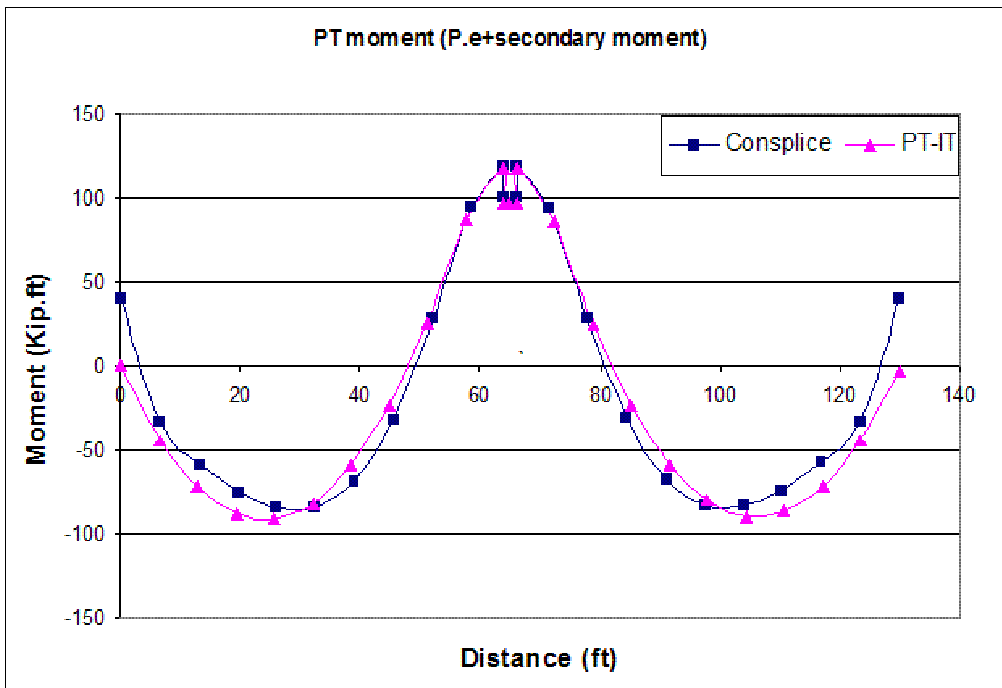


Figure 3. 51 Example 2- Moments resulting from differential shrinkage between deck and girder

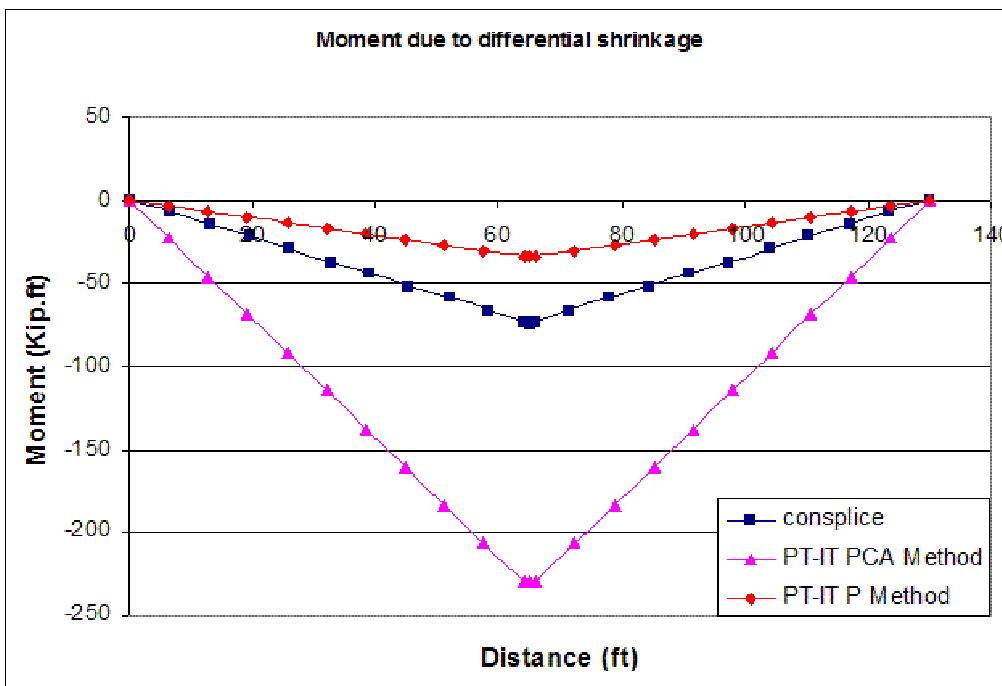


Figure 3. 52 Example 2- Moments resulting from barriers weight

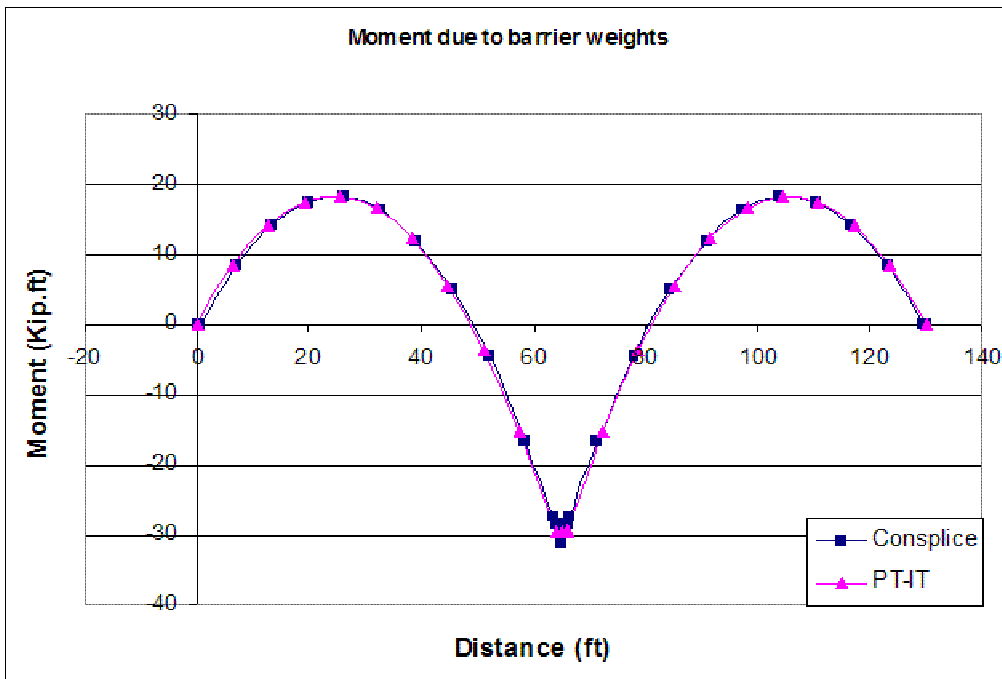


Figure 3. 53 Example 2-HL-93 Positive moment

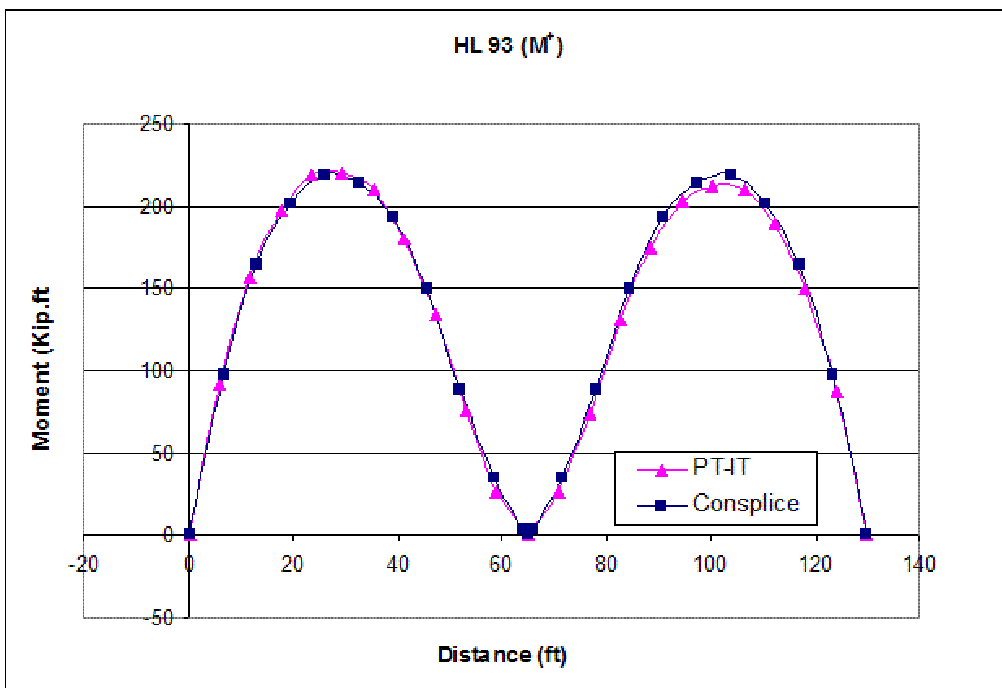


Figure 3. 54 Example 2- HL-93 Negative moment

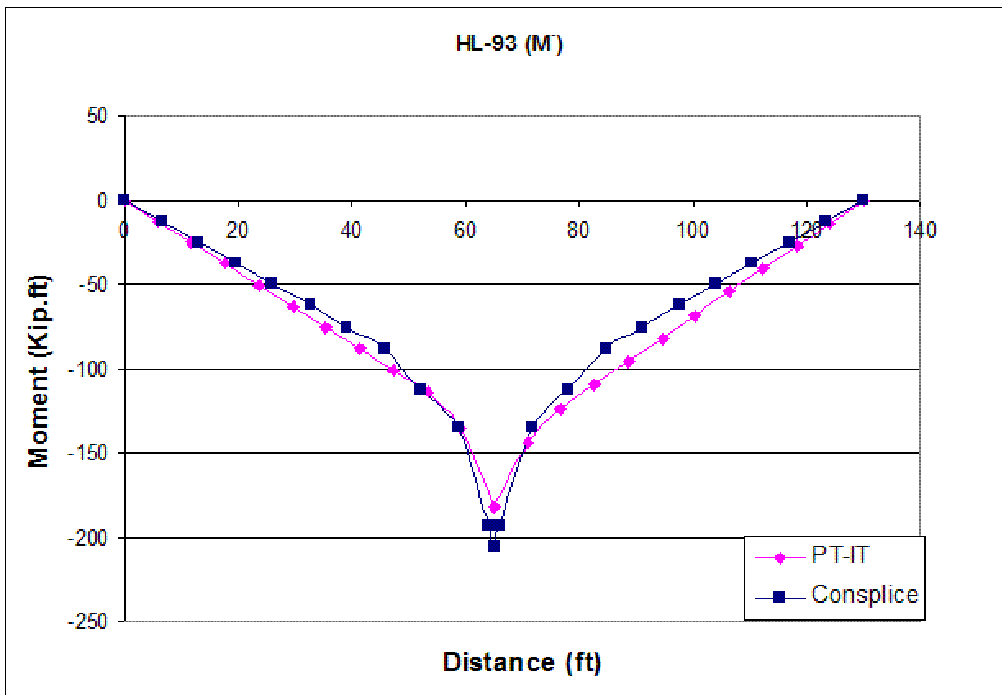


Figure 3. 55 Example 2-Factored required moment

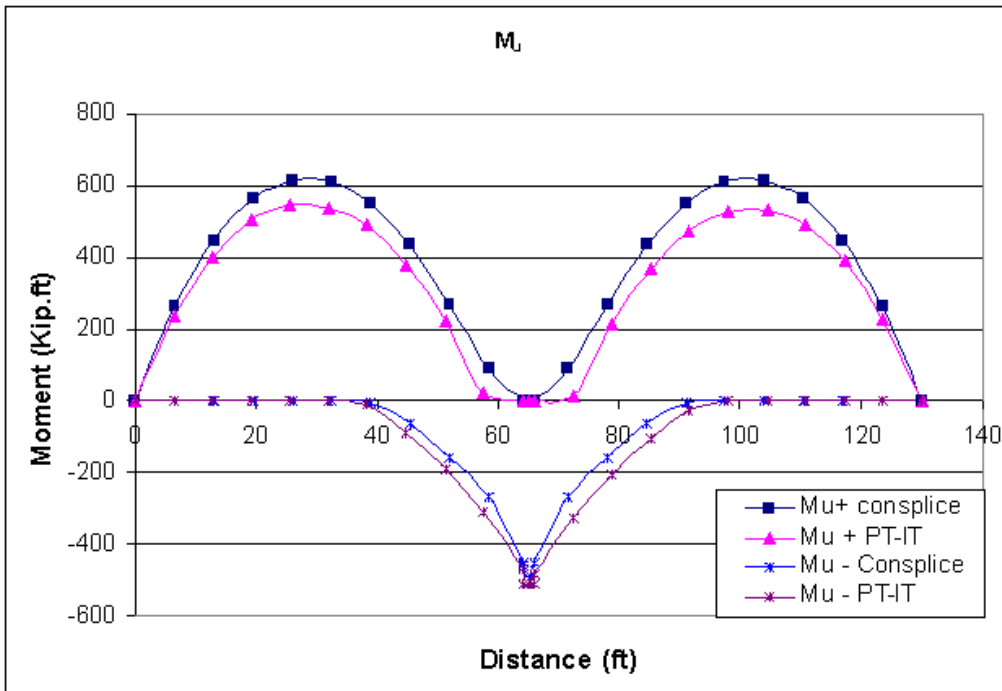


Figure 3. 56 Example 2- Φ times nominal resistance moment

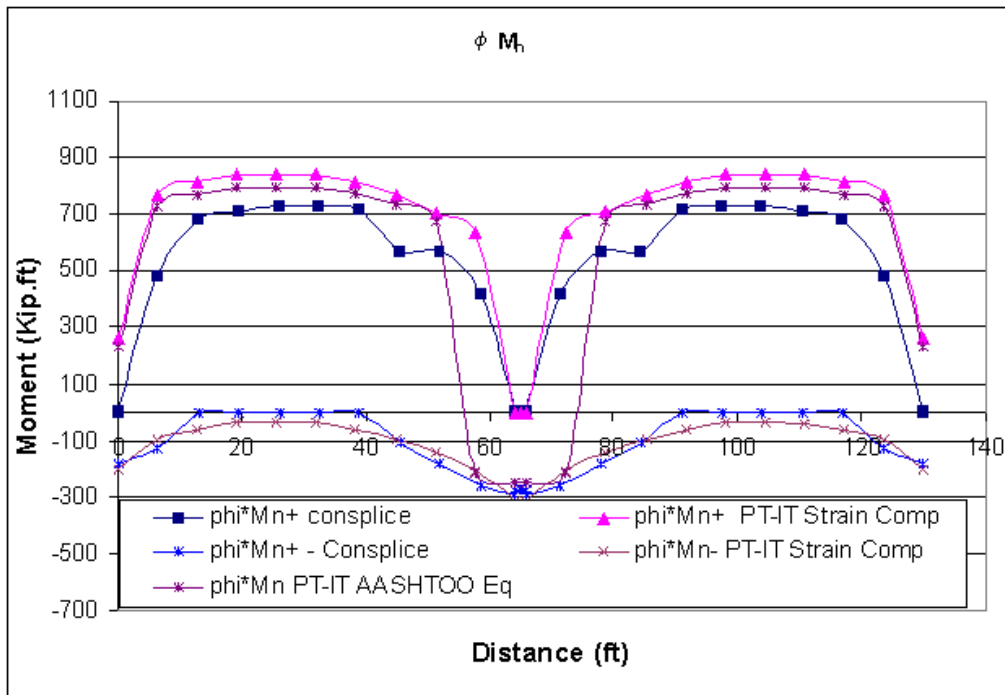


Figure 3. 57 Example 2-time-dependent deflection due to prestressing

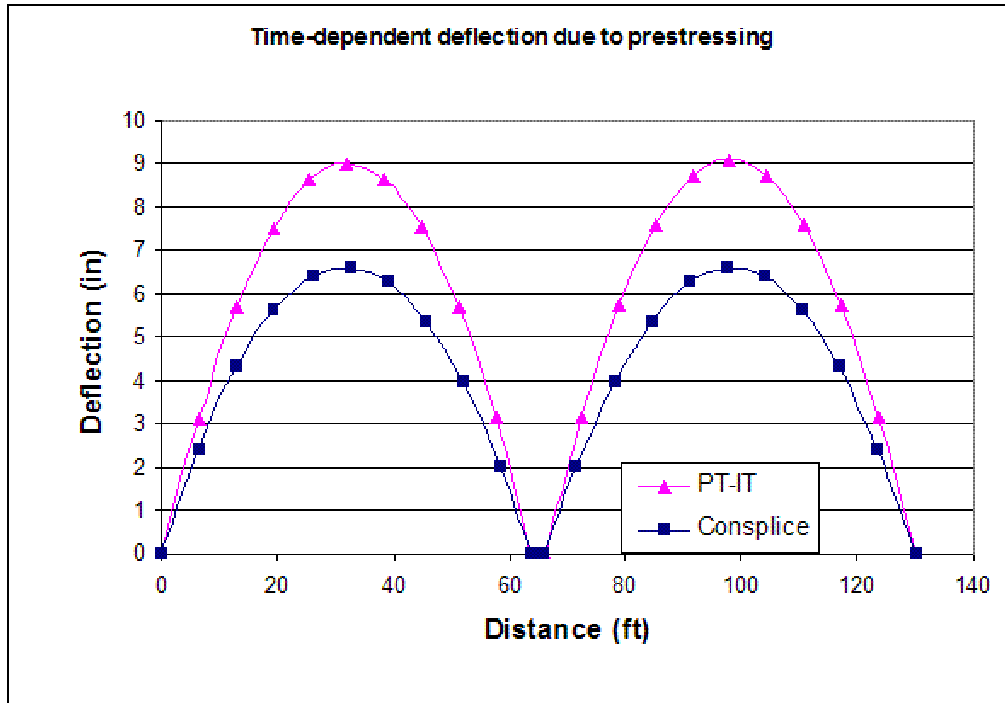


Figure 3. 58 Example 2-time-dependent deflection due to component weight and shrinkage

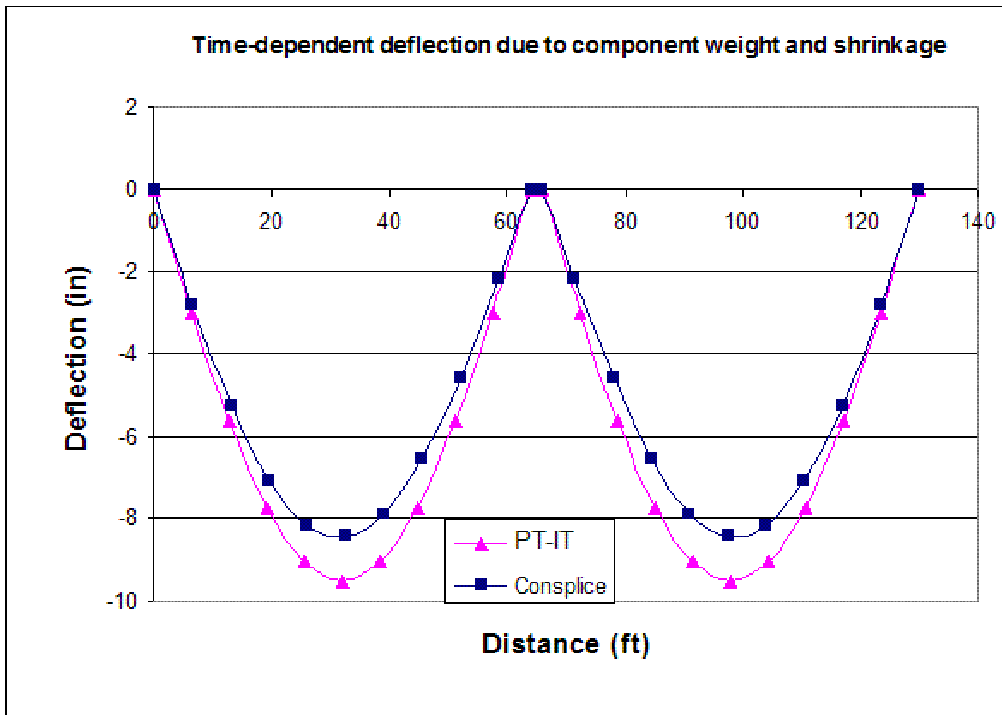
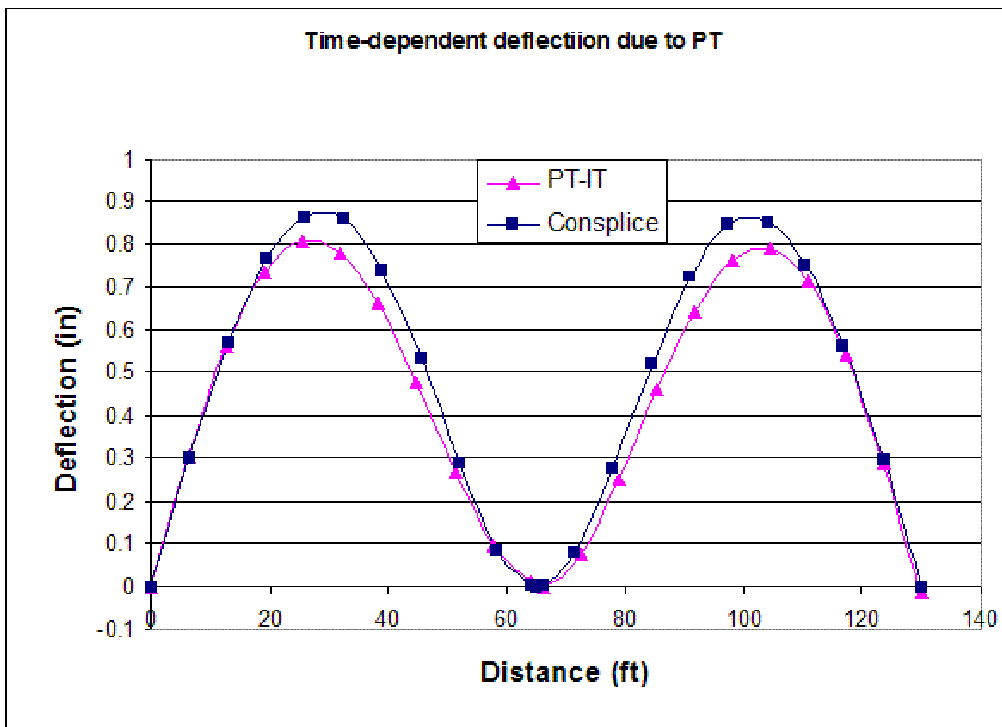


Figure 3. 59 Example 2-time-dependent deflection due to post-tensioning



B

Figure 3. 60 Example 2-time-dependent deflection due to barrier weight

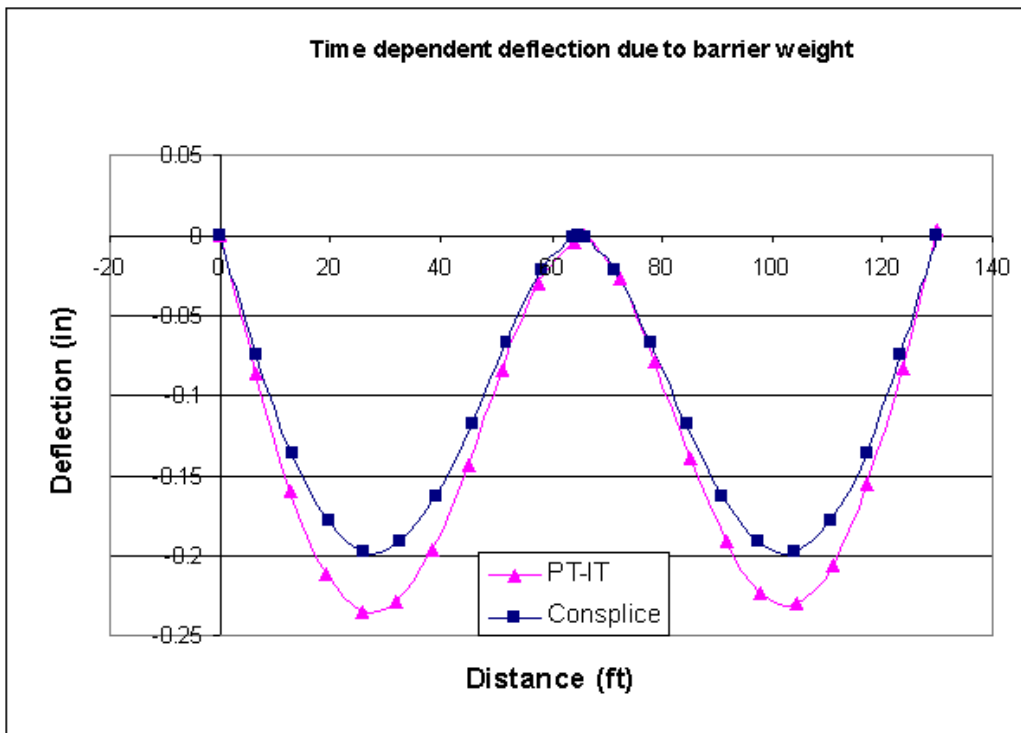


Figure 3. 61 Forces in deck and girder due to differential shrinkage

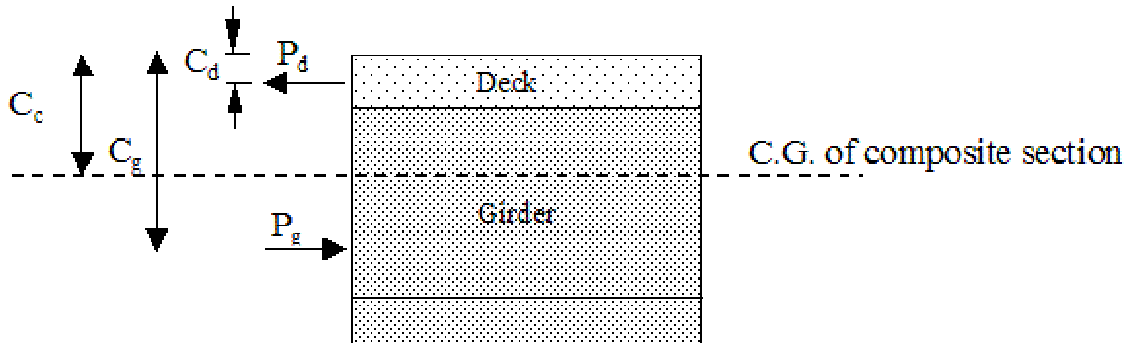


Figure 3. 62 Deformations affecting both deck and girder

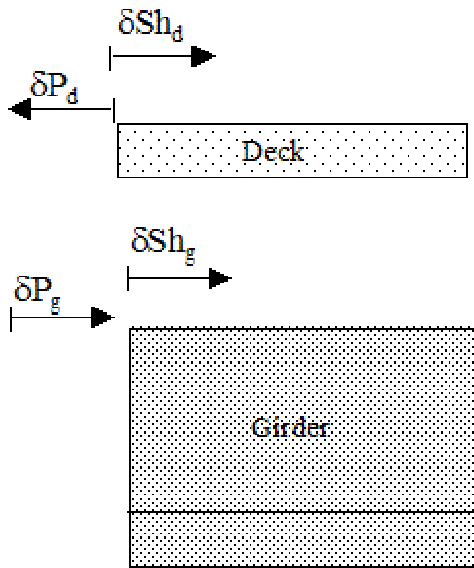


Figure 3. 63 Example 1-prediction of restraining moment due to differential shrinkage using published versus suggested CTL equation

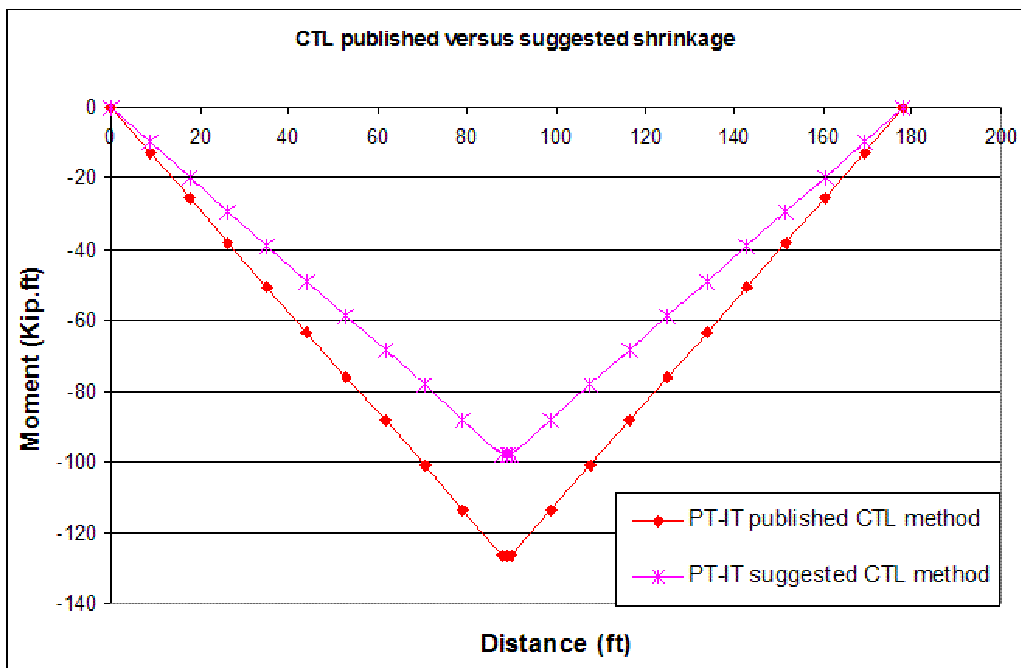


Figure 3. 64 Example 1-prediction of restraining moment due to differential shrinkage using published versus suggested P equations

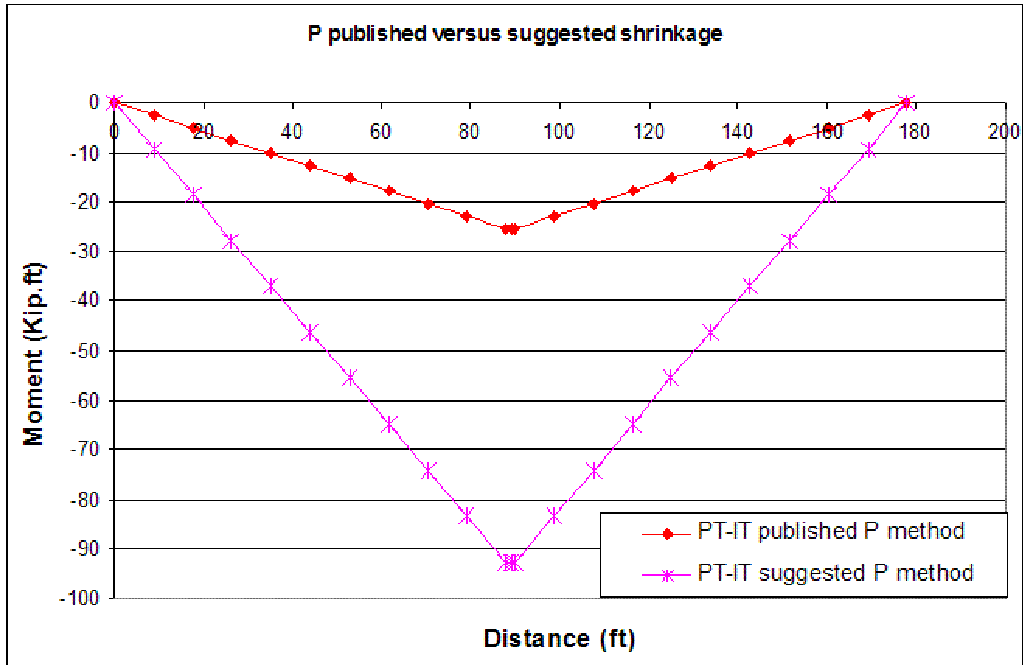


Figure 3. 65 Example 1-prediction of restraining moment due to differential shrinkage using PCA, suggested CTL, and suggested P expressions

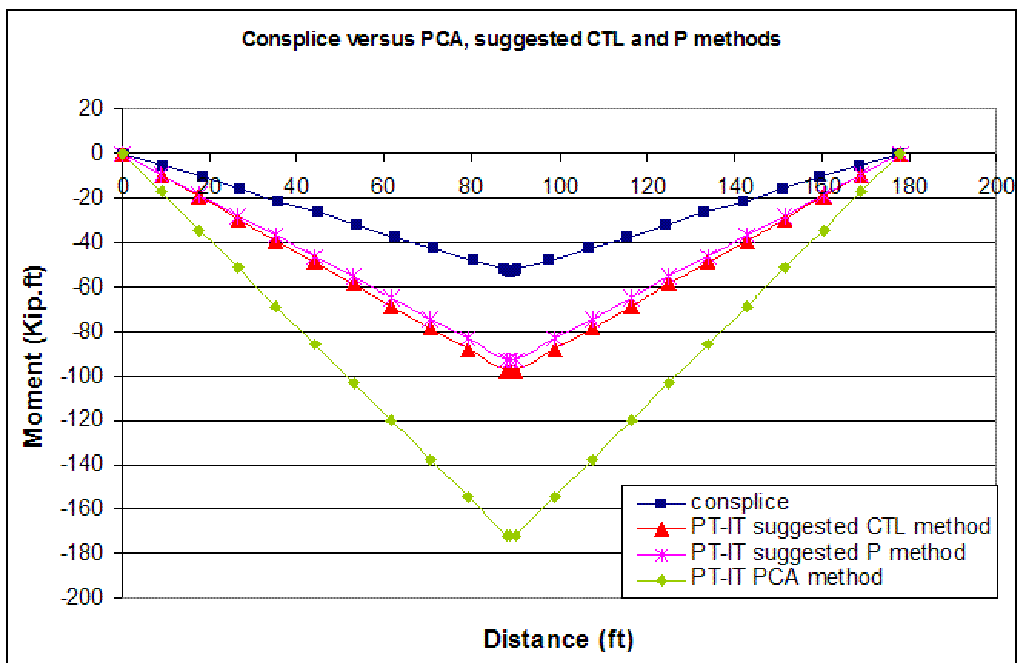


Figure 3. 66 Example 2-prediction of restraining moment due to differential shrinkage using published versus suggested CTL equations

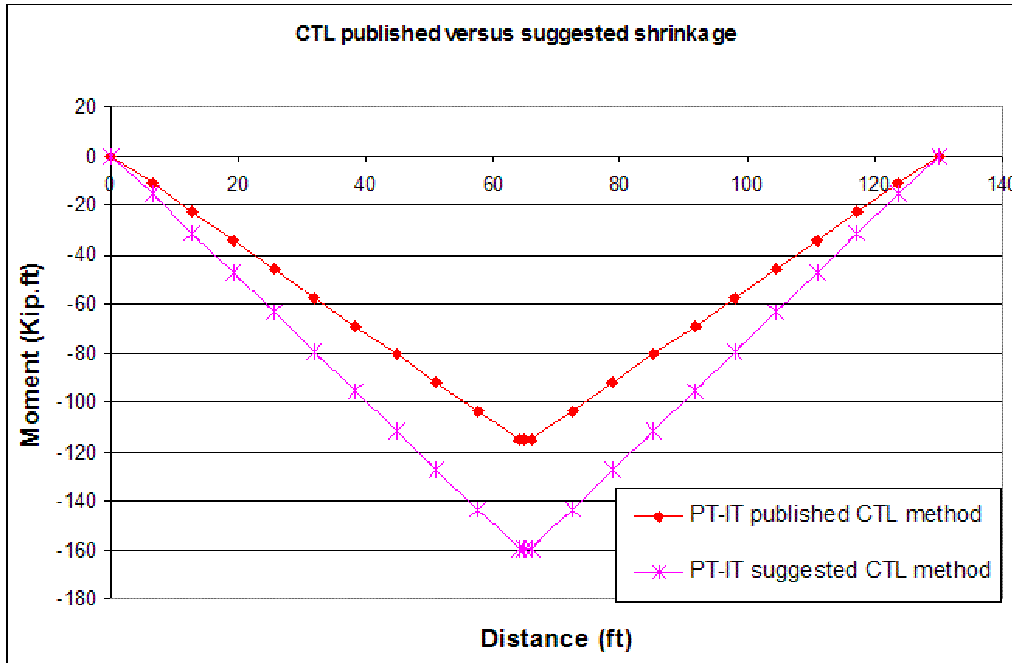


Figure 3. 67 Example 2-prediction of restraining moment due to differential shrinkage using published versus suggested P equation

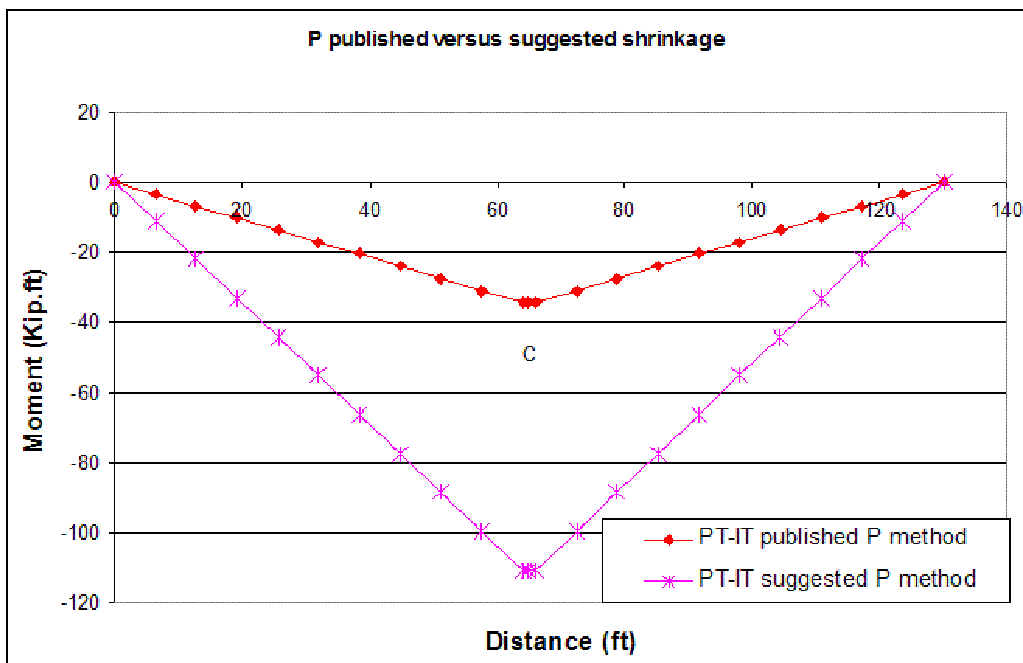


Figure 3. 68 Example 2-prediction of restraining moment due to differential shrinkage using PCA, suggested CTL, and suggested P expressions

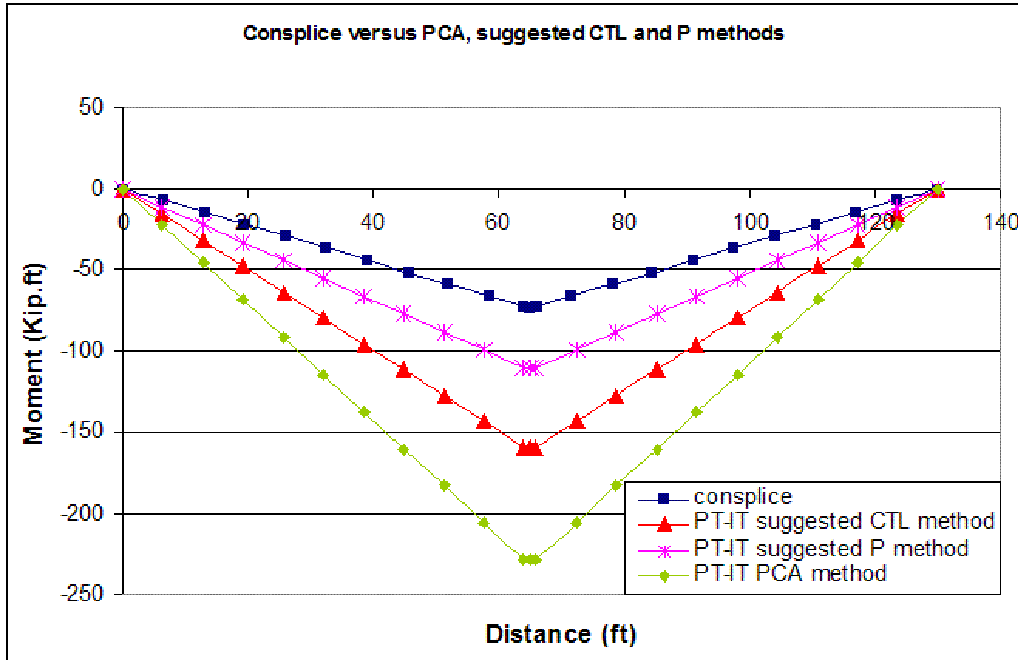


Table 3. 1 Values of the constants α and β and the time ratio for the concrete compressive strength ⁽²⁴⁾

Time ratio	Type of curing	Cement type	Constants α and β	Concrete age										Ultimate (in time)
				Days					Years					
				3	7	14	21	28	56	91	1	10		
	Moist-cured	I	$\alpha=4.0$ $\beta=0.85$	0.46	0.7	0.88	0.96	1.0	1.08	1.12	1.16	1.17	1.18	
		III	$\alpha=2.3$ $\beta=0.92$	0.59	0.8	0.92	0.97	1.0	1.04	1.06	1.08	1.09	1.09	
$(f'c)_t/(f'c)_{28}$	Steam-cured	I	$\alpha=1.0$ $\beta=0.95$	0.78	0.91	0.98	1.0	1.0	1.03	1.04	1.05	1.05	1.05	
		III	$\alpha=0.7$ $\beta=0.98$	0.82	0.93	0.97	0.99	1.0	1.0	1.01	1.01	1.02	1.02	

Table 3. 2 Values for K_1 and K_2 ⁽¹³⁾

Concrete mix	Proposed K_1 and K_2	90 th percentile K_2	10 th percentile K_2
Nebraska NE09G, NE10G, NE12G	0.975	1.211	0.788
New Hampshire NH10G, NH11G, NH12G	0.911	1.123	0.878
Texas TX08G, TX09G, TX10G	1.321	1.115	0.886
Washington WA10G, WA11G, WA12G	1.154	1.182	0.817

Table 3. 3 Shrinkage factor γ_{cp} ⁽¹³⁾

Moist-curing suration, days	Shrinkage factor γ_{cp}
1	1.2
3	1.1
7	1.0
14	0.93
28	0.86
90	0.75

Table 3. 4 Recommended values for friction and wobble coefficient

Type of duct	Range of values		Recommended for calculations	
	μ	k	μ	k
Flexible tubing, non-galvanized	0.18-0.26	5-10.10 ⁻⁴ /ft	0.22	7.5.10 ⁻⁴ /ft
Flexible tubing, galvanized	0.14-0.22	3-7.10 ⁻⁴ /ft	0.18	5.0.10 ⁻⁴ /ft
Rigid, thin-wall tubing, non-galv.	0.20-0.30	1-5.10 ⁻⁴ /ft	0.25	3.0.10 ⁻⁴ /ft
Rigid, thin-wall tubing, galv.	0.16-0.24	0-4.10 ⁻⁴ /ft	0.20	2.0.10 ⁻⁴ /ft
Greased and wrapped	0.05-0.15	5-15.10 ⁻⁴ /ft	0.07	10.10 ⁻⁴ /ft

CHAPTER 4 - RESULTS OF PARAMETRIC STUDY

Scope of Parametric Study

The objective of this parametric study was to examine the behavior of post-tensioned, prestressed, inverted-T systems (PT-IT) and determine the influence of different parameters on the design. The parametric study integrated a wide range of parameters, including assessment of different construction scenarios, effect of timing of each construction stage, and effect of concrete strength on the design for girder and deck. Different models were considered for estimating creep and shrinkage of concrete; different methods were examined to evaluate time-dependent restraint moments due to creep and differential shrinkage. The parametric study incorporated six different IT sections.

Multiple construction scenarios were considered during the course of this study, including one and two-step post-tensioning. Different scenarios were considered for one-stage post-tensioning, including the option of casting the diaphragm and deck simultaneously, then applying post-tensioning. This scenario will be referred to as Dia & Deck-PT. The second option was to cast the diaphragm to establish continuity, then cast the deck and apply post-tensioning, which will be referred to as Dia- Deck-PT. The third option for one-stage post-tensioning was to cast the diaphragm to establish continuity, apply post-tensioning to the continuous girders, and then cast the deck. This option will be referred to as Dia-PT-Deck. A two-stage post-tensioning scenario was also considered, where the diaphragm was first cast to establish continuity, first-stage post-tensioning was applied, followed by casting the deck, and the last step was applying second-stage post-tensioning. Comparison of pros and cons of each scenario are discussed later in this chapter.

Effect of timing on the behavior of the PT-IT system was determined by varying time of cutting the strands, time of establishing continuity, and time of post-tensioning. The study included IT500, IT 600, IT 700, IT 800, IT 900, and IT 1000, with concrete strengths of 6, 8, and 10 ksi. Deck concrete strength was considered to be 3, 3.5, and 4 ksi. The effect of different creep and shrinkage models was investigated, including AASHTO LRFD, ACI 209, SCC, CEB-FIP 90, and NCHRP report 496 models. Methods to estimate time-dependent restraining

moments included PCA, CTL, and P, as well as the creep-transformed section properties method. Table 4. 1 shows different parameters varied in this study.

Parametric Study Results

Different Construction Scenarios

Construction scenario is considered to be one of the most effective and critical parameters in design, as it directly affects time-dependent restraining moments due to creep and differential shrinkage, which in turn affects stress distribution in sections along the beam.

Different construction scenarios were investigated, including the two main options of applying one or two stages of post-tensioning.

Dia & deck-PT: In this scenario the deck and diaphragm are cast simultaneously, and then post-tensioning is applied, deck weight is carried by the simply-supported beam. For the case when continuity is established at early age of the girder, positive restraining moments tend to develop in the piers. Typically, secondary moments due to post-tensioning are also positive, causing high-compression stresses in the top of the girders within the spans and consequently, limiting the maximum span-to-depth ratio of the section to control stresses.

Dia-PT-Deck: For this scenario, the diaphragm is first cast, then post-tensioning is applied, and finally the deck is cast. The benefit of casting the deck after the diaphragm is cast and continuity is established, is that the weight of the deck is carried by the continuous structure, which results in lower positive moments within the span, while negative moments are developing over the piers. At the same time, the weight of the deck does not cause time-dependent restraining moments due to creep. This will increase the positive moment or reduce the negative moment in the pier (depending on whether moments in the pier are positive or negative). It will help reduce moments in the pier and consequently, reduce the probability of cracking of the deck.

The disadvantage of this option of construction is that post-tensioning will be applied at the girder section only, causing high stresses in the bottom of the girder at end adjacent to the pier. Moreover, for early age of establishing continuity where positive restraining moments are developed in the diaphragm, these high stresses will be increased.

Dia-Deck-PT: In this scenario continuity is established by casting the diaphragm, and then after the diaphragm concrete hardens, the deck is cast, post-tensioning is applied to the

whole structure, via the scenario. The weight of the deck will be carried by the continuous structure and will not cause a time dependent effect on moments in the piers. Besides, when post-tensioning is applied on the continuous structure, primary moments caused by post-tensioning at the pier will be less if they are to be applied at the girder section (less eccentricity for the post-tensioning force). This will cause less tension force at the bottom of the girders in the case when continuity is established at early girder age. The drawback of this type of scenario is that cracking of the diaphragm over the pier will occur during the period between casting the deck and post-tensioning. After post-tensioning, the deck will be under compression and consequently, the cracks will tend to close.

Two-stage post-tensioning: In this scenario, the diaphragm is cast to establish continuity, post-tensioning is applied enough to balance stresses due to the weight of the deck. Then the deck is cast, and the final stage of post-tensioning is applied to balance stresses due to the weight of the barriers and live load. The advantage of this type of construction is that the deck will be carried by the continuous beam, and less initial prestressing is needed as it controls stresses due to girder weight only, which results in less initial camber. In addition, the main part of post-tensioning is to be applied on the composite structure of the girder and the deck, which reduces the effect of tension caused by post-tensioning on the bottom of the girders at internal piers. Disadvantages of the two-stage post-tensioning scenario are obviously the extra labor, and the fact that the post-tensioning ducts have to stay ungrouted between the two stages of post-tensioning. Under real construction conditions, this time may be long enough that undesired corrosion could initiate in the tendons applied at the first stage of post-tensioning. If this option is used, care should be taken to prevent moisture from entering the un-grouted ducts between the two post-tensioning stages.

As the PCA method did not account for the case when the diaphragm is cast prior to casting the deck, a modification has been applied to account for these cases. Time-dependent restraining moments due to creep under prestressing start at the time the diaphragm is cast; restraining moment due to differential shrinkage doesn't start until the deck is cast. Consequently, the creep coefficient in the multiplier $(1-e^{-\phi})$, which is applied to restraining moment due to creep under prestressing and dead weight, is based on the increase in the creep strain from the time when diaphragm is cast. The creep coefficient in the multiplier $(1-e^{-\phi})/\Phi$,

which is applied to the restraining moment due to differential shrinkage, is based on the increase in the creep strain from the time the deck is cast.

Table 4. 2 shows a comparison of the average maximum span-to-depth ratio for different construction scenarios, including the case of a continuous IT section reported by Ambare and Peterman ⁽¹⁾ for girder concrete strength of 8 ksi. The comparison included different IT sections, considering concrete strengths of 6, 8, and 10 ksi. Values in Table 4. 2 are based on the envelope of extreme-case scenarios of establishing continuity and the envelope of estimated time-dependent restraining moments.

Figure 4. 1 shows maximum spans for different IT sections (IT 500 through IT 1000), for different construction scenarios and different concrete strengths.

Different construction scenarios were investigated for two-span girders with IT 700 cross sections of 8-ksi concrete strength, taking into account different timing for establishing continuity along the girder ages. Maximum spans are reported based on worst-case scenarios, which are earliest and latest age of establishing continuity at 14 and 224 days, respectively. Table 4. 3 includes section-reinforcement properties for different construction scenarios.

Figure 4. 2 through Figure 4. 5 show time-dependent restraining moments due to creep and differential shrinkage for different construction scenarios using PCA, CTL, P, and creep-transformed section properties methods for the case when continuity is established at 14 days. It is evident that for different methods, estimated restraining moments vary drastically. This shows the need for experimental investigation on the PT-IT system to determine the actual range of time-dependent restraining moments, and to determine which of the methods is closer to evaluating time-dependent effect on this system. The PCA method is believed to overestimate restraining moment resulting from differential shrinkage as has been noted in other studies ^{(5), (6)}.

Figure 4. 6 shows secondary moments resulting from post-tensioning for the cases when continuity is established at 14 days. In cases where post-tensioning is applied to the girder section, the resulting secondary moment is negative. The secondary moment in its nature opposes the effect of the primary moment due to post-tensioning, resulting from the resistance of the continuous member to post-tensioning deformations at the points of continuity. When post-tensioning is applied to the structure section in a parabolic profile, the primary moment will be negative when the tendon's path is under the neutral axis and positive when it is located above the neutral axis. IT sections for the neutral axis are at 34-38 % of the IT depth measured from the

bottom of the section, and maximum eccentricity of the tendon above the neutral axis is almost twice the maximum eccentricity of the tendon below the neutral axis. This makes the positive primary moment dominant and the secondary moment negative. On the other hand, when post-tensioning is applied to the composite section of the girder and the deck, the neutral axis is located around 60 % of the girder's depth from the bottom of the section. This makes the negative primary moment dominant and consequently, the secondary moment is positive. Figure 4. 7 helps illustrates the previous argument by showing the tendon's location with respect to both center of gravity of the girder and the composite section.

Figure 4. 8 shows maximum positive restraining moment in the pier, including positive live-load moment, along with cracking moment of the diaphragm section in the positive direction. Time-dependent restraining moments are calculated according to the CTL method, which usually predicts highest positive moment in the pier compared to other methods. It is clear that cracking of the diaphragm is not a concern in this case. Figure 4. 9 includes maximum positive restraining moment in the pier where time-dependent restraining moment is calculated using the P method.

The main purpose of this post-tensioning, besides increasing span-to-depth ratio, is to come up with a bridge system where top-deck cracks over the piers are greatly reduced or eliminated. Therefore, discussion of different construction scenarios will be evaluated based on these two points.

Maximum negative moment in the pier will be evaluated according to the P method, as it is the only method that accounts for cracking of the diaphragm.

Figure 4. 10 presents the maximum negative moment in the diaphragm for the Dia & Deck –PT construction scenario, including and excluding maximum negative moment due to live load. It also shows the cracking moment of the diaphragm section throughout the life of the structure. It is clear that for this construction scenario, cracking of the deck and diaphragm is not likely to occur, but in comparing span-to-depth ratios in Table 4. 2, it is evident that other scenarios provide a higher span-to-depth ratio. In terms of stresses along the girders and diaphragm, excess tension in the girder bottom ends near the pier (where prestressing doesn't apply any compression on the girder) after post-tensioning.

Figure 4. 11 shows development of maximum negative moments including and excluding live-load moments for the Dia-Deck-PT scenario, along with cracking moment of the diaphragm

section. Right after casting the deck, the diaphragm cracks under its weight and moments are redistributed along the bridge using the cracked-section moment of inertia of the diaphragm. The diaphragm stays cracked until post-tensioning is applied, where the top of the diaphragm becomes under compression, closing the cracks and causing the section to behave as uncracked. Figure 4. 12 shows time-dependent restraining moments developing in the pier. The increase in time-dependent restraining moments after applying post-tensioning is due to the fact that the cracks are closed and the section acts as uncracked.

Figure 4. 14 shows restraining moment in the pier for the Dia-PT-Deck scenario. In this case, post-tensioning is applied to the girder's section. As discussed previously, this causes negative secondary moments in the piers, which reduces the effectiveness of compression applied by the tendon to the top of the diaphragm. Under live load the deck and diaphragm crack and stay cracked throughout the structure age. Figure 4. 15 shows time-dependent restraining moments for this construction scenario, and shows that the deck and diaphragm will crack after applying live load and moments will be redistributed. Consequently, this construction scenario doesn't satisfy the criteria of eliminating cracks in the diaphragm.

Figure 4. 17 includes restraining moments in the pier for the case of two-stage PT. In this scenario, the diaphragm and deck don't crack at any time; however, tension stresses will exceed allowable stresses in the top of the diaphragm in the period between casting the deck and second-stage post-tensioning when it comes under compression.

Figure 4. 18 through Figure 4. 21 show time-dependent restraining moments due to creep and differential shrinkage for different construction scenarios using PCA, CTL, P, and creep-transformed section properties methods for the case when continuity is established at 224 days. Figure 4. 22 shows secondary moments resulting from post-tensioning for this case.

The same discussion regarding the possibility of cracking of the diaphragm and the deck for all suggested construction scenarios applies for the case when continuity is established at 224 days of girder age. Figure 4. 23 through Figure 4. 30 show Maximum negative moment in the diaphragm and time-dependent restraining moment for different construction scenarios.

As a result, it is clear that both scenarios of one-stage post-tensioning (Dia-Deck-PT) and two-stage PT have the highest span-to-depth ratio and satisfy the crack-free deck criteria. Since the option of Dia-Deck-PT incorporates less labor, it is recommended to be used for construction of PT-IT systems.

Effect of Concrete Strength

Effect of girder concrete strength

From Table 4. 2, it is clear that girder concrete strength plays a major role in maximum span-to-depth ratio. Increasing girder concrete strength from 6 to 8 ksi helps increase by 15% the span of 6-ksi girders, while increasing strength from 8 to 10 ksi increases the span by 11% of 8-ksi girders. In order to determine the effect of girder concrete strength on restraining moments in the pier, an IT 500 section was considered with deck concrete strength of 4 ksi. Table 4. 4 shows details for strands and tendons for an IT 500. Figure 4. 39 through Figure 4. 42 show time-dependent restraining moments calculated according to PCA, CTL, P, and creep-transformed section properties methods.

It is clear that with the increase of concrete strength of the girder, negative restraining moments increase. Knowing that span lengths of these girders are different, directly affects moment due to self-weight and consequently, restraining moment due to creep under weight of the girders. Analysis of different components of time-dependent restraining moment was conducted to determine the effect of different concrete strengths on time-dependent restraining moment. From Figure 4. 43, it was found that time-dependent restraining moment due to creep under prestressing decreases by 12% for 8-ksi concrete compared to that of 6-ksi concrete, and by 10% when comparing 8-and 10-ksi concrete.

While restraining moment (see Table 4. 5 and Figure 4. 44) due to girder weight increases at a ratio of 30% for 8-ksi girders compared to 6-ksi, and increases by 21% for 10-ksi girders compared to 8-ksi girders, time-dependent restraining moment increases by 14 % only for 8-ksi concrete compared to 6-ksi concrete, and increases by 7% for 10-ksi compared to 8-ksi concrete. The reason for this is that as concrete strength increases, it creeps less under permanent loads.

As concrete strength increases, it shrinks less and consequently, differential shrinkage between girders and deck increases. From Figure 4. 45, it was found that time-dependence due to differential shrinkage increases by 9% for 8-ksi girders compared to 10-ksi, and 7% for 10-ksi compared to 8-ksi concrete.

Effect of concrete strength on losses in prestressing strands and tendons is shown in Figure 4. 46 and Figure 4. 47. As concrete strength increases, fewer losses in prestressing strands and post-tensioning tendons occur.

Effect of deck concrete

For the currently used concrete deck strength (3, 3.5, and 4 ksi), concrete strength of the deck doesn't affect time-dependent restraint moment under creep and shrinkage, nor losses in stress of prestressing strands and post-tensioned tendons.

Effect of Different Creep and Shrinkage Models

The effect of using different models to predict creep and shrinkage of concrete was examined by first investigating the prediction of these models. Figure 4. 50 and Figure 4. 51 compare prediction of shrinkage strain and creep coefficient for a concrete specimen of 6-ksi strength, 2.77 volume-to-surface ratio, and 70 % humidity for AASHTO LRFD, ACI-209, NCHRP-496, SCC, and CEB-FIP-90 models. It is clear that all these models closely predict creep except the CEB-FIP-90 model, which predicts higher creep coefficient and less shrinkage strain compared to other models. The SCC model predicts less shrinkage to occur after three months of girder age.

Figure 4. 52 and Figure 4. 53 show prediction for creep and shrinkage for 10-ksi concrete, 2.77 volume-to-surface ratio, and 70% humidity. It is clear that while NCHRP-496 and ACI-209 predict close shrinkage strain for 6-ksi concrete, these predict hugely different shrinkage strain for 10 ksi. At the same time, AASHTO LRFD predicts close creep coefficient to the NCHRP model which was especially developed for high-strength concrete.

Figure 4. 54 and Figure 4. 55 compare losses in prestressing strands and post-tensioned tendons using a different model for IT600 with 6-ksi strength. The effect of using different models for creep and shrinkage affects the prediction of losses within a ratio of 7 %, and post-tensioning losses within 3 %, since a considerable amount of shrinkage and creep occurs before post-tensioning.

Figure 4. 56 through Figure 4. 59 show a prediction of time-dependent restraining moment in the pier using different methods of prediction and different creep-and-shrinkage models.

Effect of Timing

The effect of timing on the behavior of a PT-IT system in general, and the development of time-dependent restraining moment in particular, were discussed in detail in this section. This effect is discussed for the Dia-Deck-PT construction scenario, as it was recommended for construction. Timing effect includes different timing for cutting the strands, timing of establishing continuity, time of casting the deck, and time of post-tensioning.

Effect of time of cutting prestressing strands

Range of time considered for cutting the strands is between 18 hours and four days. The latest the strands are cut, the less loss of prestressing occurs. Figure 4. 60 shows that cutting strands at one day decreases loss by 1%, cutting strands when girders are two days old decreases loss by 2%, and cutting strands when girders are four days old decreases loss by 3 %. However, this small difference in stresses doesn't affect values of time-dependent restraining moments.

Effect of time of establishing continuity and casting the deck

Effect of time of establishing continuity

The effect of time of establishing continuity was studied for the Dia-Deck-PT construction scenario. It was assumed that the diaphragm is cast first to establish continuity; and two days after casting the diaphragm, the deck is cast and post-tensioning is applied 15 days after casting the deck. The effect was investigated for IT 700 with concrete strength of 8 ksi. Table 4. 6 show properties of two-span girders designed in consideration of different times of establishing continuity. A parametric study showed that the most preferable frame time for establishing continuity was between 56 and 112 days of girder age, i.e. between almost two and four months of girder age.

Figure 4. 61 through Figure 4. 65 show time-dependent restraining moment in the pier for continuity established at 14, 28, 56, 112, and 224 days of girder life. For cases when continuity is established at an early age of girder life, positive time-dependent restraining moments tend to develop in the pier. In this case, the design was controlled by positive moments developing within the span. While for cases when continuity is established after 56 days of girder age, negative time-dependent restraining moments are developed in the pier. The design is then controlled by stresses and cracking of the diaphragm and deck. Higher numbers of prestressing

strands were used with the increase of age of establishing continuity to increase positive restraining moments due to creep under prestressing that help reduce negative restraining moments resulting from differential shrinkage. Figure 4. 67 and Figure 4. 71 show overall moment in the diaphragm, including and excluding moments due to live load for different ages of establishing continuity. Figure 4. 66 shows secondary moments resulting from post-tensioning.

Effect of time of casting the deck

The effect of time of casting the deck was analyzed considering 2, 7, 15, and 21 days of time period between establishing continuity and casting the deck. Figure 4. 72 and Figure 4. 73 show effect of time of casting the deck on time-dependent restraining moment in the pier. It is clear that the later the deck is cast, the higher the negative restraining moment develops in the piers. This is because time-dependent restraining moment due to differential shrinkage increases as the age of girders increase when casting the deck. However, within the suggested frame time of 2-21 days, this increase has a minimum effect on the resultant restraining moment in the pier (see Figure 4. 74).

Effect of time of post-tensioning

It is recommended that post-tensioning be applied as soon as possible after casting the deck to close the crack in the top of the diaphragm. This could be done as soon as two days after casting the deck. The time of post-tensioning doesn't affect the value of time-dependent restraining moment, but for durability issues related to control crack initiation and development in the diaphragm, it is recommended that post-tensioning be applied to the structure as soon as possible after casting the deck.

Comparison with Experimental Data

Comparison with experimental data presented by (4) and (7) on cross sections other than IT, was included in this study to explore the applicability and accuracy of different methods to estimate time-dependent restraining moment for different sections.

Experiment 1: Mattock

Comparison of PCA test observation for an experiment conducted by Mattock⁽⁴⁾ is presented. The experimental study was restricted to the observation and evaluation of the behavior of two, half-scale continuous bridges over a period of approximately two years from the time of construction (comparison included girder 1/2 only). The long-time variation of support reactions due to creep and differential shrinkage effects were measured. Geometric properties of the bridge are shown in Figure 4. 75. The precast girders were prestressed by 28, seven-wire strands of ¼-in diameter, with an area of 0.036 in², tensioned to give an initial prestress force of 175000 lb. Weights were hung along the bridge to compensate for the extra weight of the full-scale section. Concrete strengths were 5160, 5370, and 3870 psi for girders in span 1, span 2, and the deck, respectively. Prestressed strands were cut eight days after casting the girders; the deck was cast at 28 days. More information about fabrication and instrumentation of the experiment can be found in (4).

Figure 4. 76 shows comparison of time-dependent restraining moments between experimental data and data resulting from hand calculation using PCA, P, and modified P methods, along with results obtained from the BRIDGERM program for CTL and modified CTL methods.

It was evident that the PCA method drastically overestimated time-dependent restraining moment in the pier; both P and modified P methods overestimated time-dependent restraining moment, especially 100 days after casting the deck. The modified CTL method perfectly matched experimental data up to almost 100 days from time of casting the deck, while the CTL method give a better estimation for the time after 100 days.

Experiment 2: Peterman and Ramirez

A comparison with the experiment performed by Peterman and Ramirez⁽⁷⁾ is presented in this section. The experiment in consideration was designated by Peterman and Ramirez as “Bridge 1,” in which full-span, prestressed concrete panels with two spans were fabricated and tested in the Karl H. Kettelhut Structural Laboratories at Purdue University. Each span of the bridge consisted of two prestressed concrete form panels, 21 ft long, 4 ft wide, and 6 in thick, topped with a 6-in-thick composite CIP slab. Each panel consisted of eight ½-in special uncoated low-relaxation prestressing strands. Each strand had an area of 0.167 in² and minimum ultimate

stress of 270 ksi. Reinforcement in the CIP topping over the pier contained 16 # 4 bars. Figure 4. 77 shows geometric properties of the cross section of the bridge. The four panels for the bridge were cast simultaneously; the prestress force was transferred to the panels seven days after the concrete was cast; and the CIP deck was cast when the panels were 147 days old, while stress in strands was 177 ksi. Reactions at the discontinuous ends of the bridge were monitored throughout the 50 days following casting of the deck. Restraining moment was then calculated and reported. Concrete strength of the panels was 7440 psi at 28 days; deck concrete strength was 5590 psi at 14 days of deck age (when cracks initiated in the deck) and 6150 psi at 28 days. For more information regarding the experimental procedures, the reader is referred to reference (7).

Hand calculations using PCA, P, and modified P were conducted and reported along with analysis results obtained from the BRIDGERM program for both CTL and modified CTL method.

It is important to mention that for the sake of this comparison, cracking of the deck for the P and modified P methods was considered, taking into account that it occurred at 14 days of deck age instead of considering the section cracking-moment criteria.

Figure 4. 78 shows that the PCA method overestimates time-dependent restraining moment, while CTL and modified CTL methods underestimate negative restraining moment for the first 14 days after casting the deck, and also underestimate it after 30 days. However, modified CTL is closer to the experimental results than the CTL method. P method compares very well with the experimental results; modified P method compares better with the experimental data at the beginning of the experiment and after cracking of the deck.

As a result, it is believed that P and modified P methods are more capable of capturing the behavior of shallow sections, while CTL and modified CTL methods are more capable of predicting the behavior of deeper sections. Nevertheless, the estimation for all these methods is within the acceptable range of error.

However, the need to conduct experiments on PT-IT sections is imminent to reach a decision of which method is more capable of capturing the time-dependent effect on restraining moments for the PT-IT system.

Figure 4. 1 Maximum spans for different IT sections for different construction scenarios, for girder concrete strength of 8 ksi

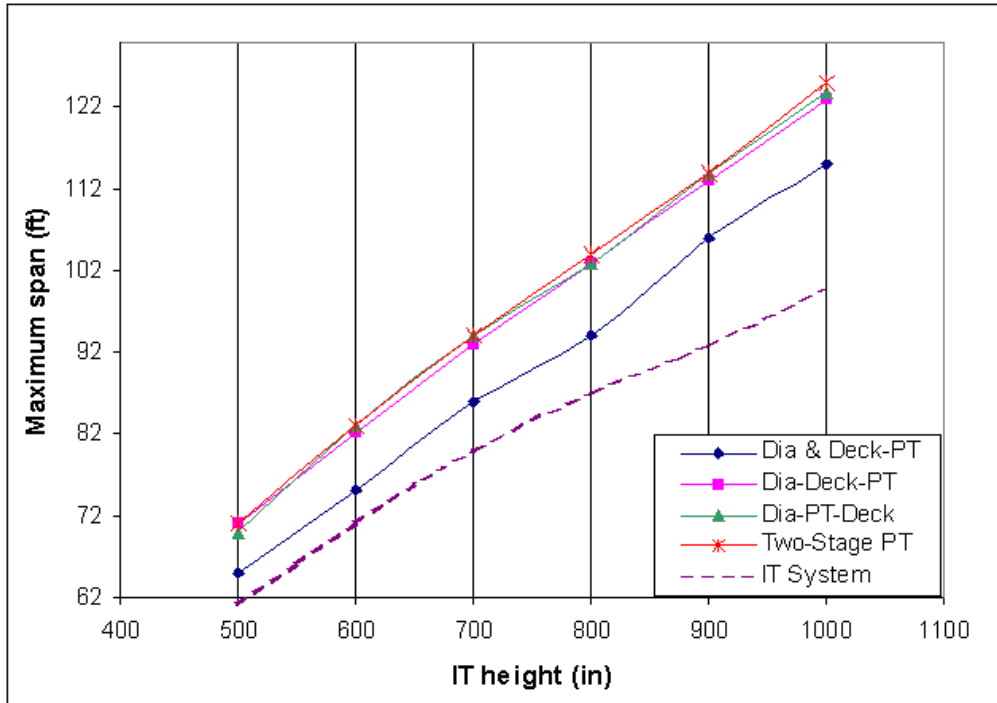


Figure 4. 2 Time-dependent restraining moments using different methods for Dia & Deck-PT construction scenario; continuity established @ 14 days of girder's age

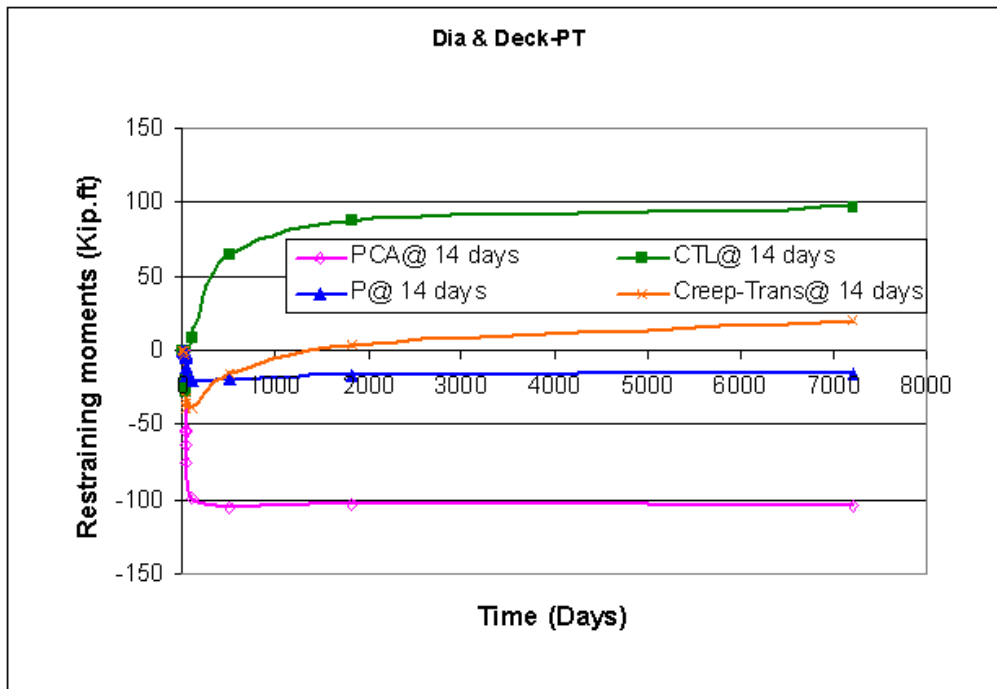


Figure 4. 3 Time-dependent restraining moments using different methods for Dia - Deck-PT construction scenario; continuity established @ 14 days of girder age

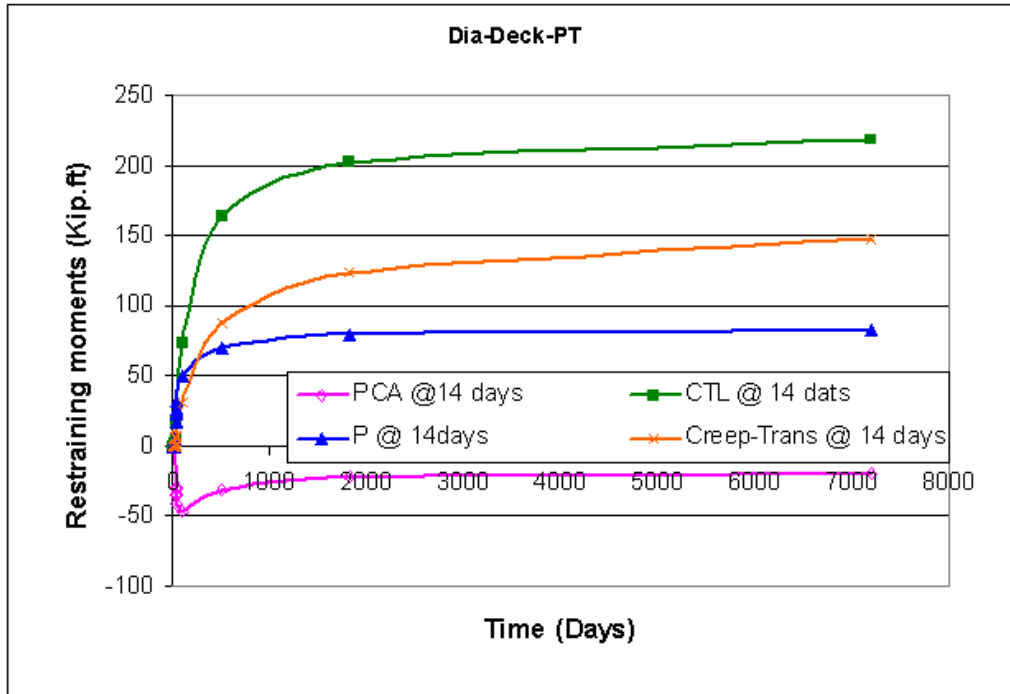


Figure 4. 4 Time-dependent restraining moments using different methods for Dia -PT - Deck construction scenario; continuity established @ 14 days of girder age

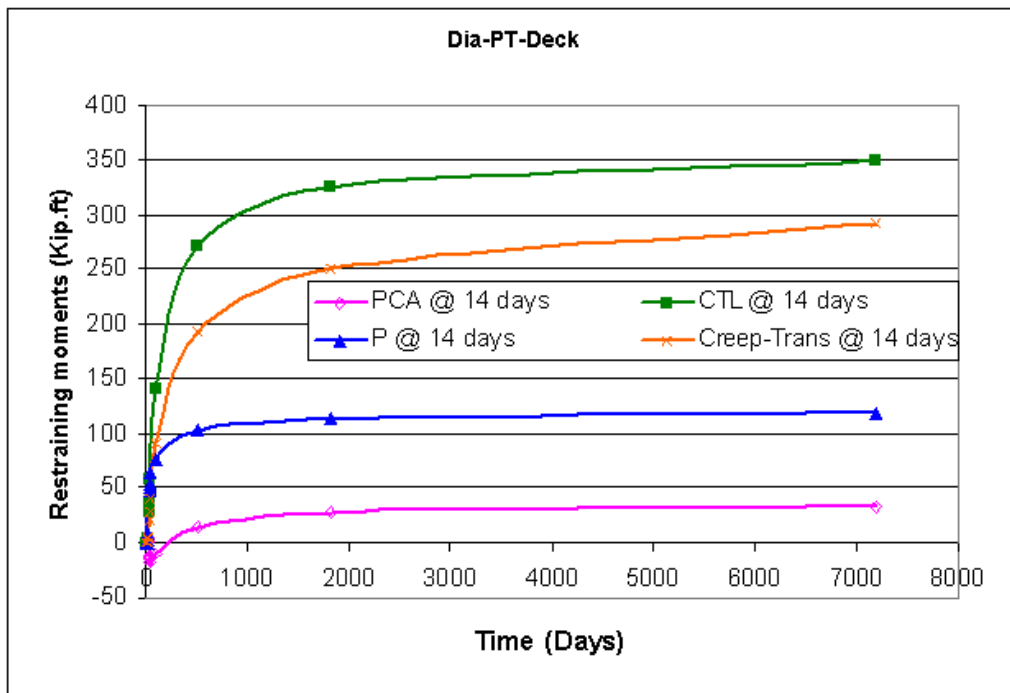


Figure 4. 5 Time-dependent restraining moments using different methods for (two-stage PT) construction scenario; continuity established @ 14 days of girder age

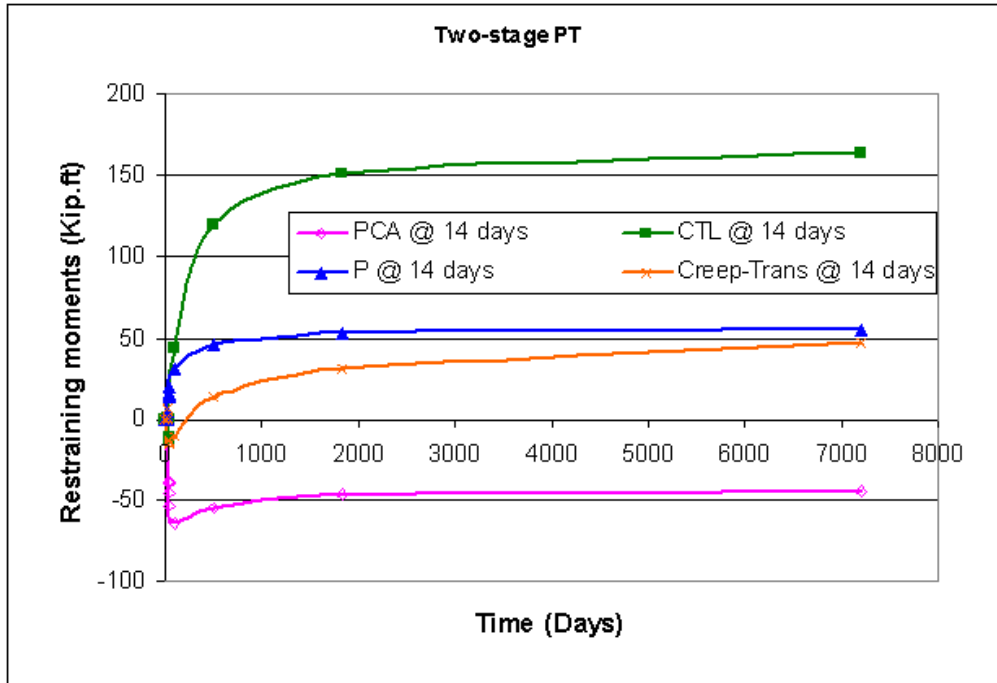


Figure 4. 6 Secondary moment due to post-tensioning for different construction scenarios; continuity established @ 14 days

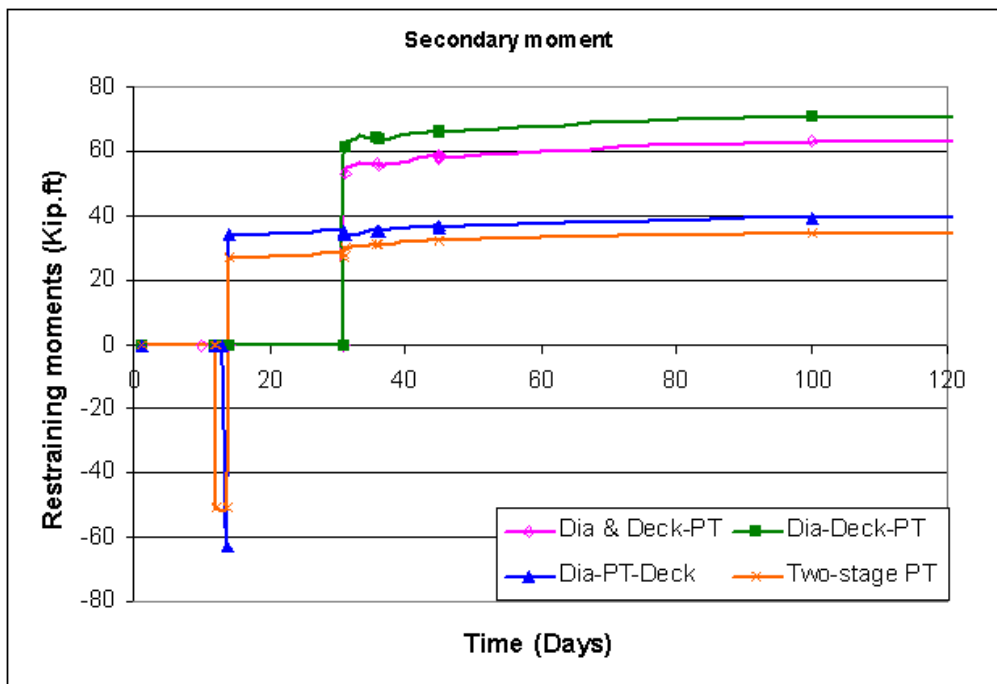


Figure 4. 7 Post-tensioning tendon path with respect to C.G. of the girder and C.G. of the composite section

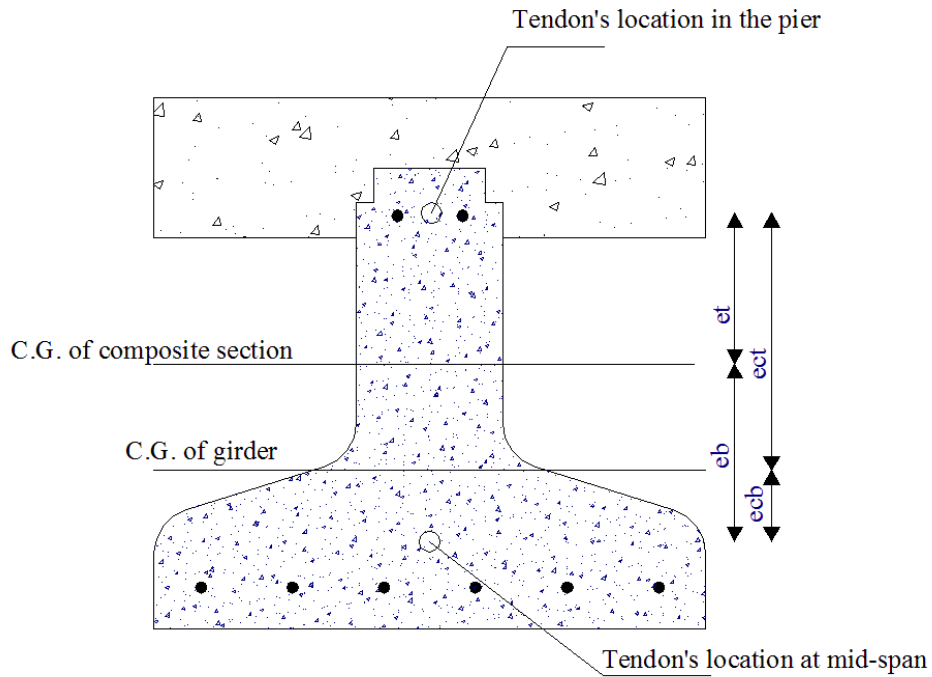


Figure 4. 8 Maximum positive restraining moment in the pier including LL, for different construction scenario according to CTL method; continuity established @ 14 days of girder age

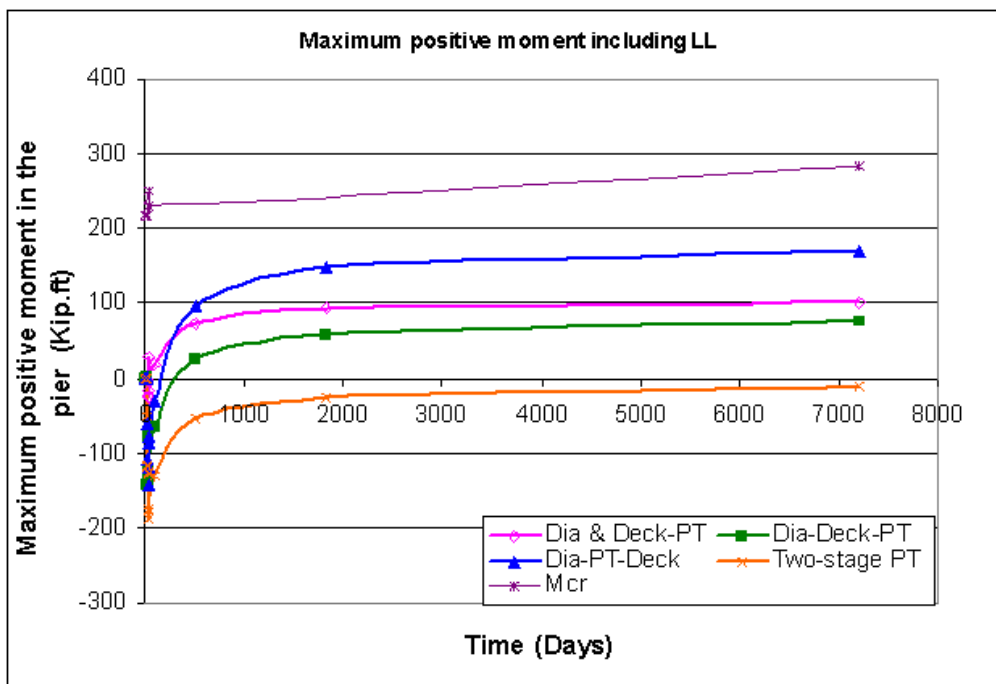


Figure 4. 9 Maximum positive restraining moment in the pier including LL, different construction scenarios, P method; continuity established @ 14 days of girder age

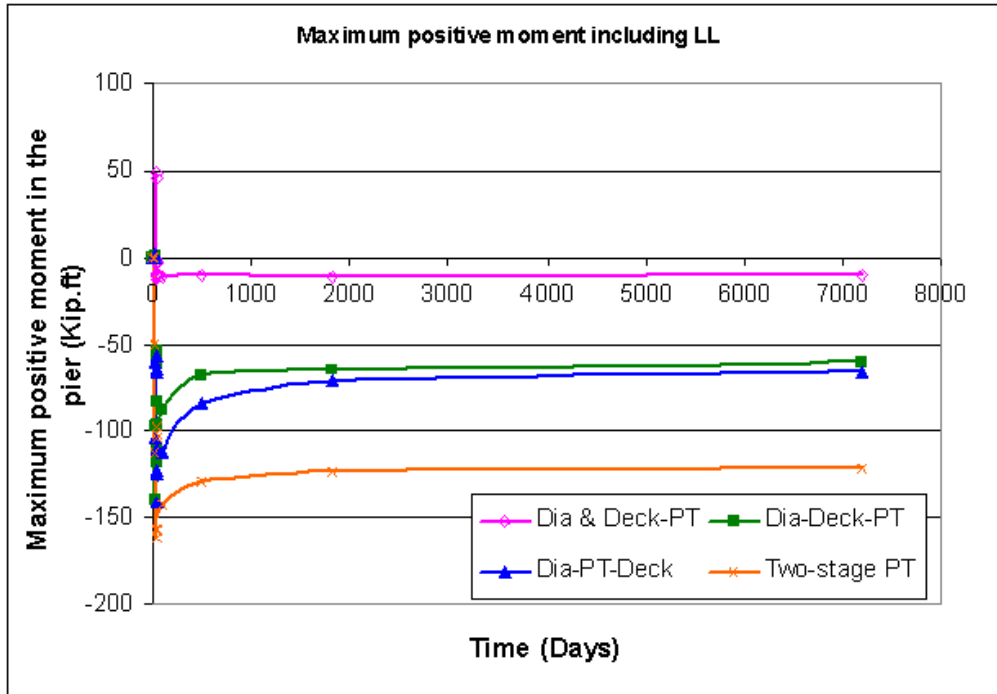


Figure 4. 10 Maximum negative restraining moment in the pier, for Dia & Deck-PT construction scenario, P method; continuity established @ 14 days of girder age

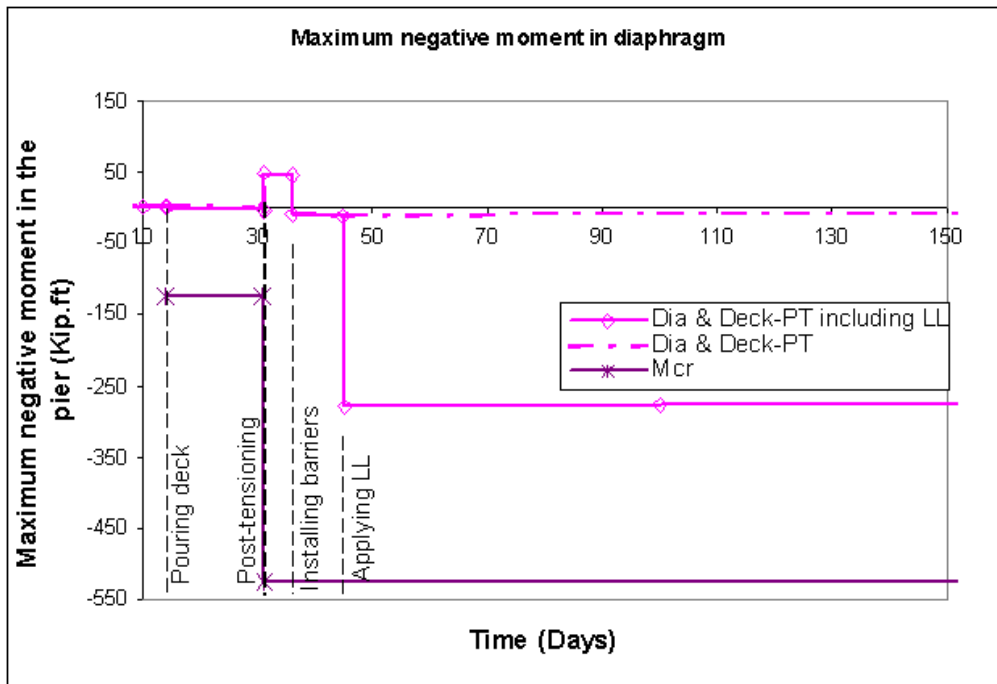


Figure 4. 11 Maximum negative restraining moment in the pier for Dia - Deck-PT construction scenario, P method; continuity established @ 14 days of girder age

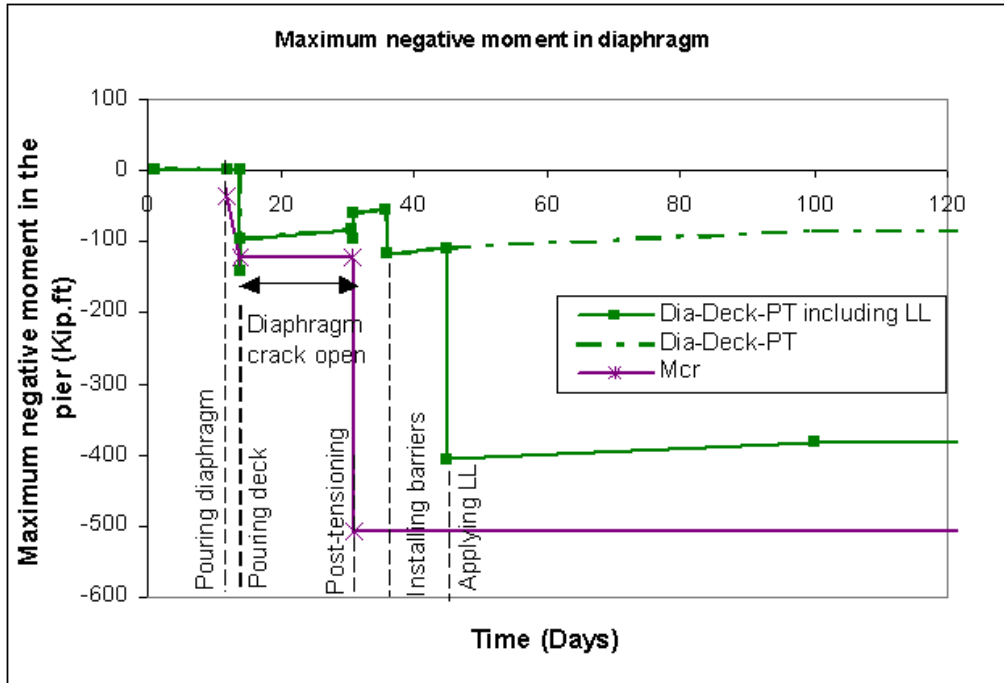


Figure 4. 12 Time-dependent restraining moment in the pier for Dia - Deck -PT construction scenario according to P method

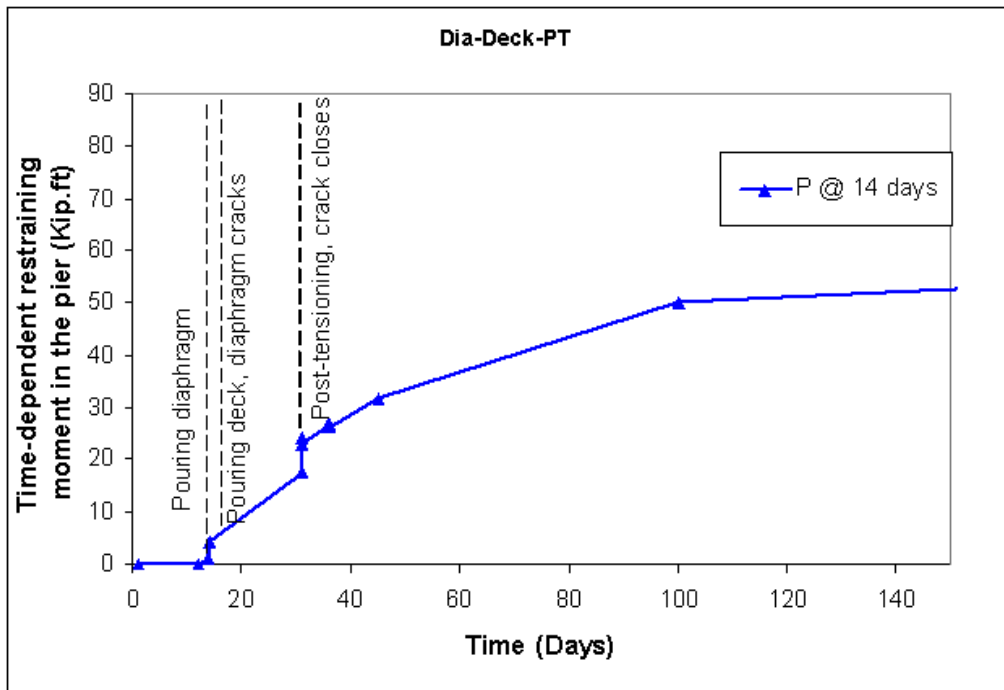


Figure 4. 13 Restraining moment in the pier for Dia - Deck -PT construction scenario resulting from time-dependent effect and secondary moment due to post-tensioning

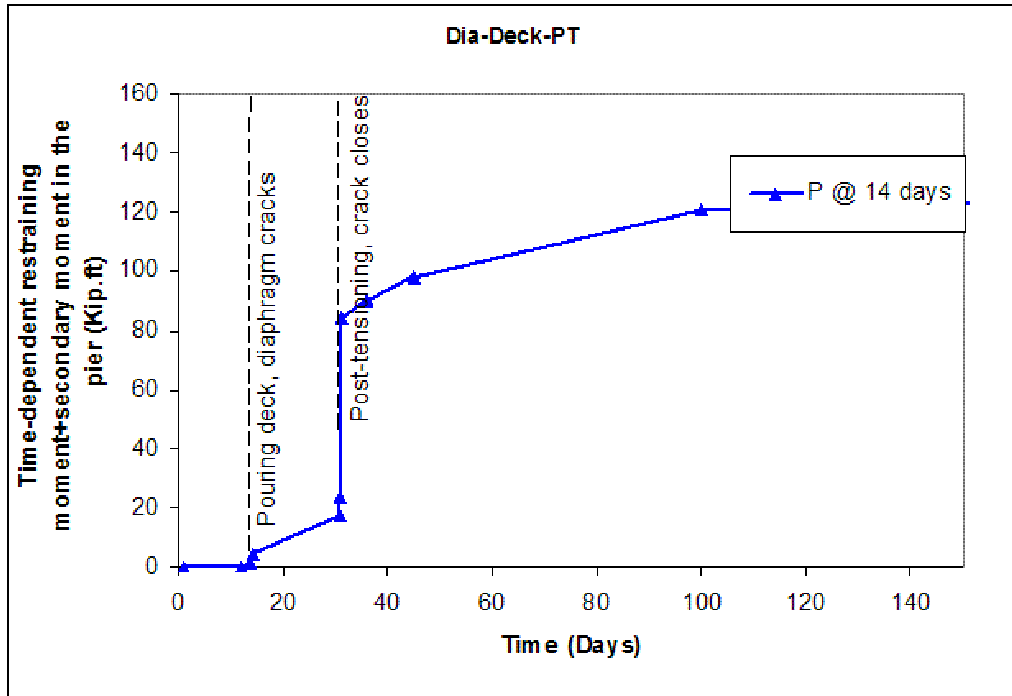


Figure 4. 14 Maximum negative restraining moment in the pier for Dia -PT - Deck construction scenario, P method; continuity established @ 14 days of girder age

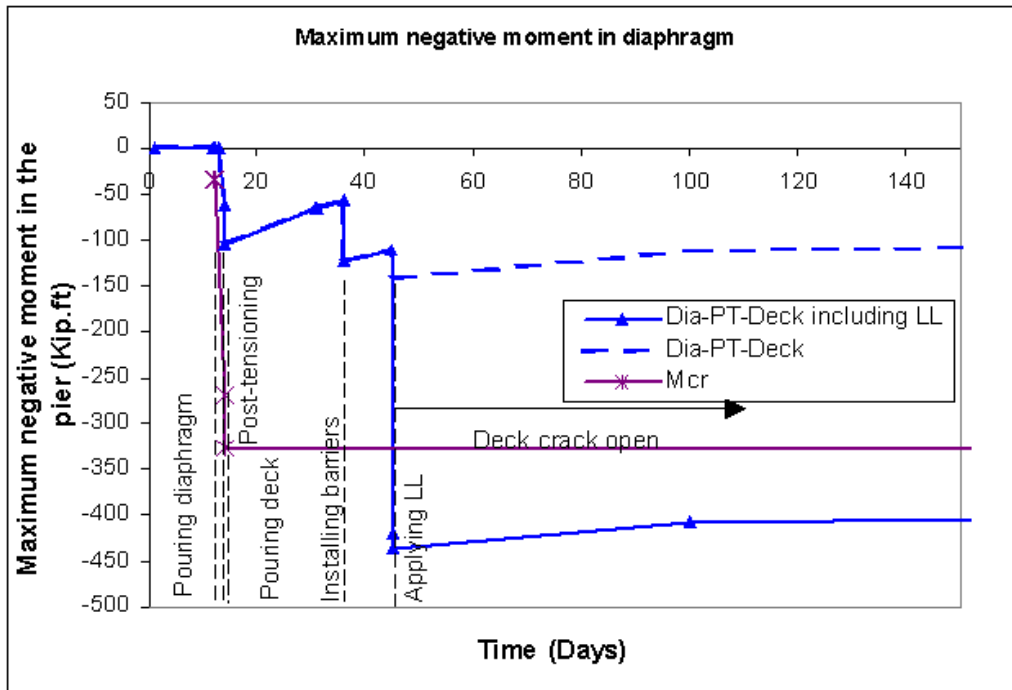


Figure 4. 15 Time-dependent restraining moment in the pier for Dia -PT - Deck construction scenario according to P method

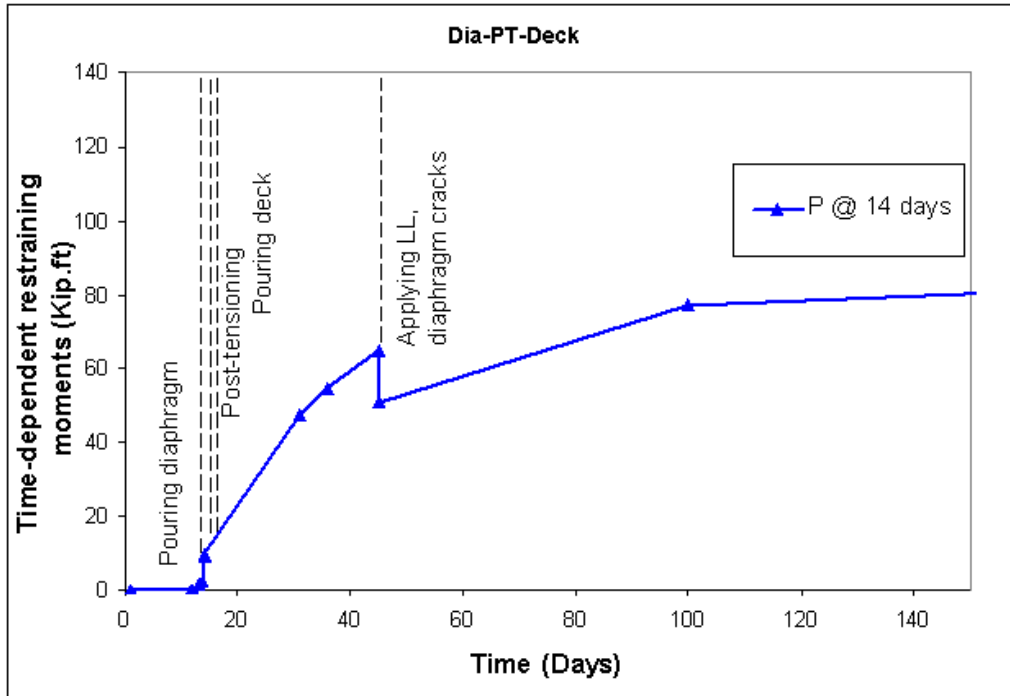


Figure 4. 16 Restraining moment in the pier for Dia – PT - Deck construction scenario resulting from time-dependent effect and secondary moment due to post-tensioning

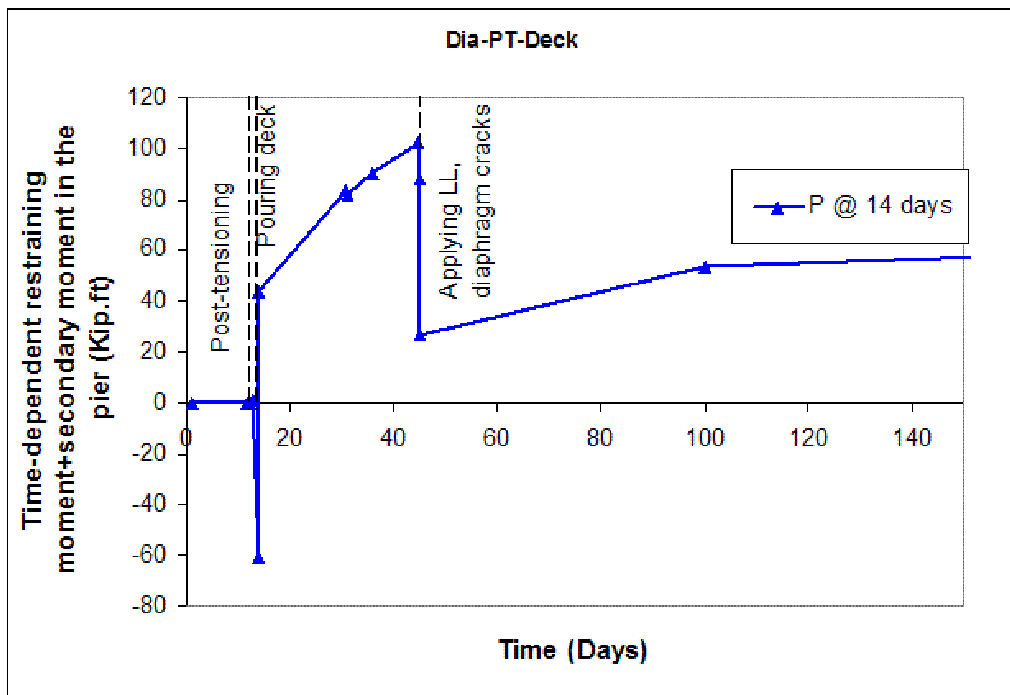


Figure 4. 17 Maximum negative restraining moment in the pier for two-stage PT construction scenario, P method; continuity established @ 14 days of girder age

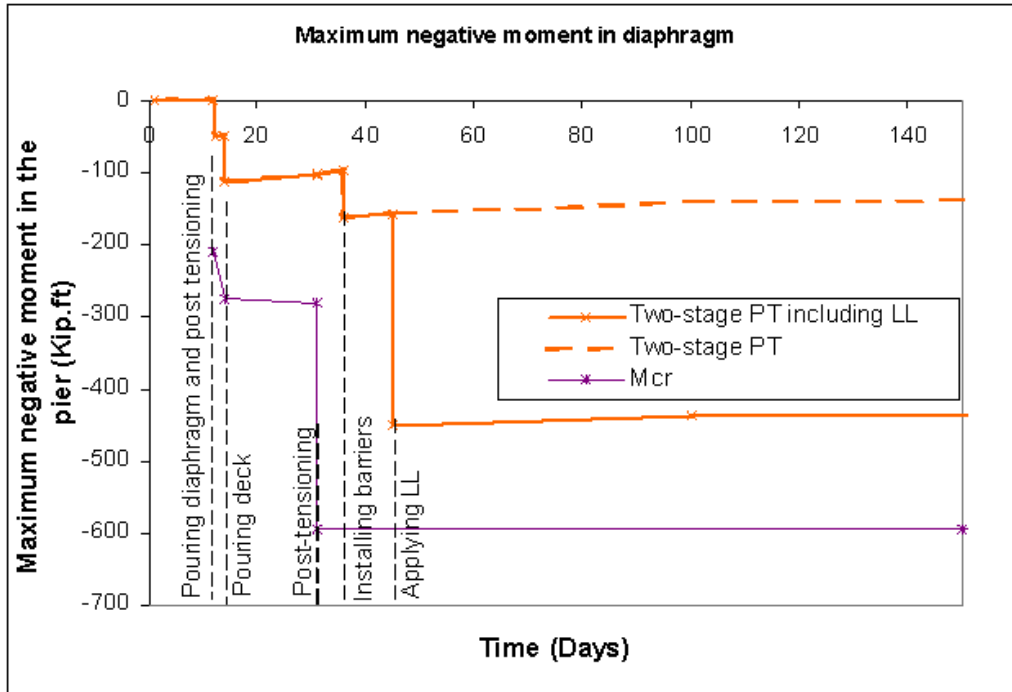


Figure 4. 18 Time-dependent restraining moments using different methods for Dia & Deck-PT construction scenario; continuity established @ 224 days of girder age

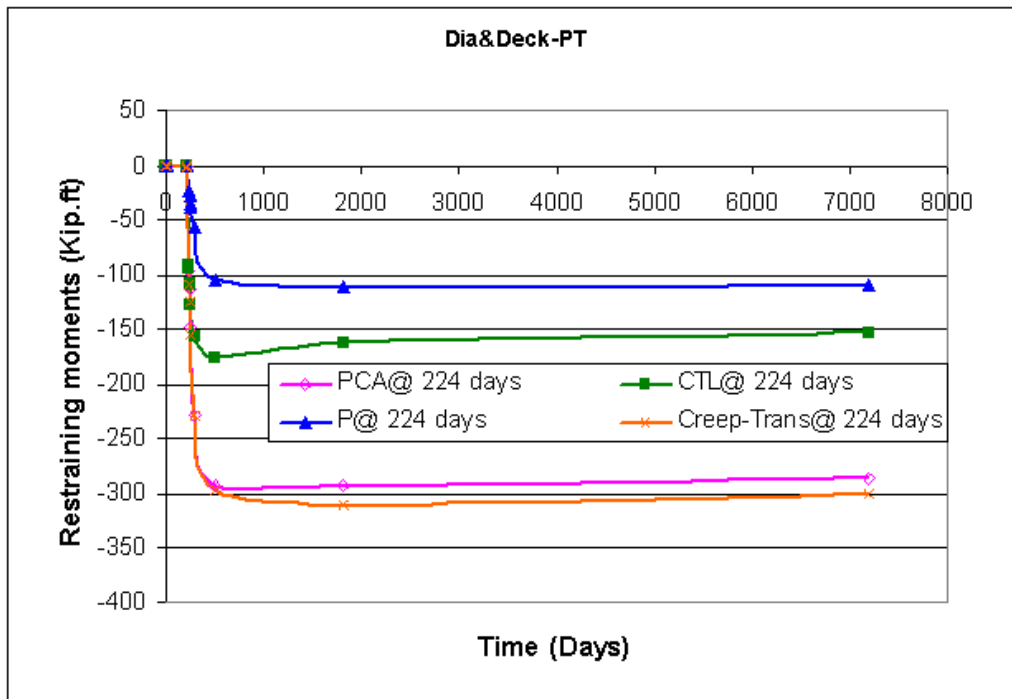


Figure 4. 19 Time-dependent restraining moments using different methods for Dia - Deck-PT construction scenario; continuity established @ 224 days of girder age

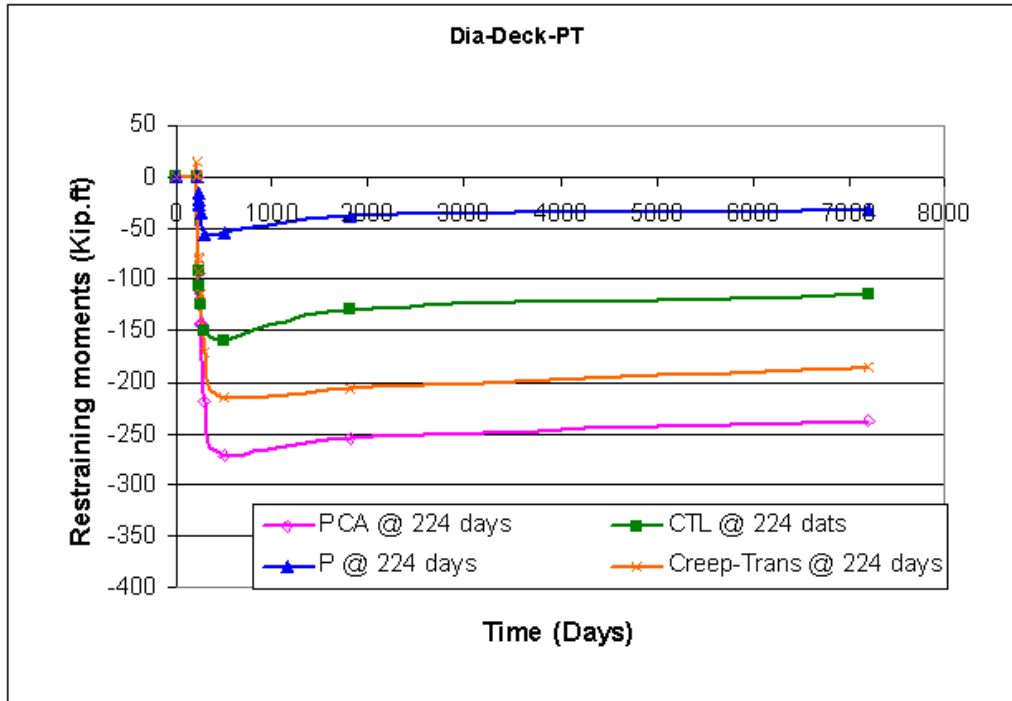


Figure 4. 20 Time-dependent restraining moments using different methods for Dia-PT - Deck construction scenario; continuity established @ 224 days of girder age

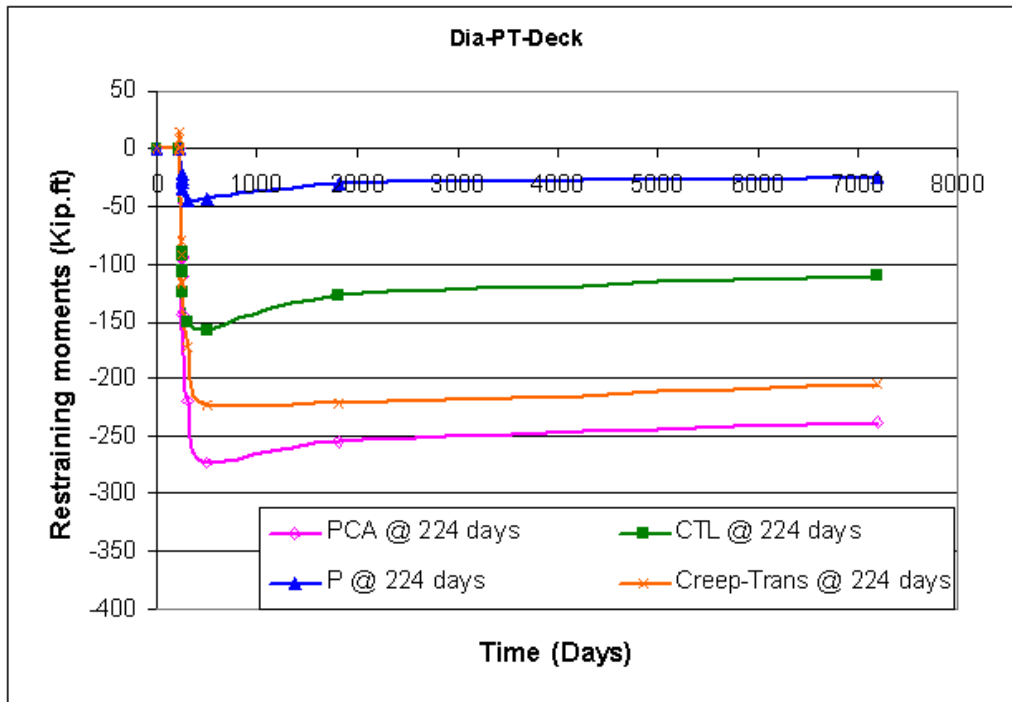


Figure 4. 21 Time-dependent restraining moments using different methods for two-stage PT construction scenario; continuity established @ 224 days of girder age

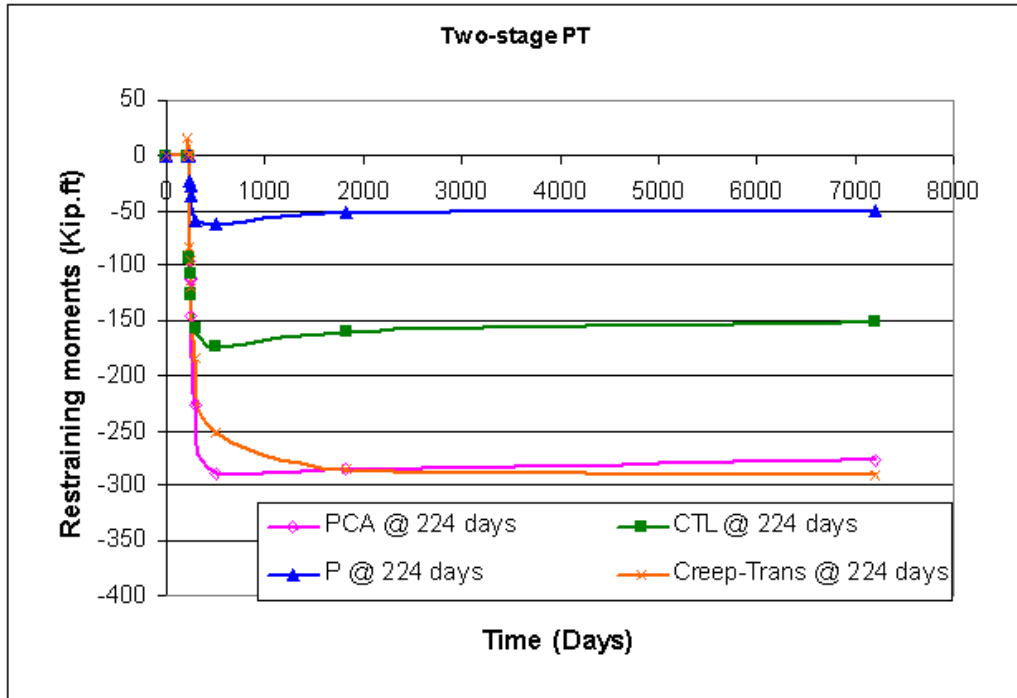


Figure 4. 22 Secondary moment due to post-tensioning for different construction scenarios; continuity established @ 224 days of girder age

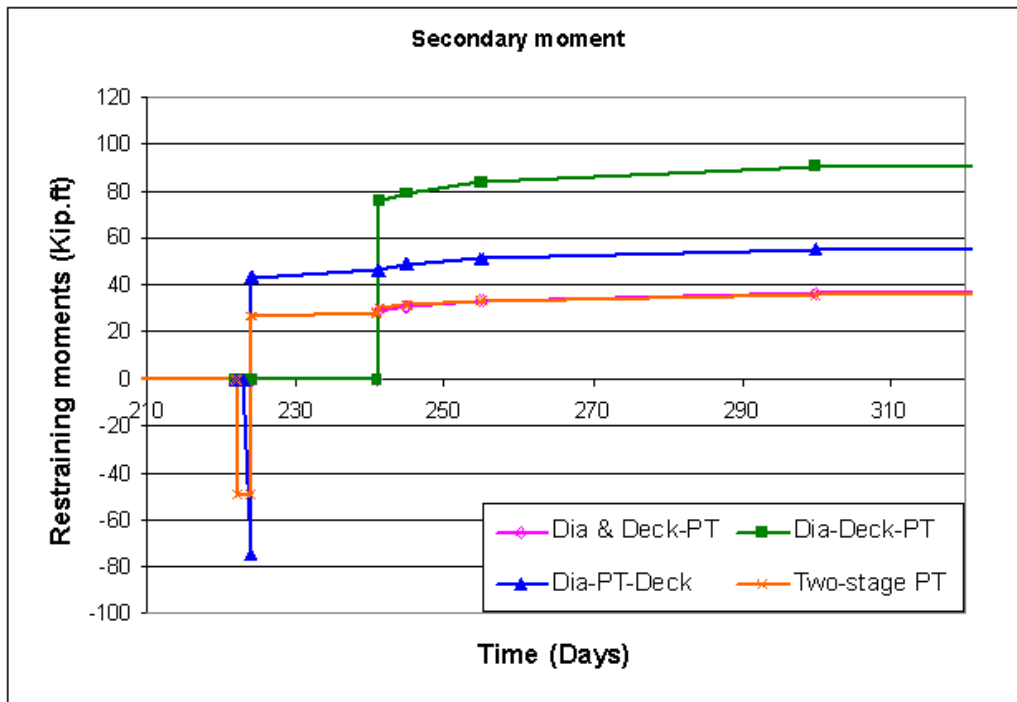


Figure 4. 23 Maximum negative restraining moment in the pier for Dia & Deck-PT construction scenario, P method; continuity established @ 224 days of girder age

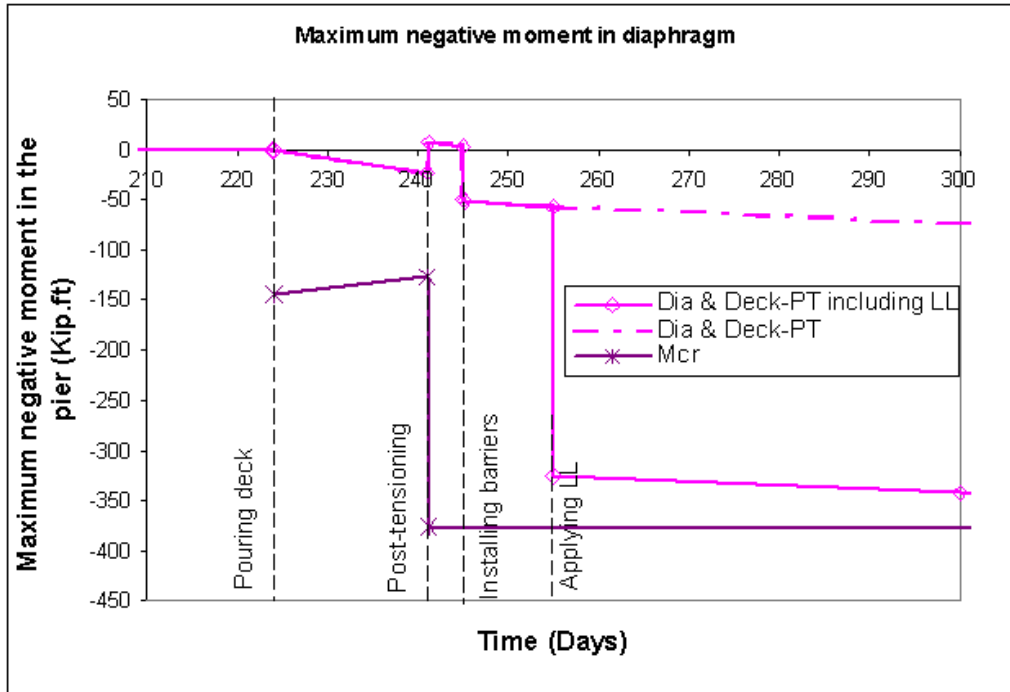


Figure 4. 24 Maximum negative restraining moment in the pier for Dia- Deck- PT construction scenario, P method; continuity established @ 224 days of girder age

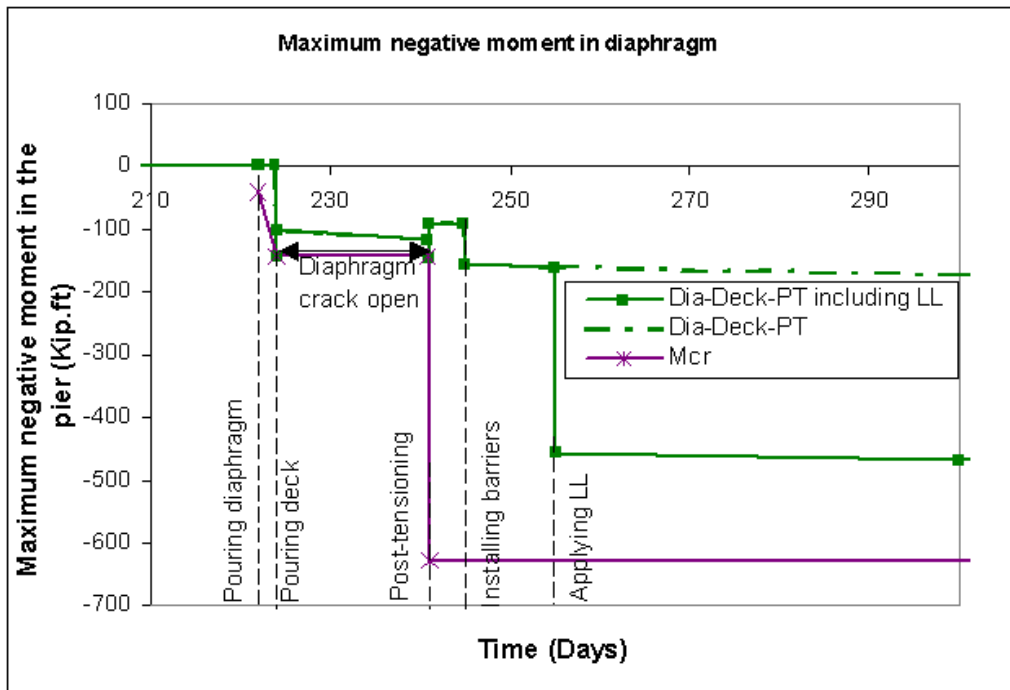


Figure 4. 25 Time-dependent restraining moment in the pier for Dia - Deck -PT construction scenario according to P method

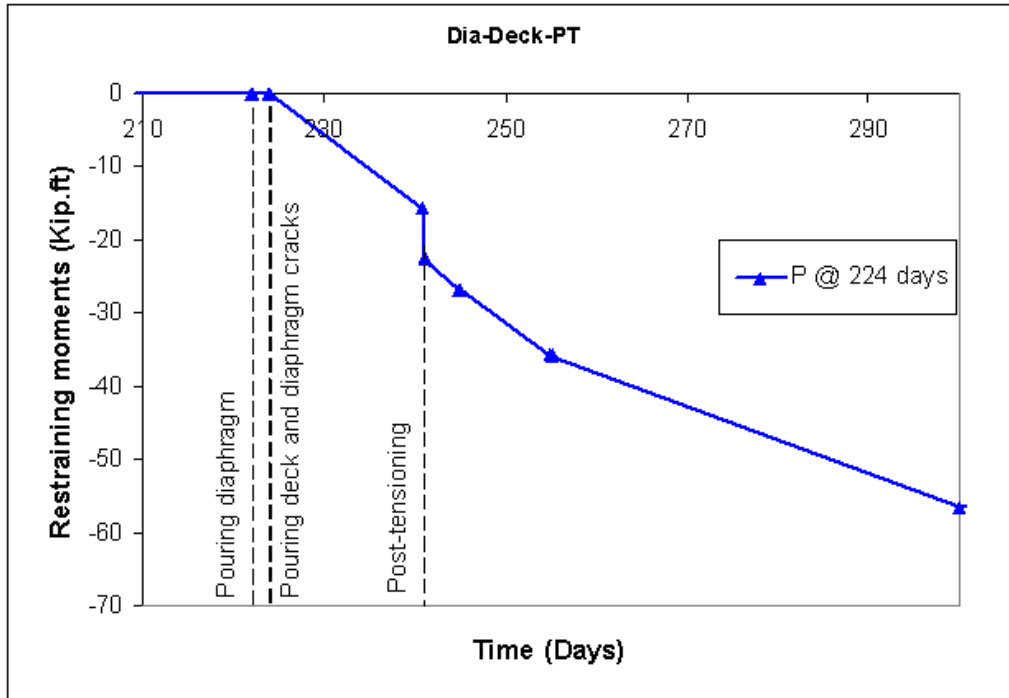


Figure 4. 26 Restraining moment in the pier for Dia - Deck -PT construction scenario resulting from time-dependent effect and secondary moment due to post-tensioning

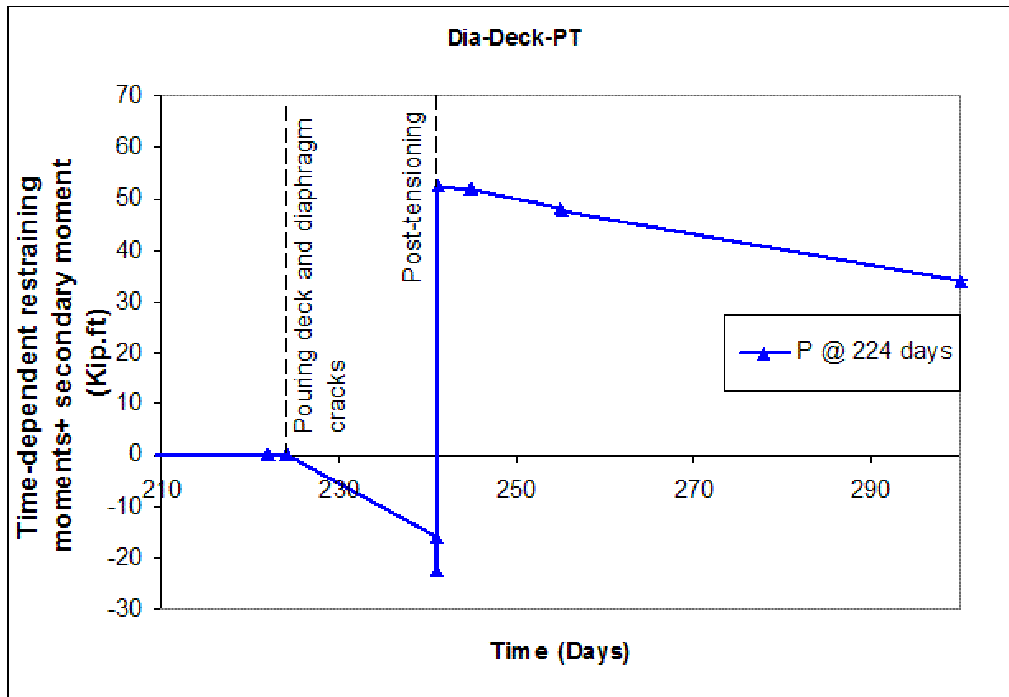


Figure 4. 27 Maximum negative restraining moment in the pier for Dia- PT- Deck construction scenario, P method; continuity established @ 224 days of girder age

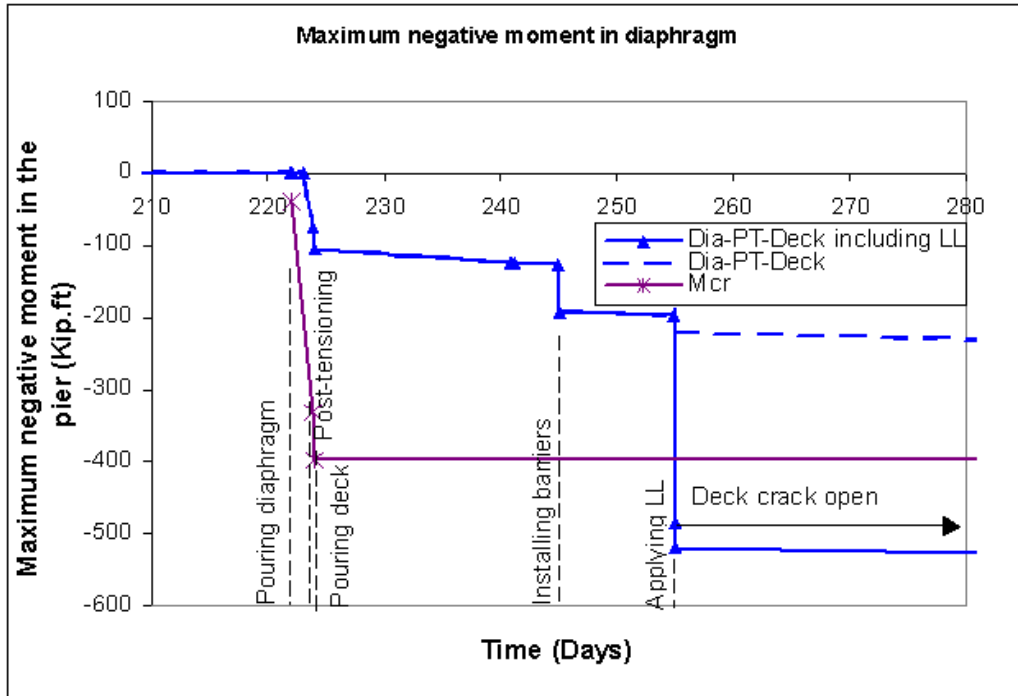


Figure 4. 28 Time-dependent restraining moment in the pier for Dia-PT- Deck construction scenario according to P method

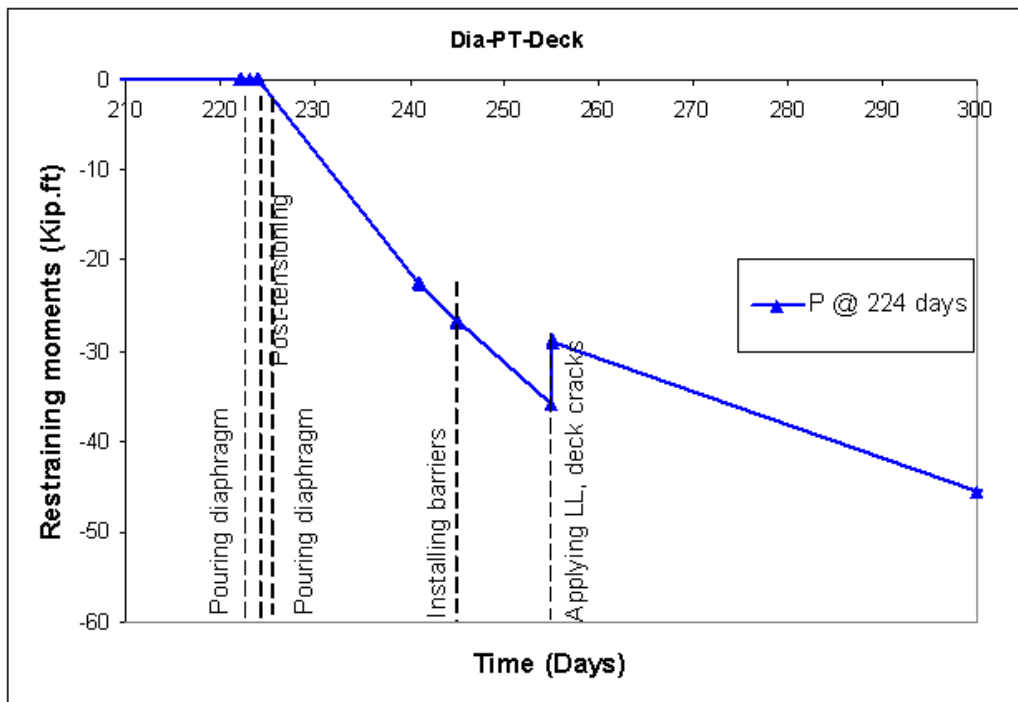


Figure 4. 29 Restraining moment in the pier for Dia -PT- Deck construction scenario resulting from time-dependent effect and secondary moment due to post-tensioning

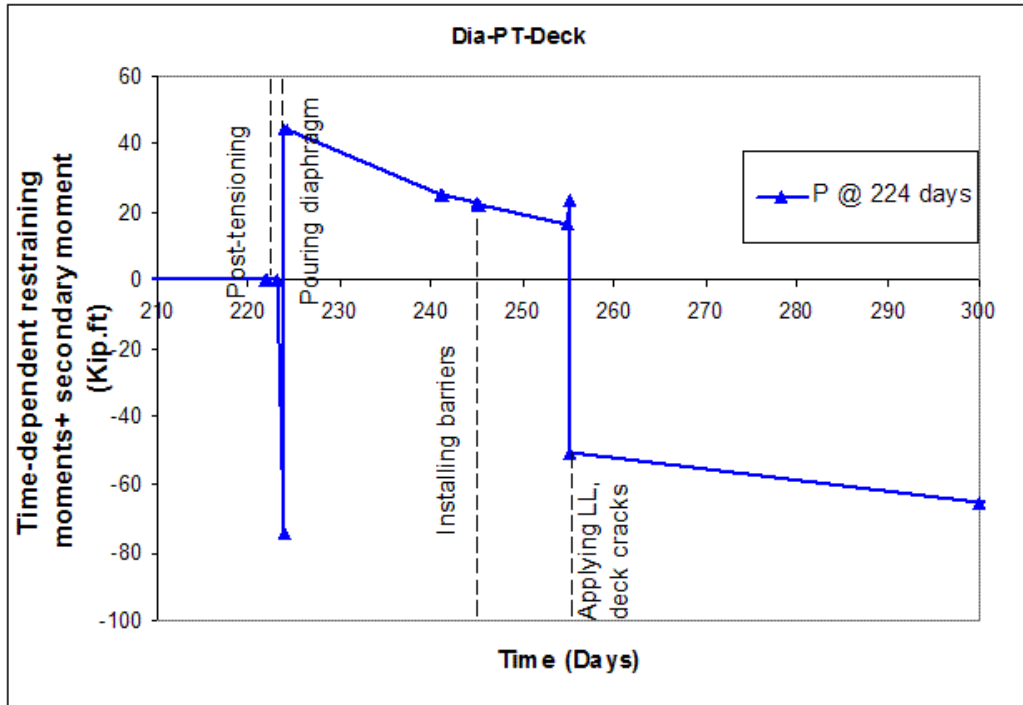


Figure 4. 30 Maximum negative restraining moment in the pier for two-stage PT construction scenario, P method; continuity established @ 224 days of girder age

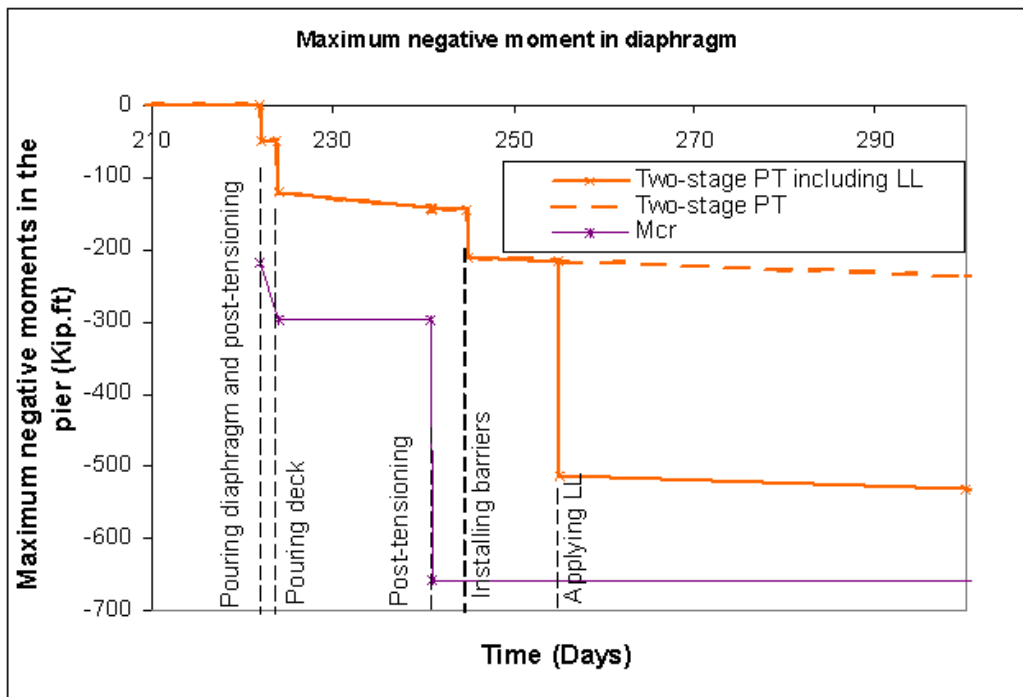


Figure 4. 31 Shear reinforcement detailing for Dia & Deck-PT construction scenario

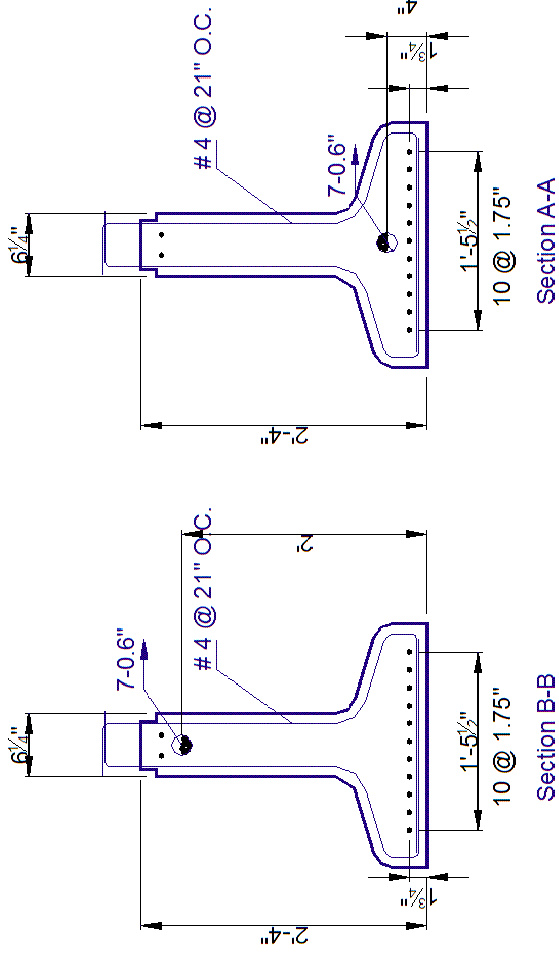


Figure 4. 32 Shear reinforcement detailing for Dia & Deck-PT construction scenario

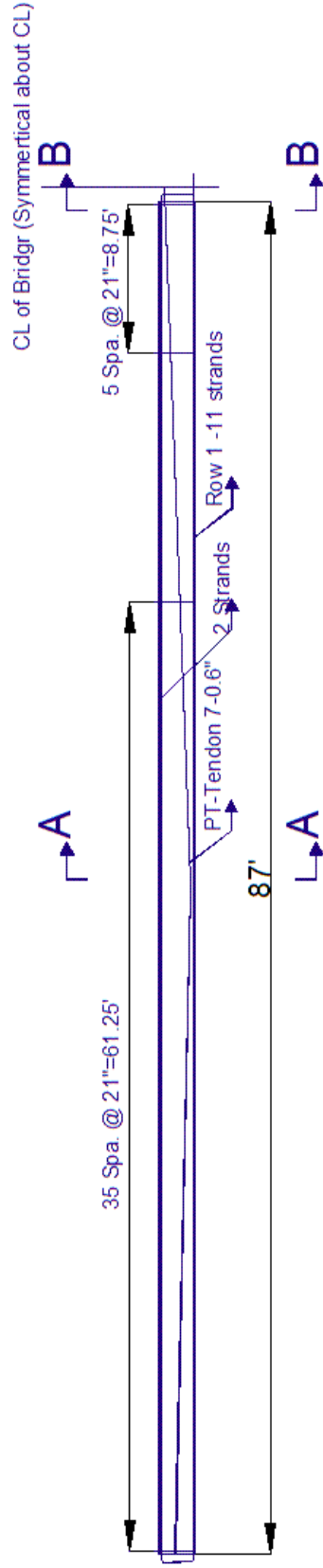


Figure 4. 33 Shear reinforcement detailing for Dia -Deck-PT construction scenario

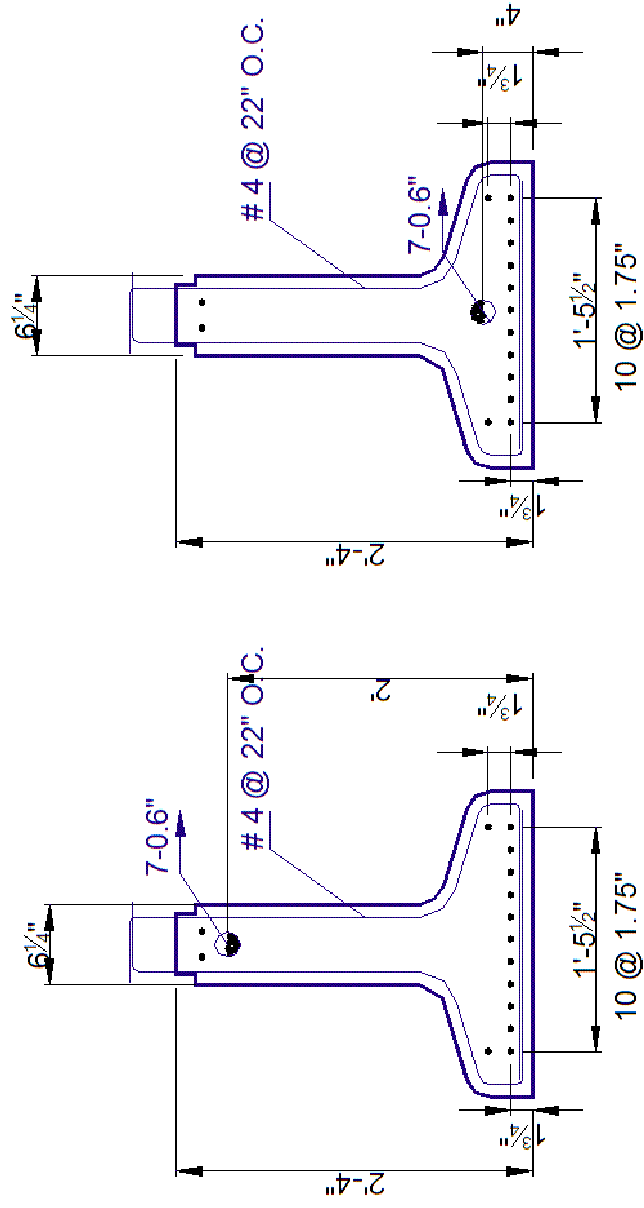


Figure 4. 34 Shear reinforcement detailing for Dia -Deck-PT construction scenario

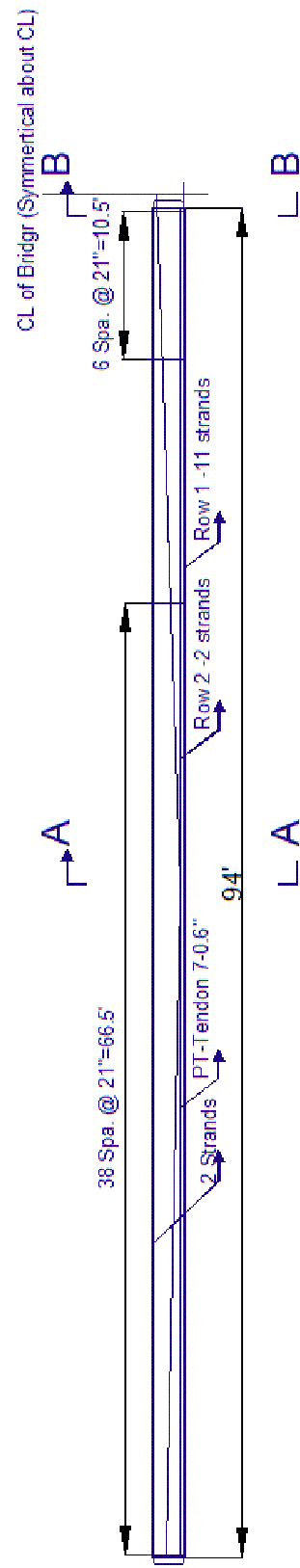


Figure 4. 35 Shear reinforcement detailing for Dia –PT - Deck construction scenario

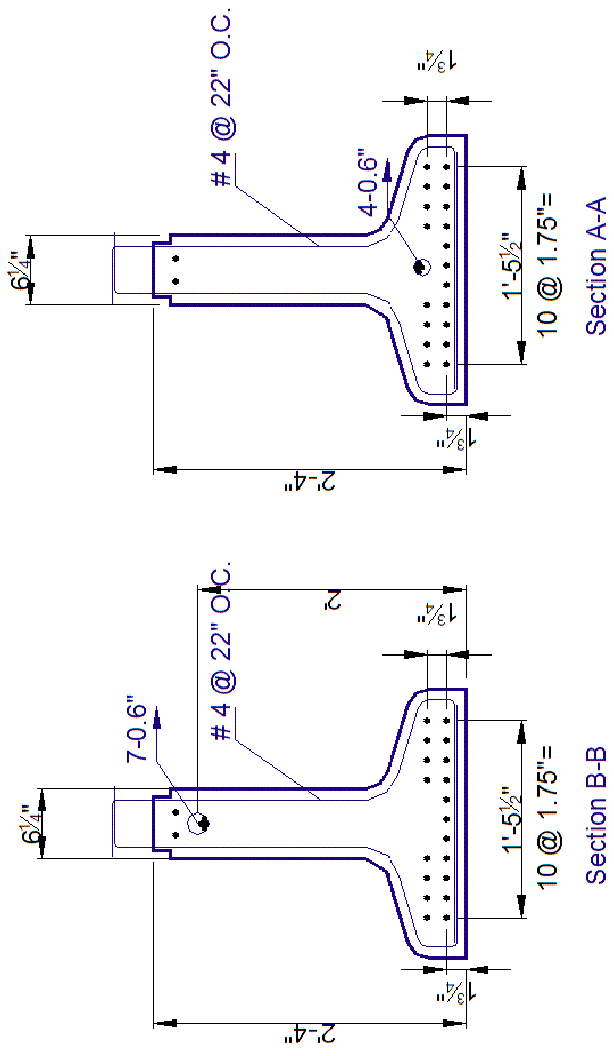


Figure 4. 36 Shear reinforcement detailing for Dia –PT - Deck construction scenario

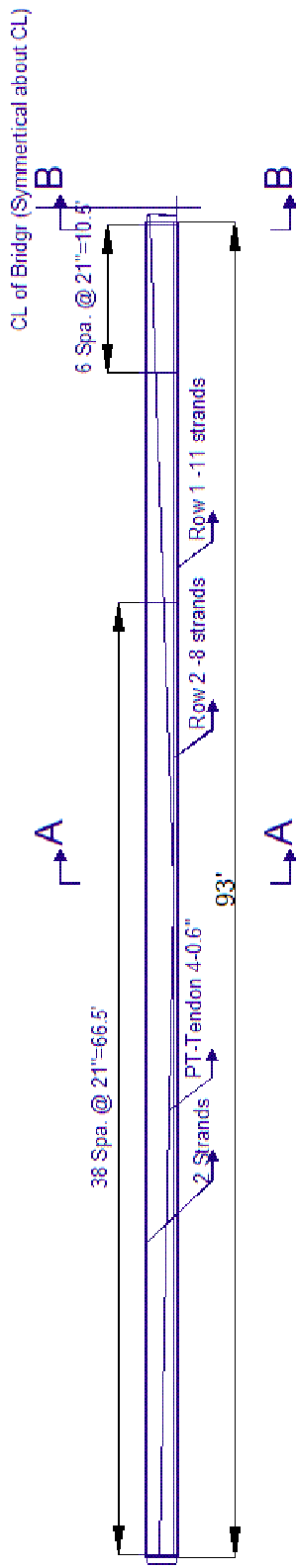


Figure 4. 37 Shear reinforcement detailing for two-stage PT construction scenario

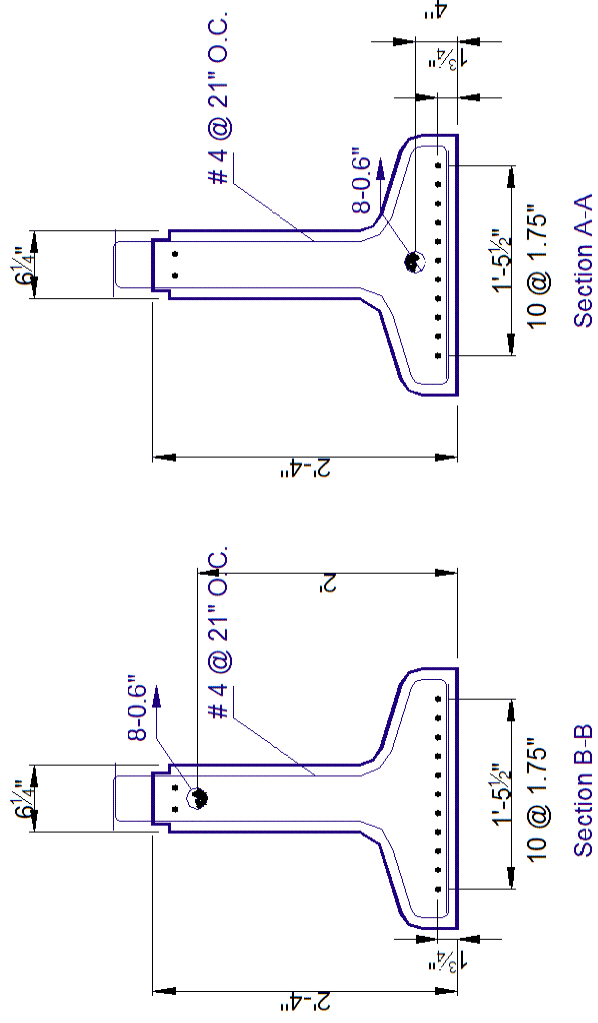


Figure 4. 38 Shear reinforcement detailing for two-stage PT construction scenario

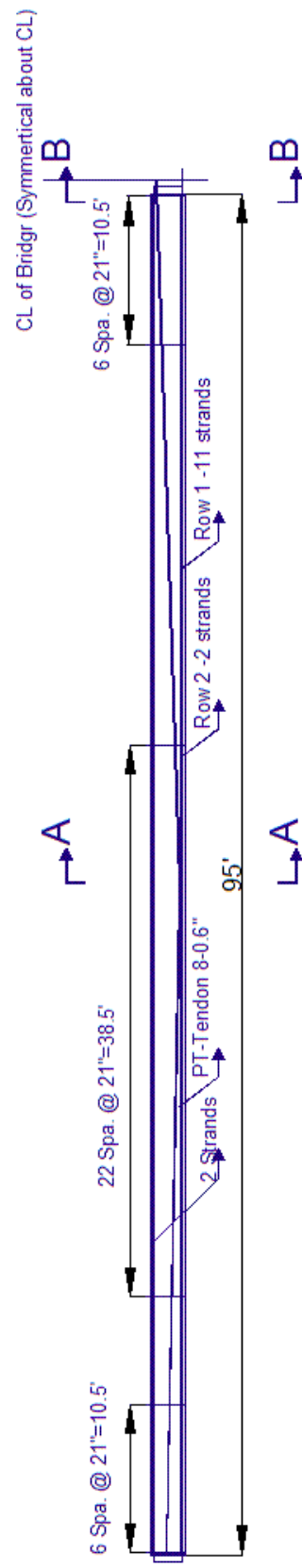


Figure 4. 39 Time-dependent restraining moment in the pier for different concrete strength of the girder using PCA method

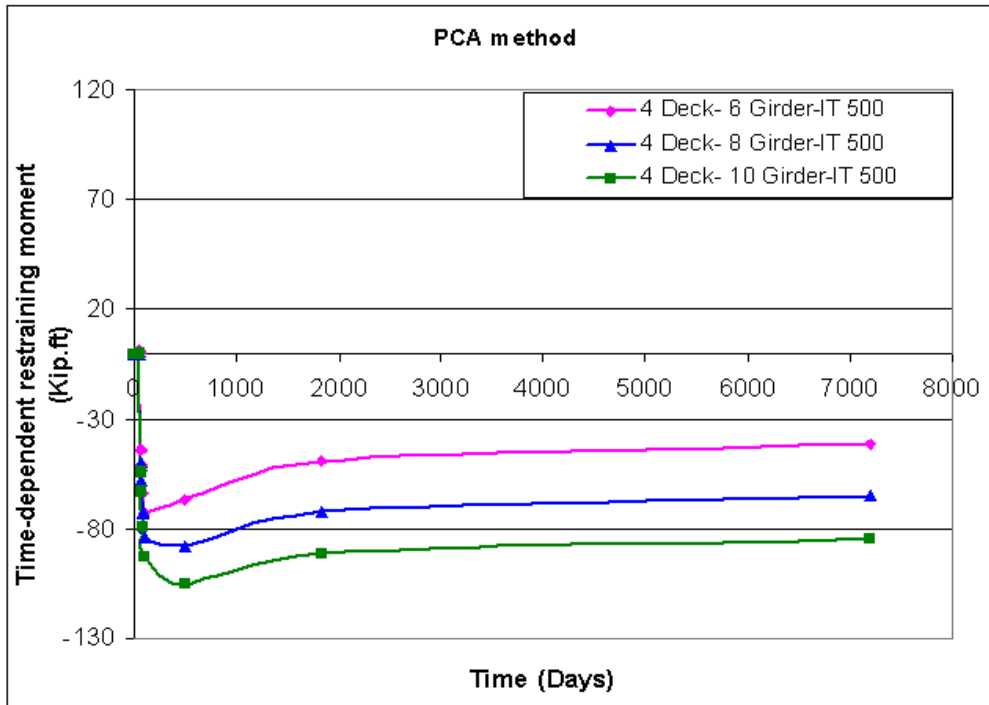


Figure 4. 40 Time-dependent restraining moment in the pier for different concrete strength of the girder using CTL method

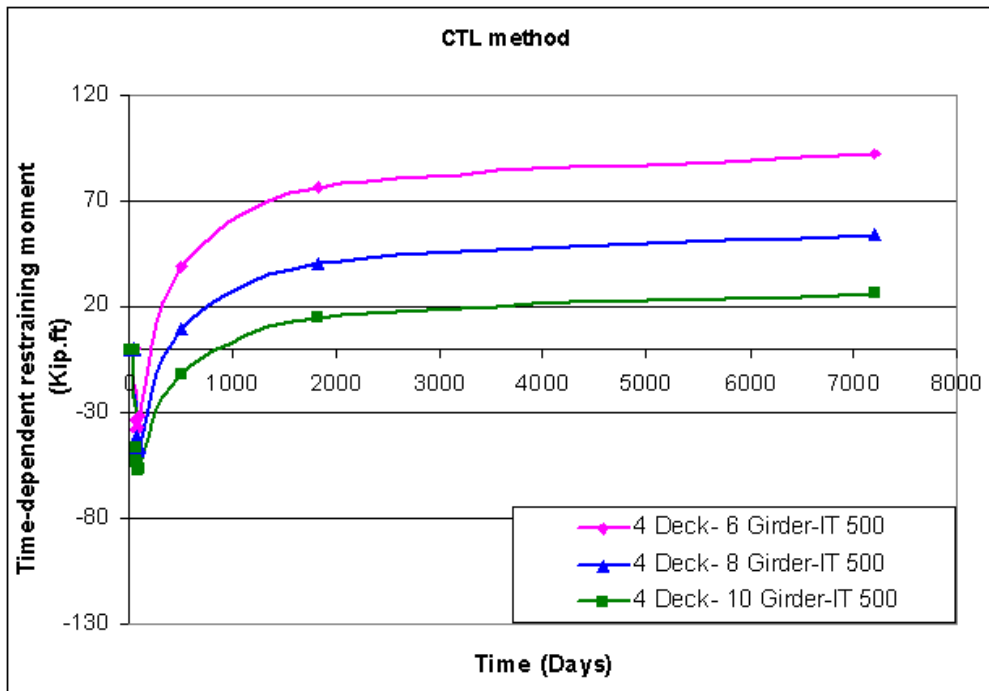


Figure 4. 41 Time-dependent restraining moment in the pier for different concrete strength of the girder using P method

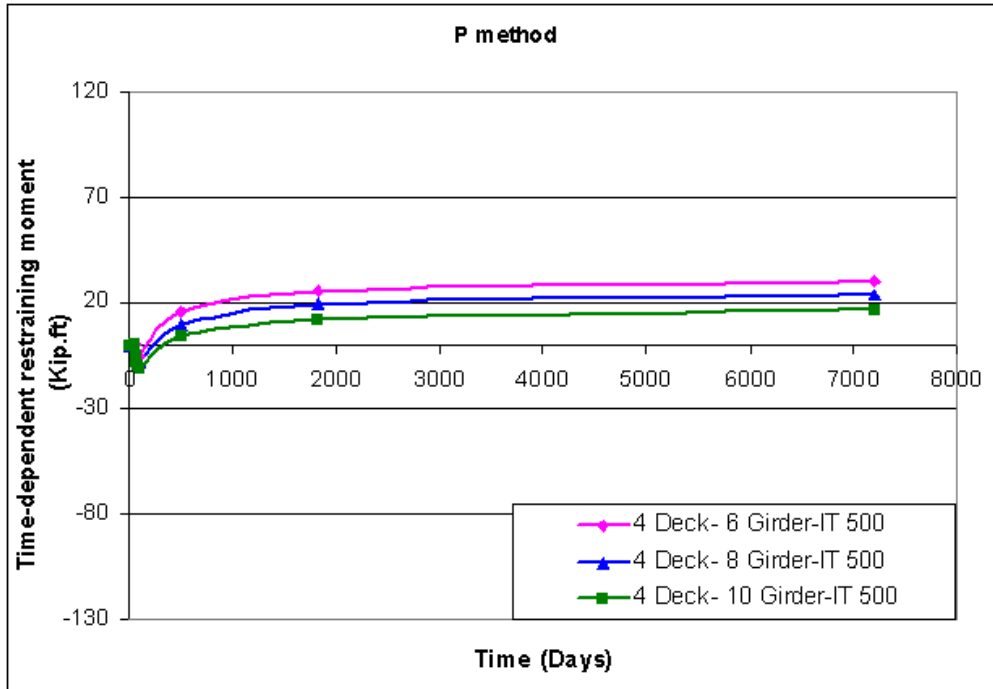


Figure 4. 42 Time-dependent restraining moment in the pier for different concrete strength of the girder using creep-transformed section properties method

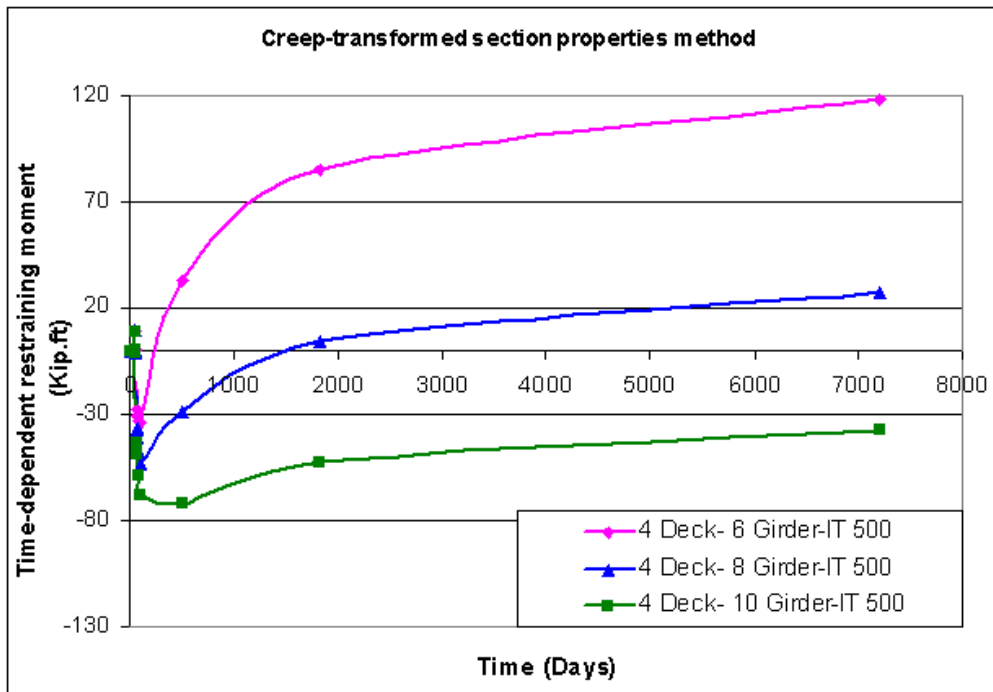


Figure 4. 43 Time-dependent restraining moment due to creep under prestressing, according to CTL method

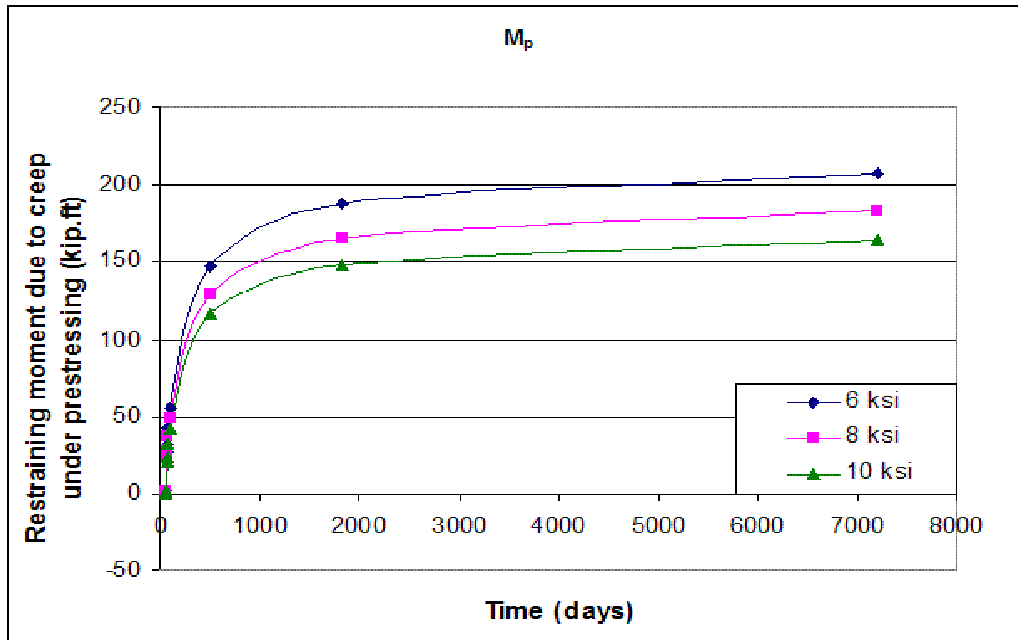


Figure 4. 44 Time-dependent restraining moment due to creep under girder weight, according to CTL method

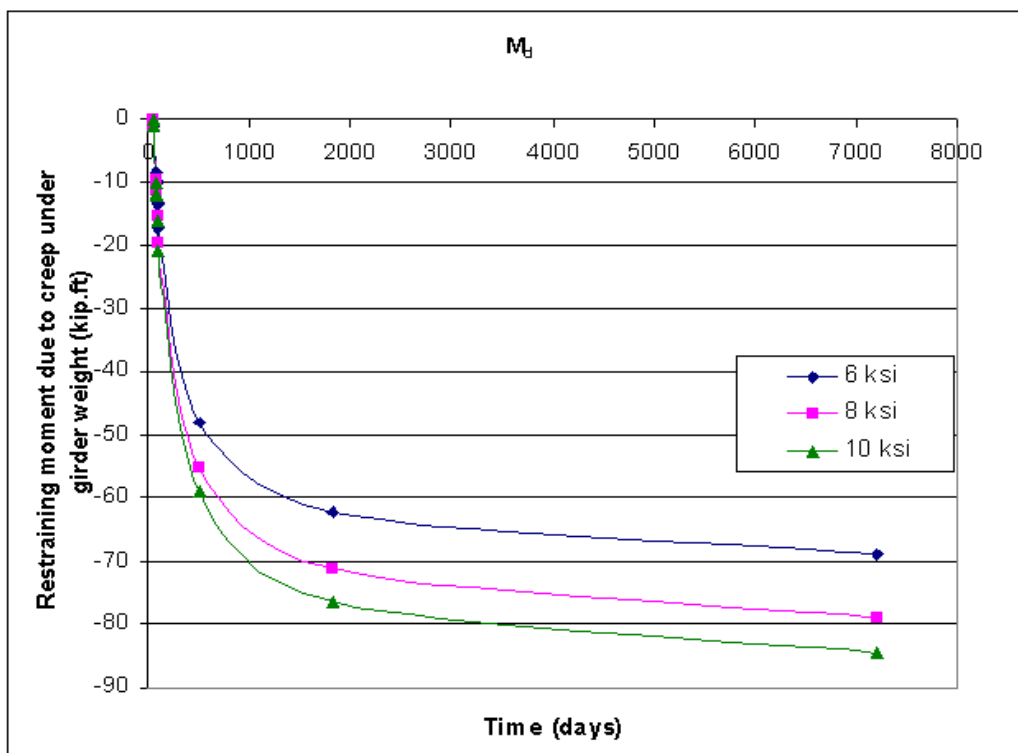


Figure 4. 45 Time-dependent restraining moment due to differential shrinkage, according to CTL method

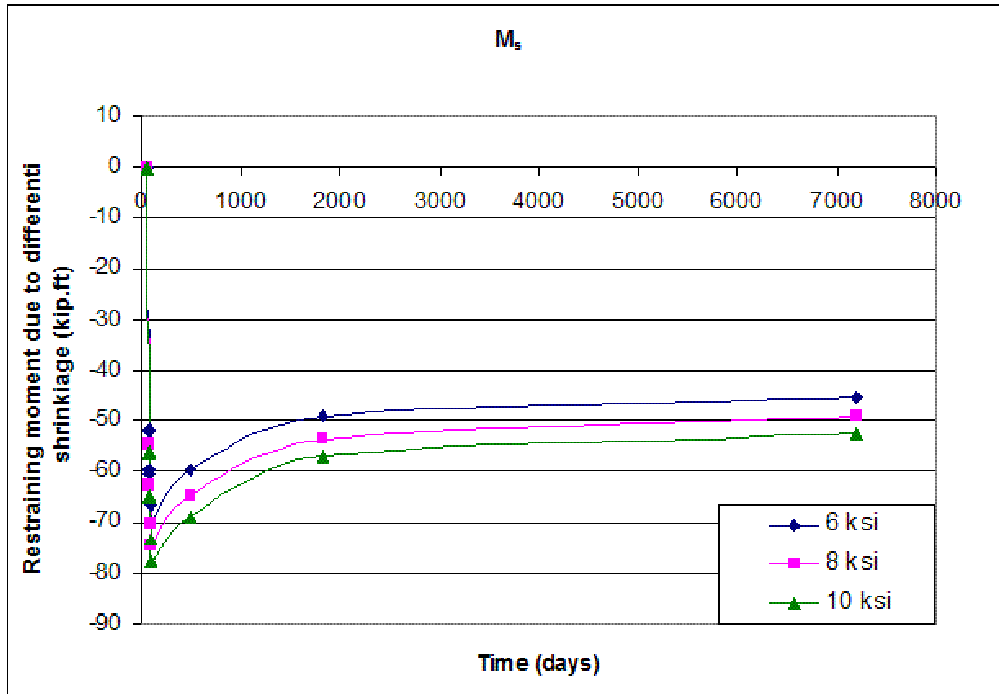


Figure 4. 46 Losses in prestressing strands for different concrete strengths

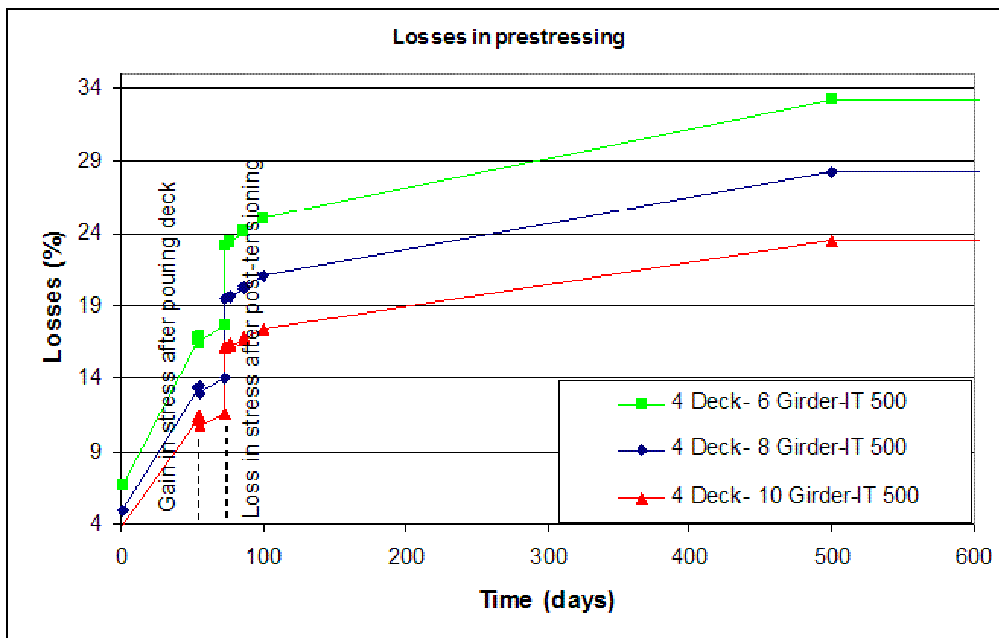


Figure 4. 47 Losses in post-tensioning tendons for different concrete strengths

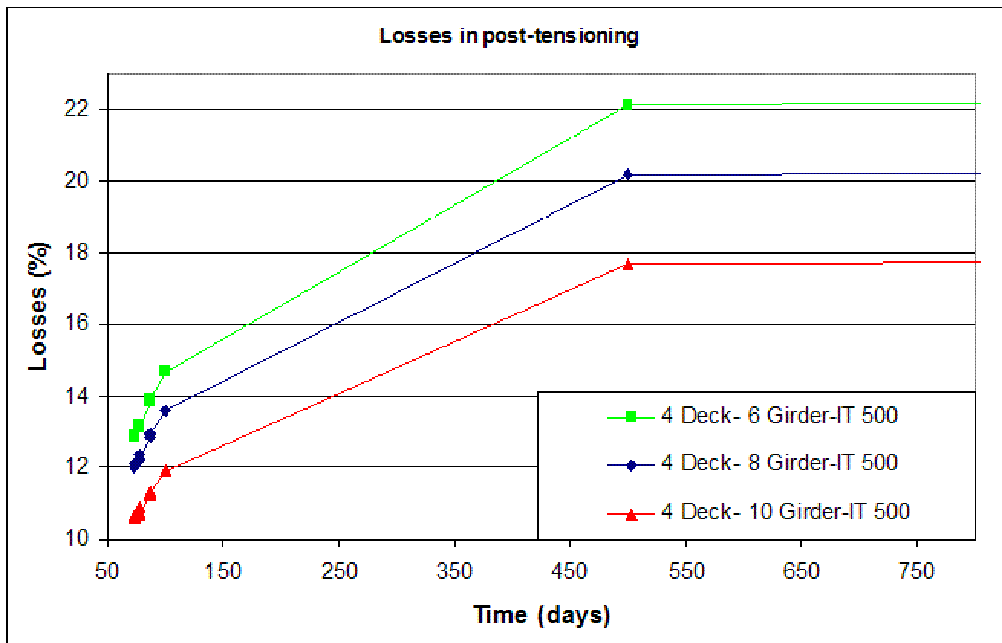


Figure 4. 48 Time-dependent restraining moment for different concrete strengths of the deck using CTL method

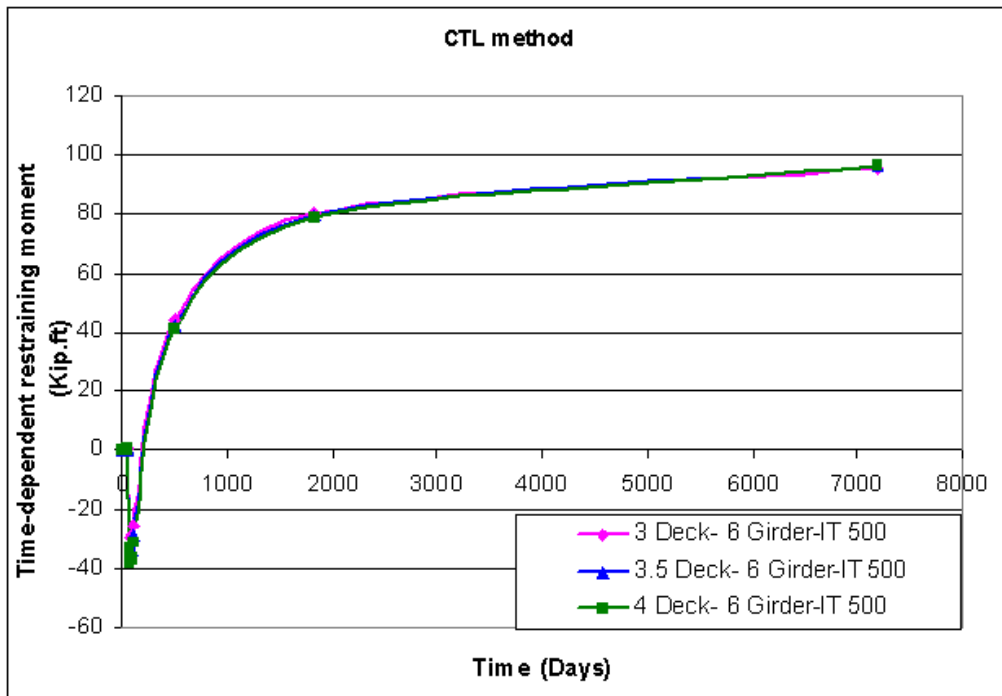


Figure 4. 49 Time-dependent restraining moment for different concrete strengths of the deck using P method

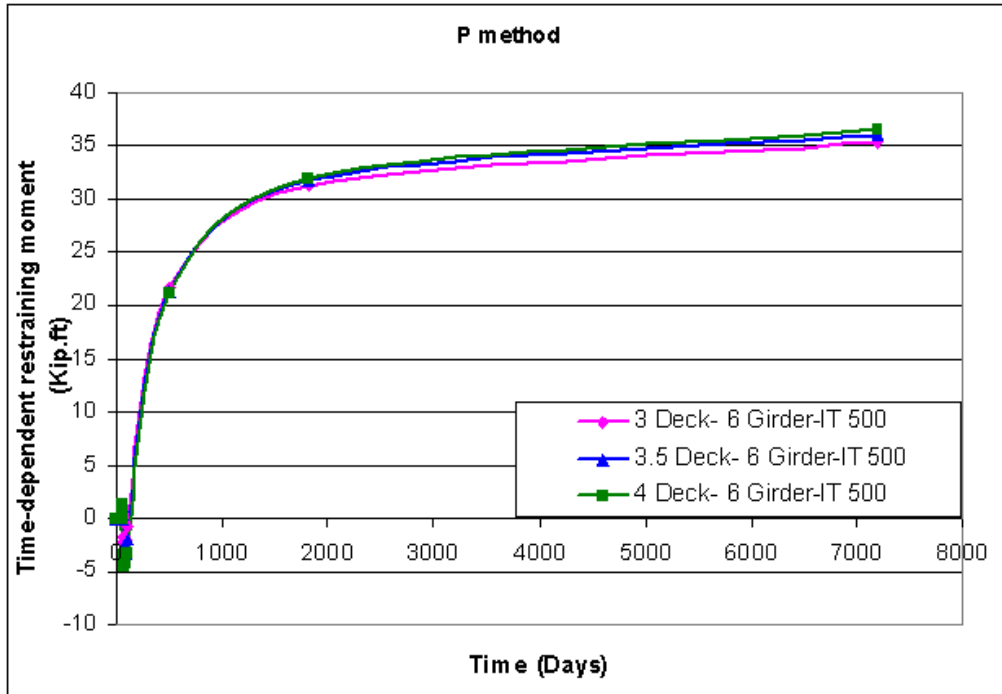


Figure 4. 50 Prediction of shrinkage strain using different models for 6-ksi concrete

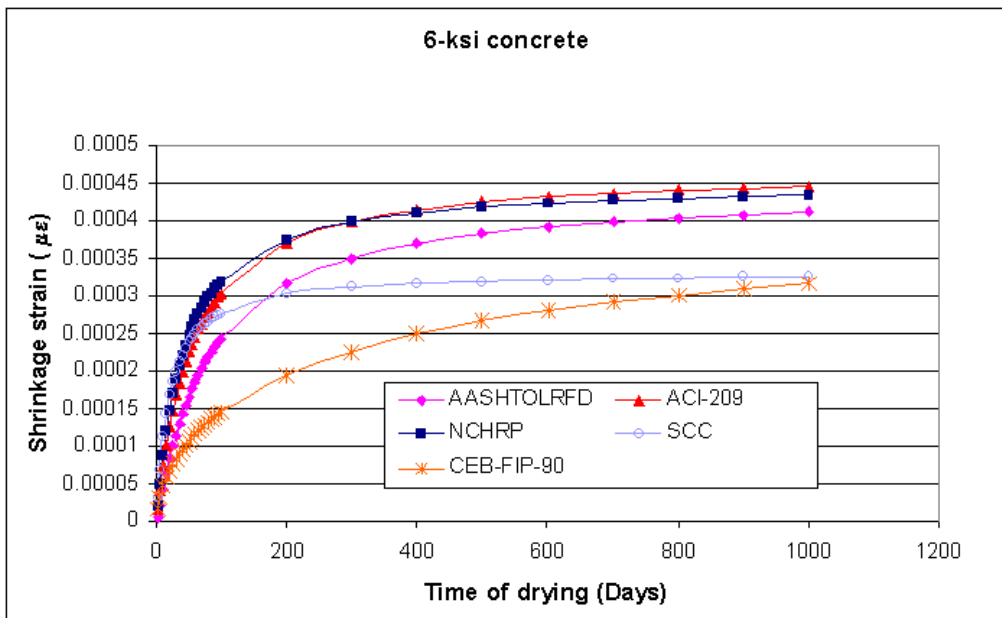


Figure 4. 51 Prediction of creep coefficient using different models for 6-ksi concrete

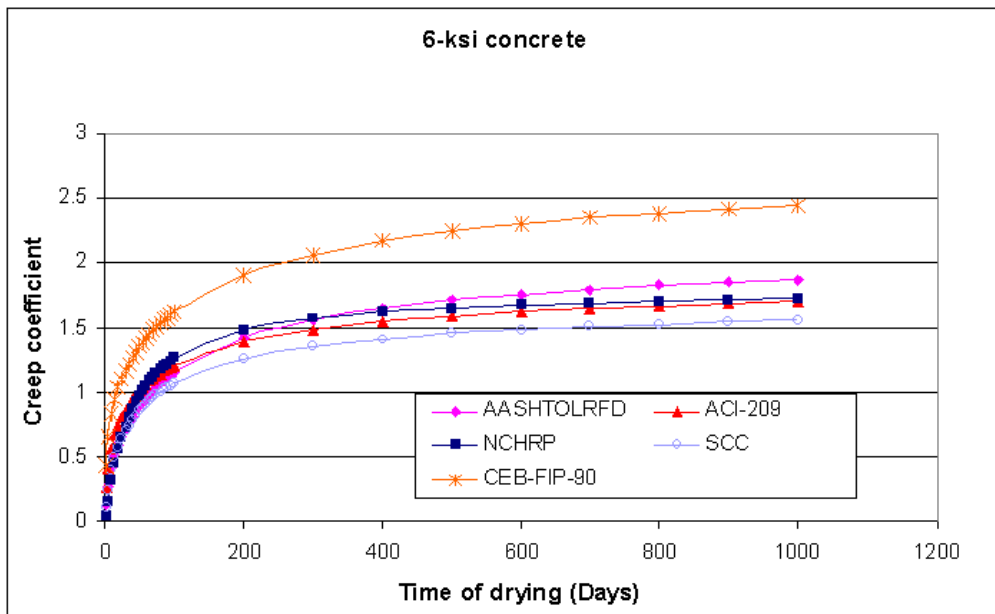


Figure 4. 52 Prediction of shrinkage strain using different models for 10-ksi concrete

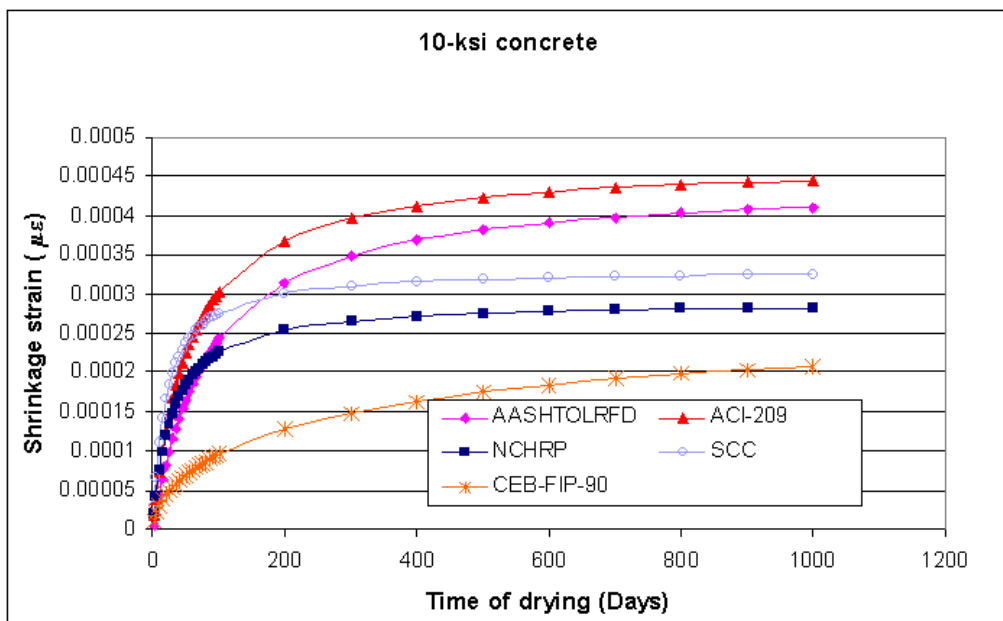


Figure 4. 53 Prediction of creep coefficient using different models for 10-ksi concrete

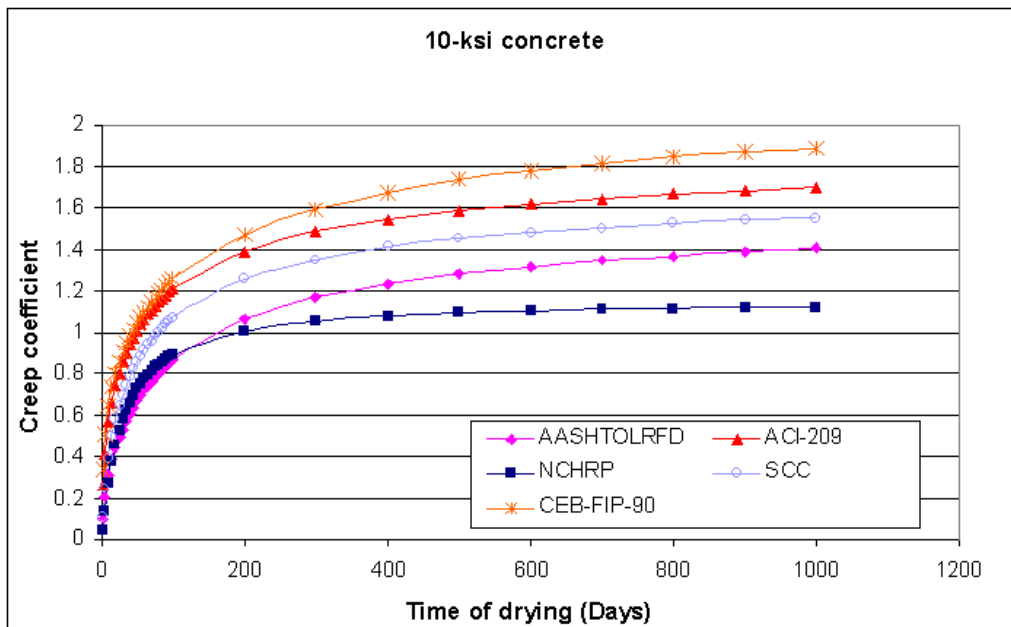


Figure 4. 54 Predicted losses in prestensioned strands using different models

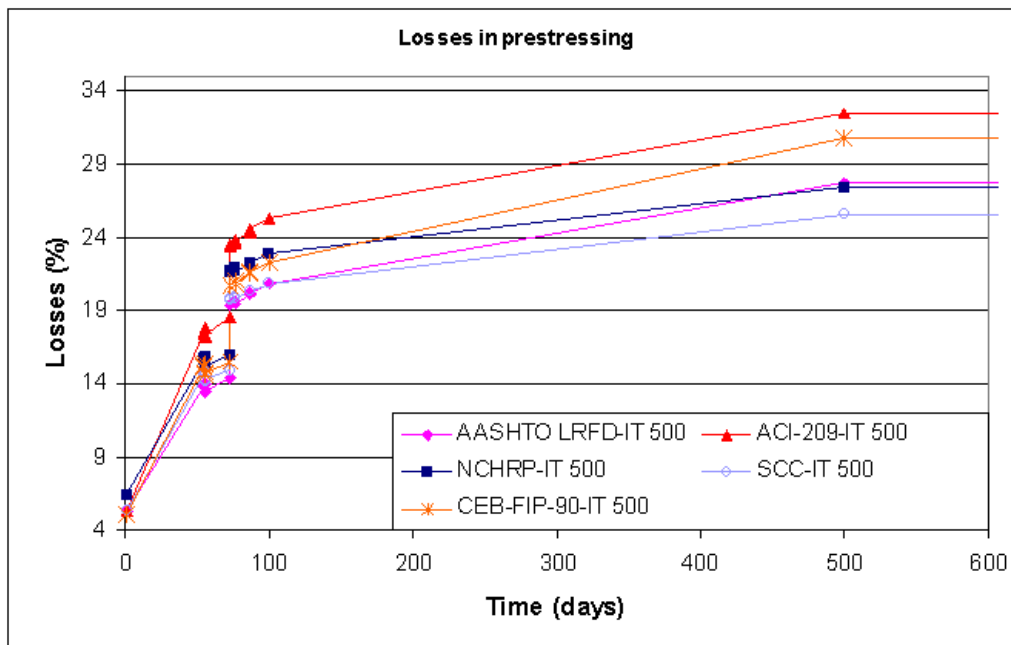


Figure 4. 55 Predicted losses in post-tensioning using different models

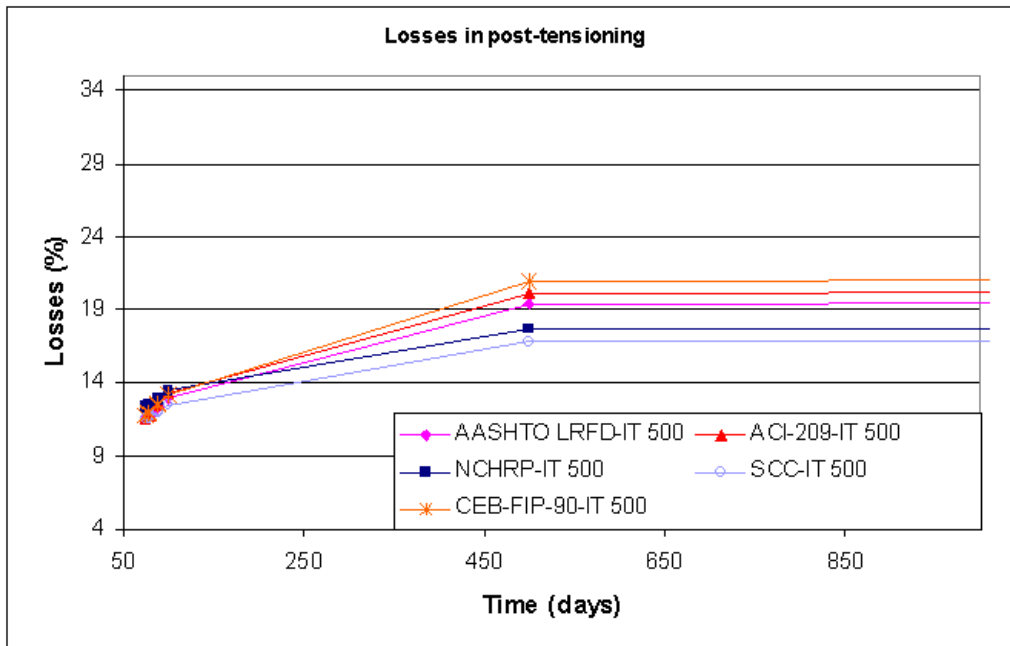


Figure 4. 56 Time-dependent restraining moment for different creep-and-shrinkage models using PCA method

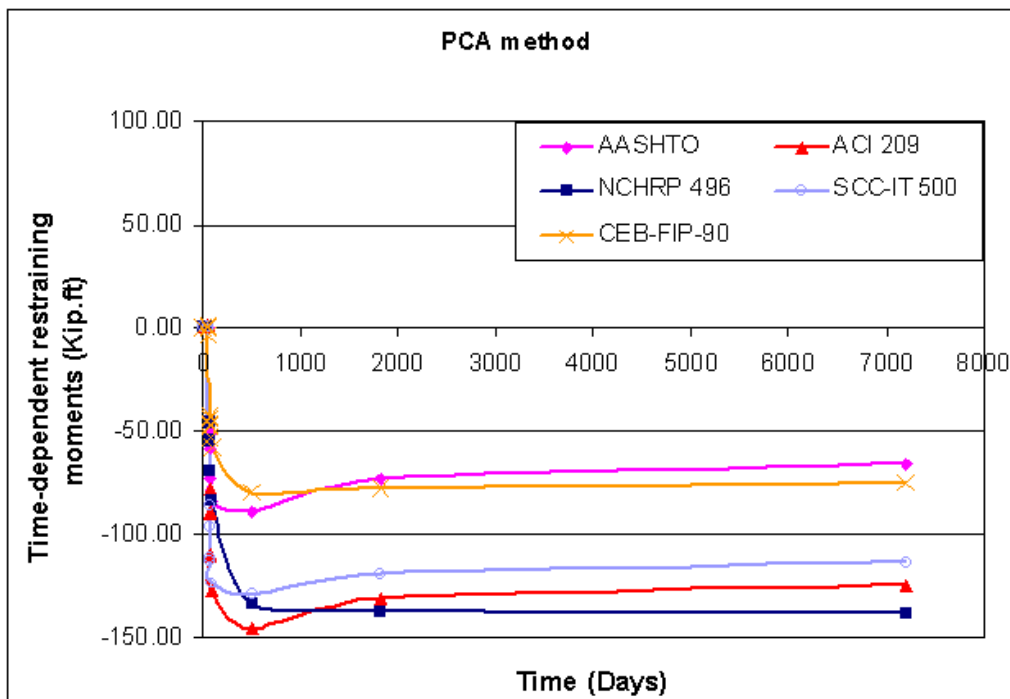


Figure 4. 57 Time-dependent restraining moment for different creep-and-shrinkage models using CTL method

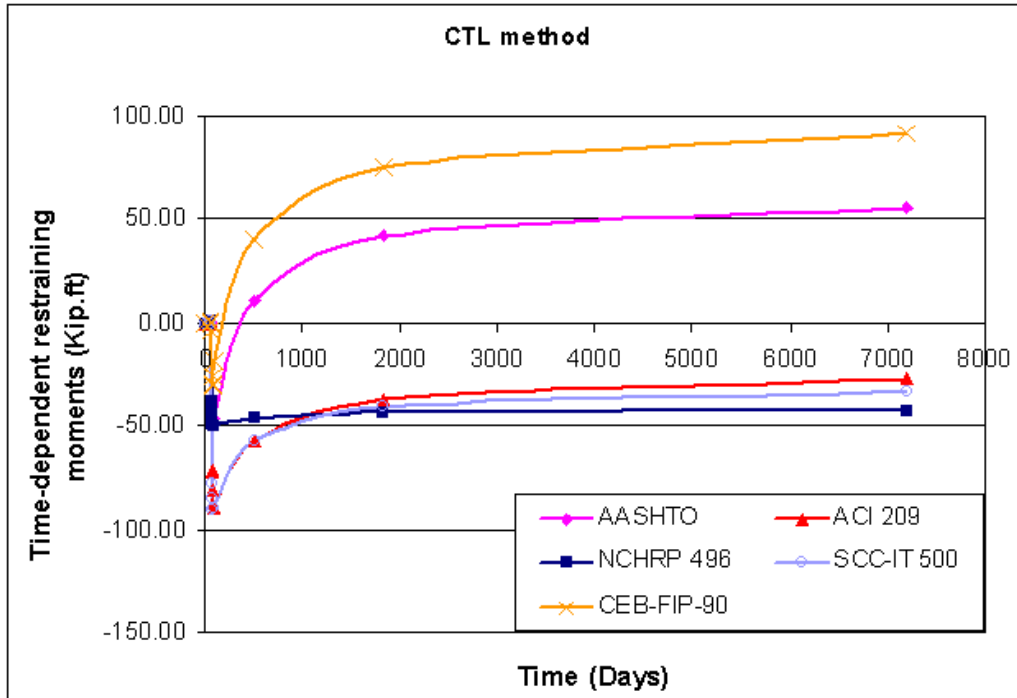


Figure 4. 58 Time-dependent restraining moment for different creep-and-shrinkage models using P method

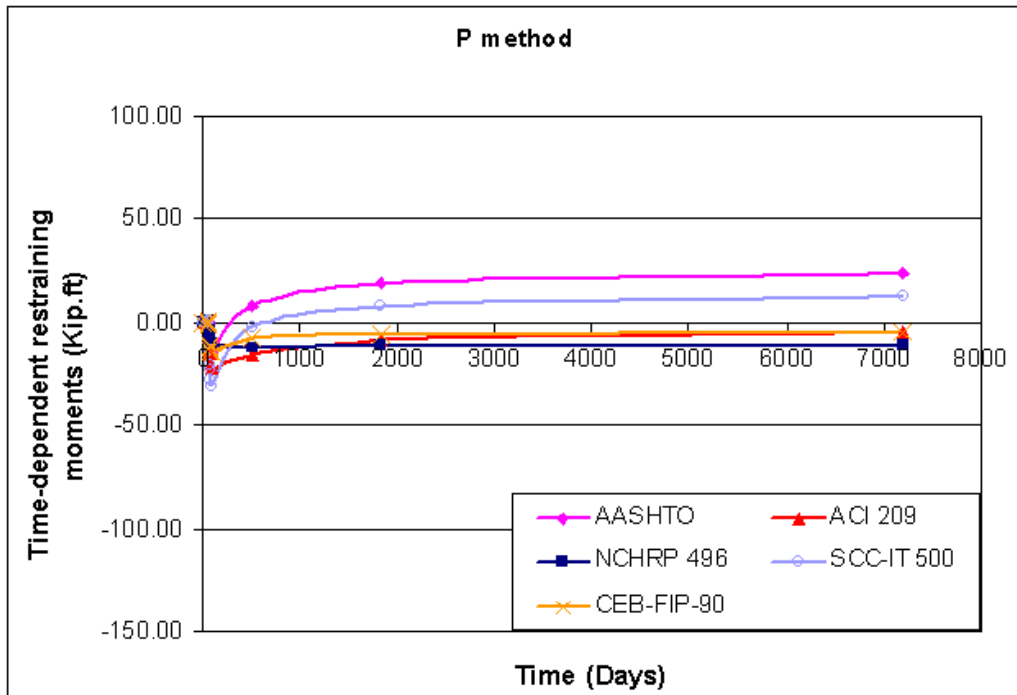


Figure 4. 59 Time-dependent restraining moment for different creep-and-shrinkage models using creep-transformed section properties method

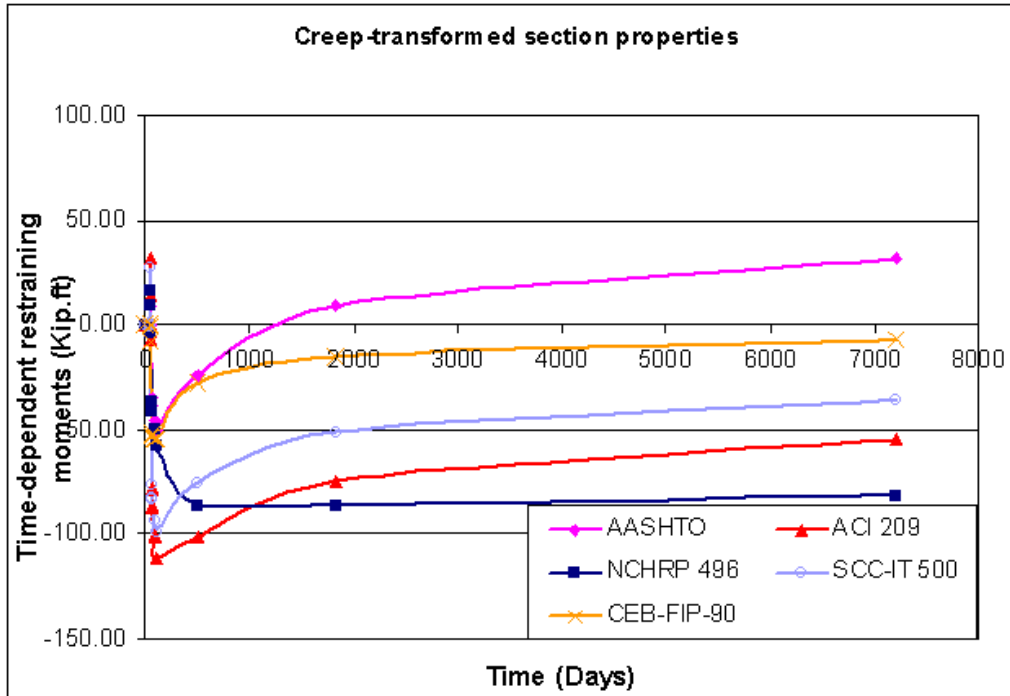


Figure 4. 60 Effect of time of cutting strands on losses in prestressing

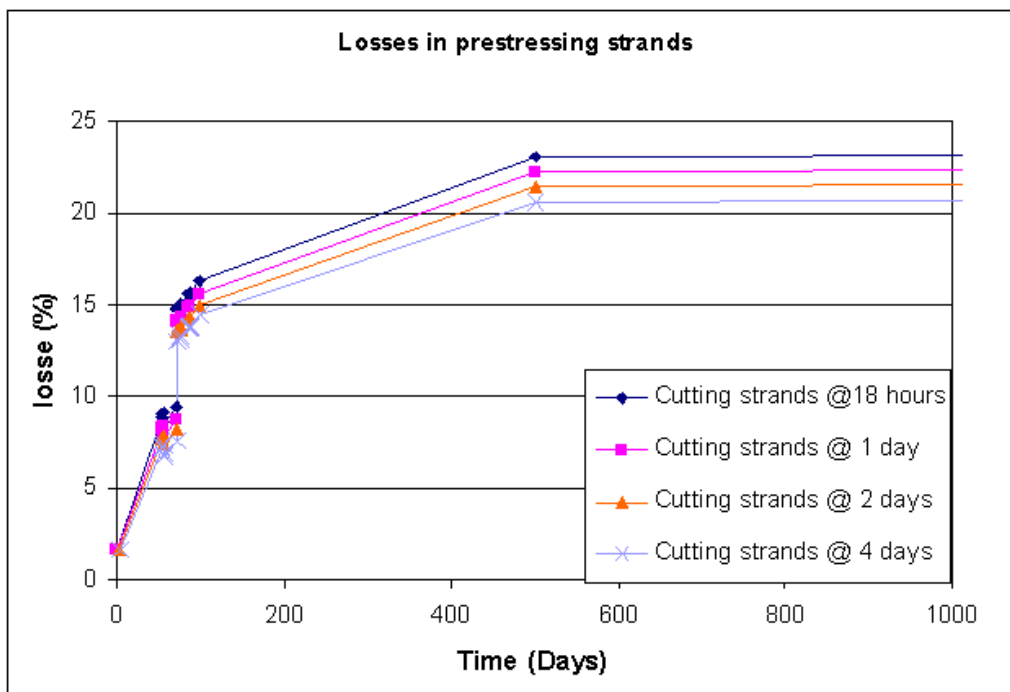


Figure 4. 61 Time-dependent restraining moment in the pier for continuity established @ 14 days of girder age

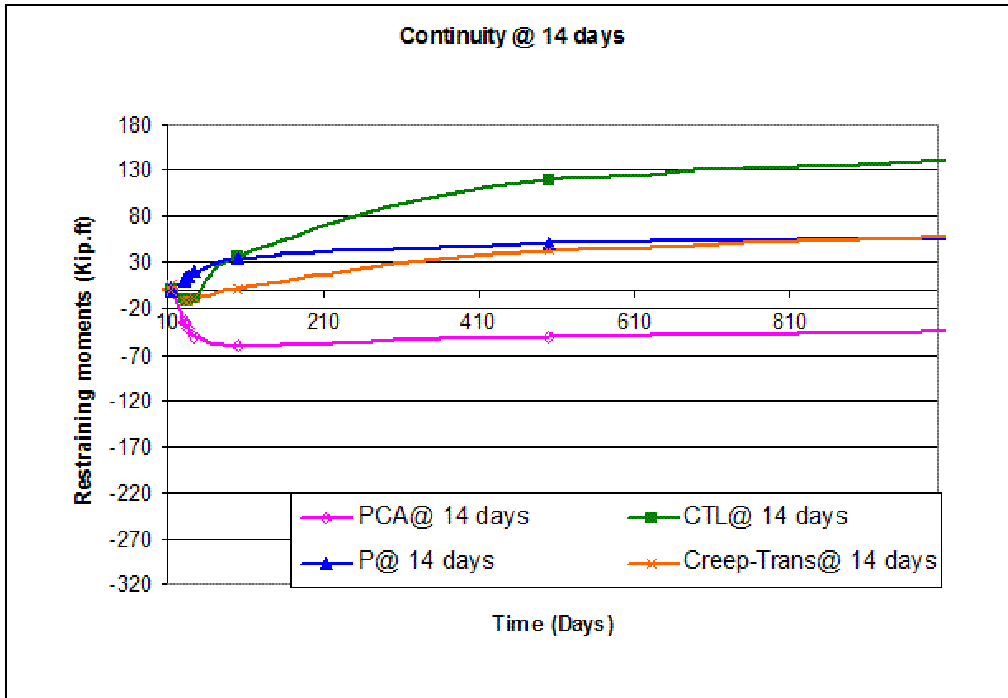


Figure 4. 62 Time-dependent restraining moment in the pier for continuity established @ 28 days of girder age

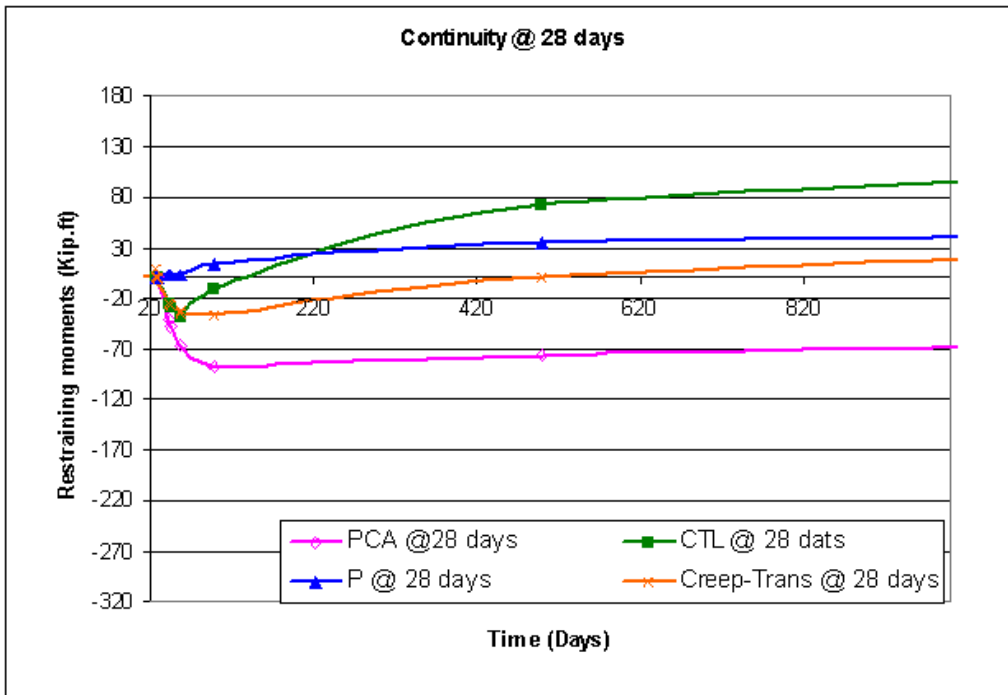


Figure 4. 63 Time-dependent restraining moment in the pier for continuity established @ 56 days of girder age

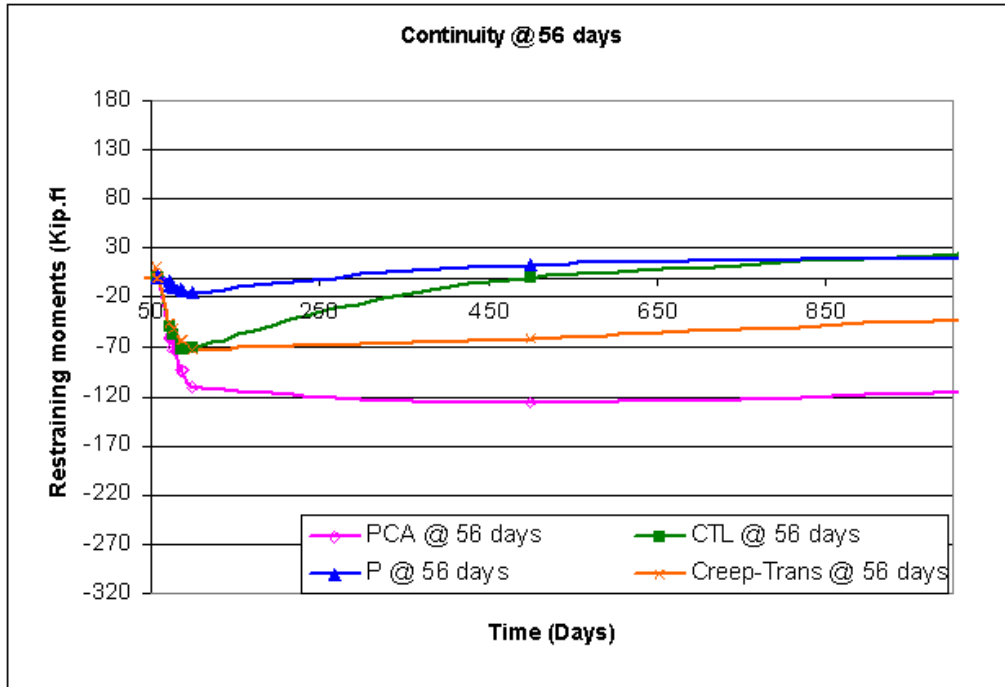


Figure 4. 64 Time-dependent restraining moment in the pier for continuity established @ 112 days of girder age

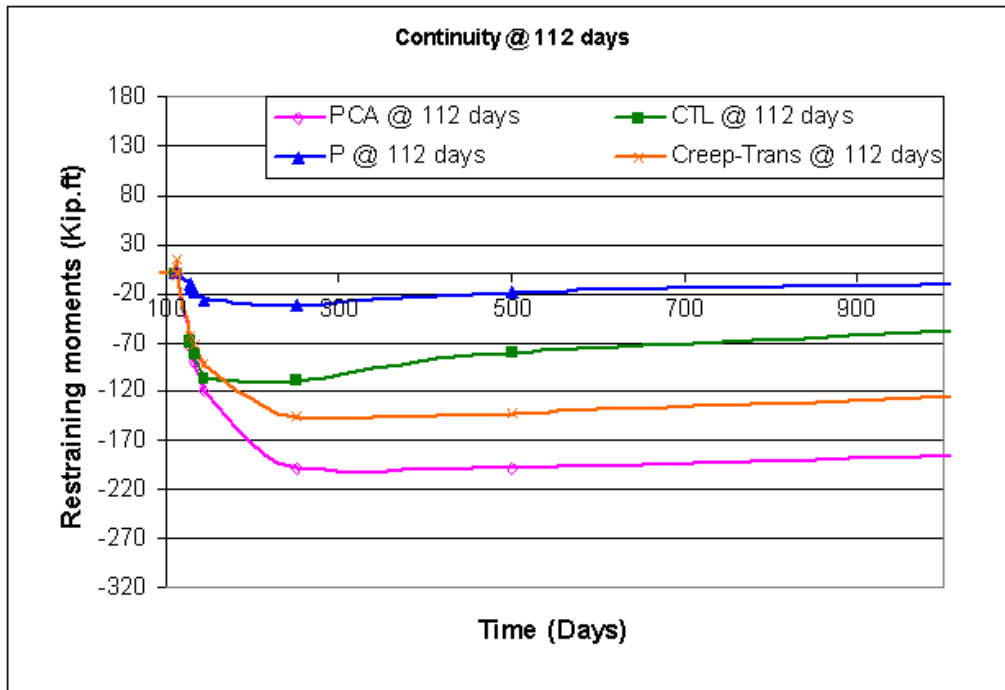


Figure 4. 65 Time-dependent restraining moment in the pier for continuity established @ 224 days of girder age

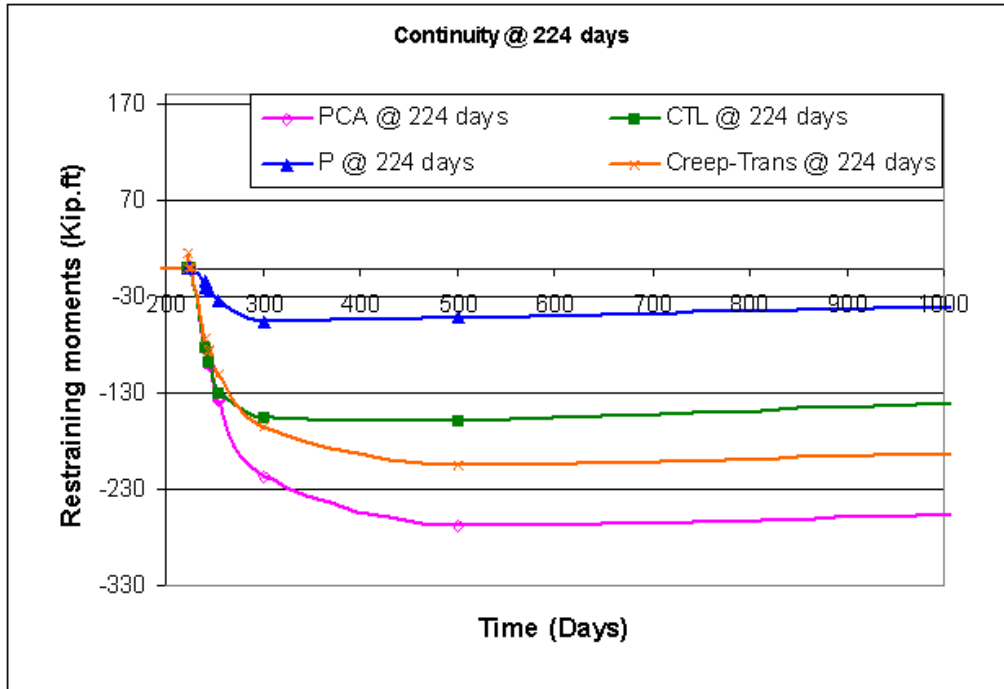


Figure 4. 66 Secondary moments due to post-tensioning for different times of establishing continuity

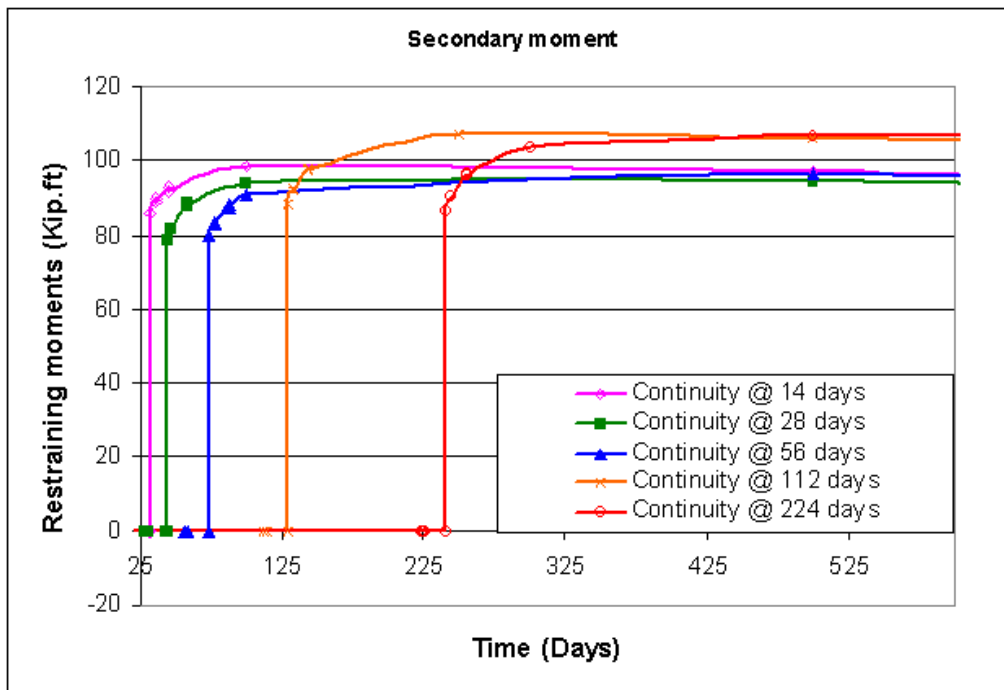


Figure 4. 67 Restraining moment in the pier for continuity established @ 14 days of girder age

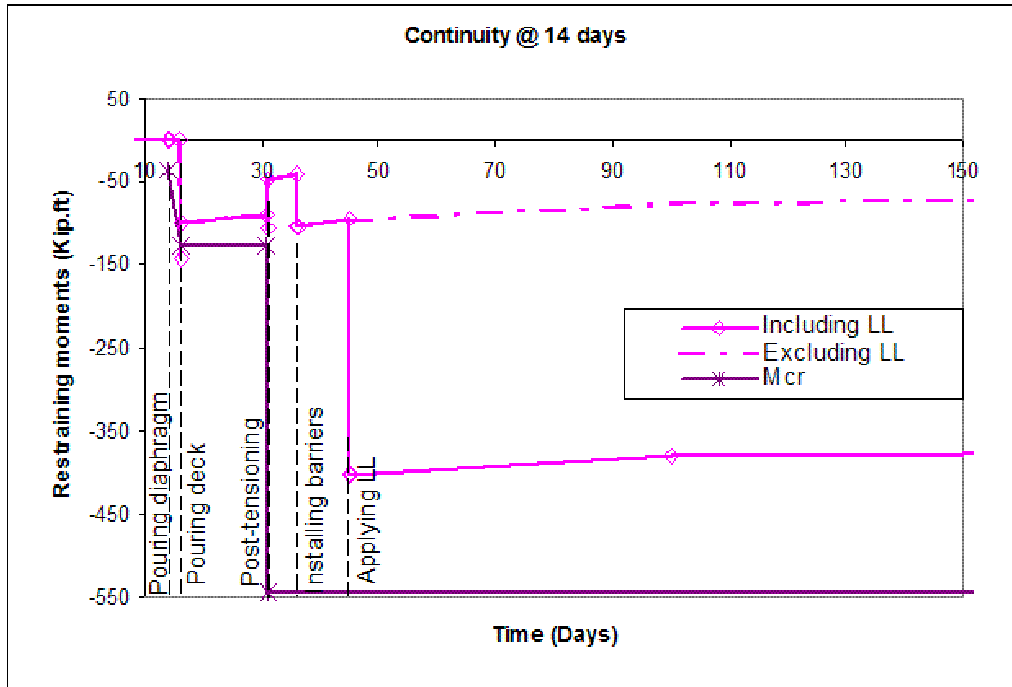


Figure 4. 68 Restraining moment in the pier for continuity established @ 28 days of girder age

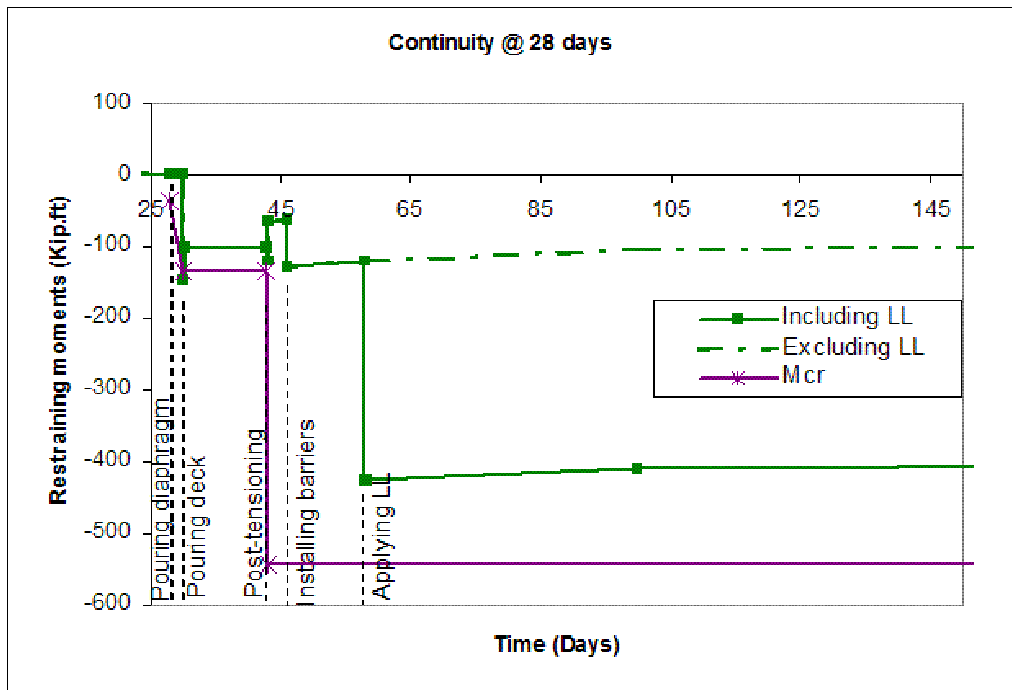


Figure 4. 69 Restraining moment in the pier for continuity established @ 56 days of girder age

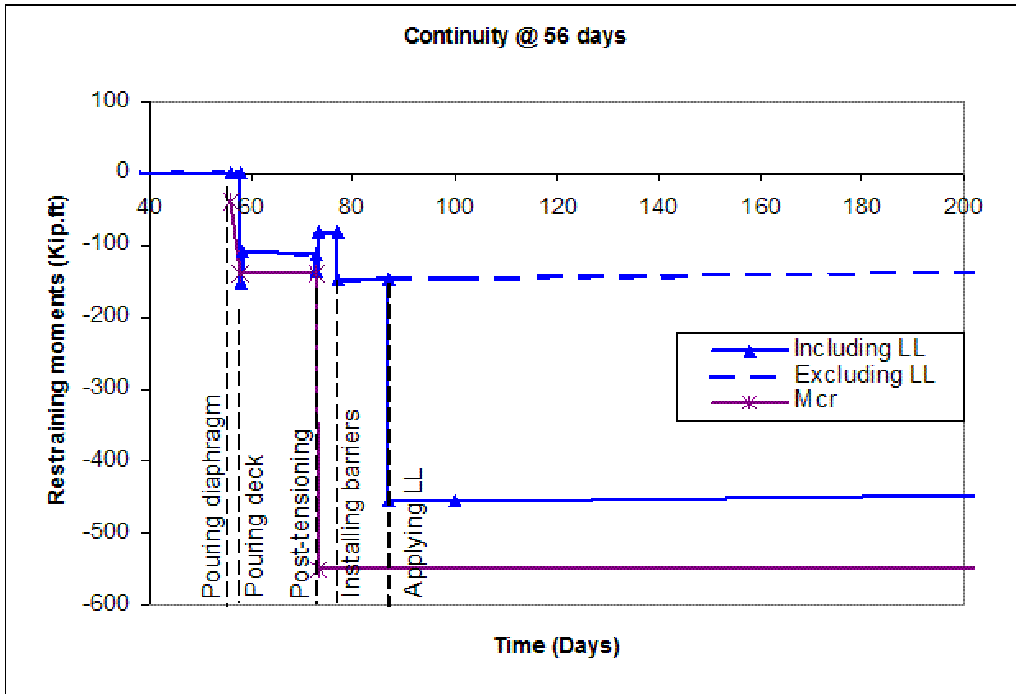


Figure 4. 70 Restraining moment in the pier for continuity established @ 112 days of girder age

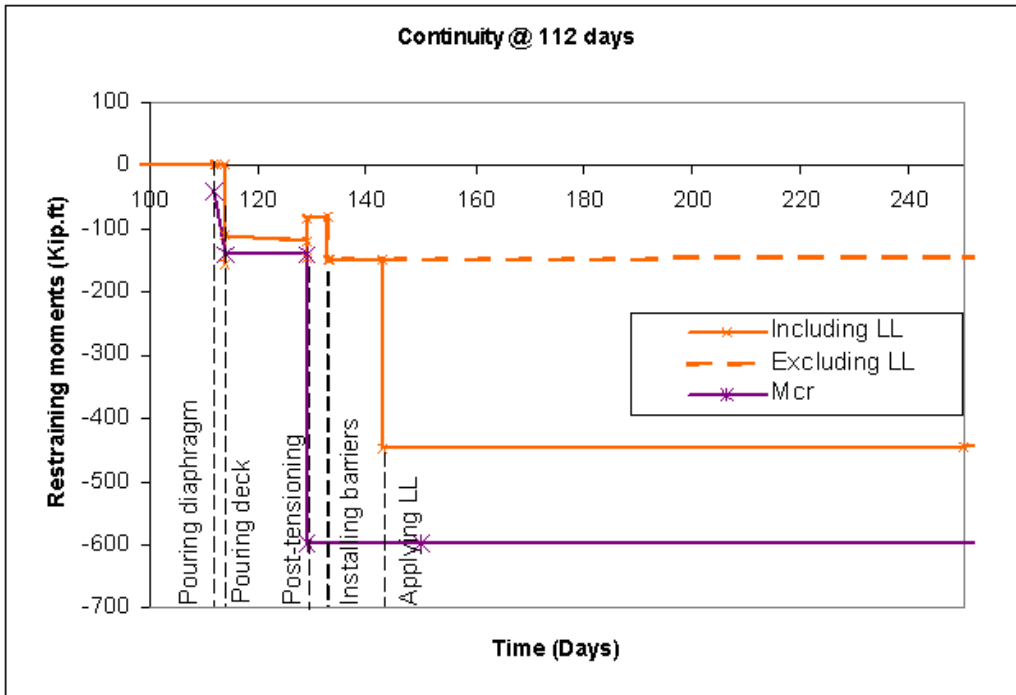


Figure 4. 71 Restraining moment in the pier for continuity established @ 224 days of girder age

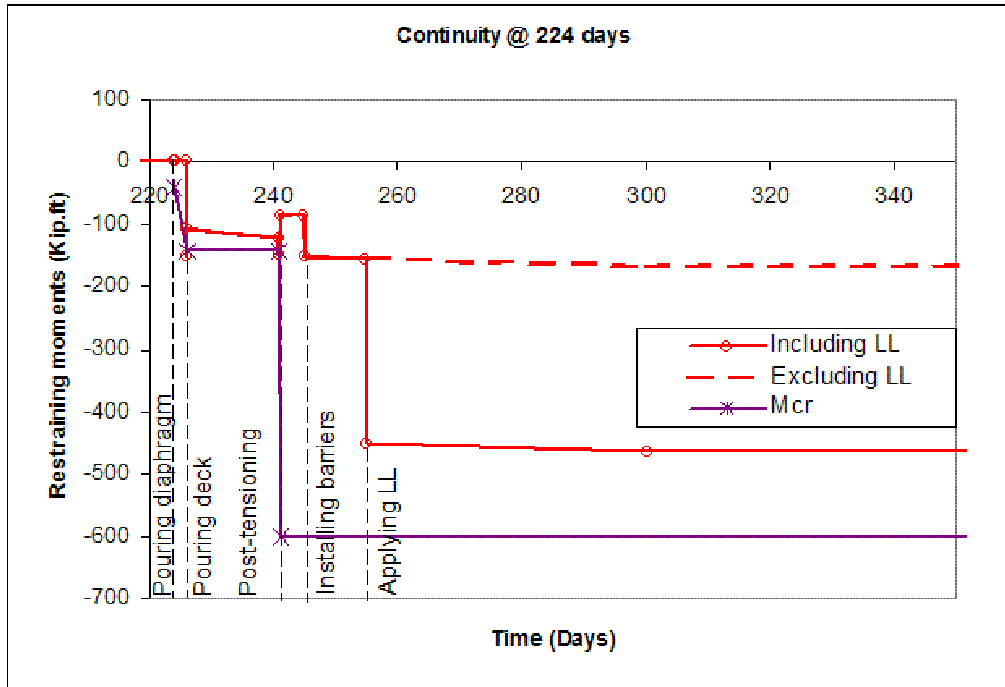


Figure 4. 72 Effect of time of casting the deck on time-dependent restraining moment using CTL method

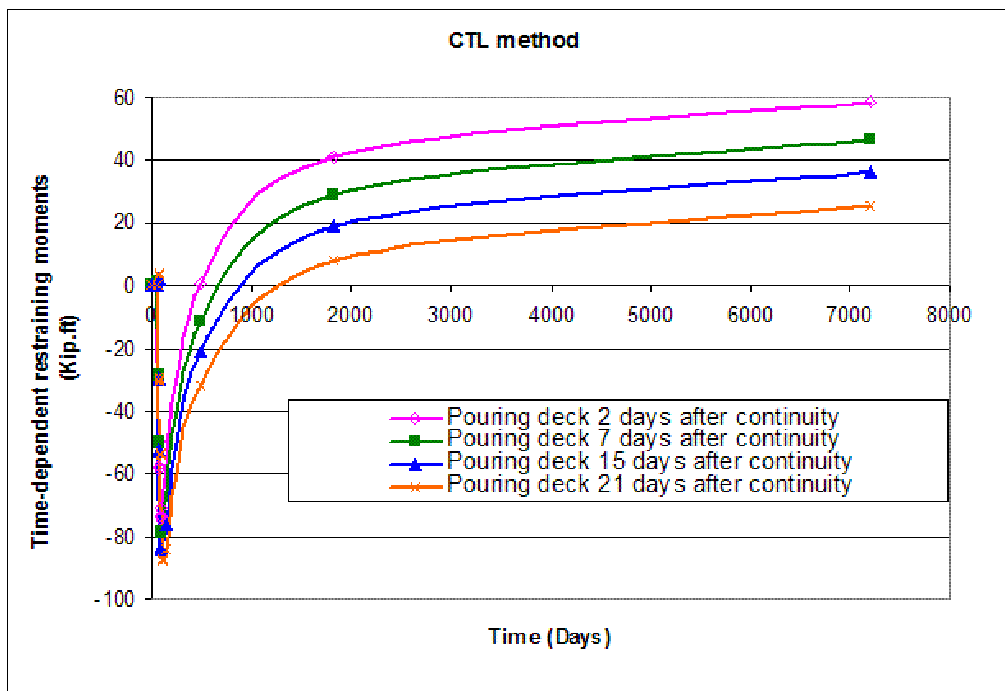


Figure 4. 73 Effect of time of casting the deck on time-dependent restraining moment using P method

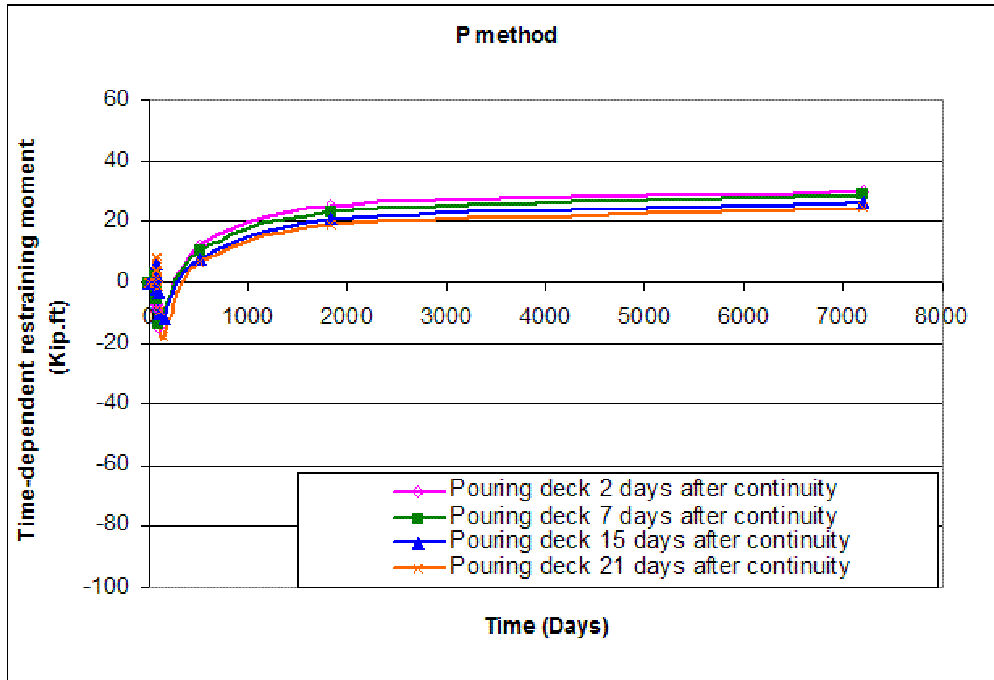


Figure 4. 74 Effect of time of casting the deck on the restraining moment in the pier

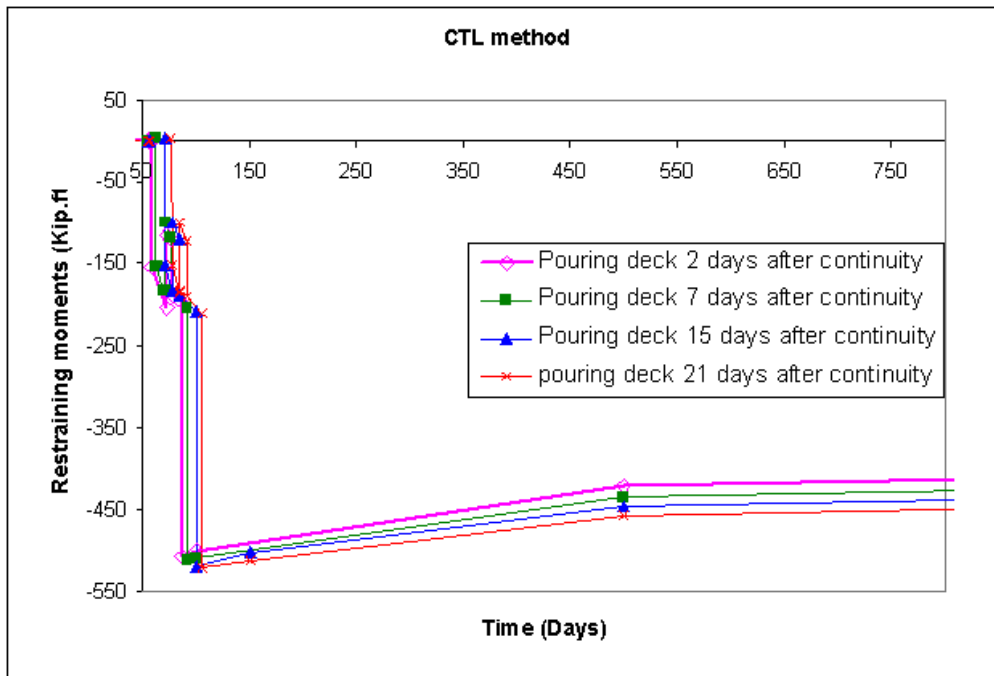


Figure 4. 75 Cross section for experiment conducted by (4)

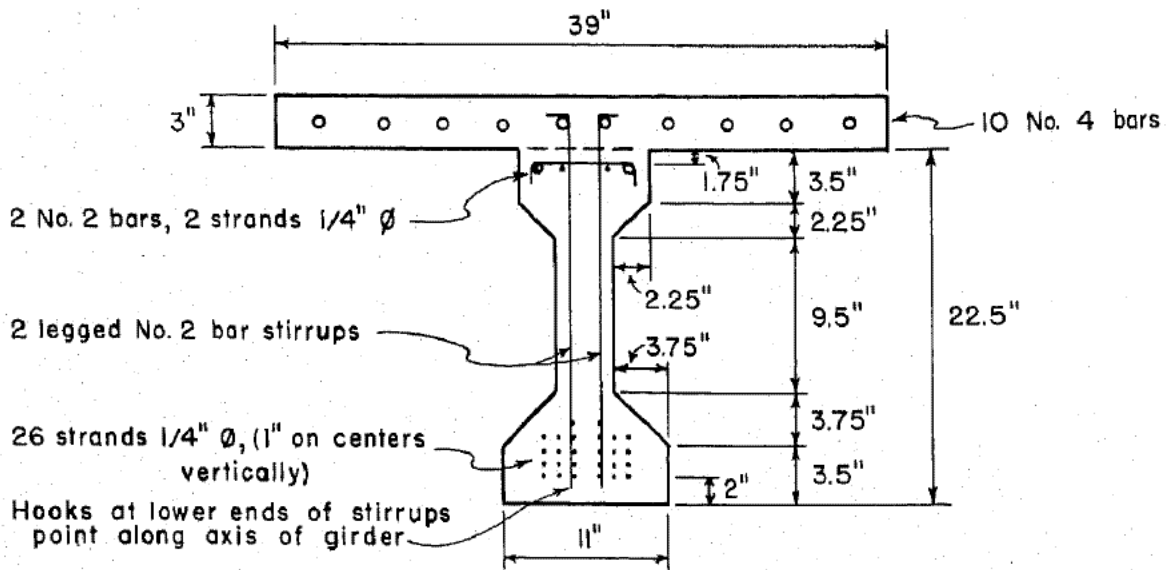


Figure 4. 76 Comparison with experimental data (4)

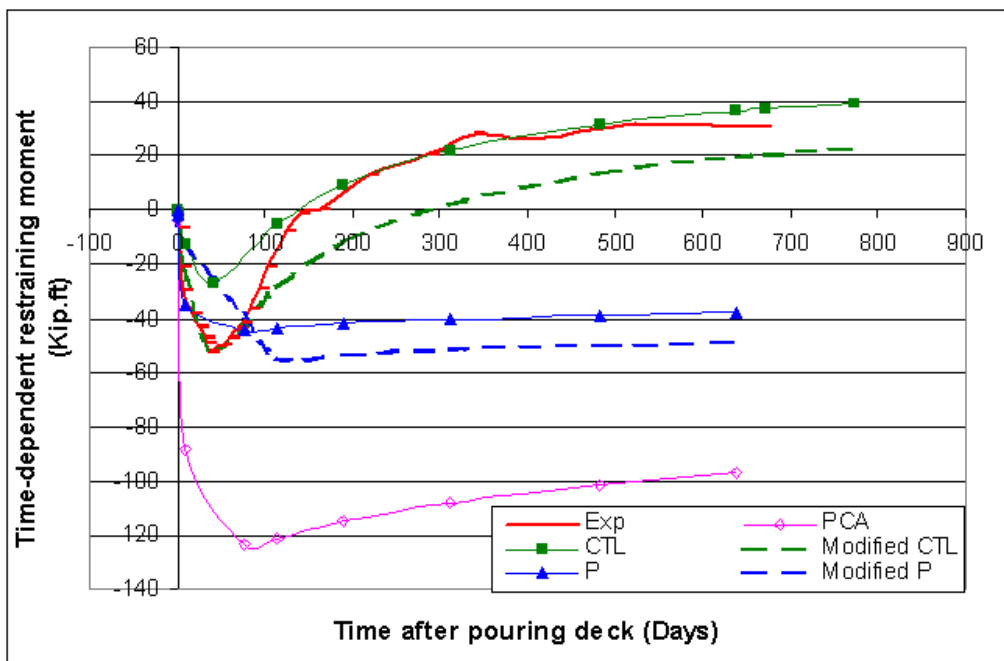


Figure 4. 77 Cross section of panels tested by (7)

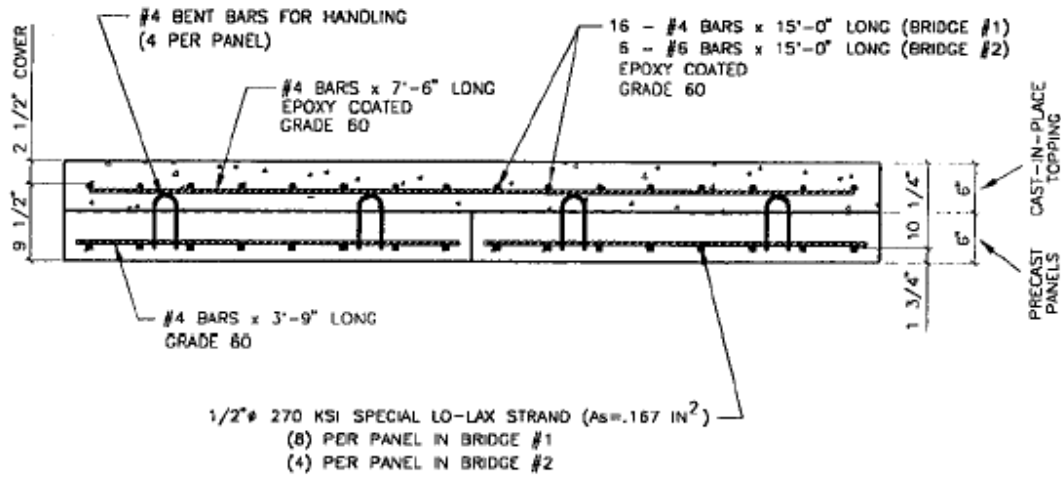


Figure 4. 78 Comparison with experimental data from (7)

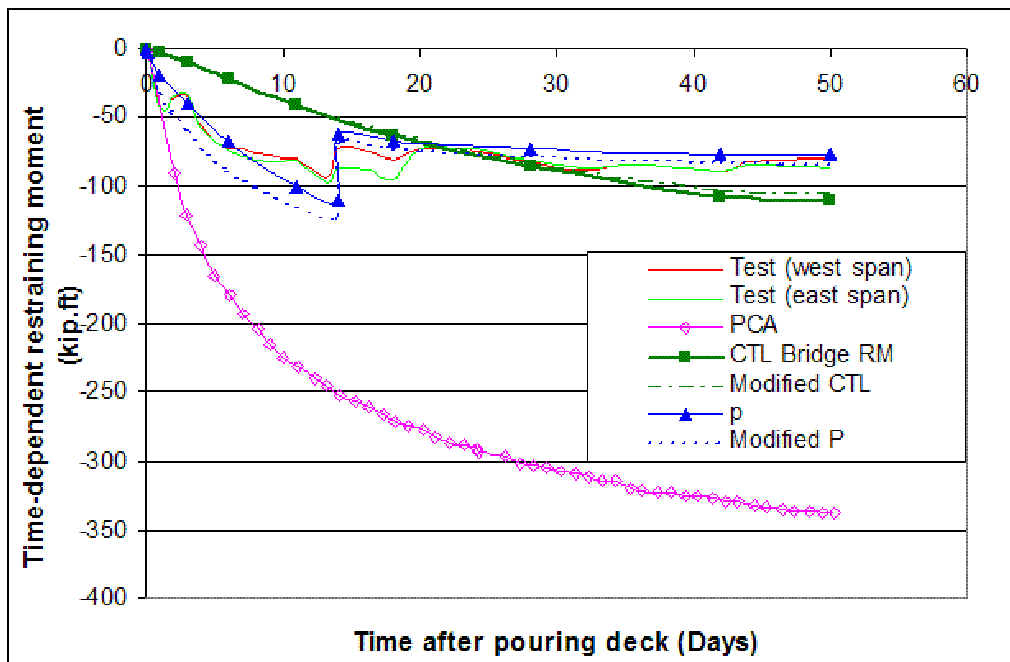


Table 4. 2 Maximum spans for different construction scenarios for IT 500-IT 1000

	IT system	PT-IT-one-stage PT									PT-IT-Two-stage PT		
		Dia & Deck-PT			Dia-Deck-PT			Dia-PT-Deck			6 ksi	8 ksi	10 ksi
	8 ksi	6 ksi	8 ksi	10 ksi	6 ksi	8 ksi	10 ksi	6 ksi	8 ksi	10 ksi	6 ksi	8 ksi	10 ksi
IT 500	61	57	65	71	62	71	78	60	71	78	62	71	79
IT 600	71	64	75	84	70	82	90	70	83	92	72	82	93
IT 700	80	75	86	95	80	93	103	78	94	103	83	94	104
IT 800	87	83	94	107	89	103	115	88	104	117	91	104	115
IT 900	93	92	106	118	99	113	127	98	114	127	100	114	128
IT 1000	100	99	115	127	107	123	138	106	124	138	108	125	138
Average (L/H)	28	26*	30*	34*	29**	33**	37**	28**	33**	37**	29**	33**	37**

* Limited by tension at the bottom of the girders within the span

** Limited by compression at the top of the girders within the span

Table 4. 3 Maximum span-to-depth ratio for different construction scenarios for IT 700

	One Stage PT						Two Stage PT	
	Dia & Deck-PT		Dia-Deck-PT		Dia -PT-Deck		14 D	224 D
	14 D	224 D	14 D	224 D	14 D	224 D	14 D	224 D
Span length (ft)	86		93		94		94	
Prestressing strands (1/2-270 K-LL)	11	11	13	13	17	13	11	9
First-stage PT (K-LL)	7-0.6"	6-0.6"	7-0.6"	9-0.6"	4-0.6"	5-0.6"	3-0.6"	6-0.6"
Second stage PT	-	-	-	-	-	-	5-0.6"	3-0.6"
Final reinforcement ratio %	0.78	0.72	0.85	0.95	0.92	0.75	0.83	0.81

Table 4. 4 Details for IT 500 for different concrete strengths

	6 ksi	8 ksi	10 ksi
Span (ft)	62	71	78
Prestressing strands	12-1/2" K-LL	12-1/2" K-LL	12-1/2" K-LL
Post-tensioned tendons	8-0.6"	9-0.6"	8-0.6"

Table 4. 5 Restraining moment in the pier due to girder weight

Concrete strength (ksi)	Moment (kip.ft)	Increase in moment (%)
6	100	31
8	131.6	
10	159.2	21

Table 4. 6 Effect of time of establishing continuity (casting diaphragm) on maximum span-to-depth ratio

	Continuity @ 14 days	Continuity @ 28 days	Continuity @ 56 days	Continuity @ 112 days	Continuity @ 224 days
Span (ft)	93	94	96	96	95
Prestressing strands	12- 1/2- 270K-LL	13- 1/2- 270K-LL	15- 1/2- 270K-LL	16- 1/2- 270K-LL	17- 1/2- 270K-LL
Post-tensioned tendons	8-0.6"	8-0.6"	8-0.6"	9-0.6"(1.953)	9-0.6"(1.953)
Span-to-depth ratio	33.3	33.6	34.3	34.3	34

CHAPTER 5 - CONCLUSION AND RECOMMENDATIONS

Conclusion

As considerable numbers of bridges need to be replaced or repaired in Kansas and other states, it is important to implement a standard method for replacement in which the capacity of the bridge is maximized and cost is minimized, while durability and safety are not compromised. Existing replacement methods do not satisfy one or more of these conditions, as previously discussed in this report.

A post-tensioned, inverted-T bridge system (PT-IT) was implemented in this study, where pretensioned inverted-T beams are post-tensioned to improve the capacity and durability of the system, increase span-to-depth ratio of the beam, and eliminate cracks in the deck over the piers.

A computer program (PT-IT) using C++ object-oriented language was developed to be used as a tool for the analysis of the PT-IT system. A user-friendly interface was also developed, using visual basic to help in data input and reading output.

A comparison between analysis results from the PT-IT program and Consplice was conducted; the comparison proved the capability of the PT-IT program to analyze the system.

An extensive parametric study was conducted to provide guidelines for designing and constructing a PT-IT system. Different construction scenarios were discussed and evaluated from maximum capacity and durability points of view. Construction sequence was found to be one of the most effective and critical parameters in design. Different construction scenarios were investigated, including two main options of applying one or two stages of post-tensioning. For one stage post tensioning, many options were evaluated. One of these was casting the deck and diaphragm simultaneously and then applying post-tensioning. In this case, deck weight was carried on the simple span beam, along with positive secondary moments due to post-tensioning; this will cause high positive stresses within the spans of the girders, which will consequently limit the span-to-depth ratio of the girders.

Another option for one-stage post-tensioning is to cast the diaphragm, then apply post-tensioning, and then cast the deck. In this scenario, the deck weight is carried by the continuous structure. This results in lower positive moments within the span, while negative moments

develop over the piers. Disadvantage of this option of construction is that post-tensioning will be applied at the girder section only. This causes high stresses in the bottom of the girder near and in the pier. Furthermore, as post-tensioning is applied on the girder section only, it will not help reduce negative stresses in the deck over the piers due to live load.

Another option for one-stage post-tensioning is when continuity is established by casting the diaphragm, and then after the diaphragm concrete hardens, the deck is cast, and finally post-tensioning is applied to the whole structure. The advantage of this construction scenario is that the weight of the deck will be carried by the continuous structure. At the same time, weight of the deck has no time-dependent effect on moments in the piers. Besides, when post-tensioning is applied on the continuous structure, primary moments caused by post-tensioning at the pier will be less, as if they were to be applied at the girder section. This will cause less tension forces at the bottom of the girders in the case when continuity is established at early girder age. The drawback of this type of scenario is that cracking of the diaphragm over the pier will occur during the period between casting the deck and post-tensioning under deck weight. After post-tensioning, the deck will be under compression and consequently, the cracks will be closed.

In the case of two-stage-post tensioning, the diaphragm is cast to establish continuity, then the first stage of post-tensioning is enough to balance stresses due to the weight of the deck. After the deck is cast, the final stage of post-tensioning is applied to balance stresses due to the weight of the barriers and live load. A disadvantage of two-stage post-tensioning is increased labor required for construction using this scenario, which reflects on the cost of construction.

Results of parametric study showed that both scenarios of one-stage post-tensioning (Dia-Deck-PT) and two-stage PT have the highest span-to-depth ratio and satisfy the crack-free deck criteria. Since the option of Dia-Deck-PT incorporates less labor, it is recommended to be used for construction of PT-IT systems.

Different methods for estimation of time-dependent restraining moment, and modifications for both CTL and P methods were suggested in this study. Comparison for CTL, P, and PCA methods with experimental results showed that the P method better estimates time-dependent restraining moment for shallow girders, while the CTL method better estimates it for deeper girders.

While PCA, CTL, P, and creep-transformed section properties methods are considered in the course of the parametric study to estimate the range in which time-dependent restraining

moment will fall, it is recommended that experimental investigations be conducted in order to determine the method that is capable of providing a better estimation of the effect of time-dependent forces on restraining moments in the piers.

Girder concrete strength plays a major role in increasing span-to-depth ratio. Increasing girder concrete strength from 6 to 8 ksi helps increase the span by 15% of 6-ksi girders, while increasing strength from 8 to 10 ksi increases the span by 11% of the 8-ksi girders.

On the other hand, deck concrete strength doesn't affect time-dependent restraint moment under creep and shrinkage, nor losses in stresses of prestressing strands and post-tensioned tendons.

Different creep-and-shrinkage models were investigated including AASHTO LRFD, ACI-209, CEB-FIP-90, SCC, and NCHRP 496. It was found that while estimation of losses in pretensioned strands and post-tensioned tendons is not significantly affected using different models, variation of time-dependent restraining moment is significant for different models.

The effect of timing on different construction stages was also discussed and addressed in the parametric study. Establishing continuity was found to be an effective parameter in the design. For early ages of establishing continuity, positive time-dependent restraining moments tend to develop in the pier, while for late age of establishing continuity, negative time-dependent restraining moments tend to form. It is recommended that continuity be established between 56 and 112 days of girder age. Time between establishing continuity and casting the deck was not found to play a major role in the time-dependent restraining moment.

It is recommended that post-tensioning be applied as soon as possible after casting the deck to close the crack in the top of the diaphragm. This could be done as soon as two days after casting the deck. The time of post-tensioning doesn't affect the value of time-dependent restraining moment, but for durability issues related to control crack initiation and development in the diaphragm, it is recommended that post-tensioning be applied to the structure as soon as possible after casting the deck.

Recommendation

Based on the results of this research, the following recommendations are made for the post-tensioned inverted-T bridge system:

- The need for full or half scale experiments on PT-IT bridge system is imminent to reach a decision of which method is more capable of capturing the time-dependent effect on restraining moments for the PT-IT system.
- Use (Dia-Deck-PT) Construction scenario for PT-IT system, this involves casting diaphragms to establish continuity, then cast the deck, and then apply post-tensioning
- Using 8 or 10 ksi concrete strength for PT-IT girders enhance span-to-depth ratio of the system
- It is recommended to cast the diaphragm between 56 and 112 days of girder age.
- Time between establishing continuity and casting the deck was not found to play a major role on the behavior of the system.
- It is recommended that post-tensioning be applied as soon as possible after casting the deck to close the crack in the top of the diaphragm. This could be done as soon as two days after casting the deck.
- The time of post-tensioning doesn't affect the value of time-dependent restraining moment, but for durability issues related to control crack initiation and development in the diaphragm, it is recommended that post-tensioning be applied to the structure as soon as possible after casting the deck.

Notations

A_g	= area of the prestressed member
A_d	= cross-sectional area of CIP slab
A_s	= steel area
b_v	= effective web width
d_v	= effective shear depth taken as the distance between the resultant of the tensile and compression forces due to flexure
e	= base of the Napierian logarithm
ec	= distance between the top of the precast member and the centroid of the composite section
E_{ci}	= modulus of elasticity of concrete at transfer
E_d	= modulus of elasticity of CIP concrete
E_g	= modulus of elasticity of the girder concrete
E_p	= modulus of elasticity of prestressing steel
f_{cgp}	= sum of concrete stresses at the center of gravity of prestressing tendons
$(f'c)_{28}$	= strength of the concrete at 28 days
f_{pce}	= compression stress in concrete due to effective prestress forces
f_{pj}	= initial stress in the tendon at the end of stressing
f_{pj}	= stress in the prestressing steel at jacking (ksi)
f_{py}	= specified yield strength of prestressing steel
f_r	= modulus of rupture
H	= average annual ambient relative humidity
h	= CIP thickness
I_d	= moment of inertia of the diaphragm region
I_m	= moment of inertia of the main span
k_s	= size factor
k_h	= humidity factor
k_f	= factor of the effect of concrete strength
k_c	= factor for the effect of the volume-to-surface ratio

k = wobble friction coefficient
 L_d = length of the diaphragm region
 L_m = length of the main span
 M_u = factored moment
 M_{dnc} = total unfactored dead load moment acting on the monolithic or noncomposite section
 $(M_d)_{precast}$ = midspan moment due to dead load of the girders
 $(M_d)_{CIP}$ = midspan moment due to CIP deck weight
 M_d = midspan moment due to dead load
 PPR = partial prestress ratio
 s = girder spacing (in)
 sc, s_{nc} = section modulus for the extreme fiber of the composite section
 t = time estimated in days from stressing to transfer
 v_p = component of prestressing force in the direction of the shear force (Kip)
 v_u = factored shear force
 x = length of a prestressing tendon from the jacking end to any point under consideration (ft)
 α = fraction of ϵ_c , which has occurred when continuity connection is established
 ΔL = anchor set (in)
 Δf_{pES} = loss due to elastic shortening
 Δf_{pR1} = loss due to relaxation of steel at transfer
 Δf_{pR2} = loss due to relaxation of steel after transfer
 Δf_{pT} = total loss of prestress
 Δf_{pES} = loss due to elastic shortening
 Δf_{pSH} = loss due to concrete shrinkage
 Δf_{cdp} = change in concrete stress at the center of gravity of prestressing steel
 ϵ_s = differential shrinkage strain
 ϵ_c = creep strain at time t due to unit stress
 ϵ_e = initial strain due to unit stress
 ϵ_{sc0} = notional shrinkage coefficient
 ϕ = creep coefficient

- Φ_u = deck's ultimate shrinkage
 Θ = angle of inclination of diagonal compressive stresses
 μ = coefficient of friction
 χ = aging coefficient

References

1. American Association of State Highway and Transportation Officials, "AASHTO-LRFD bridge design specifications, customary U.S. units," 3rd Edition, 2004, Washington, DC.
2. Collins, Michael P., Mitchell Denis "Prestressed Concrete Structures" Prentice hall, Engelwood Cliffs, New Jersey
3. Freyermuth, C., "Design of continuous highway bridges with precast prestressed concrete girders," PCI Journal, Vol. 14, No. 2, pp. 14-39, April (1969).
4. Mattock, A., "Precast-prestressed concrete bridges 5: creep and shrinkage studies," Journal of the PCA Research, Portland Cement Association, Skokie, IL, pp. 32-66, (May 1961).
5. Oesterle, R., Glikin, J., and Larson, S. "Design of simple-span precast prestressed bridge girders made continuous (final report)", Construction Technology Laboratories, Inc. for National Cooperative Highway Research Program, Transportation Research Board (NHCRP Project 12-29), Skokie, IL, May (1989).
6. Oesterle, R., Glikin, J., and Larson, S. "Design of precast-prestressed bridge girders made continuous," National Cooperative Highway Research Program Report 322, Transportation Research Board, National Research Council, Washington, DC, pp. 97, November (1989).
7. Peterman, R., and Ramirez, J. "Restraint moments in bridges with full-span prestressed concrete form panels," PCI Journal, pp. 54-73, January-February (1998).
8. Dilger, W. H., "Creep analysis of prestressed concrete structures using creep-transformed section properties," PCI Journal, Vol. 27, No. 1, pp. 98-118, January-February (1982).

9. Mirza, S. A., and Furlung, R. W., "Design of reinforced and prestressed concrete inverted-T beams for bridge structures," *Journal of the Prestressed Concrete Institute*, Vol. 30, No. 4, pp. 112-136, July-Aug. (1985).
10. Kamel, Mounir R., and Tadros, Maher K., "The inverted-T, shallow-bridge system for rural areas," *PCI Journal*, Vol. 41, No.5, pp. 28-43, September/October (1996).
11. Kamel, Mounir R., and Derrick, Deb, "A precast alternative for bridge slabs," *Concrete International*, pp. 41-42, August (1997).
12. Ambare, Sameer, and Peterman, Robert J., "Evaluation of the inverted Tee shallow bridge system for use in Kansas, (final report)" Kansas Department of Transportation (K-TRAN: KSU-00-1), Topeka, Ks, Oct (2006).
13. National Cooperative Highway Research Program, NCHRP Report 496, "Prestress losses in pretensioned high-strength concrete bridge girders," Washington, DC, (2003).
14. American Association of State Highway and Transportation Officials. "AASHTO standard specifications for highway bridges," 15th Edition, 1993, Washington, DC.
15. Prestressed Concrete Institute, "PCI bridge design manual," July (2003), Chicago, IL.
16. Jones, Harry L., and Ingram, Leonard, L. "Automated design of continuous bridges with precast prestressed concrete beams—Volume I design considerations," Texas Transportation Institute and Texas A& M University, Research Report 22-1F, October (1974).
17. Bazant, Z. P., "Prediction of concrete creep effects using age-adjusted effective modulus method," *ACI Journal, Proceedings* Vol. 69, No. 4, pp. 212-217, April (1972).
18. Rabbat, B.G., and Aswad, A. "Design of precast girders made continuous," Report to PCI Committee on Bridges, pp. 4, Oct. (1992).

19. Mirmiran, A., Kulkarni, S., Castrodale, R., Miller, R., and Hastak, M. "Nonlinear continuity analysis of precast, prestressed concrete girders with cast-in-place decks and diaphragms," PCI Journal, Sept.-Oct. (2001).
20. Miller, R., Castrodale, R., Mirmiran, A., and Hastak, M., "Connection of simple-span precast concrete girders for continuity," National Cooperative Highway Research Program Report 519, Transportation Research Board, Washington, DC, (2004).
21. Saadehvaziri, M, A., Spillers, W., and Yin, L. "Improvement of continuity over fixed piers," NJDOT Research Project (FHWA-NJ-2004-017).
22. Leap Software, Inc., "Consplce v 1.2.0" Tampa, FL
23. American Association of State Highway and Transportation Officials, "AASHTO LRFD bridge design specifications, customary U.S. units," 3rd Edition, 2006 Interim Revisions, Washington, DC.
24. American Concrete Institute (ACI), ACI Committee 209, "Prediction of creep, shrinkage, and temperature effects in concrete structures," Report ACI 209R-92, Detroit, Mich. (1992).
25. CEB-FIP Model Code 1990, Design Code, "Comite Euro-International du Beton".
26. Larson, Kyle H., Peterman, Robert J., Esmacily, Asad, "Evaluating the time-dependent deformations of pretensioned bridge girders cast with self-consolidating concrete" 2006 Concrete Bridge Conference, Oct 23-25, Grapevine, Tx.
27. Collins, Michael P., and D. Mitchell, "Prestressed concrete structures," Prentice Hall: Englewood Cliffs, N. J., (1991).

28. Magura, D. D., Sozen, M. A., and Seiss, C. P., "A study of stress relaxation in prestressing reinforcement," PCI Journal, Vol. 9, No.2, Chicago, IL, pp. 13-57, April (1964).
29. Prestressed Concrete Institute, "PCI design handbook," Fifth Edition (1999), Chicago, IL.
30. Post-Tensioning Institute, "Post-tensioning manual," Fifth Edition, November (1990), Phoenix, AZ.
31. Division of Construction Engineering and Management, Purdue University, (2001)
<http://www.new-technologies.org/ECT/Civil/itbeam.htm>.
32. PCI Committee on Prestress Losses, "Recommendations for estimating prestress losses," PCI Journal, Vol. 20, No. 4, pp. 43-75, July-August (1975).
33. Tadros, M., Al-Omaishi, N., Seguirant, S., and Galt, J., "Prestress losses in pretensioned high-strength concrete bridge girders," National Cooperative Highway Research Program (NHCRP Report 496) (2003).

Appendix A - Details of Reinforcement

The emphasis of this appendix is on details of Reinforcement

Concrete Cover

Minimum concrete cover shall be specified in AASHTO LRFD 5.12.3⁽¹⁾. As per LRFD table 5.12.3-1 concrete cover for “exterior other than above = 2 in” and “interior other than above for up to No. 11 bar=1.5 in”. as per LRFD 5.12.3 cover of steel should be modified for water-to-cement ratio (W/C) of concrete. Modification factors for water-to-cement ratio shall be 0.8 for $W/C \leq 0.4$, and 1.2 for $W/C \geq 0.5$. concrete cover for deck surface subject to tire stud or chain wear=2.5 in

Minimum Spacing of Prestressing Tendons

As per AAHSTO LRFD 5.10.3.3.1 the distance between prestressing strands including shielded ones, at each end of a member within the transfer length taken as 60 strand diameter, as specified in Article 5.11.4.1, shall not be less than a clear distance taken as 1.33 times the maximum size of the aggregate nor less than the center-to-center distance specified in Table 1 as follows 2 in. for 0.6 in. strand size and 1.75 in. for 0.5 in. Accordingly for IT sections of 23.5 in. flange width, maximum number of strands in the first row shall be taken as:

- 11 strands size 0.5 in.
- 10 strands size 0.6 in.

Maximum number of strands in the second row is limited to 6 strands to fit the post-tensioning duct.

Maximum Number of Post-Tensioning Tendons and Duct Size

As per 3.3.3 of Post-Tensioning Manual⁽³⁰⁾ “for tendons made up of a plurality of wires, bars, or strands, duct area should be at least twice the net area of the prestressing steel”. For IT section of web width of 6.3 in. Duct requires 2 in. concrete cover at each side, that leaves 2.3 in. maximum diameter for the duct

$$A_{duct} = \frac{\pi(2.3)^2}{4} = 4.155 \text{ in}^2 \Rightarrow \text{Max}(A_{ps}) = \frac{A_{duct}}{2} = 2.077$$

This is equivalent to:

- $12 \cdot 0.5 = 1.836 \text{ in}^2$
- $9 \cdot 0.6 = 1.953 \text{ in}^2$

Design and Detailing of Anchorage Zone

As per 5.10.9.1 of AASHTO LRFD ⁽¹⁾ “for anchorage zones at the end of a component or segment, the transverse dimensions may be taken as the depth and width of the section but not larger than the larger than the longitudinal dimension of the component or segment. The longitudinal extent of the anchorage zone in the direction of the tendon shall not be less than the greater of the transverse dimensions of the anchorage zone and shall not be taken as more than one and one-half times that dimension.”

For design purposes AASHTO LRFD ⁽¹⁾ considers that the anchorage zone consists of two regions:

- The general zone, for which the provisions of Article 5.10.9.2.2 apply, and
- The local zone, for which the provisions of Article 5.10.9.2.3 apply.

The extent of the general zone shall be taken as identical to that of the overall anchorage zone

According to 5.10.9.3.2 AASHTO LRFD ⁽¹⁾ the magnitude of the bursting force T_{burst} and its corresponding distance from the loaded surface d_{burst} may be determined using the strut and tie model procedures of Article 5.10.9.4, an elastic stress analysis according to Article 5.10.9.5, or the approximate method outlined in Article 5.10.9.6.3. As per Article 5.10.9.5 “Analyses based on elastic material properties, equilibrium of forces and loads, and compatibility of strains may be used for the analysis and design of anchorage zones”. Accordingly, provisions of post-tensioning manual ⁽³⁰⁾ article 5.4.1 are to be used in design.

The magnitude of the tensile splitting force can be determined from the following equation:

$$z = 0.3p \left(1 - \frac{a}{d}\right) \tag{A.1}$$

Where:

z = total splitting or bursting force

P= tendon force

a= depth of the anchor plate

d= depth of the concrete section

Sufficient vertical reinforcement acting at a unit stress of 0.6 of reinforcement yield stress to resist the computed value of z should be distributed within the distance of d/2 of the anchorage location.

As per 5.10.9.2.3 AASHTO LRFD ⁽¹⁾ “design of local zones shall be either comply with the requirements of article 5.10.9.7 or be based on the results of acceptance tests as specified in Article 5.10.9.7”.

Dimensions of local zone are specified in AASHTP LRFD 5.10.9.7.1 ⁽¹⁾ where the transverse direction of the local zone in each direction should be taken as the greater of:

- The corresponding bearing plate size, plus twice the minimum concrete cover required for the particular application and environment, and
- The outer dimension of any required confining reinforcement, plus the required concrete cover over the confining reinforcing steel for the particular application and environment.

The length of the local zone along the tendon axis shall not be taken less than:

- The maximum width of the local zone;
- The length of the anchorage device confining reinforcement, or
- For anchorage device with multiple bearing surfaces, the distance from the loaded concrete surface to the bottom of each bearing surface, plus the maximum dimension of that bearing surface.

The length of the local zone shall not be taken as greater than 1.5 times the width of the local zone.

Figure A. 1 illustrates locations of local and general zones.

The factored bearing resistance of anchorages shall be taken as:

$$P_r = \phi f_n A_b \tag{A.2}$$

for which f_n is the lesser of:

$$f_n = 0.7f_{ci} \sqrt{\frac{A}{A_g}}, \text{ and} \tag{A.3}$$

$$f_n = 2.25f_{ci}' \quad (A.4)$$

Where:

ϕ = resistance factor specified in LRFD 5.5.4.2

A = maximum area of the portion of the supporting surface that is similar to the loaded area and concentric with it and does not overlap similar areas for adjacent anchorage devices (in.²)

A_g = gross area of the bearing plate

A_b = effective net area of the bearing plate

f_{ci}' = nominal concrete strength at time of application of tendon force (Ksi)

Design and detailing of anchorage zone reinforcement and anchorage plate is discussed for tendons consisting of 5 and 9 strands of 0.6 in. diameter for IT 700. Similar procedures may be followed for other tendon combination.

For Tendon consisting of 5-0.6" strands, strength of concrete is assumed to be 8 ksi, as girders are not post-tensioned before 28 days.

Assume bearing plate of 6" width and 8" length, cross section of the plate is shown in Figure A. 2.

From equation (A.2):

$$A_b = \frac{P_r}{\phi f_n}$$

$$f_n = \min\left(0.7 \times 8 \times \sqrt{\frac{A}{A_g}}, 2.25f_{ci}'\right) = \min(5.6, 18) = 5.6 \text{ ksi}$$

$$A_b = 6 \times 8 - \frac{\pi(1.75^2)}{4} = 45.59 \text{ in}^2$$

$$P_r = 0.9 \times 5.6 \times 45.56 = 229.79 \text{ kips}$$

$$P = 5 \times 0.217 \times 0.75 \times 270 = 219.72 \text{ kips}$$

$P < P_r$ O.K.

$$T_{burst} = 0.3 \times 219.72 \left(1 - \frac{8}{28}\right) = 46.78 \text{ kips}$$

for the case of $a/d=0.29$, the transverse tensile bursting stresses will start at a distance of about $d/8$ (3.5") and will die out at about d (28") from the end face.

In order to keep the stress in the reinforcement below $0.6 f_y = 36 \text{ ksi}$

$$A_s = \frac{46.78}{36} = 1.3 \text{ in}^2$$

Hence the number of #3 closed stirrups required is:

$$\frac{1.3}{2 \times 0.11} = 5.9 = 6 \text{ stirrups}$$

we will use 6 stirrups with the first stirrup at 3.5" from the end face and the remaining stirrups spaced at 5".

In order to control spalling we will provide reinforcement to resist a tensile force of:

$$0.02P = 4.4 \text{ kips}$$

Hence the minimum number of #4 bars working at 36 ksi is:

$$\frac{4.4}{0.2 \times 36} = 0.61, \text{ Use } 2\#4. \text{ Additionally, we will provide } 4\#3 \text{ U-bars to control potential}$$

vertical splitting cracks on the end face. Assuming VSL-7E15 anchor type use spiral of 10 mm diameter, 320 mm length, 5 turns. The reinforcing details are summarized in Figure A. 3.

For Tendon consisting of 9-0.6" strands, Assume bearing plate of 6"x14" length, Figure A. 4 shows cross section of the plate

$$f_n = \min\left(0.7 \times 8 \times \sqrt{\frac{A}{Ag}}, 2.25f_{ci}'\right) = \min(5.6, 18) = 5.6 \text{ ksi}$$

$$A_b = 6 \times 14 - \frac{\pi(2.375^2)}{4} = 79.57 \text{ in}^2$$

$$P_r = 0.9 \times 5.6 \times 79.57 = 401.03 \text{ kips}$$

$$P = 9 \times 0.217 \times 0.75 \times 270 = 395.48 \text{ kips}$$

$$P < P_r \text{ O.K.}$$

$$T_{burst} = 0.3 \times 395.48 \left(1 - \frac{14}{28}\right) = 59.32 \text{ kips}$$

For the case of $a/d=0.5$, the transverse tensile bursting stresses will start at a distance of about $d/5$ (5.6") and will die out at about d (28") from the end face.

In order to keep the stress in the reinforcement below $0.6 f_y = 36 \text{ ksi}$

$$A_s = \frac{59.32}{36} = 1.65 \text{ in}^2$$

Hence the number of #3 closed stirrups required is:

$$\frac{1.65}{2 \times 0.11} = 7.5 = 8 \text{ stirrups}$$

we will use 8 stirrups with the first stirrup at 5" from the end face and the remaining stirrups spaced at 3".

In order to control spalling we will provide reinforcement to resist a tensile force of:

$$0.02P = 7.91 \text{ kips}$$

Hence the minimum number of #4 bars working at 36 ksi is:

$$\frac{7.91}{0.2 \times 36} = 1.1, \text{ Use } 2\#4. \text{ We will provide } 4\#3 \text{ U-bars to control potential vertical splitting}$$

cracks on the end face. Assuming VSL-12E15 anchor type use spiral of 15 mm diameter, 600 mm length, 6 turns. The reinforcing details are shown in Figure A. 5

Figure A. 1 General zone and local zone

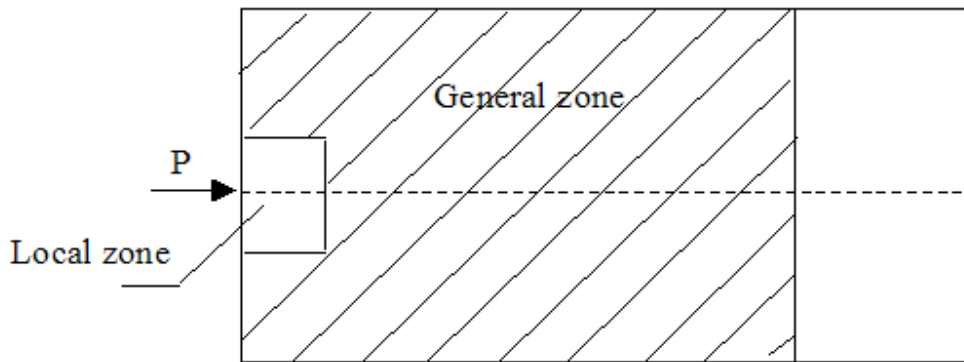


Figure A. 2 Bearing plate dimension for tendons consisting of 5-0.6" strands

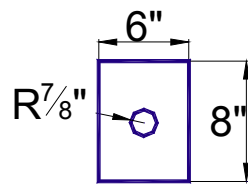


Figure A. 3 Detailing of anchorage zone for tendons consisting of 5-0.6" strands

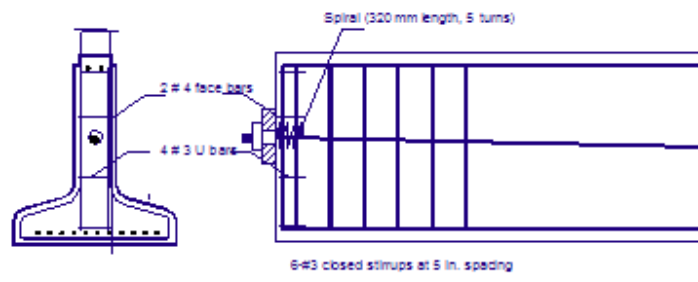


Figure A. 4 Bearing plate dimension for tendons consisting of 5-0.6” strands

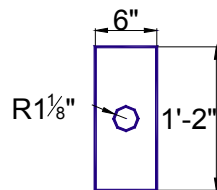
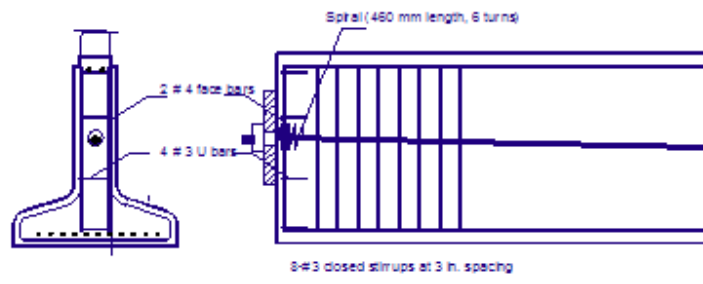


Figure A. 5 Detailing of anchorage zone for tendons consisting of 5-0.6” strands



Appendix B - Program Documentation

The purpose of developing the PT-IT program was for its use as a tool to analyze the post-tensioned, prestressed, inverted-T system. This includes analysis of shear and moment forces resulting from girder self-weight, deck weight, time-dependent restraining moments, secondary moments due to post-tensioning, and external forces. It also includes calculation of losses in pretensioned strands and post-tensioned tendons. The program also checks girder capacity and stresses according to AASHTO LRFD. ⁽¹⁾

The PT-IT program is written using C⁺⁺ language and includes 25 classes. Analysis is divided into the following major steps:

1. Reading data from the input file (*.inp.txt) may be prepared by the user and saved as a text file, or prepared using the user-friendly interface, the format of which will be automatically saved as a text file in the format that the C⁺⁺ program will read. The format of the input file is discussed in chapter 3. Input data should include results of live-load analysis (using Risa or any other program capable of performing moving load analysis). Live-load data includes maximum shear due to live load; minimum shear due to live-load; concurrent moments for maximum and minimum shear, respectively; maximum and minimum moments due to live loads; and maximum and minimum deflection due to live load as required by AASHTO LRFD. Live-load data should be saved as a text file with the following extension: *.LL.txt.
2. For each stage—
 - a. Calculate element reactions, shear, and moment due to girder self-weight, deck weight (carried on the simple span or continuous beam), secondary effect due to post-tensioning, external loads, and time-dependent restraining moment.
 - b. Calculate losses in pretensioned strands and post-tensioned tendons during the time period between each two consecutive stages.

3. For each stage, calculate stresses in the concrete according to AASHTO LRFD requirements.
4. Calculate shear reinforcement required for the girders.
5. Calculate deflection at transfer and at the last stage.
6. Save results as a text file (*.out.txt) that can be read by the interface or directly from the output file.

Header files for classes forming the PT-IT program are listed below, with a brief explanation about each class and its functions.

Class “Data”

This class is used for reading input data; creating objects along the way; and saving output data into objects to be written at the end of analysis, into the output file.

```

/* Data
   The Data class stores all problem data and provides means to access these data.
   Design Rationale:
   Memory for all data is allocated dynamically after the size of the required storage is
   known, during the input-file reading process
   Arrays of pointers (double pointers) are used for most objects. */
#ifndef Data_h
#define Data_h
#include <iostream.h>
#include "Node.h"
#include "Element.h"
#include "BCEssential.h"
#include "BCNodalLoad.h"
#include "Matrix.h"
#include "Material.h"
#include <math.h>
#include "Concrete.h"
#include "Steel.h"
#include "PreStrands.h"
#include "LinearPT.h"
#include "MSpanPT.h"
#include "Time.h"
#include "MomentandShear.h"
#include "ConcreteStresses.h"

class Data
{
private:
Node **      nodes;           // Array of pointers to node objects

```

```

Element ** elems; // Array of pointers to element objects (each span is an
// element)
Element ** diaphragm; // Array of pointers to element objects
BCEssential ** essentialBCs; // Array of pointers to essential B.C.
BCNodalLoad ** nodalLoads; // Array of ptrs to external force The array size is equal to
// the total number of external loads
Concrete ** ConcreteModels; // Array of pointers to user's defined materials
Concrete ** Beammat; // Array of pointers to elements materials
Concrete * Deckmat; // Pointer to deck material
Concrete * Diaphragmmat; // Pointer to diaphragm material
Steel * premat; // Pointer to Prestressing material
teel * postmat; // Pointer to post-tensioning material
PreStrands **prestr; // Array of pointers to prestressing strands (numbre of
// pointers==number of rows)
PostTend ** postten; // Array of pointers to post-tensioning tendons (numbre of
// pointers==number of tendons)
Section **BeamSection; // Array of pointers to element's section (one for each span)
Section *DiaphragmSection; // Pointer to diaphragm's section
ConcreteStresses ** ConStresses; // Array of pointers to save concrete service stresses
Time *time; // Pointer to the matrix which stores stages properties
Matrix * Mcr; // Pointer to the matrix which stores Cracking moments of
// the diaphragms
MomentandShear ** MandV; // Array of pointers to the matrix which stores shear and
// moments
Matrix * MPTSec; // Pointer to array which store secondary moment values
// for all stages
Matrix * VPTSec; // Pointer to array which stores shear due to secondary
// effect of post-tensioning for all stages
Matrix **PreStress; // Array to pointers which store stresses in prestressing
// strands for all stages
Matrix **PostStress; // Array to pointers which store stresses in post-tensioning
// tendons for all stages
Matrix * LiveMoment; // Pointer which stores moment due to live load
Matrix * LiveShear; // Pointer which stores shear due to live load
Matrix * ConMoment; // Pointer which stores moments concurrent to maximum
// and minimum shear
Matrix *Tprov; // Used to store tension force in reinforcement to check
// adequacy of shear reinforcement
Matrix **VerticalShear; // Used to store results of vertical shear analysis
char * title; // Title of input file
char curtype[11]; // Character to store curing type
char name[11];
int nNodes; // Total number of nodes of the model
int nElems; // Total number of elements of the model
int nEssentialBCs; // Total number of essential B.C. of the model
int nNodalLoads; // Total number of external forces.

```

```

int  TNSections;           // Total number of sections including girders and
                          // diaphragms
int  nsectionsdiaph;     // Number of sections in each Diaphragm
int  nPreStrands;        // Number of prestressing strands
int  nPostTend;          // Number of post-tensioning tendons
int  cemtype;            // Cement type
int  RestMomentMethod ;  // Number used to refer to method used to calculate time-
                          // dependent restraining moment
int  NumodofConcreteModels; // Number of concrete materials defined by the user
int  NumOutputSectionResults; // Number of section in which stresses in strands and
                          // tendons to be printed for all stages
Matrix *OutputSectionResults; // Pointer to matrix which saves section numbers for
                          // stresses to be printed
char *LossCalcMethod;    // Losses calculation method
char *ShrinkModel;       // Concrete shrinkage model
char *CreepModel;        // Concrete creep model
char *RestrMomCalcMethod; // Method used to calculate time-dependent restraining
char *ConstScenario;    // Construction scenario
char FileName[100];
double Tfspt;           // Time of first stage PT (two-stage PT scenario only)
int  Stfspt;            // Stage at which first PT is applied (two-stage PT scenario
                          // only)

public:
// Constructors and destructor
Data();
~Data();
// Functions
void readData( istream &s ); // Read input data from input file, create objects along the
                          // way
void readLLData( istream &s ); // Read LL data from input file, create Live load Moment
                          // and Shear objects
void writeData( ostream &s ); // Write the output data
Node *getNode(int node);     // Return nodes[node] (node is node id)
Element *getElem(int elem); // Return elems[elem] (elem is element id)
Element *getDiaphragm(int dia); // Return Diaphragm [dia] (dia is diaphragm id)
BCEssential *getEssentialBC(int ebc); // Return essentialBCs[ebc] (ebc is the id for the essential
                          // BC)
BCNodalLoad *getNodealLoadBC(int pbc); // Return pointBCs[pbc] (pbc is the id for the point
                          // force boundary condition)
int  getNumNodes();         // Return number of nodes
int  getNumElems();         // Return number of elements
int  getNumEssentialBCs(); // Return number of boundary condition
int  getNumNodalLoads();    // Return number of external loads
void setEqnNumber(int num); // Set nEqn = value
int  getTotalNSections();   // Return total number of sections along the bridge
int  getNsectionsdiaph();   // Return number of sections in the diaphragm

```

```

int getNumofConcreteModels(); // Return number of concrete materials defined by the user
double getTfspt(){return Tfspt;} // Return time when first PT is applied (for two-stage PT
// only)
void setTfspt(double T){Tfspt=T;} // Set stage number when first PT is applied (for two-stage
// PT only)
int getStfspt(){return Stfspt;} // Return stage number when first PT is applied (for two-
// stage PT only)
void setStfspt(int Stage){Stfspt=Stage;} // Set stage number when first PT is applied (for two-
// stage PT only)
Time * getTime(); // Return pointer to matrix which stores stages properties
PreStrands * getPrestrands(int span,int n); // Return pointer to strands in row "n" in span
// number "span"
PostTend * getPostTend(int s); // Return pointer to tendon number "n"
PreStrands ** getPrestrandsPointer(); // Return pointer of the array of pointers to strands
PostTend ** getPostTendPointer(); // Return pointer of the array of pointers to tendons
int getnPreStrands(int span); // Return number of strands in span "span"
int getnPostTend(){return nPostTend;} // Return number of tendons
Section ** getGirdersection(); // Return pointer to array of pointers of girder's section
Section * getGirdersection(int span) // Return pointer to girder's section in span "span"
Section * getDiaphragmSection(); // Return pointer to Diaphragm's section
MomentandShear * getMandV(int i) // Return pointer to Matrices storing shear and
// moment values
void SaveStress(Matrix *str1,Matrix *str2,int i); // Save stresses in strands (str1) and tendons
(str2) at stage "i"
Matrix * getLiveMoment(){return LiveMoment;} // Return pointer to the array which stores live
// load moment
double getLiveMoment(int i, int j){return LiveMoment->getEntry(i,j);} // Return value in row "i"
// and column "j" in the live load moment array
double getLiveShear(int i, int j){return LiveShear->getEntry(i,j);} // Return value in row "i" and
// column "j" in the live load shear array
void ErrorExit( int i ); // Error handler
ConcreteStresses * getConcStresses(int i); //Return array which store service concrete stresses
// at stage "i"
Matrix * getPreStress(int i){return PreStress[i];} // Return pointer to stresses in strands at stage
// "i"
Matrix * getPostStress(int i){return PostStress[i];} // Return pointer to stresses in Tendons at
// stage "i"
Matrix * getVerticalShearResults(int i){return VerticalShear[i];} // Rteurn pointer to matrix
// storing shear results at stage "i"
void setVerticalShearResults(int i,Matrix * VS); // Set values to matrix storing shear results at
// stage "i"
char * getLossCalcMethod(); // Return pointer to character storing losses
// calculation method
char * getShrinkModel(); // Return pointer to character storing
// shrinkage model
char * getCreepModel(); // Return pointer to character storing creep model

```

```

char * getRestrMomCalcMethod(); // Return pointer to character storing time-dependent
//restraining moment method
char * getConstScenario(); // Return pointer to character storing construction scenario
Matrix *getMcr(); // Return pointer to matrix storing cracking moment of the
// diaphragm
Matrix *getMPTSec(); // Return pointer to matrix storing values of secondary
// moments
Matrix *getVPTSec(); // Return pointer to matrix storing values of shear due to
// secondary effect of PT
Matrix *getConMoment() {return ConMoment;} // Return pointer to matrix storing moments
// concurrent to max and min live load shear
Matrix * getTprov() {return Tprov;} // Return pointer to matrix used to store tension in
// longitudinal reinforcement (used to check adequacy of
// shear reinforcement)
};
#endif

```

Class “Solve”

This class is used to perform all main computational part of the analysis using objects from all other classes.

```

/* Solve
The solution procedure includes
(1) Solving for moment and shear due to internal and external forces by:
    (i) finding the total number of equations
    (ii) assigning equation number to each active DOF
    (iii) assembling the global stiffness matrix and load vector
    (iv) storing of the solution data (Reactions) into node/DOF objects
(2) Calculates losses in strands and tendons between each two consecutive stages
(3) Calculate stresses in concrete
(4) Calculate deflection at transfer and final */
#ifdef Solve_h
#define Solve_h
#include <iostream.h>
#include "Matrix.h"
#include "Data.h"
class Solve
{
private:
Matrix * K; // Pointer to global stiffness matrix
Matrix * F; // Pointer to global load vector (stores the solution later)
Matrix *ThetaTabel; // Pointer to matrix contains "Theta" values from table
// 5.8.3.4.2-1 AASHTO LRFD
Matrix *BetaTabel; // Pointer to matrix contains "Beta" values from table
// 5.8.3.4.2-1 AASHTO LRFD
Matrix *Timing; // Pointer to matrix stores time when each element of the

```

```

// system and each load is added
double TDiaphragm; // Stores time when diaphragm is cast
int nEqn; // total number of equations (= total number of nodes * 2
// total number of essential BCs)
int setEqnNum( Data &dat); // calculates total number of equations
void assembleRHS(Data &dat,int i,double T); // calculates the global load vector resulting
// external loads considering simply supported spans
void assembleRHSC(Data &dat, int r,double T); // calculates the global load vector resulting
// from external loads considering continuous spans
double assembleRHSW(Data &dat,double T,int ind); // calculates the global load vector
// resulting from self weight for deck weight
void assembleRHSCrSH(Data &dat, Matrix & M); // calculates the global load vector
// resulting from effect of creep and differential shrinkage
void assembleK(Data &dat,double t); // assemble the global stiffness matrix. Also modify the
// load vector (for continuous beam)
void assembleKW( Data &dat,double T); // assemble the global stiffness matrix. Also modify the
// load vector (for simply span beam) this is used mainly to
// calculate moments due to self weight of girder and weight
// of the deck when they are carried by the simply supported
// beam
void assembleRHSMPT(double T,Data &dat, Matrix & M); //Calculate load vector resulting
// from secondary effect of PT
void saveSolution(Data &dat); // Save the solution into each active DOF
public:
// Constructors & destructor
Solve();
virtual ~Solve();
//Functions
void solve(Data &dat); // Main function that calls all sub-functions that perform
// analysis
void calcElementReactions(Data &dat,double T,double ind); // Used to calculate element
// reactions
void calcMoment_Shear(Data&dat,int j,int StageNum, double T); //Used to calculate moment
// and shear at each section along the beam
void calcDeflection(Data&dat); // Used to calculate deflection at transfer and final
void calcShearReinforcement(Data&dat); // Used to calculate amount of shear reinforcement
// needed
double getTheta(double ex, double vu); // Return value of "Theta" corresponding to strain
// ex and shear vu
double getBeta(double ex, double vu); // Return value of "Beta" corresponding to strain ex and
// shear vu
void calcTimeDependentLosses(int StageNum,Data& dat); // Calc losses in stresses in strands
// and tendons between stage "StageNum" and
// "StageNum+1" using AASHTO LRFD method
void calcTimeDependentLosses_Creep_Transformed_Method(int StageNum,Data &dat); // Calc
// losses in stresses in strands and tendons between stage

```

```

// "StageNum" and "StageNum+1" using creep-transformed
// section properties method
void calcMembersForces(Data &dat,Matrix &Mr,int Stage);// Calculate shear and forces
// resulting from time- dependent restraining moments
void CalcConcreteStresses(Data &dat);// Checks section capacity and concrete stresses at each
// stage according to AASHTO LRFD
void setTiming(Data&dat); // Set Timing matrix which contains time at which each
// member and load are added to the system
void getFEM(Data& dat,Matrix & Mat,Matrix & FEM,int stage); //Calculate fixed end moments
// (starting from given curvature)
void getPostTensioningFEM(Data &dat,Matrix & MPost,int Stage); //Calculate fixed end
// moments resulting from post-tensioning (starting by
// calculating curvature from forces in tendons)
void calcMPTSecForces(Data& dat,Matrix &MPost,int Stage); // Calculate shear and moment
// along the members resulting from secondary effect of PT
void IntegrateDef(Data &dat,Matrix & curv,Matrix & def);// Used to perform curvature
// numerical integration to obtain deflection
void Calc_strain_fspt(double t1,Data &dat,Matrix &ecg); // Calculate strain due to post
// tensioning at each location along the beam (used to
// calculate losses in PT for the case of two- stage PT
// before grouting)
};
#endif

```

Class “Element”

This is a base class from which different classes are derived and inherit the same properties with some additional properties.

```

/* Element*/
#ifndef Element_h
#define Element_h
#include <iostream.h>
#include "DOF.h"
#include "Node.h"
#include "Matrix.h"
#include "Section.h"
class Element
{
protected:

int ID; // Element id
int numNodes; // Number of nodes in element
Node ** nodes; // Array of pointers to nodes in this element
Section * Sec; // Pointer to section of element
Matrix * Fem; // Pointer to array storing fixed end moments for the
// element

```

```

Matrix * R; // Pointer to array storing reactions of the element
Matrix * V; // Pointer to array storing shear forces along the element
Matrix * M; // Pointer to array storing moment values along the element
int nsections; // Number of sections in the element
public:
// Constructors & destructor
Element(int id, Node ** nodes, Section *Sec, int n_sections);
virtual ~Element();
// Functions
int getID() const; // Return ID;
int getNumNodes() const; // Return numNodes;
int getnSections(); // Return number of sections along the element
Node ** getNodeList() const; // Return pointer array of nodes
void setFEM(Matrix &m); // Set values of fixed end moments
void setR(Matrix &re); // Set values of reactions
void setV(Matrix &v, int j); // Set values of shear forces
void setM(Matrix &m, int j); // Set values of moments
double getV(int i, int j); // Return values of shear forces
double getM(int i, int j); // Return values of moments
double getFEM(int i, int j) // Return values of fixed end moments
double getR(int i, int j); // Return values of reactions
friend ostream & operator<<( ostream &s, const Element & node ); //Function used for output
// data

// Virtual functions have to be implemented in individual element types
virtual int getNumDOFs() const = 0; // Return the total number of DOFs
virtual void getElementK( Node *bn, Node *en, double t, double l, Matrix &esm ) = 0; //Calculate
// and return element stiffness matrix.
virtual void print(ostream &out) const = 0;
virtual Section * getSection()=0; // Return pointer to element's section
virtual double getL()=0; // Return length of the element
};
#endif

```

Class “Element2”

This class is a derived class from class “Element” it creates girders elements with 2 nodes.

```

/*Element*/
#ifdef Element2_h
#define Element2_h
#include "Element.h"
#include <iostream.h>
class Element2 : public Element
{

```

```

private:
public:
// Constructor & Destructor
Element2(int id, Node ** nodes,Section * Sec,int n_section);
virtual ~Element2();
// Functions
virtual int getNumDOFs() const { return 4; } //Return the number of DOFs of the element
virtual void getElementK( Node *bn, Node*en,double t,double l,Matrix &esm);// Calculate the
// element stiffness matrix and stored in pre-allocated K

virtual void print(ostream &out) const // The function for << operator
Section * getSection(); // Return pointer to element's section
double getL(); // Return element's length
};
#endif

```

Class “Diaphragm”

This class is also a derived class from class “Element”, it is used to create diaphragm objects.

```

/* Diaphragm */
#ifndef Diaphragm_h
#define Diaphragm_h
#include "Element.h"
#include <iostream.h>
class Diaphragm : public Element
{
private:
public:
// Constructor & Destructor
Diaphragm(int id, Node ** nodes,Section * S_ec,int n_section);
virtual ~Diaphragm();
// Functions
virtual int getNumDOFs() const { return 4; }
virtual void getElementK( Node *bn, Node *en,double t,double l,Matrix &esm);
virtual void print(ostream &out) const;
Section * getSection();
double getL();
};

#endif

```

Class “Node”

The Node class stores nodes IDs, coordinates, and degrees of freedom (DOFs).

```

/* Node class */
#ifndef Node_h
#define Node_h
#include "DOF.h"
#include <iostream.h>
class Node
{
private:
    int ID; // Node ID
    DOF * DOFs; // Array of DOFs
    double * coords;
public:
    // Constructors & destructor
    Node(int id);
    ~Node();
    // Functions
    int getID() const; // Return Id;
    DOF * getDOF(int DOF) const; // Return dof[DOF];
    friend ostream & operator<<( ostream &s, Node &n ); // Define operator "<<" for output.
    void printData(ostream &out) const; // print useful info for debugging purpose
    double getCoord() const; // Return Node X;
    void setCoords( double *c );
};
#endif

```

Class “ESM”

The ESM class implements the element's stiffness matrix

```

/* ESM */
#ifndef ESM_h
#define ESM_h
#include <iostream.h>
#include "Matrix.h"
class ESM
{
private:
    double E;
    double I;
    double L;
    int BN;
    int EN;
public:
    ESM(int bn, int en, double e, double i, double l);
    ~ESM();
    // Functions
    void setEsm(Matrix &esm);

```

```

int getbn();
int geten();
friend ostream & operator<<( ostream &s, const ESM & a );
void BC(int n,int R, double value,Matrix &esm);
void getK(Matrix &K);
};
#endif

```

Class “BCEssential”

This class stores the essential boundary conditions, and its values.

```

/* BCEssential */
#ifdef BCEssential_h
#define BCEssential_h
#include "DOF.h"
#include "Node.h"
#include <iostream.h>
class BCEssential
{
private:
Node * node; //Pointer to node associated with essential BC
DOFType dof; // either UY or Theta
double value; // value = prescribed displacement value
public:
// Constructor & destructor
BCEssential(Node* n_ode, DOFType d_of, double v_alue);
~BCEssential(){};
// Functions
Node* getNode() const;
DOFType getDOF() const;
double getValue() const;
friend ostream & operator<<( ostream &s, const BCEssential & bc );
};
#endif

```

Class “DOF”

The DOF class implements a "degree of freedom" of a node. In this code, the DOFs without the prescribed value is called active, which will be assembled into the final global equation system. DOF's with prescribed values are called inactive DOF. Each node has its DOF object to define its boundary conditions.

```

/* DOF */
#ifdef DOF_h
#define DOF_h

```

```

#include <iostream.h>
enum DOFType{UY=0,Theta};
class DOF
{
private:
double value;           // The value of this degree of freedom. For essential BC
                        // (inactive DOF), it is the prescribed (displacement) value.
                        // For active DOF, it stores displacement value after system
                        // equations are solved.

int  eqnNum;           // equation number of DOF. (-1 indicates an inactive DOF)
public:
// Constructors & Destructors
DOF();
~DOF();
// Functions
bool  isActive() const           // Return active;
int   getEqnNum() const;         // Return eqnNum;
double getValue() const;        // Return value;
friend ostream & operator<<( ostream &s, const DOF & d );
void  setNotActive();           // Set active = false;
void  setEqnNum(int n);         // For active DOF, set eqnNum = n; for inactive DOF, set
                                // eqnNum = -1 (or any negative integer)

void  setValue(double v);       //Set value = value;
};
#endif

```

Class “FixedEM”

This class calculates fixed end moments resulting from uniform and concentrated loads

```

/* FixedEM */
#ifndef FixedEM_h
#define FixedEM_h
#include "DOF.h"
#include "Node.h"
#include "Element.h"
#include "Data.h"
#include <iostream.h>
enum LLoadType {UU=0, CC};
class FixedEM
{
private:
Element * elem;
Node *node;
LLoadType ltype;
double bl; //begining location from the right support
double v; //end value

```

```

public:
// Constructors & Destructor
FixedEM( Element* e_lem, LLoadType l_type, double b_l,double b_v);
FixedEM(Element* e_lem, LLoadType l_type, double b_v);
~FixedEM();
// Functions
void calcFEM(Data& dat);
};
#endif

```

Class “BCNodalLoad”

The BCNodalLoad class stores properties for uniform and concentrated forces.

```

/* BCNodalLoad */
#ifndef BCNodalLoad_h
#define BCNodalLoad_h
#include "Node.h"
#include "Element.h"
#include <iostream.h>
enum LoadType {U=0, C};
class BCNodalLoad
{
private:
Element * elem;
Node * node;
LoadType ltype;
Element ** el;
int nelelem;
double bl; //begining location from the right support
double v; //end value
public:
// Constructors & Destructor
BCNodalLoad(LoadType l_type, Element* e_lem, double b_l,double b_v);
BCNodalLoad(LoadType l_type,int numelem, Element ** e_lem, double b_v);
BCNodalLoad(LoadType l_type,Element * e_lem, double b_v);
BCNodalLoad(int numelem);
~BCNodalLoad();
// Functions
Element * getElement() const;
LoadType getLoadType() const;
double getValue() const;
int getnelem();
double getbl();
Element * getel(int i);
friend ostream & operator<<( ostream &s, const BCNodalLoad &load );
void calcFEM();

```

```
};
#endif
```

Class “MomentandShear”

This class is used to store moment and shear resulting from analysis, due to internal and external loads applied on the structure.

```
/* MomentandShear*/
#ifndef MomentandShear_h
#define MomentandShear_h
#include <iostream.h>
#include "Matrix.h"
class MomentandShear
{
private:
    Matrix *M;
    Matrix *V;
    Matrix *Deflection;
    int nSections;
    int nSpans;
    int DianSections;
    int nStages;
public:
    MomentandShear(int nSections,int nSpans,int DianSections, int nStages);
    ~MomentandShear();
    // Functions
    void setM(Matrix &m, int i,int j);
    void setV(Matrix &v, int i,int j);
    void setDeflection(Matrix &deflection, int i,int j);
    double getM(int i, int j);
    double getV(int i,int j);
    double getDeflection(int i,int j);
    void setDeflection(double val,int i,int j);
    Matrix * getM();
    Matrix * getV();
    Matrix * getDeflection();
    int MomentandShear:: getNumRows();
    int MomentandShear:: getNumCols();
    void MomentandShear::addLiveM(int i,int j, double v);
    void MomentandShear::addLiveV(int i,int j, double v);
    void printMandV();
};
#endif
```

Class “Concrete Stresses”

This class is used to store stresses of the concrete and capacity calculated as required by

AASHTO LRFD

```
/* Concrete Stresses */
#ifndef ConcreteStresses_h
#define ConcreteStresses_h
#include "Matrix.h"
#include "Concrete.h"
#include "PreStrands.h"
#include "LinearPT.h"
#include "MSpanPT.h"
#include "Time.h"
#include <iostream.h>
class ConcreteStresses
{
private:
int Nrows;
double fi;
Matrix * ReleaseAll_Comp_Stress;
double ReleaseAll_Comp_Stress_Deck;
double ReleaseAll_Tens_Stress;
Matrix * All_Comp_Stress_ServiceI_I;
Matrix * All_Comp_Stress_ServiceI_II;
Matrix * All_Tens_Stress_ServiceIII;
double All_Comp_Stress_ServiceI_I_Deck;
double All_Comp_Stress_ServiceI_II_Deck;
double All_Comp_Stress_ServiceIII_Deck;
Matrix * StrengthI;
Matrix * ServiceI_I;
Matrix * ServiceI_II;
Matrix * ServiceIII;
public:
//Constructor & Destructor
ConcreteStresses(int i,int nSpans,Concrete ** Beammat,Concrete * Deckmat,PreStrands **
PreStress,PostTend **PostStress,int TNSection,Time * time);
~ConcreteStresses();
void setStrengthI(Matrix & strengthI);
void setServiceI_I(Matrix & serviceI_I);
void setServiceI_II(Matrix & serviceI_III);
void setServiceIII(Matrix & serviceIII);
void setStrengthI (int i, int j,double k);
void setServiceI_I (int i, int j,double k);
void setServiceI_II(int i, int j,double k);
void setServiceIII (int i, int j,double k);
void printConcStresses();
double getReleaseAll_Comp_Stress(int i);
```

```

double getReleaseAll_Comp_Stress_Deck();
double getReleaseAll_Tens_Stress();
double getAll_Comp_Stress_ServicI_I(int i);
double getAll_Comp_Stress_ServicI_II(int i);
double getAll_Tens_Stress_ServicIII(int i);
double getAll_Comp_Stress_ServicI_I_Deck();
double getAll_Comp_Stress_ServicI_II_Deck();
double getAll_Comp_Stress_ServicIII_Deck();
Matrix * getStrengthI();
Matrix * getServiceI_I();
Matrix * getServiceI_II();
Matrix * getServiceIII();
};

#endif

```

Class “Meterial”

The material is a base class that provides common interface for materials. Specific material class is derived from this class and may contain its own additional interface. This is an abstract class that cannot be directly instantiated. Two classes are derived from this class “Concrete” and “Steel” classes.

```

/* Material */
#ifndef Material_h
#define Material_h
#include "Matrix.h"
#include <iostream.h>
class Material
{
protected:
char Name [15];
int ID;
double E;
public:
//Constructor & Destructor
Material(int i);
virtual ~Material();
//Functions
int getID() const; // Return Id;
char *getName();
};
#endif

```

Class “Steel”

```

/* Steel class */
#ifndef Steel_h
#define Steel_h
#include "Material.h"
#include <iostream.h>
class Steel: public Material
{
private:
double fpu;
double fy;
public:
//Constructor & Destructor
Steel(int i,double fpu, double fy);
virtual ~Steel();
double getfpu();
double getfy();
double getE();
void setfpu(double a);
void setfy(double a);
void setE(int a);
};
#endif

```

Class “Concrete”

```

/* Concrete class */
#ifndef Concrete_h
#define Concrete_h
#include "Material.h"
#include "PreStrands.h"
#include "LinearPT.h"
#include "MSpanPT.h"
#include "Matrix.h"
#include <iostream.h>
class Concrete: public Material
{
private:
char Model[20];
char CuringType[11];
char Name[20];
int CementType;
double wc;
double fpct;
double fpc28;
double fpci;
double fr;
double H;

```

```

double t;          //t is time in days
public:
//Constructor & Destructor
Concrete(int i,char * model,char *name,char * CuringType,int CementType,double fpci,double
fpc28,double wc, double h );
virtual ~Concrete();
double getfci();          // Get initial strength
double getfpct(double T); // Get concrete strength at time "T"
double getfpc28(){ return fpc28;} // Get concrete strength at 28 days
double getE(double T); // Get modulus of elasticity time "T"
double getE28(double fpc28) ; // Get modulus of elasticity at 28 days
double getE_Cr(double E1, double X, double fi); // Get creep modified modulus of elasticity at
// 28 days
double getWc(); // Get unit weight
void setWc(double a); // Set unit weight
void setfpc28(double a); // Set concrete strength at 28 days
void setCementType(int a) ; // Set cement type
void setCuringType(char*a); // Set curing type
void setName(char*a); // Set name of the concrete material
char * getCurtype(); // Get curing type
char * getName(); // Get name
int getcemtype(); // Get cement type
double getH(){ return H;} // Get humidity of the enviroment surrounding the concrete
};
#endif

```

Class “PreStrands”

This class stores properties of pretensioned strands; it allows construction of straight as well as one and two point depression strands.

```

/* PrestensionedStrands */
#ifndef PreStrands_h
#define PreStrands_h
#include <iostream.h>
#include "Steel.h"
class PreStrands
{
protected:
char ID[13];
char TenType[10];
char TenProf[10];
int Num;
float ec0;
double jacking;//ratio of the ultimate stress
double d;
double area;

```

```

float DepressFraction;
float DepressIncrement;
Steel * mat;
Matrix *Stress;
int nSections;
int NSpan;
public:
// Constructors & destructor
PreStrands(Steel *mat,int nspan,char *ID, char *TenType,char *TenProf, int Num, float ecc0);
PreStrands(Steel *mat,int nspan,char *ID, char *TenType, char *TenProf,int Num, float
ecc0,float DepressFraction);
~PreStrands();
int getNum()const;
double getecc(double x);//x is a fraction of the length
double getAngle(double x);//x is a fraction of the length
double getec0();
double getArea();
double getd();
Steel *getmat();
double getJacking();
float getDepFrac();
double CalcElasticShortening(double fcgp, double eci);
void setStress(Matrix * stress);
void setStress(int i,double v);///sets the value of stress v at the row number i
Matrix * getStress();
double getStress(int i);
int getnSections();
int getnElems();
char *getTenType();
char * getTenprof();
char * getID();
void setnSections(int n);
};

#endif

```

Class “PostTend”

This class is a base class from which two classes are derived, “Straight” and “Parabolic”

```

/* Post tensioned Tendons */
#ifndef PostTend_h
#define PostTend_h
#include <iostream.h>
#include "Steel.h"
#include "Matrix.h"

```

```

class PostTend {
protected:
char ID[15];
char TenType[10];
char TenProfile[9];
double D;
double Area;
double AnchSet;
double FricCoeff;
double WobbleCoeff;
double Jacking;
double ecc;
Steel *mat;
Matrix *Stress;
Matrix *stress;           //Helps to calculate the Friction Loss
int NSpan;
int nSections;
double Lset;
double LsetStress;
public:
// Constructors & destructor
PostTend(Steel *mat,int nSpan,char *ID,char *TenProfile,double AnchSet,double FricCoeff,
double WobbleCoeff, double Jacking,int nsections);
virtual ~PostTend();
virtual double getecc(double x)=0;//x is in (inch)
virtual double getAngle(double x)=0;//x is in (inch)
Steel * getmat();
double getArea();
double getJacking();
char * getTendProfile();
char * getTendType();
char * getID();
double returnecc();
virtual double getFrictionAngleChange()=0;
double CalcElasticShortening(int N,double fcgp, double eci);
int getnSections();
void setStress(Matrix * stress);
void setStress(int i,double v);
Matrix * getStress();
double getStress(int i);
void setstress(int i,int j,double v);
double getstress(int i,int j);
double getAnchSet(int i);
double getWobbleCoeff();
double getFricCoeff();
int getNSpans();

```

```

void setLset(double x) {Lset=x;}
void setLsetStress(double x) {LsetStress=x;}
double getLset() {return Lset;}
double getLsetStress() {return LsetStress;}
virtual int getNRow()=0;
};
#endif

```

Class “Straight”

```

/* StraightPT */
#ifndef StraightPT_h
#define StraightPT_h
#include "PostTend.h"
#include <iostream.h>
#include "Matrix.h"
class StraightPT : public PostTend
{
private:
public:
// Constructor & Destructor
StraightPT(Steel *mat,int nSpan,char *ID,char *TenProfile,double AnchSet,double FricCoeff,
double WobbleCoeff, double Jacking,double e_cc,int nsections);
~StraightPT();
// Functions
double geteicc(double x);
double getFrictionAngleChange();
int getNRow();
double getAngle(double x);
};
#endif

```

Class “ParabolicPT”

```

/* ParabolicPT */
#ifndef ParabolicPT_h
#define ParabolicPT_h
#include "PostTend.h"
#include <iostream.h>
#include "Matrix.h"
class ParabolicPT : public PostTend
{
private:
//
int NSpan;
Matrix *XY;
Matrix *xy;

```

```

Matrix *xy1; //original xy that is provided by the user
int NRow;
double contraflexure;
public:
// Constructor & Destructor
ParabolicPT(Steel *mat,int NSpan,char *ID,char *TenProfile,double AnchSet,double FricCoeff,
double WobbleCoeff, double Jacking,double contraflexure, Matrix *xy,int nsections);
~ParabolicPT();
// Functions
double getecc(double x);
double getAngle(double x);
double getFrictionAngleChange();
int getNRow(){return NRow;}
};
#endif

```

Class “Section”

```

/* Section*/
#ifndef Section_h
#define Section_h
#include <iostream.h>
#include "Material.h"
#include "Concrete.h"
#include "PreStrands.h"
#include "PostTend.h"
class Section {
private:
int CrackingInd; // Used to indicate when the diaphragm has cracked (for P
// Method)
int id; // Used to indicate when the Deck is added to the system
int ipre; /// Used to indicate when the strands is added to the system
int ipost; // Used to indicate when the post-tensioned is added to the system
double Cg; // Distance from the centroid of the section to the bottom of the
// Concrete sectio
double A; // Area of the girder's section
double Ixx; // Moment of Inertia around the X axis for the girder's Section
double VtA; // Volume to Area ratio for the Concrete Section
double H; // Overall Height of the Conceret Section
double WW; // Girder's web width
double hf; // IT flange thickness=5.51 in
double w; // Effective Width of the deck
double hd; // Height of the deck
double CgComp; // Distance from the centroid of the section to the bottom of
// the (girder and prestressing) Composite section
double Acomp; // Area of the (girder and prestressing) composite section
double IxxComp; // Moment of inertia around the X axis for the (girder and

```

```

//prestressing) composite Section
double CgComp; // Distance from the centroid of the section to the bottom of
// the composite section
double Acomp;= // Area of the composite section
double IxxComp; // Moment of inertia around the X axis for the composite
// section
double VtAComp; // Volume to area ratio for the composite section
double HComp; // Overall height of the composite section
//Properties of Creep_Transformed section properties
double CgComp_Cr;
double Acomp_Cr;
double IxxComp_Cr;
double VtAComp_Cr;
double HComp_Cr;
double As;
double Tdeck; //Time when the deck is added
Concrete *mat; // Material of the Beam
Concrete *matd; // Material of the Deck
PreStrands ** Prestrand;
PostTend ** Postten;
int nprestrands;
int nposttend;
public:
// Constructors & destructor
Section ();
virtual ~Section();
// Functions
int getID();
double getH()const{return H;}
void SetProperties(Concrete *material,double cg,double a, double ix, double vta,double
h,double ww,Concrete * Deckmaterial,double W,double h_d,int npre,PreStrands
**prestrands,int npost,PostTend **posttend);
void SetPostProperties(int npost,PostTend **posttend);
void adddeckproperties();
void Removedeckproperties();
void addPresProperties ();
void RemovePresProperties();
PreStrands * getPrestrands(int i) {return Prestrand[i];}
int getNpres() {return nprestrands;}
void addPostProperties ();
void RemovePostProperties();
void CalcNetSectProp(double t, double xpre, double xpo);
void CalcGirderTransformedSecProp(double t, double xpre);
void CalcTransformedSecProp(double t, double xpre, double xpo);
void CalcCreep_TransformedSecProp(double t, double xpre, double xpo,double
AgingCoeffg,double fig, double AgingCoeffd,double fid);

```

```

double Section::getCgComp();
double Section::getIxxComp();
double Section::getAComp();
double getCgComp();
double getIxxComp();
double getAComp();
double getCgComp_Cr();
double getIxxComp_Cr();
double getAComp_Cr();
double getCg();
double getWW();
double gethf(){return hf;}
double getIxx();
double getA();
Concrete *getmat();
Concrete *getDeckmat();
double getVtAComp();
double getVtA();
double gethdeck();
double getHComp();
double getwdeck();
void setTdeck(double T);
void setCrackingInd(){CrackingInd=1;};
void unsetCrackingInd(){CrackingInd=0;};
int getCrackingInd(){return CrackingInd;};
void setAs(double as) {As=as;}
double getAs() {return As;}
};
#endif

```

Class “TimeDepLosses”

This class is used to calculate shrinkage and creep properties of the concrete.

```

/* TimeDep.Losses class */
#ifndef TimeDepLosses_h
#define TimeDepLosses_h
#include <iostream.h>
#include "Matrix.h"
class TimeDepLosses{
private:
double VtS;
double t1;
double t2;
double ti;
double H;
double CR;

```

```

double SH;
double RE;
char CType[11]; //concrete type
char SHModel[20];
char CrModel[20];
Matrix * Aging_Coeff;
public:
TimeDepLosses(char *Shmodel, char *Crmodel, char * cType, double vts, double h);
~TimeDepLosses();
double CalcShrinkage(double Fpc, double Ti, double T1);
double CalcPartialShrinkage(double Fpc, double Ti, double T1, double T2);
double CalcPartialRelaxation(char *TType, double Fpi, double Fy, double T1, double T2);
double CalcPartialfi(double Fpc, double Ti, double T1, double T2);
double Calcfi(double Fpc, double t0, double t);
double Calcfu(double Fpc, double t0);
double getAgingCoeff(double Fpc, double t, double t0);
};
#endif

```

Class “Time”

This class saves stages properties.

```

/* Time */
#ifndef Time_h
#define Time_h
#include <iostream.h>
#include "Matrix.h"
class Time
{
private:
int N;
Matrix *time;
public:
// Constructor & destructor
Time(Matrix * ttime);
~Time();
// Functions
int getN();
double gettime(int i, int j);
};
#endif

```

Class “Matrix”

This class is used to perform manipulation for matrices

```

/* Matrix */

```

```

#ifndef Matrix_h
#define Matrix_h
#include <stdio.h>
#include <stdlib.h>
#include <iostream.h>
class Matrix{
private:
double ** entry;           // Entries of the matrix. Double point format
int   n_row;              // Number of rows
int   n_column;          // Number of columns
public:
// Constructor and destructor
Matrix(int row, int column );           //construct a nr x nc matrix
~Matrix();
// Functions
void   zero();                       // Initialize all coefficients of the matrix to zero
int   getNumRows() const;           // Return n_row;
int   getNumCols() const;          // Return n_column;
friend ostream & operator<<( ostream &s, const Matrix & a );
void   setEntry(int i, int j, double value);
void   addToEntry(int i, int j, double value);
double getEntry(int i, int j) ;
// Arithmetics
Matrix & operator +=( Matrix &a ); // (*this) = (*this) + a
Matrix & operator *=( double a ); // (*this) = (*this) * a
void mult(Matrix &b, Matrix &c); // c = (*this) * b
void trans(Matrix &a);           // a = (*this)^T
// Solver of Gaussian elimination. This is a so-called "Fully Pivoted
// Gaussian Elimination" solver. Solve the equation [*this]{x} = {b}.
// Solution is stored back into b, so the original b is destroyed.
void gauss_solver( Matrix & b );
};
#endif

```